U.S. DEPARTMENT OF COMMERCE
DANIEL C. ROPER, Secretary
BUREAU OF STANDARDS
LYMAN J. BRIGGS, Director

BUREAU OF STANDARDS JOURNAL OF RESEARCH

July 1933
Vol. 11, No. 1

UNITED STATES
GOVERNMENT PRINTING OFFICE
WASHINGTON : 1933

For sale by the Superintendent of Documents, Washington, D.C. - - Price 25 cents; $2.50 per year on subscription

For a partial list of previous research papers appearing in BUREAU OF STANDARDS JOURNAL OF RESEARCH see pages 2 and 3 of the cover

U.S. DEPARTMENT OF COMMERCE—BUREAU OF STANDARDS

RESEARCH PAPER RP573

Part of Bureau of Standards Journal of Research, Vol. 11, July 1933

AN INTERNATIONAL COMPARISON OF TEMPERATURE SCALES BETWEEN 660° AND 1,063° C.

By Wm. F. Roeser, F. H. Schofield,[1] and H. A. Moser[2]

ABSTRACT

This paper reports an intercomparison of the termperature scales (in the range 660° to 1,063° C.) in use at the National Physical Laboratory, the Physikalisch-Technische Reichsanstalt, and the Bureau of Standards since 1927. It is shown that the methods used in realizing the International Temperature Scale have yielded results differing by as much as 0.7° C. at 850° C. due primarily to a difference of 0.4° C. at the freezing point of silver, one of the basic fixed points of the International Temperature Scale. After exchanging samples of silver and thermocouples the various scales have been brought into agreement, within 0.1° C., at all points in the range covered.

CONTENTS

		Page
I.	Introduction	1
II.	Definition of scale from 660° to 1,063° C	2
III.	Methods and results	2
IV.	Summary	5
V.	Acknowledgments	6

I. INTRODUCTION

Since the adoption of the International Temperature Scale in 1927 by the Seventh General Conference of Weights and Measures, representing 31 nations, the temperature determinations of practically the entire world have been based for the first time in history upon a common set of definitions and specifications. In the definition of the International Temperature Scale values are assigned to selected fixed points, instruments are specified to be calibrated at these fixed points, and forms of equations are specified for obtaining values other than the fixed points. To a very limited degree the experimental procedure to be followed in calibrating the instruments at the fixed points is also specified.

The fact that two standardizing laboratories base their temperature determinations on the International Temperature Scale leads to the presumption but does not of itself insure that the results obtained with instruments calibrated in one of these laboratories will agree with those obtained with instruments calibrated in the other. Since the fixed points of the scale are the temperatures at which either the solid and liquid phases or the liquid and vapor phases of pure materials are in equilibrium, appreciable differences in the purity of the materials actually used, or differences in experimental technique, may lead to constant differences, which can best be determined by having all the laboratories in question calibrate a given instrument or preferably a group of instruments.

[1] National Physical Laboratory, Teddington, Middlesex, England.
[2] Physikalisch-Technische Reichsanstalt, Berlin-Charlottenburg, Germany.

Arrangements have been made by the national laboratories of Great Britain, Germany, and the United States to make intercomparisons through an exchange of instruments calibrated in each laboratory according to its regular procedure for realizing the International Temperature Scale in practice. Since three types of instrument—the resistance thermometer, the thermocouple, and the optical pyrometer—are required to cover the entire range of this scale, the work has naturally been divided into three parts. The part covering that portion of the scale which is based on the indications of a thermocouple has now been completed and is the subject of this paper. The other two parts of the work will be published subsequently.

II. DEFINITION OF SCALE FROM 660° TO 1,063° C.[3]

From 660° C. to the gold point, the temperature t is deduced from the electromotive force e of a standard platinum *vs.* platinum-rhodium thermocouple, one junction of which is kept at a constant temperature of 0° C. while the other is at the temperature t defined by the formula

$$e=a+bt+ct^2$$

The constants a, b, and c are to be determined by calibration at the freezing point of antimony, and at the silver and gold points.

The silver and gold points are defined as 960.5° and 1,063.0° C., respectively, but since the antimony point lies in the range in which temperatures are defined by platinum resistance thermometers, the freezing point of the antimony to be used is determined by resistance thermometer measurements.

III. METHODS AND RESULTS

Each of the three laboratories participating in the present work furnished two standard platinum to platinum-10 percent rhodium thermocouples. The data concerning these thermocouples and the metals used in the calibrations are given in tables 1 and 2.

The observations obtained in the three laboratories are summarized in tables 3 and 4.

After each of the laboratories had made measurements with all the thermocouples, the results showed significant discrepancies at the freezing point of silver, and further work was undertaken to determine the cause of these discrepancies.

Since the silver originally used at the Bureau of Standards was found to contain 0.069 percent impurities, a new lot of silver was obtained from the United States Bureau of the Mint. This silver is of the quality known as "inquartation silver", which contained only 0.005 percent lead, 0.002 percent copper, and 0.001 percent iron.

TABLE 1.—*Data on thermocouples used in intercomparison of temperature scales*

Thermocouples supplied by—	Thermocouples manufactured by—	Designated—	Preliminary treatment	Type of protection tube
Bureau of Standards	Bureau of Standards	G_1 and G_2	Annealed 6 hours at 1,500° C.	Porcelain.
National Physical Laboratory.	Johnson, Matthey & Co.	P_{15} and P_{17}	Annealed 1 hour at 1,500° C.	Silica.
Physikalisch-Technische Reichsanstalt.	Heraeus	$D_{3,024}$ and $D_{3,028}$	Annealed 5 minutes at 1,200° C.	Porcelain.

[3] Proc. Seventh General Conference of Weights and Measures. 1927, p. 56. [illegible] Annex IV, p. 94. B.S. Jour. Research, vol. 1, p. 635, 1928.

TABLE 2.—*Data on metals used in primary calibration of thermocouples*

BUREAU OF STANDARDS

Metal	Prepared by—	Purity	Freezing point [1]	Crucible material	Method of protection from oxygen	Depth of immersion of thermocouple
			° C.			cm
Gold	U.S. Bureau of the Mint	99.99 (?)	1,063.0	Graphite (Acheson)		11
Silver (old)	do	99.931	960.5 (?)	do	Covered with flake graphite	11
Silver (inquartation)	do	99.992	960.5	do	do	11
Antimony	Schering-Kahlbaum A.G	99.96 (?)	[2] 630.53 [3] 630.47	do	do	11
Zinc	New Jersey Zinc Co	99.992	419.50	do	do	11

NATIONAL PHYSICAL LABORATORY

Gold	Johnson Matthey & Co	99.99 (?)	1,063.0	Porcelain (Marquardt)		9
Silver	do	99.99	960.5	Silica	Melted in vacuo	13
Antimony	Schering-Kahlbaum A.G	99.97	630.42	Graphite	Covered with powdered graphite	11
Zinc	New Jersey Zinc Co	99.97	419.43	do	do	8

PHYSIKALISCH-TECHNISCHE REICHSANSTALT

Gold (1928)	Heraeus		1,063.0			[4]
Gold (1931)	Gold- und Silberscheideanstalt	99.99	1,063.0	Porcelain		7
Silver	Heraeus	99.99	960.5	Graphite (Acheson)	Graphite cover	9
Antimony (1928)	Schering-Kahlbaum A.G		630.35	Graphite	do	11
Antimony (1931)	do	99.97	630.48	do	do	11
Zinc	do	99.9	419.45	do	do	10

[1] The values for the freezing points of gold and silver are defined. Those for antimony and zinc are determined by use of platinum resistance thermometer.
[2] In 1929.
[3] In 1931.
[4] Wire method.

TABLE 3.—*Summary of observations*

GOLD POINT, 1,063.0° C.

Laboratory	Year	Emf in microvolts (cold junctions at 0° C.)					
		$D_{3,024}$	$D_{3,026}$	G_1	G_2	P_{16}	P_{17}
P.T.R.	1928	10,256	10,257				
B.S.	1929	10,256.0	10,257.3	10,307.8	10,312.7	10,316.9	10,314.7
N.P.L.	1930	10,254	10,253.5	10,307.5	10,312	10,316	10,314
P.T.R.	1931	10,261	10,257	10,305	10,314	10,314	10,314
B.S.	1931			10,307.3	10,313.0	10,313.2	10,312.0
P.T.R.	1931		10,258				

SILVER POINT, 960.5° C.[1]

P.T.R.	1928	9,082	9,080				
B.S.	1929	9,075.5	9,075.7	9,117.5	9,121.9	9,124.7	9,122.8
N.P.L.	1930	9,077.5	9,074	9,126.5	9,129.5	9,127.5	9,128.5
P.T.R.	1931	9,078	[2] 9,064	9,117	9,123	9,121	9,124
B.S.	1931			9,117.3	9,121.9	9,121.0	9,119.9
P.T.R.	1931		[3] 9,080				
B.S.	1931			9,118.2	9,121.8		
B.S.	1931			[4] 9,123.5	[4] 9,127.0		

ANTIMONY POINT, 630.50° C.[5]

P.T.R.	1928	5,513.5	5,512.5				
B.S.	1929	5,512.1	5,512.1	5,537.3	5,539.3	5,537.3	5,535.8
N.P.L.	1930	5,514.8	5,513.8	5,536.8	5,539.8	5,535.8	5,536.8
P.T.R.	1931	5,512.2	5,512.2	5,540.2	5,541.2	5,536.2	5,537.2
B.S.	1931			5,536.7	5,539.4	5,535.6	5,534.4

ZINC POINT, 419.45° C.[6]

P.T.R.	1928	3,422.5	3,422.1				
B.S.	1929	3,423.2	3,423.3	3,437.4	3,438.1	3,435.3	3,434.4
N.P.L.	1930	3,425.2	3,424.2	3,437.7	3,438.2	3,436.7	3,436.2
P.T.R.	1931	3,424	3,419	3,437	3,438	3,434	3,434
B.S.	1931			3,437.0	3,438.0	3,434.1	3,433.4

[1] Additional measurements with other thermocouples at the B.S. and the P.T.R. showed that the emf at the freezing point of the inquartation silver was 5.5 μv higher than that of the 1st lot of B.S. silver and 3.5 μv higher than that of the P.T.R. silver.
[2] This thermocouple was found to be inhomogeneous after this measurement.
[3] This value was obtained after annealing this thermocouple for 1 minute at 1,200° C.
[4] These values were obtained using a new lot of silver. (See p. 2.)
[5] The freezing points of the various samples of antimony ranged from 630.35° to 630.53° C., but all values in this table have been adjusted to 630.50° C.
[6] The freezing points of the various samples of zinc ranged from 419.43° to 419.50° C., but all values in this table have been adjusted to 419.45° C.

TABLE 4.—*Average emfs of thermocouples*

Freezing point	Temperature	Average emf in microvolts		
		P.T.R.	N.P.L.	B.S.
	° C.			
Gold	1,063.0	10,293.8	10,292.8	10,293.7
Silver (first lot)	960.5	[1] 9,107.5	9,110.6	[2] 9,105.8
Silver (second lot)[3]	960.5	9,111.0		9,111.3
Antimony	630.50	5,530.0	5,529.6	5,528.7
Zinc	419.45	3,431.1	3,433.0	3,431.7

[1] The value 9,064 obtained with $D_{3,026}$ in 1931 is not included in this average.
[2] This value was obtained with the silver which contained 0.039 percent impurities.
[3] The values given here were obtained by applying corrections to the values in the line above.

The following conclusions have been drawn from these experiments:

(*a*)[4] The freezing point of the "inquartation silver" is 0.5° C. (5.5 μv) higher than that of the silver previously used at the Bureau of Standards and listed as "first lot" in table 4.

(*b*)[5] The freezing point of the "inquartation silver" is 0.3° C. (3.5 μv) higher than that of the Heraeus silver listed in table 2.

(*c*)[4] The freezing point of the "inquartation silver" is within 0.01° C. (0.1 μv) of that of a sample (kindly loaned to us by Dr. A. L. Day) used in the gas thermometer work of Day and Sosman which led to the acceptance of 960.5° C. as the freezing point of pure silver.

(*d*)[4] The freezing point of any particular lot of silver protected from access of oxygen by graphite is within 0.05° C. (0.6 μv) of that of the same silver in porcelain in vacuo (pressure 0.03 to 0.005 mm Hg).

From this it is evident that the results of the Bureau of Standards and of the Physikalisch-Technische Reichsanstalt given in tables 3 and 4 for the first lots of silver should be increased 5.5 and 3.5 μv, respectively. When this is done the observations of the three laboratories at the freezing point of silver are brought into exceedingly close agreement.

The differences between the thermoelectric temperature scales of the various laboratories based on both the old and new silver are given in detail in table 5.

IV. SUMMARY

The results indicate that previous to this intercomparison the maximum difference in the range 660° to 1,063° C. of the temperature scales of the National Physical Laboratory and the Bureau of Standards has been 0.7° C. at 850° C. due primarily to a difference of 0.42° C. at the freezing point of silver. The maximum difference between the scales of the National Physical Laboratory and the Physikalisch-Technische Reichsanstalt has been 0.4° C. at 850° C., due primarily to a difference of 0.27° C. at the freezing point of silver. After exchanging samples of silver these differences have been reduced to about 0.1° C. The mean values obtained with six thermocouples at the three National Laboratories are in agreement to this extent. The results obtained with a single couple may differ to a greater extent, possibly several tenths of a degree. Such differences are presumably to be attributed to small inhomogeneities in the couples and to lack of temperature uniformity in the furnace and are therefore of the nature of accidental errors.

[4] B.S. Jour. Research, vol. 10 (RP557), p. 661, May 1933.
[5] Zeits. für Instrumentenkunde, vol. 52, p. 201, 1932.

TABLE 5.—*Average temperature-emf relation for thermocouples*

Temperature °C.	Emf in microvolts				
	N.P.L.	P.T.R. based on inquartation silver	P.T.R. based on P.T.R. silver	N.B.S. based on inquartation silver	N.B.S. based on old silver
419.45	3,433.0	3,431.1	3,431.1	3,431.7	3,431.7
630.50	5,529.6	5,530.0	5,530.0	5,528.7	5,528.7
660.00	5,835.7	5,836.0	5,834.8	5,835.0	5,833.1
700.00	6,255.2	6,255.4	6,252.8	6,254.8	6,250.7
750.00	6,786.7	6,786.7	6,782.9	6,786.5	6,780.4
800.00	7,326.0	7,326.0	7,321.4	7,326.1	7,318.9
850.00	7,873.2	7,873.3	7,868.5	7,873.6	7,866.0
900.00	8,428.4	8,428.5	8,424.0	8,428.9	8,421.7
950.00	8,991.4	8,991.7	8,988.0	8,992.0	8,986.2
960.50	9,110.6	9,111.0	9,107.5	9,111.3	9,105.8
1,000.00	9,562.2	9,562.8	9,560.4	9,563.0	9,559.3
1,050.00	10,141.0	10,141.9	10,141.4	10,141.9	10,141.0
1,063.00	10,292.8	10,293.8	10,293.8	10,293.7	10,293.7

V. ACKNOWLEDGMENTS

The authors wish to acknowledge the assistance received from the following at the institutions named:

National Physical Laboratory.—J. A. Hall (assistant) for the resistance thermometer determination of the freezing point of antimony. C. R. Barber (junior observer) for assistance in the thermocouple measurements.

Bureau of Standards.—F. R. Caldwell for the resistance thermometer determination of the freezing point of antimony.

WASHINGTON, March 21, 1933.

U.S. Department of Commerce—Bureau of Standards

RESEARCH PAPER RP574

Part of Bureau of Standards Journal of Research, Vol. 11, July 1933

A STUDY OF SOME FACTORS INFLUENCING THE STRENGTH AND STABILITY OF EXPERIMENTAL PAPERS MADE FROM TWO DIFFERENT SULPHITE PULPS

By Royal H. Rasch,[1] Merle B. Shaw, and George W. Bicking

ABSTRACT

A study on a semicommercial scale was made at the Bureau of Standards of the manufacture of bond papers from pulps prepared commercially by the sulphite process. Two kinds of bleached sulphite pulp were used in these experiments; one was of domestic and the other of foreign manufacture. A series of 43 experimental papers was made from the pulps in which the variables of beating and sizing were studied.

Since this study was confined to the bond type of papers, in which strength is an important requirement, the beating treatment was conducted in such manner as to develop the maximum strength consistent with other desired properties. This was accomplished satisfactorily by means of a 4-hour beating in the case of one pulp, and a 5-hour beating in the case of the other. The beater roll was lowered gradually during the course of the beatings. The beaten stock was brushed lightly in the Jordan. In strength the experimental papers compared favorably with the average good grade of sulphite bond.

Papers made from either type of sulphite pulp underwent marked changes in properties when subjected to the accelerated aging test, which consists in heating the paper in air at 100° C. for 72 hours. The moderate stability of the best papers produced as indicated by this test, was commensurate with the medium degree of fiber purity. While all the papers are relatively unstable, careful adjustment of the acidity of the rosin-sized papers resulted in marked improvement in stability without sacrifice of the degree of sizing. The correct adjustment of acidity appears to be at a pH of 5.0. It is indicated that the amount of rosin used in engine sizing the sulphite papers made was not an important consideration as far as the effect on their stability was concerned.

When unsized or rosin-sized papers were surfaced sized with glue or starch there was an improvement in tensile properties and a decrease in tearing strength in approximate proportion to the amount of size taken up by the basic paper. In general, no very marked increase in folding endurance resulted on surface sizing with either glue or starch. A glue-sized currency-type paper made from the stronger of the two fibers under study was of very high folding endurance, but not sufficiently so to meet the United States Government specification for this kind of paper. In general, glue sizing improved slightly the stability of the papers. It was indicated that for optimum stability the alum in the tub sizing bath should be kept at the minimum necessary to serve satisfactorily as a preservative of the glue.

CONTENTS

	Page
I. Introduction	8
II. Paper-making processes	8
III. Test methods	8
IV. Tests of paper-making fibers used	9
V. Manufacturing details and test data for papers	9
1. Unsized papers	9
(*a*) Effect of beating on development of strength properties	9
(*b*) Effect of beating on the alpha cellulose content and copper number	14
(*c*) Stability of unsized papers	15
2. Beater-sized papers	16
(*a*) Rosin-sized	16
(*b*) Starch-sized	19
3. Surface-sized papers	19
VI. Acknowledgment	23

[1] Research associate representing the Brown Co., Berlin, N.H.

I. INTRODUCTION

The present report deals with a study of some effects of cellulosic impurities and paper-making processes on the strength and stability of sulphite bond papers. It is the second in a series of studies designed to extend present information relative to the paper-making value of various fibers. The purpose and plan of the investigation as a whole are stated more in detail in the previous article.[2]

The sulphite process consists, briefly, in cooking wood chips under pressure in a solution of calcium bisulphite containing uncombined sulphurous acid. Spruce is the wood generally employed, although hemlock is also well adapted to the process. Associated with the cellulose, which makes up about half of the raw wood, are incrusting materials such as lignins (to the extent of 25 or 30 percent), pentosans, gums, waxes, resins, etc. The hydrolytic action of the bisulphite liquor at high temperature and pressure renders the bulk of the impurities soluble so that they may be washed out. For the higher grades of papers the fibers are bleached to a white color by treatment with calcium hypochlorite.

Included in the present study are two types of commercial bleached sulphite pulp, one of domestic and the other of foreign make, prepared for manufacture of bond and ledger papers.

II. PAPER-MAKING PROCESSES

The methods of beating, paper-machine operation, and sizing followed very closely those described in the initial publication of this investigation,[3] and in previous bureau publications.[4] The reader is referred thereto for details of the operations.

III. TEST METHODS

In testing the papers produced the official paper testing methods of the Technical Association of the Pulp and Paper Industry were used for the determination of weight, bursting strength, thickness, folding endurance, tensile breaking strength, tearing strength, opacity, ash, resin, starch, and glue.[5] The procedures for alpha cellulose content and copper number were described in detail in a previous publication.[6] Determinations of the titratable acidity were made on extracts of ground paper (Kohler-Hall method) [7] and directly on suspensions of the ground paper. Both procedures were outlined in a previous publication.[8] The pH of the paper extracts was determined electrometrically using the quinhydrone electrode. The stability was measured by exposing the paper specimen under test to a current of air at 100° C. for 72 hours and then determining to what extent the paper was altered in its properties, particularly

---

[2] R. H. Rasch, M. B. Shaw, and G. W. Bicking, Highly-Purified Wood Fibers as Paper-Making Material, B.S. Jour. Research, vol. 7 (RP372), pp. 765–782, November 1931.

[3] See footnote 2.

[4] M. B. Shaw and G. W. Bicking, Research on the Production of Currency Paper in the Bureau of Standards Experimental Paper Mill, B.S. Tech. Paper No. 329, and Further Experimental Production of Currency Paper in the Bureau of Standards Paper Mill, B.S. Jour. Research, vol. 3 (RP121), pp. 899–926, December 1929.

[5] Paper Testing Methods, prepared by the Committee on Paper Testing of the Technical Association of the Pulp and Paper Industry, Lockwood Trade J. Co., New York, 1929.

[6] J. O. Burton and R. H. Rasch, The Determination of the Alpha Cellulose Content and Copper Number of Paper, B.S. Jour. Research, vol. 6 (RP295), pp. 603–619, April 1931.

[7] S. Kohler and G. Hall, Acidity in Paper, Paper Industry, vol. 7, pp. 1–5, October 1925.

[8] R. H. Rasch, Accelerated Aging Test for Paper, B.S. Jour. Research, vol. 7 (RP352), pp. 465–475, September 1931.

folding endurance and alpha cellulose content. For more complete details the reader is referred to previous discussions of the method.[9] [10] The method used for determining pentosans was similar to the usual ones involving the distillation of the sample with dilute hydrochloric acid, except that precipitation was accomplished by the use of thiobarbituric acid instead of phloroglucinol.[11]

IV. TESTS OF PAPER-MAKING FIBERS USED

Representative samples of the pulps used for this work were tested with results as given in table 1. The pulps, which will be referred to throughout this paper as A and B are shown by the tests to be representative high-grade sulphite pulps. A is slightly better than B as regards content of alpha cellulose.

TABLE 1.—*Tests of paper-making fibers used*

	Alpha-cellulose content	Copper number	Pento-sans	Resin	Ash
Pulp A:	*Percent*		*Percent*	*Percent*	*Percent*
Original sample	[1] 84.6	3.10	3.50	0.9	0.22
Sample heated at 100° C. for 72 hours	81.9	3.64			
Pulp B:					
Original sample	[1] 82.4	3.20	2.86	.6	.19
Sample heated at 100° C. for 72 hours	80.3	3.90			

[1] The same determination made on ¼-inch squares of the pulp sheet gave a result of 85.9 and 83.8 percent, respectively. Many methods for the determination of alpha-cellulose content, including the tentative standard method of the American Chemical Society, specify that the sample shall be in the form of squares.

V. MANUFACTURING DETAILS AND TEST DATA FOR PAPERS

1. UNSIZED PAPERS

(a) EFFECT OF BEATING ON DEVELOPMENT OF STRENGTH PROPERTIES

The general method of beating characterized by a gradual lowering of the beater roll has been described in detail in earlier publications.[12] This procedure, so advantageous in the development of high-strength currency paper, was deemed to be equally applicable in obtaining optimum results with the sulphite pulps under study. Beating is one of the most important operations in paper making. The duration of beating and the manipulation of the beater roll are among the variables in the beating operation which have their marked effect on the physical properties of the paper, such as strength, opacity, hardness, etc. This is especially true of sulphite fibers which "hydrate" with comparative ease. Overbeating results in a sheet of low tearing strength and low opacity, and also effects an undesirable hardness or "tinny" character in the sheet. Underbeating results in a soft, bulky, weak sheet of poor formation.

The effect of duration of beating was studied both with hand sheets and with the paper machine product. Hand sheets were made from

[9] See footnote 2, p. 8, and footnote 8, p. 8.
[10] R. H. Rasch, G. O. Stone, Procedure for Estimation of Stability of Paper by Heating, Paper Trade J., vol. 95, no. 4, pp. 40–42, July 28, 1932.
[11] Dox and Plaisance, J. Am. Chem. Soc., vol. 38, p. 2156, 1926.
[12] See footnote 4, p. 8.

stock taken at different intervals during the beatings and were tested for strength.[13]

Typical illustrations are given in figure 1 of the effect of beating on the folding endurance, tearing strength, and bursting strength. It is apparent that A attains maximum folding endurance in about 6 hours and B in 5 hours. The bursting strength develops in similar fashion. Beginning at an early stage in the beating the tearing strength decreases gradually with further beating.

Unsized papers were made on the paper machine from fibers beaten 4, 5, and 7 hours, respectively. The data relative to the operation of the beater and the test results of the machine-made papers are given in tables 2 and 3. In the case of both pulps 7 hours was considered too long. A 4-hour beating of pulp A gave the best result as

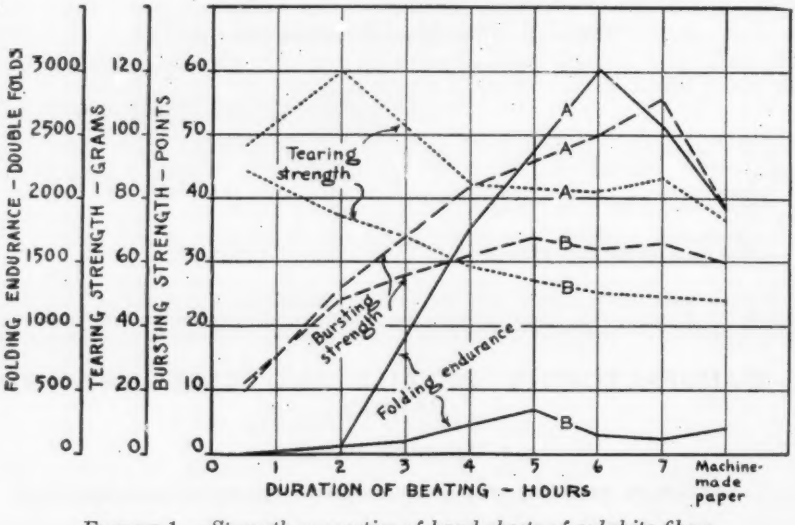

FIGURE 1.—*Strength properties of hand sheets of sulphite fibers.*

regards opacity, feel, and general appearance. A 5-hour beating with less drastic roll setting was judged to be more advantageous in the case of pulp B, which was somewhat less susceptible to "hydration."

The schedule of roll settings adopted for the beatings is given in table 4. In each case the treatment as outlined therein was followed by a light brushing in the Jordan.

The papers made from pulp A are very high in folding endurance for this type of fiber. Otherwise the papers made from pulps A and B approximate in strength the average commercial sulphite bonds.

Figures 2 and 3 are photomicrographs of the beaten fibers and are of interest in illustrating the differences in the two pulps. Figure 2 shows the fibers of pulp A, which are long, clean, and uniform in comparison to those of pulp B (fig. 3). In the latter case the shrunken and shriveled appearance of many of the fibers is noteworthy. Fibrillae can be seen on the fibers in both figures.

[13] M. B. Shaw, G. W. Bicking, and L. W. Snyder, The Preparation of Fiber Test Sheets, B.S. Jour. Research, vol. 5 (RP190), pp. 105–114, July 1930.

FIGURE 2.—*Sulphite wood fiber A.* ×100.

FIGURE 3.—*Sulphite wood fiber B.* ×100.

TABLE 2.—*Data on unsized and beater-sized papers (pulp A)*

UNSIZED PAPERS

Paper machine run no.	Beating interval, hours	Freeness of stock		Rosin size, amount based on dry fiber, percent	Alum, amount based on dry fiber, percent	Starch size, amount dry starch based on dry fiber, percent	Acidity of stock at head box	Physical tests															Chemical tests										Heat tests [1]		
		After beating	At head box					Weight, 25 by 40 inches, 500 sheets, pounds	Bursting strength, points [2]	Ratio bursting strength to weight, percent	Thickness, inch	Folding endurance, double folds [3]		Tensile properties				Tearing strength		Opacity, percent	Water resistance, seconds		Ash, percent	Sizing materials, percent		Acidity, percent [4]			Alpha cellulose, percent	Copper number	Folding endurance in percent of initial	Tearing strength in percent of initial	Decrease in alpha cellulose content, percent	Increase in copper number
												Machine direction	Cross direction	Breaking load [5]		Elongation at rupture, percent		Machine direction	Cross direction		Indicator	Curl		Resin	Starch	Extract, Kohler-Hall method	Fiber suspension	pH of extract						
							pH							*kg*	*kg*			*g*	*g*																
867	7	113	68	0	0	0		56.2	37	66	0.0033	1,600	2,200	9.2	5.4	2.8	7.6	69	63	71			0.18	0.8			0.021			2.94	57	73		0.26
868	5	136	100	0	0	0		58.9	38	65	.0037	2,000	2,100	9.3	5.6	2.6	6.9	79	74	76				1.0			.020			3.28	60	68		
869	4	195	110	0	0	0		53.8	36	67	.0033	1,600	2,000	8.6	5.7	2.2	6.5	62	72	76			.15	.8			.024			3.16	63	75	2.7	.25
872	4	176	98	0	0	0		56.5	34	60	.0034	2,000	1,800	9.0	6.3	2.0	5.7	60	67	77			.18	.9		0.012	.020			3.08	63	89		
873	4	194	93	0	0	0		62.0	39	63	.0037	2,500	2,200	10.4	5.8	2.3	6.6	68	69	80				.8										
871	4	192	125	0	3.0	0	4.0	56.2	32	57	.0034	1,400	1,700	8.8	5.7	2.3	5.8	61	64	76			.20	.8		.004	.172	3.9	81.4	2.90	1	36	9.6	.82
870	4	185	128	0	1.0	0	5.0	55.9	33	60	.0036	1,700	2,000	9.1	5.6	2.1	6.4	64	58	76			.22	.7		.060	.120	4.3	82.9	3.19	11	58	6.5	.12

[1] Samples heated at 100° C. for 72 hours.
[2] For test specimen 15 mm wide and 90 mm between jaws.
[3] For test specimen 15 mm wide and 100 mm between jaws.
[4] Acidity expressed as percent SO_3.
[5] Bursting pressure in pounds per square inch through a circular orifice 1.2 inches in diameter.

TABLE 2.—*Data on unsized and beater-sized paper (pulp A)*—Continued

ROSIN-SIZED PAPERS

Paper machine run no.	Beating interval, hours	Freeness of stock		Rosin size, amount based on dry fiber, percent	Alum, amount based on dry fiber, percent	Starch size, amount dry starch based on dry fiber, percent	Acidity of stock at head box	Physical tests														Chemical tests								Heat tests			
		After beating	At head box					Weight, 25 by 40 inches, 500 sheets, pounds	Bursting strength, points	Ratio bursting strength to weight, percent	Thickness	Folding endurance, double folds		Tensile properties				Tearing strength		Opacity, percent	Water resistance, seconds		Ash, percent	Sizing materials, percent		Acidity, percent			Alpha cellulose, percent	Copper number	Folding endurance in percent of initial	Tearing strength in percent of initial	Decrease in alpha cellulose content, percent	Increase in copper number
														Breaking load		Elongation at rupture, percent								Resin	Starch	Extract, Kohler-Hall method	Fiber suspension	pH of extract					
												Machine direction	Cross direction	Machine direction	Cross direction	Machine direction	Cross direction	Machine direction	Cross direction		Indicator	Curl											
							pH							*kg*	*kg*			*g*	*g*														
881	4	168	90	2	3.3	0	4.0	56.2	35	62	0.0035	1,400	900	8.9	5.3	2.0	5.4	70	74	77	30	33	0.49	2.2	----	0.067	0.176	4.2	81.5	3.36	9	69	6.7	0.54
880	4	170	104	2	1.9	0	4.4	55.3	35	63	.0035	1,700	1,100	8.7	5.0	1.9	5.5	67	66	78	30	32	.42	2.4	----	.058	.145	4.5	81.9	2.82	19	68	5.7	1.01
879	4	170	105	2	1.2	0	5.0	53.9	33	62	.0033	1,300	700	8.3	4.9	2.0	5.7	58	60	78	22	26	.40	2.5	----	.043	.117	4.8	81.8	3.08	28	75	4.9	.82
882	2	240	82	2	1.3	0	5.0	57.0	33	57	.0039	1,000	1,100	7.6	5.1	1.9	5.3	76	72	80	34	29	.36	2.2	----	.037	.114	4.8	-----	3.20	29	78	----	.69
875	4	210	104	1	1.1	0	5.0	55.4	33	59	.0034	1,500	1,000	8.6	5.2	1.9	5.6	62	67	76	27	28	.25	1.5	----	.056	.137	4.6	81.3	3.05	14	69	5.4	.48
874	4	180	108	0.5	1.0	0	5.0	57.3	34	59	.0035	1,400	1,400	9.1	5.2	1.8	5.3	68	68	78	26	25	.31	.9	----	.053	.135	4.5	81.0	2.83	9	62	5.3	.64
878	4	190	88	2	0.6	0	6.0	56.1	35	63	.0033	1,400	1,600	8.9	5.6	2.3	6.1	68	58	77	30	30	.35	1.5	----	.037	.065	5.1	81.3	3.09	46	84	3.3	.68

STARCH-SIZED PAPERS[6]

876	4	206	113	0	1.0	4.5	5.0	55.8	44	79	0.0033	2,100	2,200	10.1	6.2	2.4	6.4	52	56	75	8	9	0.31	0.8	1.1	0.040	0.120	4.5	81.5	3.15	12	60	3.7	0.41
877	4	185	94	1	1.0	4.5	5.0	54.6	40	73	.0033	1,800	1,700	10.1	6.0	2.4	6.6	52	59	75	25	26	.35	1.4	1.0	.067	.120	4.5	81.6	3.15	19	74	4.0	.54

[6] Starch prepared by process of oxidation.

NOTE.—All physical tests made under conditions of 65 percent relative humidity and 70° F.

TABLE 3.—*Data on unsized and beater-sized papers (pulp B)*

UNSIZED PAPERS

Paper machine run no.	Beating interval, hours	Freeness of stock		Rosin size, amount based on dry fiber, percent	Alum, amount based on dry fiber, percent	Acidity of stock at head box	Physical tests														Chemical tests							Heat tests [1]			
		After beating	At head box				Weight, 25 by 40 inches, 500 sheets, pounds	Bursting strength, points [5]	Ratio bursting strength to weight, percent	Thickness, inch	Folding endurance, double folds [2]		Tensile properties				Tearing strength		Opacity, percent	Water resistance, seconds		Ash, percent	Resin, percent	Acidity, percent [4]			Alpha cellulose, percent	Copper number	Folding endurance in percent of initial	Tearing strength in percent of initial	Decrease in alpha cellulose content, percent	Increase in copper number
													Breaking load [3]		Elongation at rupture, percent									Extract, Kohler-Hall method	Fiber suspension	pH of extract					
											Machine direction	Cross direction	Machine direction	Cross direction	Machine direction	Cross direction	Machine direction	Cross direction		Indicator	Curl											
						pH							*kg*	*kg*			*g*	*g*														
886A	7	103	70	0	0	-----	56.6	29.8	53	0.0036	260	150	7.8	4.6	2.0	5.5	50	46	77	----	----	0.16	0.5	----	----	----	80.9	3.10	43	88	1.8	0.50
886B	7	103	85	0	0	-----	57.6	28.8	50	.0036	200	160	7.7	4.8	2.1	6.3	54	51	79	----	----	----	----	----	----	----	80.5	----	47	78	2.6	----
885A	4	158	65	0	0	-----	53.9	29.1	54	.0035	270	420	7.3	4.6	2.3	4.9	53	48	78	----	----	.18	.6	----	----	----	80.6	3.28	38	81	2.4	.26
885B	4	158	103	0	0	-----	54.2	28.2	52	.0035	300	250	7.4	4.8	2.0	5.5	50	51	78	----	----	----	----	----	----	----	80.7	----	40	81	1.9	----
887	5	159	69	0	0	-----	54.2	28.0	52	.0034	140	440	7.9	5.0	1.9	5.6	51	50	77	----	----	.16	.6	----	----	----	----	----	42	78	----	----
895	5	134	62	0	0	-----	55.0	31.2	57	.0035	270	450	7.8	4.9	1.7	6.2	43	50	78	----	----	.21	.7	0.010	0.010	----	79.5	3.34	37	99	2.3	.32
889	5	146	82	0	3.2	4.1	54.7	27.7	51	.0030	280	250	7.4	4.2	2.0	5.3	42	44	----	----	----	.29	.6	.076	.151	3.9	79.6	3.08	7	65	6.6	.59
888	5	149	84	0	1.0	5.0	54.4	27.7	51	.0030	390	210	7.7	4.3	1.9	5.6	47	47	78	----	----	.29	.9	.045	.086	4.5	79.8	3.34	11	69	4.1	.38

ROSIN-SIZED PAPERS

893	5	133	90	2	3.4	4.1	56.9	31.1	55	0.0036	390	140	8.1	3.9	1.8	5.3	52	51	81	24	30	0.38	2.2	0.083	0.139	4.3	79.7	3.52	15	75	6.4	0.39
892	5	149	78	2	2.0	4.4	55.9	30.0	54	.0035	350	140	8.0	4.1	1.8	5.3	52	50	79	24	30	.33	2.0	.071	.123	4.4	79.1	3.46	21	85	5.5	.44
891	5	162	66	2	1.4	5.0	55.7	31.0	56	.0035	250	140	7.9	4.3	1.9	5.6	42	48	80	26	27	.40	2.6	.038	.088	4.8	80.0	3.52	35	95	4.6	.44
894 [6]	5	132	69	2	1.4	5.0	55.3	32.0	58	.0034	700	310	8.6	4.3	2.0	6.3	62	52	78	24	27	.35	2.5	.040	.094	4.8	80.0	3.30	27	79	5.0	.76
897	5	152	65	1	1.3	5.0	56.2	30.5	54	.0035	180	290	7.7	4.9	1.9	5.4	48	52	----	24	25	.37	2.0	.034	.088	4.9	79.2	3.18	31	86	3.9	.79
896	5	146	66	0.5	1.2	5.0	55.2	31.1	56	.0034	520	330	7.7	4.7	1.8	6.9	46	48	78	14	16	.34	1.6	.049	.116	4.5	80.4	2.94	19	94	3.8	.75
890	5	157	76	2	1.1	6.0	55.4	26.3	47	.0035	200	150	7.7	4.2	1.6	5.3	44	48	----	27	26	.27	2.0	.023	.045	5.5	79.5	3.40	34	87	3.5	.59

[1] Samples heated at 100° C. for 72 hours.
[2] For test specimen 15 mm wide and 90 mm between jaws.
[3] For test specimen 15 mm wide and 100 mm between jaws.
[4] Acidity expressed as percent SO_3.
[5] Bursting pressure in pounds per square inch through a circular orifice 1.2 inches in diameter.
[6] The furnish for this run was 50 percent pulp A and 50 percent pulp B.

NOTE.—All physical tests made under conditions of 65 percent relative humidity and 70° F.

TABLE 4.—*Schedule of roll settings for beating sulphite pulps*

Pulp A			Pulp B		
Beating interval		Position of roll [1]	Beating interval		Position of roll [1]
Hours	*Minutes*		*Hours*	*Minutes*	
0	0	[2] 10	0	0	[2] 10
0	15	[3] 10	0	15	[3] 10
0	30	2	0	30	3
1	0	1	1	0	2
1	30	½	1	30	1½
2	0	0	2	0	1
3	0	0	2	30	½
4	0	0	3	0	½
			3	30	0
			4	30	0
			5	0	0

[1] Indicated as turns of the handwheel with which the position of the roll relative to the bed plate is changed. At the zero setting the bed plate is just barely cleared. One turn of the handwheel raises or lowers the roll 0.008 inch.
[2] Lighter-bar up.
[3] Lighter-bar down.

(b) EFFECT OF BEATING ON THE ALPHA CELLULOSE CONTENT AND COPPER NUMBER

The pulp used for this experiment, while neither A nor B, was a sulphite pulp similar to B in all respects. A 2 percent suspension of fibers was beaten in a small laboratory beater. Portions of the stock were taken out at the following intervals: (1) after a brief slushing, (2) after 2¼ hours of beating, (3) after 4¼ hours of beating, and (4) after 6¼ hours of beating. Hand sheets were made from each of these portions and air dried at room temperature. The alpha cellulose content was determined on squares of the sheets, also on ground specimens. The data, which are presented in table 5, indicate that the beating caused little change in the chemical properties measured by these tests. The apparent increase in the alpha cellulose content of the squares with increased duration of beating is a result of decreased absorptiveness of the sheet and thus incomplete extraction by the mercerizing solution, which is further evidence of the desirability of grinding pulp specimens for this test.

TABLE 5.—*Effect of beating on the alpha cellulose content and copper number of a sulphite pulp* [1]

Sample	Duration of beating	Alpha cellulose content		Copper number	
		¼-inch squares	Ground fiber	¼-inch squares	Ground fiber
	Hours	*Percent*	*Percent*		
1	0	84.3	81.8	3.34	3.45
2	2¼	86.1	80.4	3.34	3.31
3	4¼	88.0	80.2	3.33	3.31
4	6¼	88.8	80.8	3.35	3.07

[1] The beating was done in a laboratory beater.

(c) STABILITY OF UNSIZED PAPERS

The effect of beating on the stability of the paper was studied. Hand sheets were made from stock beaten to various extents in the beater used for machine runs. Folding endurance was determined on hand sheets heated for 72 hours at 100° C. and on the unheated paper according to the usual procedure. The data obtained are presented in figure 4 for pulps beaten up to the points of maximum.

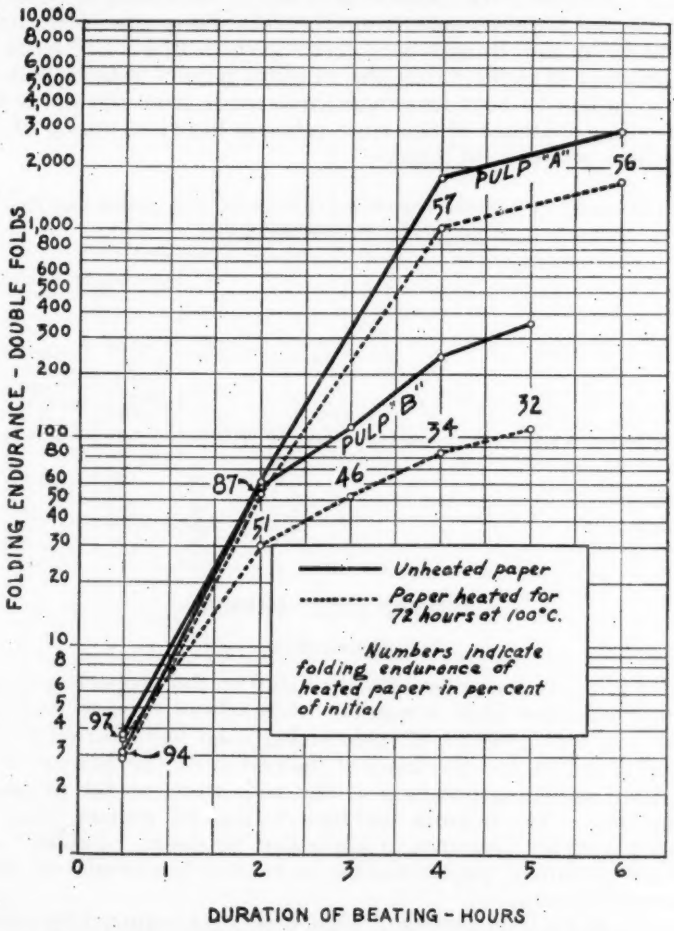

FIGURE 4.—*Effect of beating on stability of sulphite fibers*

folding endurance. The hand-made papers prepared from pulps beaten only one half hour undergo no appreciable change on heating, whereas those prepared from pulps beaten up to maximum strength decrease in folding endurance to 56 percent of initial, for pulp A, and to 32 percent of initial, for pulp B, as a result of the heat treatment. The results are in substantial agreement with those of similar experiments made by Richter.[14]

[14] Durability of Purified Wood Fibers, Ind. Eng. Chem., vol. 23, no. 4, pp. 371-380, April 1931.

In regard to the stability of unsized machine-made papers, it will be noted in tables 2 and 3 that the paper made from pulp A retained about 60 percent of the initial folding endurance after the heat treatment, and that the paper made from pulp B retained about 40 percent. Varying the beating time at 4, 5, and 7 hours, respectively, resulted in no apparent effect on the stability. Unsized papers made from either fiber lost 2 to 3 percent in alpha cellulose content under the heat test. In table 6 comparison is made of the chemical purity and stability of the papers made from the sulphite pulps with unsized papers made in the Bureau mill from various fibers of higher commercial grade. It is clear that the sulphite papers were considerably less stable under the heat test than those made from the purer fibers. This is further evidence of the close relation between purity of paper fibers and the stability of papers.

TABLE 6.—*Stability of unsized papers made from sulphite pulps and from fibers of higher commercial grade*

Fiber	Alpha cellulose	Copper number	After heat treatment at 100° C. for 72 hours		
			Folding endurance in percent of initial	Decrease in alpha cellulose content	Increase in copper number
	Percent				
Fiber A	97.7	0.29	95	0.6	0.05
Fiber B	93.4	.62	97	.8	.09
Fiber C	91.5	.65	99	.4	.15
Sulphite wood fiber A	83.5	3.08	58	2.7	.25
Sulphite wood fiber B	79.5	3.34	37	2.3	.32

2. BEATER-SIZED PAPERS

(a) ROSIN-SIZED

In order to study the effect of rosin sizing on the properties of papers made from sulphite fiber a number of machine runs were made in which acidity and amount of rosin sizing used were varied while the factors involved in the mechanical operation of the beater, such as beating time and manipulation of the roll, were, as far as possible, kept constant. As controls for the rosin-sized papers, runs were made using varying amounts of alum and no rosin. Tables 2 and 3 contain the pertinent paper-making data and the results of tests of the papers produced.

In run no. 881 a large excess of alum over that required for adequate sizing was purposely added. The pH of this paper was 4.2. A very adverse effect on stability, as regards decrease in folding endurance and alpha cellulose content under the heat test occurred. Reduction in the use of alum resulted in the expected improvements in stability. For example, in run no. 878, in which only 0.6 percent alum was employed, the stability of the rosin-sized paper approached closely to that of the paper containing neither rosin nor alum. This paper, having a pH value of 5.1, was fairly well sized; however, it is believed that about 1.0 percent alum would be a safer amount to use. With this fiber, as with the purer wood fibers previously studied, pH 5.0

appears to be about the correct acidity for maximum stability consistent with adequate sizing.

No very marked difference in stability could be detected among the papers sized with different amounts of rosin. It is clear, however, that the rosin-sized papers were more stable toward heat than papers of corresponding acidities containing no rosin. This finding is contrary to that made in the study of the purer wood fibers, since rosin-sized papers made from those fibers were less stable than the unsized papers.[15] As a possible reason for this apparent disagreement, it is suggested that below a certain stability range rosin sizing may actually have a protective effect, similar to that of glue in surface sizing, which more than offsets an accompanying deteriorative effect. The indi-

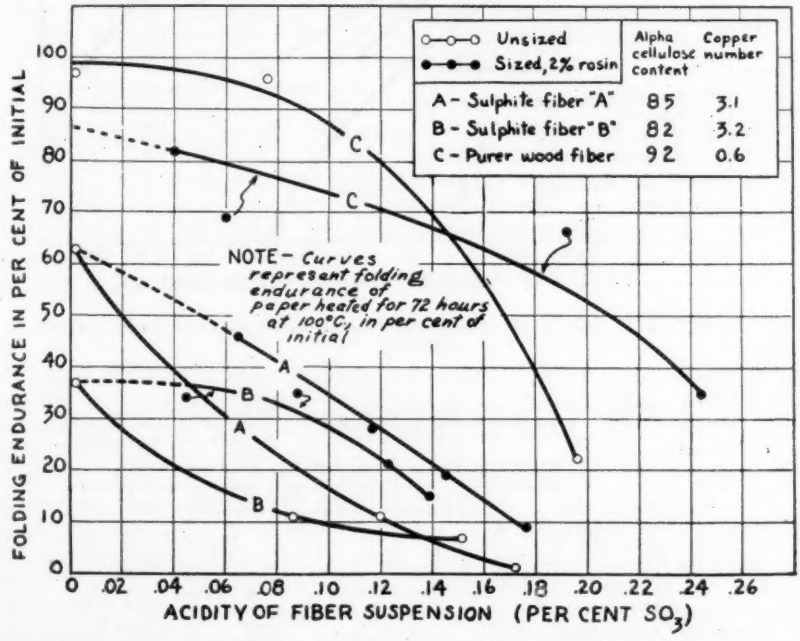
Unsized
Sized, 2% rosin
Alpha cellulose content
Copper number
A - Sulphite fiber "A" 85 3.1
B - Sulphite fiber "B" 82 3.2
C - Purer wood fiber 92 0.6
NOTE - Curves represent folding endurance of paper heated for 72 hours at 100°C., in per cent of initial
FOLDING ENDURANCE IN PER CENT OF INITIAL
ACIDITY OF FIBER SUSPENSION (PER CENT SO_3)
0 .02 .04 .06 .08 .10 .12 .14 .16 .18 .20 .22 .24 .26
0 10 20 30 40 50 60 70 80 90 100

FIGURE 5.—*Effect of acidity of unsized and rosin-sized sulphite bond papers on stability.*

cations are that, within the range studied (one half to 2 percent), the amount of rosin employed in sizing sulphite papers is not an important consideration as far as stability is concerned.

The same experiments in varying rosin size and acidity were made using pulp B. The data relative to the preparation and tests of papers made from this pulp are given in table 3. Results as to the effect of acid and rosin on the stability of papers made with pulp B agree in most particulars with those for pulp A papers.

Figures 5 and 6 are of interest in illustrating some of the points brought up in the above paragraphs. They show the effects of acidity (fiber-suspension method), rosin, and the quality of the fibrous raw material on the stability of the papers produced.

[15] See footnote 2, p. 8.

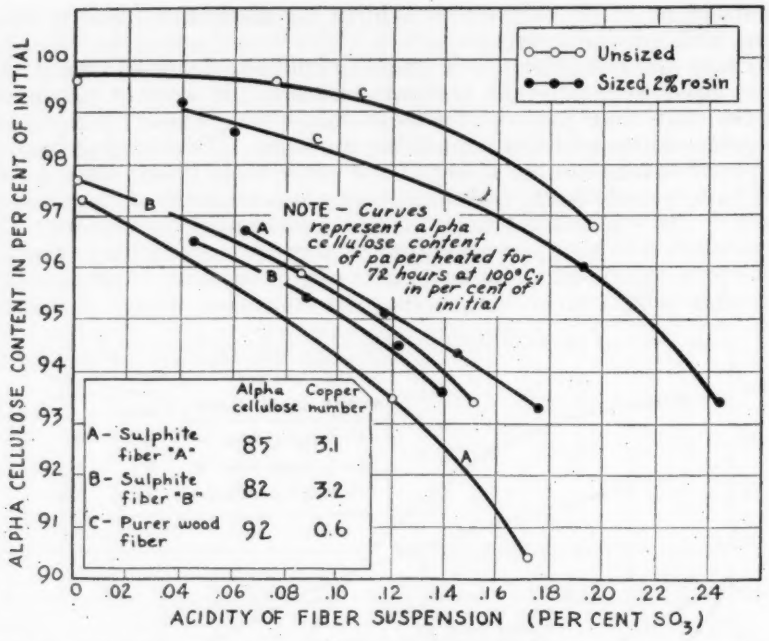
Unsized
Sized, 2% rosin
NOTE – Curves represent alpha cellulose content of paper heated for 72 hours at 100°C, in per cent of initial
Alpha cellulose
Copper number
A – Sulphite fiber "A" 85 3.1
B – Sulphite fiber "B" 82 3.2
C – Purer wood fiber 92 0.6
ALPHA CELLULOSE CONTENT IN PER CENT OF INITIAL
ACIDITY OF FIBER SUSPENSION (PER CENT SO_3)

FIGURE 6.—*Effect of acidity of unsized and rosin-sized sulphite bond papers on stability.*

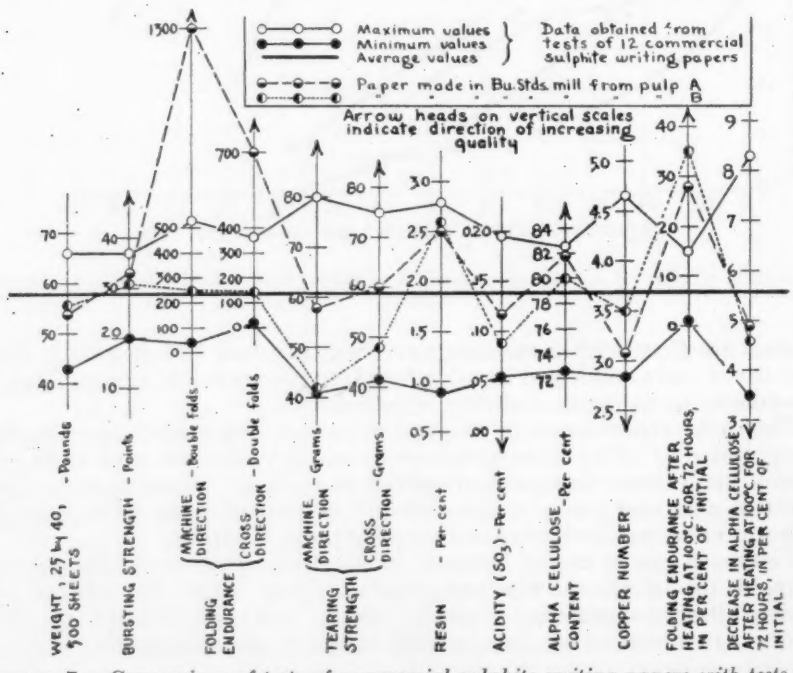
Maximum values
Minimum values
Average values
Data obtained from tests of 12 commercial sulphite writing papers
Paper made in Bu. Stds. mill from pulp A B
Arrow heads on vertical scales indicate direction of increasing quality
WEIGHT, 25 by 40, 500 SHEETS – Pounds
BURSTING STRENGTH – Points
FOLDING ENDURANCE (MACHINE DIRECTION – Double folds; CROSS DIRECTION – Double folds)
TEARING STRENGTH (MACHINE DIRECTION – Grams; CROSS DIRECTION – Grams)
RESIN – Per cent
ACIDITY (SO_3) – Per cent
ALPHA CELLULOSE CONTENT – Per cent
COPPER NUMBER
FOLDING ENDURANCE AFTER HEATING AT 100°C. FOR 72 HOURS, IN PER CENT OF INITIAL
DECREASE IN ALPHA CELLULOSE AFTER HEATING AT 100°C. FOR 72 HOURS, IN PER CENT OF INITIAL

FIGURE 7.—*Comparison of tests of commercial sulphite writing papers with tests of experimental papers.*

Figure 7 is of interest in affording a comparison of the strength, chemical purity, and stability of two rosin-sized papers made in the Bureau mill from pulps A and B with the maximum, minimum, and average values selected from the tests of 12 different commercial, rosin-sized sulphite papers. With the exception of the folding endurance of the paper made from pulp A, which is very high, the strength tests of the experimental papers are in good agreement with those of the average commercial papers. In regard to acidity, however, it should be pointed out that the average commercial sheet has an acidity of 0.14 percent SO_3. This is unnecessarily high and is reflected in the poorer stability of the commercial paper as compared with the experimental paper having optimum acidity. The alpha cellulose content and copper number tests indicate that the experimental sheets have a higher chemical purity than the average commercial papers.

(b) STARCH-SIZED

Two runs were made in which starch, manufactured commercially by a so-called oxidation process, was added to the beater. In one case rosin size was not used and in the other case 1 percent was employed. The data relative to these papers are given in table 2. The retention of starch was rather low, amounting to about a fourth of that added to the beater, but improvements in folding endurance and tensile properties were realized. The presence of starch did not adversely affect the stability of the papers.

3. SURFACE-SIZED PAPERS

Three different basic papers were used for the tub sizing experiments, an unsized paper containing no alum, and two papers sized respectively with one half and 1 percent rosin. The acidity sought in the case of the rosin-sized base papers was pH 5.0. On test, however, they were found to be somewhat more acid. This fact is to be considered in connection with the stability of these papers. Papers made from pulp A were sized, respectively, with glue, glue containing alum, and starch containing alum. Papers made from pulp B were sized with glue containing alum. Data relative to the preparation and testing of these papers are given in table 7. Control samples corresponding to each of the surface sizing runs were tested individually for strength and stability. The control samples were taken immediately before and after each surface sizing treatment so as to be as representative as possible of the portion of paper sized.

TABLE 7.—*Data on surface-sized papers*

GLUE-SIZED PAPERS, PULP A

Basic paper, machine run no.	Surface sizing run no.	Rosin size, amount rosin based on dry fiber, percent	Acidity of stock at head box	Acidity of surface sizing bath	Physical tests												Chemical tests										Heat tests [1]		
					Weight, 25 by 40 inches, 500 sheets, pounds	Bursting strength, points [2]	Ratio bursting strength to weight, percent	Thickness, inch	Folding endurance, double folds [3]		Tensile properties				Tearing strength		Opacity, percent	Water resistance, seconds		Ash, percent	Sizing materials, percent			Acidity, percent [4]			Alpha cellulose content, percent	Copper number	Folding endurance in percent of initial	Tearing strength in percent of initial	Decrease in alpha cellulose content, percent	Increase in copper number
									Machine direction	Cross direction	Breaking load [3]		Elongation at rupture, percent		Machine direction	Cross direction		Indicator	Curl		Resin	Glue	Starch	Extract, Kohler-Hall method	Fiber suspension	pH of extract					
											Machine direction	Cross direction	Machine direction	Cross direction																
		(6)	*pH*	*pH*	*kg*						*kg*				*g*	*g*															
872B		0			56.5	33.8	60	0.0033	1,300	2,300	9.4	6.1	1.9	5.5	60	67	77			0.18	0.9			0.012	0.020		83.5	3.08	54	92	2.7	0.25
872B					60.6	46.5	77	.0035	1,500	1,800	11.0	8.1	2.6	6.5	52	52	77	6		.26	.9			.031	.038	5.2	82.5	2.96	71	94	1.0	.19
874B	225				57.3	32.1	56	.0035	1,700	1,400	9.0	5.1	1.8	5.2	72	68	78	26	25	.31	.9			.053	.135	4.5	81.0	2.83	9	62	5.3	.64
874B		0.5	5.0		59.2	47.3	80	.0035	1,800	1,500	10.9	6.3	2.4	6.5	56	51	75	34	33	.24	1.3	1.58		.062	.137	4.5	81.9	2.86	23	87	2.7	.46
875B					56.6	32.9	58	.0034	1,600	1,000	8.4	5.2	1.8	5.5	62	71	76	27	28	.25	1.5			.056	.137	4.6	81.3	3.05	14	69	5.4	.48
875B	226	1	5.0		56.0	40.6	73	.0034	1,400	1,300	9.3	6.0	2.2	5.8	48	55	76	27	32	.39	1.7	.82		.063	.137	4.5	81.8	2.74	17	82	4.9	.44
872C		0	(6)		53.4	34.6	65	.0033	1,500	1,500	8.4	5.9	2.0	5.9	60	62	77			.18	.9			.012	.020		83.5	3.08	65	87	2.7	.25
872C					55.0	39.3	71	.0033	1,600	1,700	10.1	7.3	2.3	6.2	46	47	71	24	29	.39	1.0	2.21		.033	.078	5.0	83.0	2.72	54	94	1.4	.64
874C	228		5.0		54.7	32.2	59	.0033	1,200	800	8.4	5.1	1.6	5.5	64	66	78	26	25	.31	.9			.053	.135	4.5	81.0	2.83	9	61	5.3	.64
874C		.5			55.1	41.4	75	.0033	1,400	1,100	9.6	5.8	2.3	6.0	42	52	74	26	31	.39	1.5	1.15		.081	.131	4.3	81.8	2.90	11	83	4.4	.39
875C	229			4.3	55.5	33.7	61	.0034	1,200	900	8.8	5.2	1.9	5.9	63	66	76	27	28	.25	1.5			.056	.137	4.6	81.3	3.06	20	71	5.4	.48
875C		1	5.0		56.3	38.4	68	.0033	1,000	1,200	9.6	5.7	2.3	6.4	55	55	77	25	33	.36	1.8	.84		.074	.152	4.4	81.9	2.94	17	73	5.1	.45
	230			4.3																										

STARCH-SIZED PAPERS,[7] PULP A

872A		0	(6)		59.5	33.5	56	0.0035	1,700	2,300	9.2	6.7	2.0	5.7	61	70	77			0.18	0.9			0.012	0.020		83.5	3.08	56	87	2.7	0.25
872A	222			4.5	59.0	43.2	73	.0034	1,900	2,100	10.4	7.5	2.8	6.3	48	51	72	30	31	.20	.8		1.65	.036	.034	5.1	82.6	2.86	44	94	2.8	.28
874A		0.5	5.0		60.1	36.2	60	.0037	1,200	2,000	9.8	5.4	2.0	5.3	68	71	78	26	25	.31	.9			.053	.135	4.5	81.0	2.83	8	63	5.3	.64
874A	223			4.5	58.5	41.5	71	.0034	1,500	1,500	10.1	5.7	2.4	5.8	54	50	75	32	30	.25	1.2		1.25	.082	.153	4.3	81.2	2.85	5	80	5.5	.62
875A		1	5.0		54.2	31.6	58	.0033	1,700	1,000	8.6	5.2	2.0	5.5	60	65	76	27	28	.25	1.5			.056	.137	4.6	81.3	3.05	10	66	5.4	.48
875A	224			4.5	58.9	37.9	64	.0035	1,300	1,300	10.0	5.6	2.0	6.1	55	62	78	34	32	.24	1.5		.79	.081	.180	4.3	80.8	2.76	8	72	5.7	.50

GLUE-SIZED PAPERS, PULP B

895		0	(6)		55.0	31.2	57	0.0035	270	450	7.8	4.9	1.7	6.2	43	50	78			0.21	0.7			0.010	0.010		79.5	3.34	37	99	2.3	0.32
895	232			4.5	58.8	41.1	70	.0036	520	490	8.5	6.3	2.0	6.8	48	45	74	8	12	.32	.5	1.84		.041	.040	5.2	80.7	3.31	44	79	2.2	.28
896		0.5	5.0		55.2	31.1	56	.0034	520	330	7.7	4.7	1.8	6.9	46	48	78	14	16	.34	1.6			.049	.116	4.5	80.4	2.94	19	94	3.8	.75
896	233			4.5	55.7	35.5	64	.0032	270	340	8.5	5.5	2.2	6.3	46	48	77	31	29	.34	1.2	1.15		.068	.127	4.4	80.0	3.22	26	78	2.9	.38
897		1	5.0		56.2	30.5	54	.0035	180	290	7.7	4.9	1.9	5.4	48	52		24	25	.37	2.0			.034	.088	4.9	79.3	3.18	31	86	3.9	.79
897	234			4.5	57.8	33.8	58	.0033	260	280	8.6	5.2	2.2	5.5	48	47	79	33	27	.36	1.6	.71		.049	.094	4.5	79.1	2.86	35	84	3.2	.68

[1] Samples heated at 100° C. for 72 hours.
[2] For test specimen 15 mm wide and 90 mm between jaws.
[3] For test specimen 15 mm wide and 100 mm between jaws.
[4] Acidity expressed as percent SO_3.
[5] Bursting pressure in pounds per square inch through a circular orifice 1.2 inches in diameter.
[6] No alum added.
[7] Starch prepared by process of oxidation.

NOTE.—All physical tests made under conditions of 65 percent relative humidity and 70° F.

In general, surface sizing resulted in marked improvement in tensile properties, the magnitude of which was roughly related to the amount of glue or starch taken up on sizing. No great improvement in folding endurance resulted. Of the 12 papers, 5 showed no improvement in this respect, while only 4 showed an increase of 10 percent or more. The tearing strength of papers made from pulp A was lowered about 20 percent by the surface sizing. Papers made from pulp B, having a very low tearing strength initially, were unchanged by sizing. The uniformity of the paper in respect of folding endurance in the two directions was improved very greatly by surface sizing. On the average, the values for the folding endurance in the machine and cross directions differed from each other, in the case of the basic papers, by about 40 percent. This difference was reduced to 12 percent on surface sizing. In regard to effects of sizing materials on the strength of papers, the characteristics of the fibers or papers treated should be considered. For example, it is known that while the folding endurance of weak rag papers may be materially increased by surface sizing them, such treatment may decrease the folding endurance of very strong rag papers. Therefore, other sulphite fibers of different characteristics from those used in this study might react differently to sizing treatments as far as strength is concerned.

All the papers of the series were relatively low in stability, with the exception of tub sizing run no. 225, a waterleaf sheet sized with glue containing no alum, which retained 71 percent of the initial folding endurance and decreased but 1 percent in alpha cellulose content after the accelerated aging test. In general, the papers engine sized with rosin and surface sized with glue lost considerably over half of the initial folding endurance and decreased several percent in alpha cellulose content. These are indications of only moderately stable paper. A slight improvement in stability resulted from surface sizing with glue. Starch sizing apparently offered no improvement in stability. When alum was not used in the sizing bath the papers appeared to be slightly more stable than when it was present.

The results of this study are further evidence of the close relation between the cellulosic purity of paper fibers and the stability of papers; the moderate stability of the best papers produced was commensurate with the medium degree to which the fibers had been purified. Under a system of classification of printing and writing papers, relative to their permanence qualities, which has been suggested by the Bureau of Standards, the best of the sulphite papers produced in this study would fall in class III, as representative of papers of fair purity for routine correspondence and other records requiring moderate life.[16]

Since some of the various types of fibers included in the program of study may have certain inherent characteristics that would make them adapted to the manufacture of currency paper, it is planned to make currency-type papers from each of them so that their printing and wearing properties may be studied and compared. In table 8 test results for waterleaf and glue-sized papers are given for currency-type paper made from the stronger of the two sulphite fibers discussed in this article. While the papers are of very high strength, they do not meet the United States Government strength requirements for currency paper.

---

[16] B. W. Scribner, Permanence Standards for Printing and Writing Papers, Trans. A.S.M.E., vol. 52, no. 19, P.I., pp. 52-55, May-August 1930. Also, Paper Mill and Wood Pulp News, vol. 53, p. 13, June 21, 1930.

TABLE 8.—*Tests of currency-type papers made from sulphite fibers*

Paper machine run no.	873	873
Surface sizing run no.	----	231
Weight (500 sheets 17 by 22 inches) ..... pounds	23.2	23.4
Weight (500 sheets 25 by 40 inches) ..... do	62.0	62.5
Thickness ..... inch	0.0037	0.0036
Bursting strength ..... points [1]	39.1	50.4
Folding endurance:		
Machine direction ..... double folds	2,500	2,200
Cross direction ..... do	2,200	2,400
Tearing strength:		
Machine direction ..... grams	68	53
Cross direction ..... do	69	52
Glue ..... percent	0	1.96
Opacity ..... do	80.0	77.0

[1] Approximately pounds per square inch.

VI. ACKNOWLEDGMENT

The authors are indebted to M. J. O'Leary [17] and G. O. Stone [18] for assistance in these studies.

WASHINGTON, April 27, 1933.

[17] Assistant paper maker.
[18] Assistant research associate representing the National Research Council.

U.S. Department of Commerce—Bureau of Standards

RESEARCH PAPER RP575

Part of Bureau of Standards Journal of Research, Vol. 11, July 1933

PERMISSIBLE CURVATURE OF PRISM SURFACES AND INACCURACY OF COLLIMATION IN PRECISE MINIMUM-DEVIATION REFRACTOMETRY

By L. W. Tilton

ABSTRACT

Care in the optimum translational adjustment of a prism in order to permit the symmetrical use of all apertures is always necessary on account of aberrations inherent in lens systems. Such prism adjustments are advisable also because of slight curvatures of most prism surfaces. When prisms are at all times correctly located with respect to the axes of collimator, telescope, and spectrometer, the departures of the surfaces from planeness may then be appreciably greater than has hitherto been recognized as allowable. Moreover, it is shown that the latitude in collimation becomes sufficiently large to permit making all necessary refocusings with the telescope, even when using objectives with the usual type of color correction. Tolerances, corresponding to an error of $\pm 1 \times 10^{-6}$ in index of refraction, are evaluated for curvature of prism surfaces, translational adjustment of the prism, eccentricity of prism-table axis, and collimator refocusing.

CONTENTS

	Page
I. Introduction	26
II. Symmetrical use of the prism and the lens systems	29
1. Lens aberration and "obliquity" errors	30
2. Methods of refracting-angle measurement and curvature of prism surfaces	30
3. Minimum-deviation measurement and curvature of prism surfaces	31
III. Relations between curvature of prism surfaces and prism-position adjustment	32
1. Effect of asymmetric tabling when prism surfaces are curved (collimated incident light)	32
(*a*) Making refracting-angle measurements	32
(*b*) Making minimum-deviation measurements	34
(*c*) Combined effects of asymmetric tabling on refractive-index determinations	38
(*d*) Tolerance in curvature of prism surfaces	41
(*e*) Tolerance in asymmetric tabling	42
(*f*) Refocusing of telescope required because of prism-surface curvature	43
2. Effect of eccentric prism-table axis when prism surfaces are curved (collimated incident light)	43
(*a*) Making refracting-angle measurements	44
(*b*) Making minimum-deviation measurements	45
(*c*) Combined effects of table-axis eccentricity on refractive-index determinations	46
(*d*) Tolerance in table-axis eccentricity	46
IV. Relations between inaccurate collimation and prism-position adjustment	47
1. Effect of asymmetric tabling when incident light is uncollimated (flat prism surfaces)	48
2. Effect of eccentric prism-table axis when incident light is uncollimated (flat prism surfaces)	50
(*a*) Experimental determination and azimuthal adjustment of eccentricity of table-axis	52
(*b*) Tolerance in collimation adjustment corresponding to a table-axis eccentricity of 0.2 mm	52
V. Relation of prism aberration to collimation and to curvature of surfaces	53
VI. Summary and discussion	56

I. INTRODUCTION

The errors of a goniometrical nature which occur in the practice of precise prism refractometry may be classed as pertaining either (*a*) to the spectrometer only and to its use as a goniometer, or (*b*) to the prism and its relation to the instrument. The most important errors of the first category are those pertaining to the divided circle and in the second group the proper orientation of a prism in azimuth has often been considered a serious matter. Both of these subjects have been discussed by the author in former papers.[1] In this paper consideration is given chiefly to other interrelations of prism and spectrometer, and the stipulations which are customarily made regarding the planeness of prism surfaces are discussed. In particular, the accuracy necessary in the translational adjustment of the prism with respect to the instrument is considered.

The adjustments of the spectrometer itself are in general well understood, but they require particular mention in two instances. The customarily assumed necessity for securing exact collimation has not been conclusively demonstrated and, on the other hand, it is not apparent that the eccentricity of the prism-table axis can be safely neglected under all the conditions which occur in practice. Both collimation and axis eccentricity are, however, closely related to prism quality and to translations of the prism, and consequently these two adjustments of the spectrometer are discussed in this paper because they cannot be adequately considered apart from a treatment of other matters relating more particularly to the prism.

Although planeness of prism surface is the only prism quality explicitly considered, a high degree of homogeneity is necessarily assumed, especially in treating of the subject of prism aberration and its bearing on the permissible inaccuracies of collimation. It is also presupposed that the working conditions are such that the properties of the prism are satisfactorily constant during the measurements; and many other obvious matters are not mentioned.

In all cases the individual tolerances are here evaluated to correspond to an error of $\pm 1 \times 10^{-6}$ in index of refraction. While these tolerances are given as consistent with "sixth decimal place" refractometry, it should be remembered that, in order to limit the combined errors rigorously to one unit of the sixth place, the separate contributions must be confined to still smaller magnitudes.

For convenience of reference the definitions of the various symbols are summarized here as follows:

$A \equiv$ refracting angle of an isosceles portion of a prism (measured between planes tangent at the mid-points of the effective prism surfaces);

$A_e \equiv$ erroneous value of refracting angle as measured when prism is incorrectly placed on the prism table;

C and $C' \equiv$ intersections of incident and emergent chief rays for prism in the "left-hand" position and in the "right-hand" position, respectively (C' sometimes coinciding with C);

[1] L. W. Tilton, B.S.Jour. Research, vol. 2 (RP64), p. 909, 1929; vol. 6 (RP262), p. 59, 1931.

c and $c' \equiv$ cosines of incidence angles on first and second faces of prism as oriented for minimum deviation; that is,

$$c \equiv \cos \frac{A+D}{2} \text{ and } c' \equiv \cos (A/2);$$

D, D_e, and $D_c \equiv$ angles of minimum deviation produced, respectively, by a prism correctly placed, asymmetrically tabled, and tabled with respect to an eccentric table axis;

$E \equiv_\lambda$ distance through which, after refracting-angle measurement, the prism vertex should be translated toward the table axis preparatory to deviation measurement for a wave length λ;

$e_A \equiv$ linear asymmetry of prism position (when making refracting-angle measurements) measured from prism-table axis to the intersection of normals erected at the surface centers of the effective isosceles portion of the prism;

$e_D \equiv$ linear asymmetry of prism position (when making minimum-deviation measurements) measured from prism-table axis to the intersection of the incident and emergent chief rays;

e_{AR} and $e_{AL} \equiv$ errors in tabling a prism for refracting-angle measurement as measured perpendicularly to the line of sight at the right- and left-hand telescope pointings;

e_{DR} and $e_{DL} \equiv$ errors in tabling a prism for minimum-deviation measurement as measured perpendicularly to the line of sight at the right- and left-hand pointings;

$e_m \equiv$ maximum error (measured perpendicularly to the telescope pointings) that is made in translational adjustment of a prism;

$\epsilon \equiv$ linear eccentricity of prism-table axis with respect to axis of the spectrometer;

$\eta \equiv$ phase difference in complete periods or cycles;

$f \equiv$ focal length of telescope objective;

$f_c \equiv$ focal length of collimator objective;

$f'_c \equiv$ adequate collimator focal length which permits refractive-index measurement without chromatic refocusing of collimator;

$f_{tp} \equiv$ combined focal length of telescope objective and prism;

$F_c \equiv$ actual collimator tube length or distance from collimator slit to objective;

$\Delta F_c \equiv$ error in focusing collimator; that is, $\Delta F_c = (f_c - F_c)$;

$\Delta F_A \equiv$ required refocusing of telescope for refracting-angle measurements (on curved-surface prisms) by auto-collimation;

$\Delta F_D \equiv$ required refocusing of telescope for minimum-deviation measurements; that is, $\Delta F_D = (f_{tp} - f)$;

$\varphi \equiv$ azimuth of eccentricity of prism-table axis;

$L \equiv$ length or horizontal dimension of an effective prism face or surface;

$\lambda \equiv$ wave length of light;

$n \equiv$ relative index of refraction of a medium, the subscripts C and F specifying the wave lengths 6,563 and 4,861 A, respectively;

$n' \equiv$ Rayleigh's symbol for nc'/c;

$\delta n_{\Delta A}$ and $\delta n_{\Delta D} \equiv$ partial errors in index of refraction attributable to error in measurements of A and D, respectively;

Δn_e, Δn_ϵ, and $\Delta n_{\Delta F_c} \equiv$ combined errors in index of refraction attributable to asymemtric tabling, eccentricity of prism-table axis, and inaccurate collimation, respectively;

N_A and $N_D \equiv$ number of measurements of refracting angle and minimum deviation, respectively, made with independent translational adjustments of the prism;

$\nu \equiv$ optical constringence, that is, $\nu = \dfrac{n-1}{n_2 - n_1}$;

$O \equiv$ horizontal projection of the vertical axis of the spectrometer;

$P.E.e_o \equiv$ probable error of a single translational adjustment of a prism made perpendicularly to the telescope axis;

$P.E.n_A$ and $P.E.n_D \equiv$ partial probable errors in index of refraction attributable to probable error of tabling as it affects measurements of A and D, respectively;

$P.E.n_e \equiv$ combined probable error in index of refraction attributable to probable errors in asymmetry of tabling the prism;

r_1 and $r_2 \equiv$ radii of curvature of faces of a prism (positive when convex toward incident light);

$r \equiv$ an average of the radii of curvature of faces of a prism; that is, $r = 0.5\ (r_1 - r_2)$;

$S \equiv$ position of source;

S_1 and $S_2 \equiv$ virtual positions of source (for left- and right-hand pointings, respectively) when prism is properly tabled and table-axis eccentricity is zero;

S_L and S_R ≡ virtual positions of source (for left- and right-hand pointings) when prism is not in correct position with respect to the spectrometer axis;

s ≡ sagittal departure (in wave lengths) from flatness for any prism surface, s' referring to a limited portion of the surface having a diameter of 1 cm;

$T_{1/r}$ ≡ tolerance in average prism-surface curvature which corresponds to a probable error of $\pm 1 \times 10^{-6}$ in refractive index;

$T_{P.E._{e_0}}$ ≡ tolerance in probable error of translational adjustment of a prism (made perpendicularly to the telescope axis) which corresponds to a probable error of $\pm 1 \times 10^{-6}$ in refractive index;

T_e ≡ tolerance in table-axis eccentricity which corresponds to an error of $\pm 1 \times 10^{-6}$ in refractive index;

$T_{\Delta F_c}$ ≡ tolerance in inaccuracy of collimation which corresponds to an error of $\pm 1 \times 10^{-6}$ in refractive index;

ϑ_A and ϑ_D ≡ azimuth of asymmetry of prism position (for refracting-angle and minimum-deviation measurement, respectively) referred to the bisector of the refracting angle (positive toward base of prism);

u and u' ≡ object and image distances measured from first surface of lens (or prism);

v ≡ image distance measured from second surface of lens (or prism);

x ≡ distance from collimator objective to prism;

y ≡ semiwidth of (cross-sectional) aperture of the pencil incident on the prism; and

y' ≡ projection of semidiameter of incident pencil along the first face of the prism; that is, $y' \equiv y/c$.

II. SYMMETRICAL USE OF THE PRISM AND THE LENS SYSTEMS

The necessity of proper translational adjustment of the prism with respect to the axis of the spectrometer has been noticed to some extent by several writers. Hastings,[2] originally, exercised considerable care in tabling his prisms in order to eliminate errors due to aberration which he recognized as existing in every objective, and later he made further statements about the intersection of lines of collimation and prism-face centers. Müller [3] had both curvature of prism surfaces and lens aberration in mind when speaking of prism positions on the table, at least when referring to measurements of refracting angles. Macé de Lépinay [4] refers to errors in focusing the collimator and to the

[2] C. S. Hastings, Am. J. Sci., vol. 15, pp. 269–275, 1878; vol. 35, pp. 65–68, 1888.
[3] G. Müller, Publicationen des Astrophysikalischen Observatoriums zu Potsdam, vol. 4, p. 163, 1885.
[4] J. Macé de Lépinay, J. de Physique (2), vol. 6, pp. 190–196, 1887. See, also, Annales de Chimie et de Physique (7), vol. 5, pp. 225–226, 1895.

curvatures of surfaces as reasons for adjusting the prism so that when measuring deviations the chief ray of the beam of incident light passes through the centers of the prism surfaces. It seems, however, that the majority of observers have given inadequate attention to these matters, and some recent manuals, in treating of refractive index goniometry, have neglected them entirely.[5] Moreover no one seems to have realized that strictly symmetrical conditions permit the use of curved surfaces on prisms and a useful latitude in collimation. Therefore, on account of the advantages in observing the principle of symmetry, and also because of its fundamental importance for good work, even in the fifth decimal place of refractive index, it is well to discuss this topic in detail.

1. LENS ABERRATION AND "OBLIQUITY" ERRORS

In general, comparatively small prisms and large telescope apertures are used in prism refractometry, and it is especially under these conditions that the greatest care must be taken to make the effective apertures symmetrical about vertical lines through the lens and prism-surface [6] centers. Otherwise, the presence of aberration in the lens system, a departure from flatness of the prism surfaces, or an unusually defective collimator adjustment may vitiate the results.

Furthermore, even with perfect lenses, flat prism surfaces, and perfect adjustment of collimator tube length, an error in pointing is still introduced, according to Guild,[7] by inaccurate focusing of the eyepiece, whenever oblique cones of rays are produced within the telescope through using the objectives [8] unsymmetrically. This causes an "obliquity" error in angular measurement unless the asymmetry is of a compensating nature at each of the two pointings.

2. METHODS OF REFRACTING-ANGLE MEASUREMENT AND CURVATURE OF PRISM SURFACES

The difficulties in connection with the unsymmetrical use of apertures and with oblique reflections from imperfect prism surfaces are, in fact, so great that the split-beam method of measuring a refracting angle, A, is probably inadequate in precise refractometry even with the application of troublesome corrections, such as those given by Cornu [9] or Carvallo [10] for (1) the absolute error in collimation, and (2) the changes in focus necessitated by the curvatures of prism surfaces; and this statement is made with due consideration of the apparent advantage of the procedure in that $2A$ is directly determined, thus halving certain errors in A.

With any method of refracting-angle measurement, the curvature of prism surfaces must be regular to give fair imagery by reflection. Curvatures must also be of the same character (both convex or both

[5] The Dictionary of Applied Physics, vol. 4, Macmillan & Co., Ltd., London, is a noteworthy exception and for this credit is due to J. Guild, of the National Physical Laboratory.

[6] If large prisms are used and the whole telescopic apertures filled, then for curved prism surfaces, it is still necessary to use prism apertures which are symmetrical about definite vertical lines, conveniently those through the surface centers.

[7] J. Guild, Proc., Phys. Soc., London, vol. 28, p. 244, 1916; or Nat. Phys. Lab., Collected Researches, vol. 13, p. 232, 1916. See also W. Uhink, Zeits. f. Instrumentenk., vol. 52, pp. 435–442, 1932.

[8] Obviously, the unsymmetrical use of an eyepiece causes no errors because both image and fiducial lines are equally displaced.

[9] A. Cornu, Annales de l'Ecole Normale Superieure (2), vol. 9, pp. 76–87, 1880.

[10] E. Carvallo, Annales de l'Ecole Normale Superieure (3), vol. 7, supplement, pp. 77–88, 1890.

concave) and approximately [11] of the same magnitude to obviate refocusing of the telescope between two successive pointings. When a prism satisfies these conditions and is leveled and "centered" so that the face-center normals intersect the vertical axis of a properly adjusted spectrometer, the prim angle measured by autocollimation (and possibly by collimator and rotating table [12] also) will be sensibly that between planes tangent at the mid-points of the prism surfaces. This value of the prism angle is, however, not the refracting angle actually used at minimum deviation except for isosceles prisms. Only an isosceles portion of a prism can be used for minimum deviations and the refracting angle A, as considered in this paper, is formed by planes tangent at the mid-points of the effective surfaces of the isosceles portion. The circumcenter of the horizontal projection of this usable portion of the prism must coincide with the spectrometer axis during refracting-angle measurements.[13]

3. MINIMUM-DEVIATION MEASUREMENT AND CURVATURE OF PRISM SURFACES

If, after refracting-angle measurement, the prism be properly translated so that, when measuring minimum deviation, the axes of the telescope and collimator again intersect the effective prism surfaces at their mid-points, then the measured deviation will correspond very closely [14] to that for a plane-surface prism of the refracting angle determined by the tangent planes at these mid-points. For a prism with curved surfaces this particular plane-surface-prism deviation is defined as the correct value.

For other prism positions, which may be termed asymmetric (axis of telescope or collimator not intersecting effective prism-surface center) different measured values of refracting angle and of minimum deviation are to be expected, depending on the amount of asymmetry of position, the curvature of the surfaces, and perhaps on the lack of collimation. It is, of course, realized that these variations in the measured values depend, also, on certain differential errors (lens aberration and obliquity) due to variations in the unsymmetrical use of the optical system. However, with small asymmetries of prism position (see figs. 4 and 6), and fairly well corrected objectives, it may be considered that these differential errors are negligible [15] in comparison with the primary effects which are to be discussed. Also, as will be found in section V, it can be assumed that the aberration of the prism is likewise of minor importance. From this standpoint the result of asymmetric prism position will now be considered in detail, first in connection with curvature of surfaces, section III, and then in its relation to lack of collimation, section IV. For convenience and simplicity of treatment, asymmetry of prism position will be considered

[11] See footnote 17, p. 32, and footnote 27, p. 42.

[12] Although the lens system is used unsymmetrically in the prism-rotation method of angle measurement with a collimator, it will be noticed that the asymmetry can (for isosceles prisms) be identical for the successive pointings. The reflections at oblique incidence are, however, unfavorable because of aberration introduced by imperfect prism surfaces. W. Voigt (Zeits. f. Kryst., vol. 5, pp. 122–124. 1880) has discussed a special case of the error caused by incorrect translational adjustmert when measuring by this method the refracting angle of a prism having curved surfaces.

[13] See footnote 20, p. 34.

[14] References to prism-aberration errors are made in section V.

[15] In all cases which are considered in detail in this paper, these neglected differential errors pertaining to the lens systems may, if necessary, be eliminated by the use of centrical (preferably rectangular) diaphragms of adjustable aperture. The first order errors caused by using asymmetric apertures of prisms having curved surfaces are, of course, not obviated by the use of such diaphragms.

as arising from two separate causes (1) asymmetry of tabling; that is, failure to correctly translate and adjust the prism with reference to the axis of the prism table; and (2) that incorrectness of prism position which may result solely because of eccentricity of the prism table axis.

III. RELATIONS BETWEEN CURVATURE OF PRISM SURFACES AND PRISM-POSITION ADJUSTMENT

In this section it will be assumed (1) that the spectrometer is equipped with perfectly corrected objectives (see footnote 15), (2) that the aberration introduced by the prism is negligibly small (see sec. V), (3) that the instrument and the prism are correctly adjusted in the usually mentioned particulars, including the accurate adjustment of the slit in the focal plane of the collimator objective, and (4) that the optical axes of both telescope and collimator intersect the principal axis of rotation of the instrument.[16]

With these assumptions the light incident on the prism when measuring deviations is strictly parallel and, if the prism surfaces are plane, the observing telescope may be used as correctly focused for infinity. Under these ideal conditions no particular care is required in translational adjustments when tabling prisms and no errors ensue from eccentricity of the prism table axis. It is quite otherwise, however, when the prism surfaces are curved, and the effects of asymmetric tabling and of eccentric table axis will be considered separately, with the additional general assumption (5) that the prism surfaces are both convex, or concave, and have radii which are approximately equal[17] and very large compared to the dimensions of the prism.

1. EFFECT OF ASYMMETRIC TABLING WHEN PRISM SURFACES ARE CURVED (COLLIMATED INCIDENT LIGHT)

In discussing asymmetric tabling and prism-surface curvature it will further be specifically assumed (6′) that the asymmetry is small compared with the prism and that the prism-table axis is not only parallel to but coincides with that of the spectrometer.

(a) MAKING REFRACTING-ANGLE MEASUREMENTS

Referring first to refracting-angle measurement, attention will be confined to the autocollimation method[18] with rotating telescope, and in figure 1 the axis of the prism table coincides with the axis of the spectrometer at O, while the intersection of the face-center normals of the isosceles portion of the prism is at C. The fiducial mark in the image plane of the telescope is replaced by its virtual positions at S_L and S_R, the centers of curvature of the prism surfaces, and S_Lt_L and S_Rt_R are normals to the prism surfaces at their centers.

[16] In this directional adjustment of a telescope or a collimator no elaborate attempt need be made to use, in practice, a true optical axis but merely the line from the image plane fiducial mark, or from the slit center, approximately through the appropriate principal point of the objective. These lines may vary somewhat in azimuth as the tube lengths are changed and so do not exactly intersect the vertical axis of the spectrometer except, possibly, for one particular tube length. All pointings are thus to be regarded as slightly erroneous, but no direct effect of this remains in the resultant angles provided the tube lengths remain constant between pointings. (Slight inaccuracies in prism-position adjustment may result.) The introduction of assumption (4) serves, however, to simplify the discussion in this and in the following section.

[17] The radii must be equal only to the extent that during refracting-angle measurement a satisfactory compromise focus of the telescope can be found. Excellence of definition is not of great importance because the precision of tabling (see fig. 4(*b*)) insures approximate symmetry of the aberration about a vertical axis. See footnote 27, p. 42.

[18] The general assumption (3) of collimated incident light must, of course, be interpreted here as "autocollimated" light for the particular surfaces concerned.

The refracting angle (in radians) whose measure is required is

$$A = \pi - \angle t_L C t_R \tag{1}$$

but since the telescope revolves about O, it takes the directions $T_L O S_L$ and $T_R O S_R$, irrespective of the tube length or of the obliquity of the eccentric pencils, and consequently

$$A_e = \pi - \angle T_L O T_R \tag{2}$$

is the angle which is determined. From equations (1) and (2), and from the figure, it is evident that

$$\Delta A = \angle t_L S_L T_L + \angle T_R S_R t_R \tag{3}$$

is the error in angle, namely, $A_e - A$.

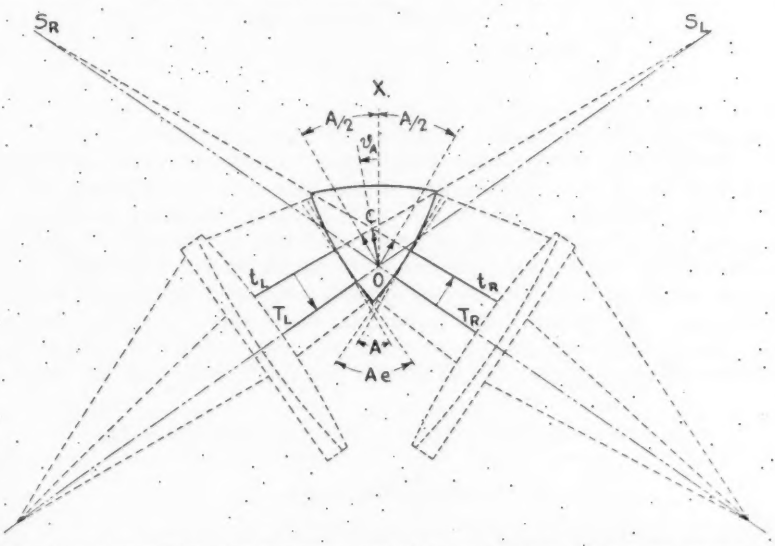

FIGURE 1.—*Autocollimation measurement of the refracting angle of an asymmetrically tabled prism having curved surfaces.*

When the intersection of the face-center normals, $t_L C S_L$ and $t_R C S_R$, at the prism "center" C, is not coincident with the vertical axis of the goniometer at O, then the telescope pointings which are necessarily along $T_L O$ and $T_R O$ toward the virtual sources S_L and S_R are not parallel to the normals. Thus the chief error in determining the definite refracting angle A is directly proportional to the curvature of the prism surfaces and also to $OC \cos \vartheta_A$ which is the longitudinal component of the error in tabling. Of the other errors which occur because of the unsymmetrical use of the telescope objectives, some are independent of prism surface curvature but all may be minimized by reducing the asymmetry of tabling.

If from O, parallel to the bisector of the refracting angle of the prism, a reference line, OX, is drawn, the positive direction being toward the third side of the prism, then OC, the asymmetry of prism position, may conveniently be considered as a vector having a length e_A and an azimuth ϑ_A with respect to this reference line. The lengths of the components of OC, perpendicular to $t_L C$ and $t_R C$, respectively, are $e_A \cos (A/2 - \vartheta_A)$ and $e_A \cos (A/2 + \vartheta_A)$ where $A/2$ is an essentially positive quantity. Consequently equation (3) may be easily rewritten [19] as

[19] To rewrite equation (4) in seconds of arc apply the factor 206.3×10^3.

$$\Delta A = \frac{2e_A \cos \frac{A}{2} \cos \vartheta_A}{r} \tag{4}$$

where $r = 0.5\ (r_1 - r_2)$ is an average radius of curvature, positive for convex surfaces. Then by the use of the appropriate elemental differential equation for the minimum-deviation method, namely

$$\frac{o\,n}{o\,A} = -\frac{\sin \frac{D}{2}}{2 \sin^2 \frac{A}{2}} \tag{5}$$

one obtains

$$\delta n_{\Delta A} = \frac{-e_A \sin \frac{D}{2} \cos \vartheta_A \cos \frac{A}{2}}{r \sin^2 \frac{A}{2}} \tag{6}$$

as the partial effect of prism surface curvature on index.

A consideration of equation (4) and the conditions of its derivation shows that for a given refracting angle this error is independent of prism-table rotation. Thus equation (4) applies not only to "direct" measurements of any refracting angle, but also to "reverse" determinations of the same angle by measurements on its explement. If, however, all three angles of any prism are measured for a given tabling adjustment,[20] the prism table remaining stationary or being conveniently rotated between measurements on each angle, the asymmetry of tabling affects each angle differently but from their sum the error

$$\Delta A_1 + \Delta A_2 + \Delta A_3 = \frac{2e_A}{r}\left(\cos \frac{A_1}{2} \cos \vartheta_{A1} + \cos \frac{A_2}{2} \cos \vartheta_{A2} + \cos \frac{A_3}{2} \cos \vartheta_{A3}\right) \tag{7}$$

vanishes completely since

$$\vartheta_{A2} = \vartheta_{A1} + \pi + \frac{A_1 + A_2}{2} \text{ and } \vartheta_{A3} = \vartheta_{A2} - \pi + \frac{A_2 + A_3}{2},$$

and by a series of trigonometric transformations it can be shown that the total factor in parentheses equals zero. This result, which is quite obvious from geometrical considerations, is of value when making a precise test of a goniometer with a prism polished on all three faces.

(b) MAKING MINIMUM-DEVIATION MEASUREMENTS

As already mentioned, the prism-face-center normals should not intersect the table axis during deviation measurements. The refracting edge or vertex of an isosceles portion of the prism, as placed for angle measurement, should be moved toward the table axis a distance

$$E\lambda = \frac{L}{2} \tan \frac{A}{2} \sec \frac{D}{2} \sin \frac{A+D}{2} \tag{8}$$

[20] In general it is the circumcenter of the horizontal projection of the entire prism which must coincide with the vertical axis of the spectrometer during prism-angle measurements. Only for equilateral prisms are all three of these prism angles equivalent to refracting angles for index measurement. See sec. II, 2.

L being the length of a face of the isosceles prism. The axes of telescope and collimator then always pierce the centers of the effective surfaces when the minimum-deviation conditions are fulfilled and thus this correct installation of the prism may also be termed symmetrical. Equation (8) is equivalent to that given by Carvallo,[21] who also demonstrated that, in passing from deviation on the left to that on the right, the conditions of symmetry are preserved without further prism translation.

In practice, when more than one wave length is used for refractive index measurements, it is advisable to know whether or not a prism requires retabling between the various deviation measurements.

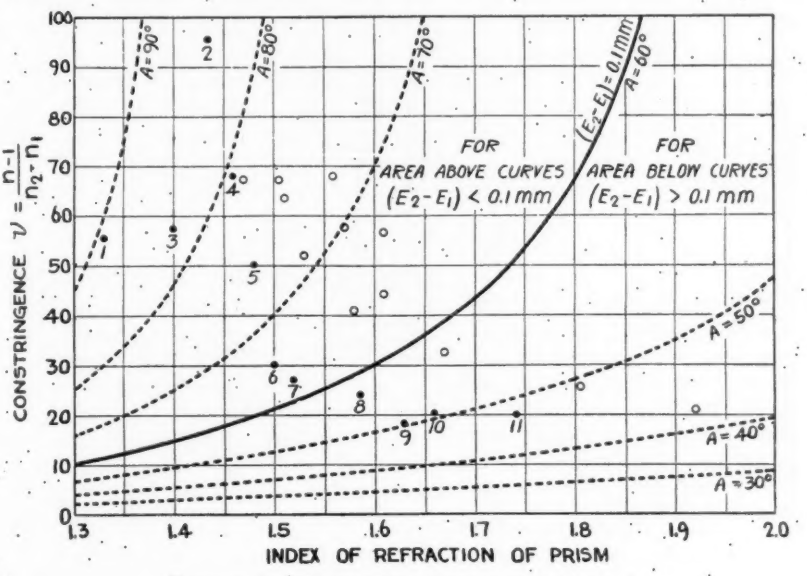

FIGURE 2.—*Chromatic tolerance in retabling.*

These contours of $(E_2-E_1)=0.1$ mm show, for various refracting angles, the chromatic limits for a given translational prism adjustment for minimum-deviation measurements. A prism surface length of 2 cm is used and a precision of ± 0.1 mm in prism translation is assumed. If, for any spectral interval $(\lambda_2-\lambda_1)$, the corresponding constringence of a substance lies above the ΔE curve for the appropriate A, then no retabling is advisable between observations on spectral lines separated by a comparable interval. For the particular interval (n_F-n_C), the open circles designate typical optical glasses and the dots show approximate locations of other substances as follows: 1, water; 2, fluorite; 3, *n*-octane; 4, fused quartz; 5, linseed oil; 6, benzene; 7, tungoil; 8, aniline; 9, carbon disulphide; 10, *m*-bromonaphthalene; 11, methylene iodide.

Accordingly, equation (8) has been used in computing these chromatic variations. A prism-surface length of 2 cm has been used and results are expressed in figure 2 for several values of prism angle. The ordinate ν is a general expression (see fig. 2) inversely proportional to the partial dispersion between any two wave lengths. For the sodium lines index and the special spectrum interval from 4,861 to 6,563 A (F to C of hydrogen) this becomes that particular measure of optical constringence which was introduced by Ernst Abbé and is now widely used for expressing dispersion data. For this spectrum interval the locations of several transparent media are shown by circles and dots on figure 2. In using this figure it should be remembered that (1) prisms in excess of approximately 2 cm surface length are seldom if

[21] See pp. 89–92 of paper cited in footnote 10, p. 30.

ever required for index measurements; [22] (2) the attainable precision of a single adjustment of prism position is $P.E. = \pm 0.1$ mm or less (see sec. III, 1 (*c*) below); (3) as shown by figure 4 a precision as high as $P.E. = \pm 0.1$ mm in this prism adjustment is seldom necessary; and (4) the partial dispersion $(n_F - n_C)$ is, for most transparent media, approximately one half the partial dispersion for the whole range of the visible spectrum. Consequently, it may be concluded that comparatively few prisms, of angle $A = 60°$ or less, require any translational readjustment on the prism table during dispersion measure-

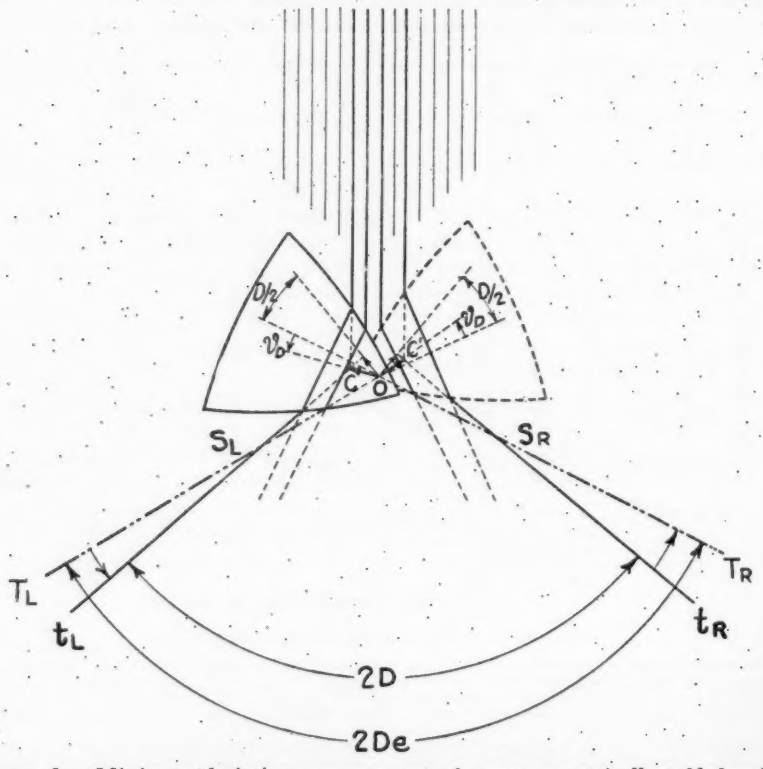

FIGURE 3.—*Minimum-deviation measurement of an asymmetrically tabled prism having curved surfaces.*

Images of the source are formed at S_L and S_R when the prism is oriented for deviation left and right, respectively. C and C' are the intersections of the prolongations of those rays which traverse the prism surface centers and in correct tabling for deviation measurement these points must coincide at O. The emergent rays CS_Lt_L and $C'S_Rt_R$ have the angular separation $2D$, the measurement of which is desired, but the telescope pointings are necessarily along T_LS_L and T_RS_R toward the virtual sources and the axis of the spectrometer at O.

ments within the range of the visible spectrum, if the initial adjustment is made for some wave length near the midrange.

To facilitate the investigation of errors in minimum-deviation measurements which result from incorrect or asymmetric prism tabling, reference will be made to figure 3 where the coincident axes are again represented at O while C and C' are the points of intersection of those particular incident and emergent chief rays which pass through the surface centers during deviation left and deviation right,

[22] See p. 76 of second paper cited in footnote 1, p. 26.

respectively. The collimator is supposed replaced by a source at an infinite distance, u, and at the corresponding image distance, v, from the prism is located the virtual source, S_L, to be imaged in the telescope at the left-hand pointing. A similar virtual source, S_R, is shown for the right-hand pointing.

Obviously, for a given orientation, only a single ray traverses the prism exactly at minimum deviation but the extreme divergence of the emergent rays with which one is concerned is usually only a matter of seconds. Consequently it is evident [23] that one prism orientation serves sufficiently well for all such rays.

If the observing telescope measured correctly the deviation of the ray which passes through the prism-surface centers, that is one half the angle, $2D$, between t_LC and the similar line t_RC', then no error would be caused by the curvature of surfaces because these particular rays traverse the prism precisely as if the surfaces were flat and thus (with collimated incident light) the effective lateral translation of the prism as it is oriented about O between left and right deviation would be to this extent immaterial. The telescope, however, swings through the angle $T_LOT_R=2D_e$ between left and right pointings, and therefore

$$2\Delta D=\angle T_LS_Lt_L+\angle t_RS_RT_R \tag{9}$$

expresses the error in double deviation.

With the same convention previously used regarding the azimuth, ϑ_D, of the asymmetry $OC=OC'$, this distance may be resolved into components of length $e_D\cos(D/2+\vartheta_D)$ and $e_D\cos(D/2-\vartheta_D)$, perpendicular respectively to t_LC and t_RC', where $D/2$ is considered essentially positive. Neglecting prism thickness and the distance from the prism to the objective, the virtual object distance for telescope pointings is $OS_L=OS_R$, or approximately the image distance, v, as given by the formula for oblique refraction (primary plane) through a thin lens in air, namely

$$\frac{1}{v}=\frac{1}{u}+\frac{nc'-c}{c^2}\left(\frac{1}{r_1}-\frac{1}{r_2}\right) \tag{10}$$

where in this application u is infinite, n is the index of refraction of the prism, c and c' (cosines of incidence angles) are $\cos\frac{A+D}{2}$ and $\cos(A/2)$, respectively, and $r_2=-r_1$ approximately. Consequently

$$v=\frac{r}{2}\cdot\frac{\sin\frac{A}{2}\cos^2\frac{A+D}{2}}{\sin\frac{D}{2}} \tag{11}$$

and equation (9) becomes

$$\Delta D=\frac{2e_D\sin\frac{D}{2}\cos\vartheta_D\cos\frac{D}{2}}{r\sin\frac{A}{2}\cos^2\frac{A+D}{2}} \tag{12}$$

where, again, r is positive for convex surfaces.

[23] For tolerance in prism orientation see fig. 5, p. 73 of second paper cited in footnote 1, p. 26.

Using the value of v expressed in equation (11) as the focal length of the prism at minimum deviation, the required refocusing of the telescope, of focal length f, is

$$\Delta F_D = f_{tp} - f = \frac{-2f^2 \sin \frac{D}{2}}{r \sin \frac{A}{2} \cos^2 \frac{A+D}{2} + 2f \sin \frac{D}{2}} \tag{13}$$

where f_{tp} is the combined focal length of telescope objective and prism, and separation has been neglected. Consequently, equation (12) may be written as

$$\Delta D = \frac{-e_D \Delta F_D}{f^2} \cos \vartheta_D \cos \frac{D}{2} \tag{14}$$

if the relatively unimportant second term in the denominator of (13) is neglected. For the case of convex surfaces and the special conditions, $\vartheta_D = \pi$ and $e_D = E$ as expressed in equation (8), it is found that equation (14) is equivalent to that given by Carvallo [24] as

$$\Delta D = -\frac{p}{f^2} \delta f \sin \frac{A+D}{2} \tag{15}$$

where p is the perpendicular from the center to a side of the prism, and $\delta f = -\Delta F_D$.

By combining equation (12) with the appropriate elemental equation

$$\frac{o\,n}{oD} = \frac{n}{2 \tan \frac{A+D}{2}} \tag{16}$$

one obtains

$$\delta n_{\Delta D} = \frac{e_D \sin \frac{D}{2} \cos \vartheta_D \cos \frac{D}{2}}{r \sin^2 \frac{A}{2} \cos \frac{A+D}{2}} \tag{17}$$

as another partial effect of prism-surface curvature on index.

(c) COMBINED EFFECTS OF ASYMMETRIC TABLING ON REFRACTIVE-INDEX DETERMINATIONS

Equations (6) and (17) may be added to give

$$\Delta n_e = \frac{\sin \frac{D}{2}}{r \sin^2 \frac{A}{2}} \left(\frac{e_D \cos \vartheta_D \cos \frac{D}{2}}{\cos \frac{A+D}{2}} - e_A \cos \vartheta_A \cos \frac{A}{2} \right) \tag{18}$$

as the total index error which occurs because of asymmetric tabling of prisms having curved surfaces.

For a prism having a given angle, refractive index, and curvature of surfaces, the sign and the magnitude of the error expressed by equation (18) are, of course, dependent on the lengths $e_A \cos \vartheta_A$ and $e_D \cos \vartheta_D$. In particular, it may be remarked that, under the assump-

[24] See p. 81 of paper cited in footnote 10, p. 30.

tions which have been made in this section, translational prism adjustment at right angles to the bisector of the refracting angle (that is, at an azimuth $\vartheta = \pm\frac{\pi}{2}$) has no effect [25] on measurements of refractive index.

If translational adjustments are made by centering the image of the prism in the exit pupil of the telescope while the latter is correctly pointed for measurements, then from diagrams similar to figures 1 and 3 it can easily be shown that

$$\left.\begin{aligned} e_A \cos \vartheta_A &= \frac{e_{AR}+e_{AL}}{2} \sec \frac{A}{2} \\ \text{and} \\ e_D \cos \vartheta_D &= \frac{e_{DR}+e_{DL}}{2} \sec \frac{D}{2} \end{aligned}\right\} \tag{19}$$

where e_{AR}, e_{AL}, e_{DR}, and e_{DL} are the tabling errors, measured perpendicularly to the line of sight, which are made at each of the right- and left-hand pointings required in angle and in deviation measurements. All four of these centerings in the line of sight can be made with approximately the same precision and, if e_m is the maximum error to be made, then equation (18) can be rewritten as

$$\Delta n_e = \pm \frac{e_m \sin \frac{D}{2}}{r \sin^2 \frac{A}{2}} \left(\sec \frac{A+D}{2} + 1 \right) \tag{20}$$

to express the limiting errors in index for the most unfavorable case which may occur.

Next, a typical value for e_m is required. Obviously, some care must be taken if this error is to be small, say within the limits of ± 1 mm, and if the precision sought is to correspond to a valid accuracy. The author mounts vertical threads near the centers of the objectives so that they intersect those effective axes of the telescope and collimator which are properly directed (see assumption (4) and footnote 16 of sec. III), and he uses a prism table provided with two sets of horizontal ways which are operated by slow-motion screws. Then, while viewing a magnified image of the exit pupil of the telescope, one may center any prism aperture (less than 2 or 3 cm in width) with a probable error not exceeding ± 0.08 mm for a single translational adjustment. Consequently, a limiting value for e_m may be taken as approximately ± 0.4 mm and for a 60° prism of index 1.5 it may be found from equation (20) that r must be as large as 1,280 m to obviate index error greater than $\pm 1 \times 10^{-6}$.

Similar calculations for special cases with even larger estimated values for e_m are probably responsible in part for the widely prevalent idea that extremely flat prism surfaces are absolutely essential for accurate refractive-index measurements. Fortunately, such a large error as e_m is to be expected but once in a thousand of such prism adjustments, and, moreover, as shown by equation (18), there are

[25] It should be remembered, however, that in practice a neglect of lateral translational adjustment leads to appreciable aberrational and obliquity errors (see sec. II, 1).

two terms which have opposite signs and will, in the great majority of cases, compensate to some appreciable degree. Thus probability has an important bearing on the practical matter of establishing a tolerance in curvature for prism surfaces. Therefore it is suggested that a useful tolerance in this curvature should correspond to the production of a given probable error in index through measurements on a prism so adjusted that the probable error of each of the four independent single translations (made perpendicularly to the telescope axis) is $P.E.e_0$.

Corresponding to the actual errors of equation (19), the probable errors are

$$\left.\begin{aligned} P.E.e_A \cos \vartheta_A &= \pm \frac{P.E.e_0}{\sqrt{2}} \sec \frac{A}{2} \\ P.E.e_D \cos \vartheta_D &= \pm \frac{P.E.e_0}{\sqrt{2}} \sec \frac{D}{2} \end{aligned}\right\} \tag{21}$$

and these may be substituted for actual errors in equations (6) and (17) to express the separate probable errors in index, $P.E.n_A$ and $P.E.n_D$, which result from probable errors in prism tabling during single refracting-angle and deviation measurements, respectively. $P.E.n_A$ and $P.E.n_D$ may then be combined as

$$P.E.n_e = \pm \frac{P.E.e_0}{\sqrt{2}} \frac{\sin \frac{D}{2}}{r \sin^2 \frac{A}{2}} \sqrt{1+\sec^2 \frac{A+D}{2}} \tag{22}$$

to express the effect of tabling probable error in a single complete refractive-index determination instead of the actual error of equation (18) or the maximum error of equation (20).

If N_A measurements of angle and N_D measurements of deviation are made with readjustments of prism position, the quantity under the radical sign of equation (22) becomes

$$\frac{1}{N_A}+\frac{1}{N_D} \sec^2 \frac{A+D}{2}$$

and obviously it is advantageous to choose N_A and N_D so that approximate equality of these two terms is obtained. Thus, for any desired precision in index measurements to be made on a given prism with a definite available degree of tabling precision, one may easily decide to what extent the prism tabling should be repeated during such repetitions as may for other reasons be included on the observational program.

Equation (22) also serves as a suitable basis for determining (1) tolerances in curvature for prism surfaces which are to be centered or tabled with a given precision, and (2) tolerances in imprecision of tabling prisms having given curvature of surfaces.

(d) TOLERANCE IN CURVATURE OF PRISM SURFACES

From equation (22) the tolerance in curvature is

$$T_{1/r} = \pm \frac{1.41 \times 10^{-6} \sin^2 \frac{A}{2}}{P.E.e_0 \sin \frac{D}{2} \sqrt{1+\sec^2 \frac{A+D}{2}}} \tag{23}$$

if the error in index is specified as $P.E.n'_e = \pm 1 \times 10^{-6}$ for a single determination of refractivity. Equation (23) has been used in computing reference contours which are shown in figure 4 (*a*) and labeled

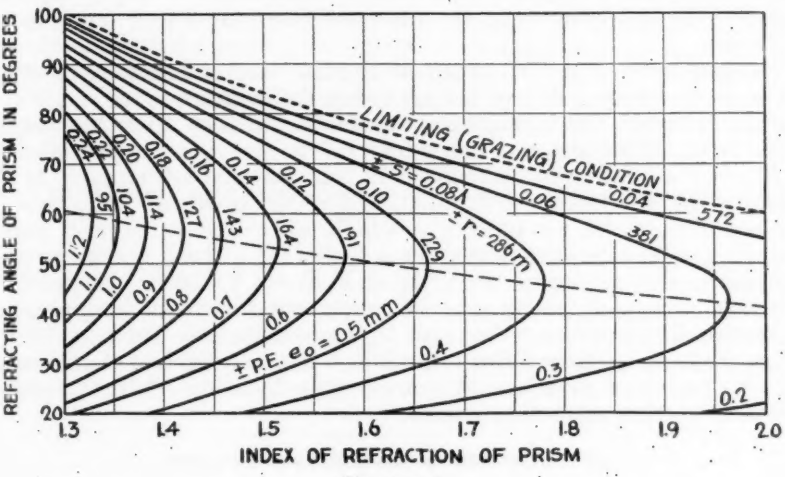

FIGURE 4

(*a*) Tolerance contours for approximately equicurvature of prism surfaces.—These contours of permissible curvature (read designations on upper arms of curves) are computed for translational adjustments of a prism which are made with a precision $P.E.e'_0 \equiv \pm 0.1$ mm. Departures from flatness are expressed as radius of curvature in meters and also as the sagitta, s', between the curved surface and a plane which passes through the circumference of a surface area having a diameter, $d' \equiv 1$ cm. If the curvatures are those specified, an idex of refraction may be measured with a precision $P.E.n'_e \equiv \pm 1 \times 10^{-6}$.

(*b*) Tolerance contours for precision of prism translation.—If the prism surfaces depart from flatness by only 0.02λ for an area of 1 cm diameter ($r = \pm 1{,}145$ m) then these same curves show (as designated on their lower arms) the precision necessary in the installation of a prism on the spectrometer table when an index precise to $\pm 1 \times 10^{-6}$ (probable error) is to be measured.

in the upper portion of the diagram.[26] The particular value $P.E.e'_0 = \pm 0.1$ mm, used in these computations, was selected because it is a unit value corresponding closely to a precision reached experimentally with the use of simple auxiliary prism-tabling devices. Since the planeness of prism surfaces is conveniently tested by comparison with a standard flat surface, the tolerances have been expressed as departures, s', in wave lengths ($\lambda = 0.546\ \mu$) from flatness for a surface having a diameter, d', of 1 cm; that is, s' represents departures of the curved surfaces from a plane tangent to the central point of this

[26] By taking with respect to A the partial derivative of the tolerance in curvature (equation 23 expressed in terms of the variables A and n), the most favorable conditions is found to be

$$\tan\left(A+\frac{D}{2}\right) \tan^2 \frac{A+D}{2} = 2$$

and this is expressed in fig. 4 by an undesignated dashed line.

limited area. The general relation between the sagitta, s, the diameter, d, and radius of curvature, r, is $s=d^2/8r$, an expression which, in connection with equation (22), shows that the limiting permissible sagitta for any area of surface varies directly as d^2 and directly as $P.E.n_e$, the permissable probable error in index, but varies inversely as $P.E.e_0$.

Tolerances or precisions may thus be readily evaluated from figure 4 (a) for any given conditions according to the equation

$$\frac{P.E.n_e}{P.E.n'_e}=\frac{P.E.e_0}{P.E.e'_0}\cdot\frac{s}{s'}\cdot\frac{d'^2}{d^2}$$

where unprimed symbols refer to actual conditions for any given case and the primes denote the specific conditions for which figure 4 (a) is drawn.

For example, if a 60° prism of fluorite, index 1.434, with 2 cm surfaces, is being polished for an index determination to $\pm 1\times 10^{-6}$ (probable error), the surfaces are satisfactory if they show like departures from planeness not exceeding 0.7 λ, provided a precision of $P.E.e_0=\pm 0.1$ mm can be realized in translational adjustment of the prism. Or, if $P.E.e_0=\pm 0.2$ mm and a 50° prism of index $n=1.9$ has surfaces of 2.5 cm in length which have like curvatures corresponding to an over-all sagitta of 2 λ each ($|r|=74$ m), the index may nevertheless be measured correctly to $P.E.=\pm 1\times 10^{-5}$. In practice, however, serious difficulty may be encountered with the larger values of permissible curvature because in such cases two surfaces of the same prism frequently differ too much [27] in the degree of their curvature to permit a satisfactory compromise focusing of the telescope when measuring refracting angles.

(e) TOLERANCE IN ASYMMETRIC TABLING

From equation (22) the tolerance in imprecision of tabling is

$$T_{P.E.e_0}=\pm\frac{1.41\times 10^{-6}\sin^2\frac{A}{2}}{\frac{1}{r}\sin\frac{D}{2}\sqrt{1+\sec^2\frac{A+D}{2}}} \qquad (24)$$

if the probable error in index is to be $\pm 1\times 10^{-6}$ for a single determination of refractivity. Equation (24) has been used in computing reference curves which coincide with those shown in figure 4(a) but, in this case, they are redesignated in the lower portion of the diagram and considered as figure 4(b). The choosing of the curvature for these computations was somewhat arbitrary. The value of $|r|=1{,}145$ m which is used corresponds to a departure from flatness of 1/50 wave length ($\lambda=0.546\ \mu$) at the circumference of an area having a diameter of 1 cm (or 1/8 λ for an area 1 inch in diameter) and is a fairly high degree of planeness even for precise optical surfaces of small prisms. The curves of figure 4(b) thus show approximately the maximum freedom in probable error of translational prism adjustment which is consistent with probable errors of unity in the sixth decimal place of refractive index. Evidently precision of prism

[27] For a 400-mm collimator the permissible difference in radii may, however, be at least as large as 0.3r when $|r|=100$ m and as large as 1.0 r when (average) $|r|=500$ m. See footnote 17, p. 32

installation to fractions of a millimeter should invariably be obtainable, the necessary precision being higher for larger curvatures and relatively much higher for media of high index than for those of low index. Incidentally, it may also be mentioned that correct tabling to small fractions of a millimeter is desirable from a purely goniometrical viewpoint, as shown by equation (4), if accurate or even precise measurements are to be made on angles between (planes tangent to) curved surfaces.

Since the probable errors in index, according to equation (22), are directly proportional to those probable errors which may be made in tabling, it becomes evident from figure 4 that the customary total neglect of prism position may cause serious error even in the fifth decimal place of indices for prisms having only very slight surface curvature. It is principally because of this required high precision in tabling, and the consequent enforced symmetrical use of all optical surfaces, that it seems at all permissible, as suggested in section II, to neglect the consideration of tolerances for the accuracy of eyepiece focusing and for residual aberrations in fairly well corrected optical systems.

(f) REFOCUSING OF TELESCOPE REQUIRED BECAUSE OF PRISM-SURFACE CURVATURE

In connection with the discussion of collimation, to be considered in sections IV and V, it is of interest to determine the maximum refocusing of the telescope which is required on account of the use of prisms with curved surfaces. For minimum-deviation measurements equation (13) serves, and for the refocusing in angle measurement by autocollimation, ΔF_A, the similar equation is

$$\Delta F_A = \frac{f^2}{r-(f-z)} \tag{25}$$

where z is the distance from a prism surface to the telescope objective. The quantity $(f\text{-}z)$ is negligible in comparison with r and if the latter be taken as positive for convex reflecting surfaces the refocusing is positive for an increase in telescope tube length. From the formulas (13) and (25), it may be ascertained that with $f=400$ mm the range of curvatures shown in figure 4 (a) will necessitate telescope refocusings of from 0.3 to 1.7 mm when making refracting-angle measurements and from 2.5 to 6.5 mm for deviation observations on 60° prisms ranging from 1.3 to 1.9 in index. These refocusings are of the same order of magnitude as those which are found in section IV, 2 (b) as permissible changes in collimator tube length. It is not apparent, however, that these required changes in the telescope tube length can produce any further errors comparable with those which are discussed in this section as effects of the curvature of prism surfaces.

2. EFFECT OF ECCENTRIC PRISM-TABLE AXIS WHEN PRISM SURFACES ARE CURVED (COLLIMATED INCIDENT LIGHT)

In treating of the eccentricity of prism-table axis and of its relation to the measurement of prisms having curved surfaces, the special assumption (6′) of part 1 of this section is no longer valid because the table axis in this case is not coincident with that of the instrument but merely parallel thereto as covered by general assumption (2). Instead it will now be assumed (6″) that the table-axis eccentricity

is small and that the prism is correctly placed [28] with respect to the axis of the table.

(a) MAKING REFRACTING-ANGLE MEASUREMENTS

When "directly" measuring a refracting angle (by autocolimation) with a rotating telescope, eccentricity of table axis has no significance as distinguished from asymmetry of table position of the prism because no table rotation is involved. The corresponding error in index may, therefore, be determined at once by comparing with equation (6) and adopting a new reference system. If linear eccentricity of table axis is denoted by ϵ, and φ represents its azimuth with respect to the (fixed) collimator axis, the positive direction being that of the incident light, then the partial error in index, namely, that part due to erroneous refracting-angle measurement, is expressible as

$$\delta n_{\Delta A} = \frac{\epsilon \sin \frac{D}{2} \cos (\varphi - \sigma) \cos \frac{A}{2}}{r \sin^2 \frac{A}{2}} \tag{26}$$

where σ is the angle through which the prism is oriented from the customary symmetrical installation in which the bisector of A makes an angle of 180° with the collimator axis during refracting-angle measurements. Consequently it is possible without knowing ϵ or φ to eliminate eccentric table-axis error from the average of "direct" and "reverse" measurements on $(\pi - A)$ and $(\pi + A)$, respectively, by choosing for these two prism installations two values of σ which differ by π. Also, it should be noted that, in case φ is known but cannot be satisfactorily adjusted (see 2(*a*) of sec. IV), σ may often be chosen in such manner as to eliminate or effectually minimize table-axis error in "direct" goniometry of prisms having curved surfaces.

Obviously, if the collimator does not prevent the telescope from making a complete revolution, the three angles of a prism may be "directly" measured without table rotation and their sum obtained free from eccentric table-axis error just as for the analogous case of asymmetric tabling expressed by equation (7). When, however, the prism table is rotated between prism-angle measurements so that in each case the bisector of A and the collimator axis form an angle of 180°, then (see equation (4)) the sum of the three angles exceeds 180° by the amount

$$\Delta\Sigma = \left\{ \xi - \frac{412.5 \times 10^3 \epsilon \cos\varphi}{r} \left(\cos \frac{A_1}{2} + \cos \frac{A_2}{2} + \cos \frac{A_3}{2} \right) \right\} \text{sec.}, \tag{27}$$

where ξ is the excess in seconds due to the pyramidal error of the prism and the remaining term must also be considered when seeking to accurately check the performance of a goniometer by applying this test to "direct" measurements.

---

[28] That is, "centered" over the table axis during refracting-angle measurements (see sec. II, 2) and then displaced according to equation (8) for deviation measurements.

(b) MAKING MINIMUM-DEVIATION MEASUREMENTS

In order to derive an expression for the error in minimum-deviation measurement when the prism-table axis is eccentric, figure 5 has been drawn. The principal difference between this case and the one represented in figure 3 is that here O represents only the axis of the instrument and for both right- and left-hand deviations the eccentric axis of the prism table now coincides at $C=C'$ with the intersection of those rays which traverse the prism surface centers. As previously, the correct angular deviation is one half the angle between t_LC and t_RC, although the telescope swings through the angle $T_LO\ T_R$. Therefore

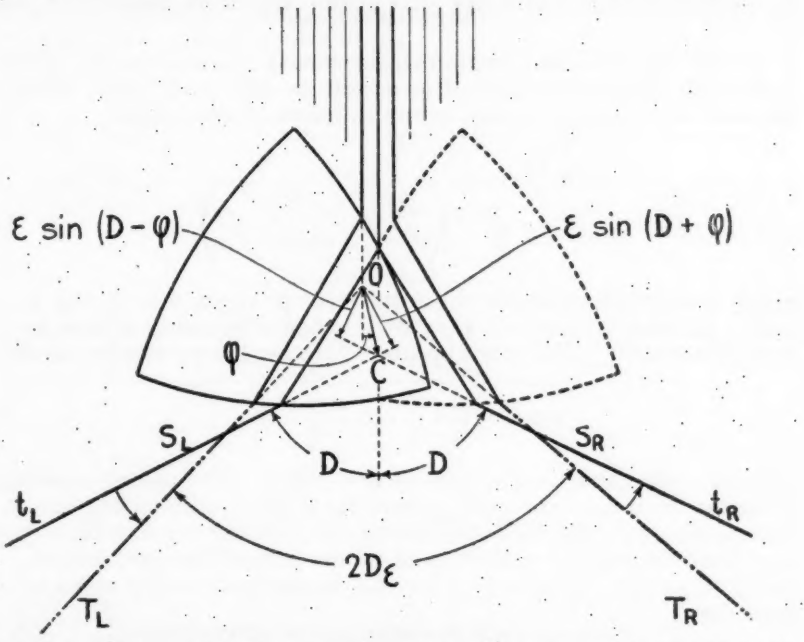

FIGURE 5.—*Minimum-deviation measurement of a prism symmetrically tabled with respect to an eccentric prism-table axis when the prism surfaces are curved*

The incident and emergent chief ray intersections, shown on figure 3 at C and C', are here coincident with the eccentric prism-table axis at C. The telescope pointings include the angle $2D_\epsilon$ instead of $2D$ which would be measured if the table axis and the spectrometer axis were coincident at O.

$$2\,\Delta D = -\angle t_L S_L T_L - \angle T_R S_R t_R \tag{28}$$

is the error in double deviation.

According to the convention adopted for expressing the azimuth of the eccentricity of the table axis, φ in figure 5 is a positive angle in the first quadrant, and it is evident that OC may be resolved into the components $\epsilon \sin (D+\varphi)$ and $\epsilon \sin (D-\varphi)$, perpendicular, respectively, to t_LC and t_RC, where D is considered as essentially positive. Consequently, using equations (11) and (28), it is found that

$$\Delta D = \frac{-2\,\epsilon \sin\frac{D}{2}\cos\varphi \sin D}{r \sin\frac{A}{2}\cos^2\frac{A+D}{2}} \tag{29}$$

and then from equation (16) one obtains

$$\delta n_{\Delta D}=\frac{-\epsilon \sin \frac{D}{2} \cos \varphi \sin D}{r \sin^2 \frac{A}{2} \cos \frac{A+D}{2}} \tag{30}$$

as the partial error in index resulting from that error in minimum-deviation measurement which arises because of curved prism surfaces and eccentricity of prism-table axis.

(c) COMBINED EFFECTS OF TABLE-AXIS ECCENTRICITY ON REFRACTIVE-INDEX DETERMINATIONS

Usually in refracting-angle measurements σ is zero and the value of $\epsilon \cos \varphi$ is, of course, identical in equations (26) and (30). Then by the addition of these partial errors in index, there results

$$\Delta n_{\epsilon}=\frac{\epsilon \sin \frac{D}{2} \cos \varphi}{r \sin^2 \frac{A}{2}}\left(\cos \frac{A}{2}-\frac{\sin D}{\cos \frac{A+D}{2}}\right) \tag{31}$$

which is an expression for the total error in index due to any eccentricity of table axis which may exist when measuring prisms having curved surfaces. This error becomes zero for the particular condition

$$\sin D=\cos \frac{A}{2} \cos \frac{A+D}{2} \tag{32}$$

and also whenever the value of $\varphi=\pm 90°$. The latter possibility indicates an important and general method of eliminating errors of this nature, provided that φ is known and that the prism table support may itself be rotated with respect to the base of the instrument. In part 2 of section IV a method for the determination of φ and ϵ will be mentioned.

(d) TOLERANCE IN TABLE-AXIS ECCENTRICITY

From equation (31) a tolerance in table-axis eccentricity is

$$T_{\epsilon}=\pm \frac{1\times 10^{-6} \sin^2 \frac{A}{2}}{\frac{1}{r} \sin \frac{D}{2} \cos \varphi} \cdot \frac{\cos \frac{A+D}{2}}{\cos \frac{A}{2} \cos \frac{A+D}{2}-\sin D} \tag{33}$$

for an error of $\pm 1\times 10^{-6}$ in index measurements on prisms having surface curvature $1/r$. Figure 6 gives an idea of the extent to which unfavorably oriented table-axis eccentricity ($\varphi=0$ or $180°$) may be tolerated, according to equation (33), when using prisms whose surfaces have precisely as much curvature as may for other reasons (see fig. 4 (*a*)) be permitted. In other words, that variable value of $1/r$ which is defined by equation (23) has been used in solving equation (33) for figure 6.

The degree of permissible table-axis eccentricity, for refractive-index determinations, thus proves to be satisfactorily large in general and especially so for 60° prisms in the range 1.4 to 1.6 of refractive index. This is mainly the result of compensating effects of errors in refracting-angle measurement and of those made in observations of minimum deviation. Such liberal tolerances in table-axis eccentricity are, however, by no means desirable for all other purposes. A well-built goniometer for precise work should not have table-axis eccentricity in excess of 0.1 or 0.2 mm because, for example, with $\epsilon = 0.2$ mm and $r = 572$ m ($s = 0.04\ \lambda$ for 1 cm), the error in the sum of the measured angles of a 60° prism, according to equation (27), may be as large as 0.4 seconds unless one uses averages of measurements made both on the angles and on their explements.

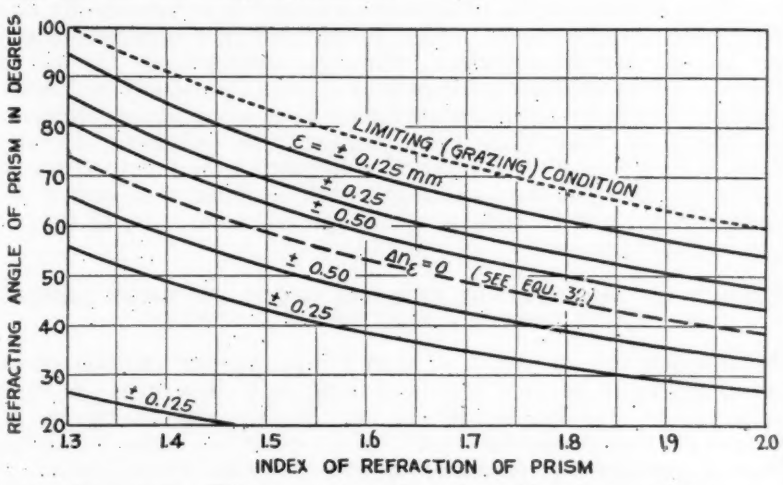

FIGURE 6.—*Tolerance contours for prism-table-axis eccentricity*

If prism surfaces have no equicurvature in excess of the values shown in figure 4 (*a*), then table-axis eccentricity is permissible to the extents shown here even when its azimuth is 0 or 180° with respect to the collimator axis. These tolerances apply only to complete refractive-index determinations. For accurate goniometry of prisms having only slight curvature of surfaces this eccentricity should not exceed 0.2 mm.

IV. RELATIONS BETWEEN INACCURATE COLLIMATION AND PRISM-POSITION ADJUSTMENT

Parallel light over a prism table is probably never realized not only on account of the difficulty in securing, except by chance, a perfect optimum adjustment of collimator tube length for the existing conditions of a particular moment but also because of aberration inherent in the lens system. This collimation adjustment of a spectrometer has been considered of such importance that ordinary care has been deemed inadequate, presumably on account of depth of focus, and special procedures have been recommended, such, for example, as Schuster's [29] method of alternately refocusing the telescope and the collimator on appropriately produced slit images, or the refocusing in pairs [30] of three telescopic systems of which one is the collimator in question.

[29] Schuster, Phil. Mag. (5), vol. 7, p. 95, 1879.
[30] See p. 765 of volume cited in footnote 5, p. 29.

Possibly current ideas on the necessity of equal refocusing of both collimator and telescope are traceable to Cornu [31] and Carvallo,[32] who showed that, when measuring angles by the split-beam method, the corrections for curvature of prism surfaces were eliminated by refocusing both tubes to equal extents. Considerable attention may also have been directed to precise collimation because imperfections of this nature were considered by Macé de Lépinay and Buisson as having caused the discrepancies between certain spectrometrically and interferometrically determined indices.[33]

It seems quite necessary then to investigate the effects of erroneous collimation of the incident light. Only minimum-deviation measurements, however, need consideration because the autocollimating method of refracting-angle measurement (which, as indicated in sec. II, is preferable for work of highest accuracy) is automatically eliminated from the discussion. As a simplification, the general assumtions of the previous section, namely, assumptions (1) to (5), inclusive, will be used here, except that (3) must obviously be modified to include merely an approximate rather than an accurate collimation adjustment, so that there exists an error in collimator focusing, $\Delta F_c = f_c - F_c$, where F_c is the actual collimator tube length (from slit to objective) and f_c is the focal length of the collimator objective; also assumption (5) will be reduced to the special case $r = \infty$, or that the prism surfaces are plane.

1. EFFECT OF ASYMMETRIC TABLING WHEN INCIDENT LIGHT IS UNCOLLIMATED (FLAT PRISM SURFACES)

Assumption (6′) of part 1, section IV, concerning the coincidence of axes, will again be used here, and in figure 7 these axes are represented at O. The intersection of the incident and emergent chief rays is at C for deviation left and at C' for deviation right. A distant source, S, replaces the collimator; S_1 and S_2 are the virtual sources for pointings when a prism is properly centered at O, and the correct double deviation is $2D = \angle T_1 O T_2$. Points at S_L and S_R represent the virtual sources when the tabling is asymmetric. The paths in air of the rays for left and right deviations then lie on lines from S to C to t_L and S to C' to t_R, respectively, and the measured double deviation is $2D_e = \angle T_L O T_R$. The additional angle designations

$$\left.\begin{aligned} \alpha_1 &= \angle O\ S\ C' \\ \beta_1 &= \angle C\ S\ O \\ \alpha_2 &= \angle T_R S_R t_R \\ \beta_2 &= \angle t_L S_L T_L \end{aligned}\right\} \tag{34}$$

and

$$\left.\begin{aligned} 2d &= \angle t_L S_L \text{ to } t_R S_R \end{aligned}\right\}$$

will be employed for convenience. Then, from figure 7

$$2d = 2D_e + \alpha_2 + \beta_2 \tag{35}$$

[31] See p. 87 of paper cited in footnote 9, p. 30.
[32] See pp. 85–88 of paper cited in footnote 10, p. 30.
[33] For brief remarks and references see p. 915 of first paper cited in footnote 1, p. 26.

and, since $\alpha_1+\beta_1$ is the effective change of orientation in the incident light between left and right pointings,

$$2d=2D+\alpha_1+\beta_1 \tag{36}$$

whence

$$\Delta D=\frac{\alpha_1-\alpha_2+\beta_1-\beta_2}{2} \tag{37}$$

may be written to express the error in measured deviation.

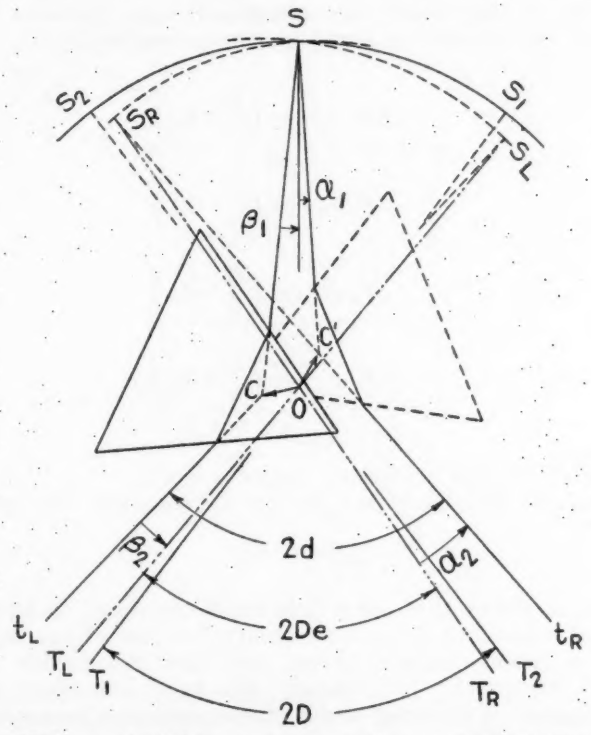

FIGURE 7.—*Minimum-deviation measurement of an asymmetrically-tabled prism when using uncollimated incident light*

Although the telescope pointings are along T_LO and T_RO toward the virtual sources S_L and S_R, investigation shows that the (double) minimum deviation thereby measured is equal to that for a symmetrically tabled prism (not shown) for which C and C' would coincide at O, the axis of the spectrometer, and for which the virtual sources are represented at S^1 and S^2.

If the azimuth, ϑ_D, of the asymmetry $OC=OC'$ (of length e_D), is again referred to the bisector of the prism, as in figure 3, part 1 (b) of section III, then the lengths of the components perpendicular [34] to the emergent rays are again $e_D \cos (D/2+\vartheta_D)$ and $e_D \cos (D/2-\vartheta_D)$, respectively, for the left- and right-hand deviations. Similarly for the incident rays the values are the same but their order is reversed.

[34] Since the angles α and β are of the order of a few seconds in magnitude, all of the various incident and emergent rays may for this purpose be considered as parallel.

The prism is approximately equidistant ($OS=OS_1=CS_L$, etc.) from the source S and all of the virtual sources, the object distance of the source from the prism being

$$-u_p=-v_c-x=\frac{f^2_c-f_c\Delta F_c}{\Delta F_c}-x \tag{38}$$

where v_c represents the distance from the collimator objective to the image of the source, and x is the distance from the collimator objective to the prism table axis. The term x can be ignored for the small values of ΔF_c which are considered, and likewise the term $-f_c\,\Delta F_c$ may be omitted as small in comparison with f^2_c. Then the equations

$$\left.\begin{aligned}\alpha_1&=\frac{\Delta F_c\, e_D\cos\left(\frac{D}{2}+\vartheta_D\right)}{f^2_c}\\ \alpha_2&=\frac{\Delta F_c\, e_D\cos\left(\frac{D}{2}-\vartheta_D\right)}{f^2_c}\\ \beta_1&=-\frac{\Delta F_c\, e_D\cos\left(\frac{D}{2}-\vartheta_D\right)}{f^2_c}\\ \text{and}\quad \beta_2&=\frac{\Delta F_c\, e_D\cos\left(\frac{D}{2}+\vartheta_D\right)}{f^2_c}\end{aligned}\right| \tag{39}$$

specify the values of the various angles α and β.

These values (39) when substituted in equation (37) reduce the latter to

$$\Delta D=0 \tag{40}$$

a result which shows that, to a first approximation, no care in collimation of the incident light is necessary because of the asymmetric tabling of a (plane-surface) prism, provided the double minimum deviation is measured. Incidentally, this is an important reason for the measurement of $2D$ even under circumstances where it is possible to make precise settings on the direct undeviated slit image.

2. EFFECT OF ECCENTRIC TABLE AXIS WHEN INCIDENT LIGHT IS UNCOLLIMATED (FLAT PRISM SURFACES)

As in part 2, section III, the special assumption (6′) relating to coincident axes must again be supplanted by (6″) which specifies correct tabling with respect to the axis of the table. Figure 8 and the notation illustrative of this case are already familiar from the preceding discussions and full details are unnecessary. The correct double deviation, $2D$, is $\angle T_1OT_2$ and also, since no change in orientation of incident light occurs between pointings, $2D=\angle t_LCt_R$. The measured double deviation, $2D_\epsilon$, is $\angle T_LOT_R$, and the angles $t_RS_RT_R$ and $T_LS_Lt_L$ will be designated as γ and δ, respectively. Then from figure 8

$$2D_\epsilon=2D+\gamma+\delta \tag{41}$$

and hence

$$\Delta D = \frac{\gamma + \delta}{2} \tag{42}$$

is the error in minimum-deviation measurement.

The orientation, φ, of the table-axis eccentricity, OC is of course constant for both left and right deviations, and the lengths of the

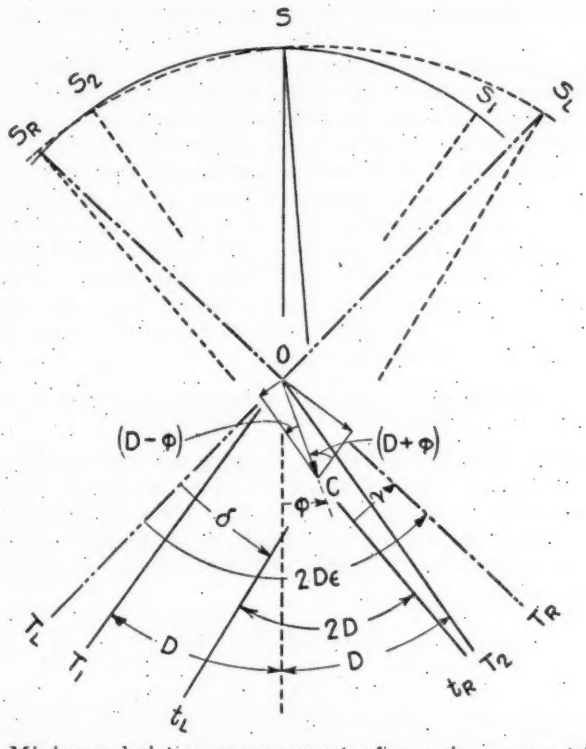

FIGURE 8.—*Minimum-deviation measurement of a prism symmetrically tabled with respect to an eccentric prism-table axis when using uncollimated incident light.*

As in figure 5 the chief ray intersections are again coincident with the eccentric prism-table axis at C, the prism outlines being omitted. In practice the eccentricity, $\epsilon = OC$, is small in proportion to the dimensions of the prism; the distance to the source, S, is very large; the virtual sources are sensibly coincident with their positions for an eccentricity of zero; and the angles γ and δ do not exceed a few seconds in magnitude. The resulting error in the measured deviation becomes zero when ϵ has an aximuth, φ, of $\pm 90°$.

components of OC perpendicular to the emergent rays, left and right, respectively, are $\epsilon \sin (D+\varphi)$ and $\epsilon \sin (D-\varphi)$. With these lengths and equation (38) the error in deviation as given in equation (42) becomes

$$\Delta D = \frac{\Delta F_c \, \epsilon \sin D \cos \varphi}{f_c^2} \tag{43}$$

where, as previously in this section, ΔF_c is positive for a decrease in collimator tube length.

(a) EXPERIMENTAL DETERMINATION AND AZIMUTHAL ADJUSTMENT OF ECCENTRICITY OF TABLE AXIS

If, for a known comparatively large value of ΔF_c, ΔD is experimentally determined for a few orientations of the prism table support, using a prism with plane surface, equation (43) may then be used to determine φ and ϵ. Obviously the instrument should finally be adjusted so that $\varphi = \pm 90°$. If this adjustment can be made it seems that table-axis eccentricity can produce no first order errors in refractive-index measurements even when collimation is somewhat inaccurate.

By using equation (43) in this way, the writer computed a value of $\epsilon = 0.16$ mm for a spectrometer which he was using and then the prism-table support was oriented so that φ (as simultaneously computed) became approximately $+90°$. Later, a small pin was mounted on the prism table and a wire was mounted on the telescope in such manner that its bent and sharpened point hung just above the pin point. Then, while observing with a suitably mounted microscope of low power, the pin and wire points were adjusted so that no translation occurred as prism table and telescope were rotated through 180°. In fair agreement with the computations, the approximate values $\epsilon = 0.2$ mm and $\varphi = +100°$ were then directly determined from the relative positions of the points.

(b) TOLERANCE IN COLLIMATION ADJUSTMENT CORRESPONDING TO A TABLE-AXIS ECCENTRICITY OF 0.2 MM

Nevertheless, since these values, φ and ϵ, are usually unknown, it is useful to determine the accuracy in collimation of incident light which is necessary in order to insure that index errors are negligible even when a fairly high value of ϵ exists at an azimuth $\varphi = 0$ or 180°. Consequently equations (16) and (43) have been used in expressing this error in index

$$\Delta n_{\Delta F_c} = \frac{\Delta F_c \, \epsilon \sin D \cos \frac{A+D}{2} \cos \varphi}{2 f^2_c \sin \frac{A}{2}} \tag{44}$$

and therefore

$$T_{\Delta F_c} = \pm \frac{2 \times 10^{-6} f^2_c \sin \frac{A}{2}}{\epsilon \cos \varphi \sin D \cos \frac{A+D}{2}} \tag{45}$$

is the corresponding tolerance in collimation adjustment. Figure 9 (*a*) gives values [35] of $T_{\Delta F_c}/f^2_c$ for $\cos \varphi = \pm 1$, and $\epsilon = 0.2$ mm (the latter being the maximum value suggested in sec. III, pt. 2 (*d*), as generally permissible). For a collimator with any particular f_c (measured in millimeters), the permissible error in tube length is readily found by applying the factor f^2_c to the values given just

[35] By taking with respect to n the partial derivative of the tolerance in inaccuracy of collimation (equation (45), expressed in terms of the variables A and n) the most favorable condition is found to be

$$2 \cot D = \tan \frac{A+D}{2}$$

and this is expressed in fig. 9 by an undesignated dashed line.

above these curves. For the special case, $f_c = 400$ mm, the curves as drawn in figure 9 (*a*) become contours of $\pm \Delta F_{400} = 1.0$, 1.4, 1.9, 2.4, and 2.9 mm.

From these results it is evident that the values of table-axis eccentricity which are otherwise allowable or likely to occur on an accurate goniometer, do not necessarily impose severe tolerances in collimation adjustment when measuring refractive indices even if φ is unknown and may, therefore, have one of the unfavorable values, 0 or π. It should be remembered, however, that this tolerance varies directly as the square of the collimator focal length. This suggests a possible reason for not limiting the focal lengths of precision spectrometer collimators to the comparatively small dimensions which would be quite adequate [36] in the matter of requisite metrological accuracy.

In order to use a constant collimator tube length for all wave lengths of the visible spectrum, the collimator should be focused at

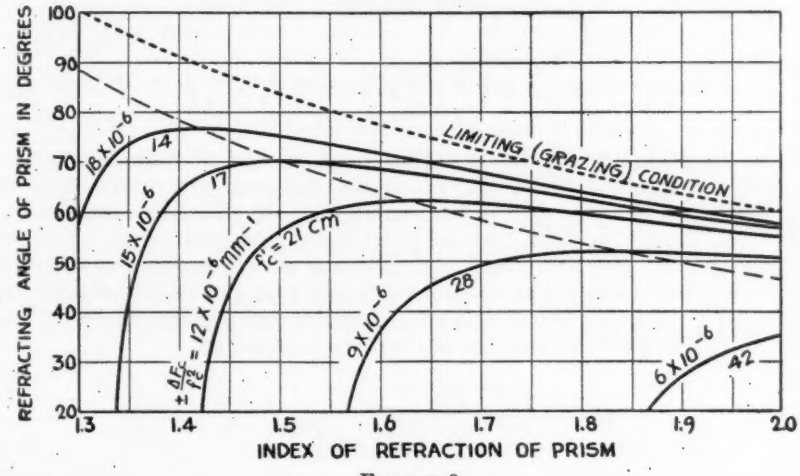

FIGURE 9

(*a*) Tolerance contours for adjustment of collimator tube length.—If unfavorably oriented table-axis eccentricity does not exceed 0.2 mm, then any collimator may be inaccurately focused to the extent shown by these contours (read designations just above the curves and multiply by (f^2_c).

(*b*) Contours for minimum f_c consistent with no chromatic refocusing of an achromatic collimator.—In the visible region a constant collimator tube length is usable if its focal length is at least as large as the values shown just below these same curves.

the middle of the linear range of required tube lengths. An adequate value of f_c for this purpose is given by the equation $f'_c \geqq 0.0025 (\Delta F_c/f^2_c)$, where the values of $(\Delta F_c/f^2_c)$ are those computed by equation (45) or read from the curves of figure 9 (*a*) and 0.0025 is taken as one half the total range of longitudinal chromatic aberration for an achromatic objective of unit focal length. Accordingly the curves of figure 9 also serve (*b*) as contours of adequate collimator focal length (read designations just below curves).

V. RELATION OF PRISM ABERRATION TO COLLIMATION AND TO CURVATURE OF SURFACES

A matter to be investigated before a final decision regarding the requisite precision in adjusting collimator tube length and the limit-

[36] See p. 76 of second paper cited in footnote 1, p. 26.

ing permissible values of prism-surface curvature, is that of the aberration introduced by the prism. Does the whole beam or pencil remain sensibly symmetrical about the chief ray after refraction by the prism, or is sufficient asymmetrical aberration introduced to vitiate the accuracy of deviation measurements? Wadsworth [37] examined the special case of a prism with plane surfaces and, corresponding to $\lambda/16$ as the limiting permissible relative retardation, he found a very liberal tolerance in the requirements for collimator focusing. It is however not at once apparent that the effects of prism surface curvature can be ignored, and a more general case will now be considered.

For a homogeneous prism of negligible thickness, oriented for minimum deviation, Rayleigh [38] gives, for rays in the primary plane, an equivalent of the equation

$$\frac{c^2}{v}=\frac{c^2}{u}+(nc'-c)\left(\frac{1}{r_1}-\frac{1}{r_2}\right)+\frac{3y'\sin\frac{A+D}{2}\,(n'-1)}{2}\left\{2(n'+1)\left(\frac{c'}{u'}\right)^2-(2n'+1)\left(\frac{1}{r_1}+\frac{1}{r_2}\right)\frac{c'}{u'}+n'\left(\frac{1}{r_1^2}+\frac{1}{r_2^2}\right)\right\} \tag{46}$$

where, in addition to the notation used in the similar first-order-imagery equation (10), u' is the image distance after refraction at the first surface, $y'\equiv L/2$ is the semiwidth of effective aperture as measured along the first face of the prism, and $n'\equiv nc'/c$. If there is imposed the condition $r_2=-r_1$ (the one which in practice must be approximately satisfied if prisms with but two polished surfaces are to be used for index measurement) then by comparison of equations (10) and (46) the longitudinal aberration reduces to

$$\Delta v=-\frac{3yv^2\sin\left(\frac{A+D}{2}\right)}{c^3}\left\{(n'^2-1)\left(\frac{c'}{u'}\right)^2+\frac{n'(n'-1)}{r^2}\right\} \tag{47}$$

where $y=y'c$ is the semiwidth of the (cross-sectional) aperture of the incident pencil at the first face of the prism.

By neglecting the aberration itself in the equation which expresses the refraction at the first face of the prism and by replacing u with one term of equation (38), u' is expressible approximately as

$$u'=-\frac{f_c^2\,rn'c'}{cr\Delta F_c-f_c^2(n'-1)} \tag{48}$$

and instead of equation (47) one may then write

$$\Delta v=-\frac{3ynv^2\sin\frac{A}{2}}{c^3}\left\{\frac{(n'^2-1)[rc\Delta F_c-f_c^2(n'-1)]^2}{f_c^4\,r^2n'^2}+\frac{n'(n'-1)}{r^2}\right\} \tag{49}$$

to express the longitudinal aberration.

---

[37] F. L. O. Wadsworth, Astrophys. J., vol. 17, pp. 9–11; 1903.

[38] Lord Rayleigh, Phil. Mag. (5), vol. 9, pp. 46–47, 1880. A change in signs has been made to conform to the convention that distances measured from the vertices of refracting surfaces are positive in the direction of travel of the light.

To find the corresponding restrictions imposed upon refocusings of the collimator it is convenient to use the equation of transformation from longitudinal aberration to phase difference in the form

$$\eta = \frac{1}{\lambda v^2}\int_0^y \Delta v\, y\, dy \qquad (50)$$

similar to that given by Martin,[39] where η is the phase difference in periods or cycles. After substituting equation (49) in (50) and adopting the Wadsworth value of $|\eta| = 1/16$ period as the permissible limit of phase difference the corresponding particular limits in refocusing of the collimator are readily established as

$$\Delta F_c = \pm \frac{nc'f^2_c}{c}\sqrt{\frac{\lambda}{2L^3n(n^2-1)\sin(A/2)} - \frac{nc'}{r^2c^2(nc'+c)}} + \frac{f^2_c(nc'-c)}{rc^2} \qquad (51)$$

where $2y$ has been replaced by Lc, the projection of $2y$ along the prism face, and where, for sixth decimal place refractometry, L need not exceed $\operatorname{cosec}\frac{A}{2}$ centimeters.[40] The successful use of such small prisms depends on realizing something closely approximating optimum metrological power and thus, to the extent[41] that $\lambda/16$ approximates the corresponding limit in relative retardation, equation (51) establishes, at least from the standpoint of prism aberration, a safe limit for inaccuracy of collimation when seeking a precision of $\pm 1 \times 10^{-6}$ in a measurement of refractive index.

For a prism with plane surfaces, $r = \infty$, equation (51) reduces to

$$\Delta F_c = \pm \frac{nc'f^2_c}{Lc}\sqrt{\frac{\lambda}{2Ln(n^2-1)\sin A/2}} \qquad (52)$$

in exact agreement with the above-mentioned result by Wadsworth. Furthermore, by making $\Delta F_c = 0$ in (51), to correspond to the special case of curved surfaces and collimated light, one may solve for $1/r$ and obtain

$$1/r = \pm \frac{ncc'}{L}\sqrt{\frac{\lambda}{2Ln(n^2-1)\sin(A/2)}\cdot\frac{(nc'+c)}{(nc'-c)^2(nc'+c)+n^3c'^3}} \qquad (53)$$

which are the particular limits in prism surface curvature within which the relative retardation for collimated light does not exceed $\lambda/16$.

[39] L. C. Martin, Trans. Optical Soc., London, vol. 23, p. 66, 1921-22.

[40] See p. 76 of second paper cited in footnote 1, p. 26.

[41] For telescopic instruments Wadsworth concluded (Astrophys. J., vol. 16, pp. 270, 279, 1902) that 1/15 was a fair value for the ratio of the limit of metrological precision to that of resolution and then he used this ratio in making his estimate of $\lambda/16$ as the permissible limit of relative retardation consistent with optimum accuracy of measurement. It should now be mentioned that, optically, the writer (see p. 64 of second paper cited in footnote 1, p. 26.) has found it easy to obtain values as small as 1/25 or 1/30 for the above-mentioned ratio between metrological and resolution limits and that the corresponding limit of relative retardation is only about $\lambda/32$. The necessity for such freedom from aberration may be questioned because of mechanical and, perhaps, other considerations, but nevertheless it is interesting to note that the use of this very high standard would simply replace 2 by 4 in the denominator of the first term under the radical in equation (51). The term over r^2 is negligible and, accordingly, this change would decrease the values of ΔF_c, as listed in table 1, by approximately 30 percent but would not affect the conclusions which are drawn therefrom.

Numerical data on the prism-aberration tolerance in collimation, equation (51), are given in table 1. The values of $T_{\Delta F_c}/f^2_c$, as adopted for the curves of figure 9(a), have again been computed and one wave length, $\lambda = 5{,}461$ Å, is adequate in showing the order of magnitude of this tolerance. For r the positive values according to equation (23) have been read from figure 4 (a). The results given in table 1 do not differ by as much as 5 percent from similar results computed for plane-surface prisms from equation (52). It is evident that this prism-aberration tolerance in collimation is very large in comparison with that which has been considered in figure 9 (a) as a result of possible table-axis eccentricity. Moreover, equation (53) shows that prism aberration is not a factor which compels reconsideration of those tolerances in prism-surface curvature which are based on an easily attainable degree of precision in the tabling of prisms and according to equation (23) are expressed in figure 4 (a).

TABLE 1.—*Prism-aberration limits for inaccuracy of collimation*

[Values of $\frac{\Delta F_c}{f_c^2} \times 10^5$ computed from equation (51)]

	$n=1.3$	$n=1.5$	$n=1.7$	$n=1.9$
$A=80°$	+66	+110		
	−63	−104		
$A=60°$	+42	+38	+42	+64
	−40	−37	−40	−60
$A=40°$	+27	+22	+20	+20
	−26	−21	−19	−19

NOTE.—By comparing the values of this table with the contours of figure 9 (a) it is found that these permissible inaccuracies of collimation exceed by at least one order of magnitude those tolerances which are based on table-axis eccentricity.

VI. SUMMARY AND DISCUSSION

The necessity of flat prism surfaces has been greatly emphasized in prism refractometry, and accurate collimation has been generally considered of major importance. Perhaps this is mainly because the split-beam method of angle measurement, which was formerly in use by many of the most careful observers, involves the inherent weaknesses of asymmetry which make it impracticable for accurate work even with the best surfaces which can be realized and with optimum adjustment of the collimator. Under such circumstances it is not surprising that undue stress has been placed on the importance of accurate collimation and that it has been considered impossible to make accurate refractive index measurements on prisms having curved surfaces.

Starting with the imperative necessity of using all lens and prism apertures symmetrically, even under the most favorable conditions, it is then found that a strict observance of this principle permits useful tolerances in curvature of prism surfaces and in collimation adjustment. The most exacting requirement in the case of prism surfaces is that the curvatures on a given prism must be equal to the extent that a satisfactory compromise focus of the autocollimating telescope can be realized for making refracting-angle measurements between planes tangent to the effective prism-surface centers. The magnitude of curvature which can be permitted is limited by the precision with

which prisms can be translated on the table of the spectrometer. When many prisms are required for refractive-index measurements a specification for approximately equi-curvature of not exceeding, say, $\lambda/3$ for 1 cm diameter of surface greatly facilitates their preparation as compared with a specification for say $\lambda/20$.

Accurate collimation is not required because of asymmetric tabling, provided the "double deviation" is observed, and there are no important limitations on collimator refocusing because of the aberration of prisms having surfaces with curvatures which are otherwise permissible. Tolerances in collimation may, however, be limited by eccentricity of the prism-table axis. Nevertheless, if the latter does not exceed 0.2 mm (or if its azimuth can be favorably oriented) then all wave lengths of the visible spectrum may be used for index measurements on 60° prisms with a constant collimator tube length (not less than 22 cm), and all of the refocusings be easily and quickly made with the telescope. In making large numbers of high-precision index measurements, this new observational procedure which eliminates the customary and troublesome collimation adjustments is a time-saving feature of self-evident value.

For such procedure the collimator should be initially adjusted to a mean between the extremes of the various focal lengths corresponding to the different wave lengths which are to be used. Obviously, the necessary range of refocusing of the telescope is twice the longitudinal chromatic aberration of either of the (identical) objectives for the spectral region which is concerned but the resulting linear error in focusing the collimator for parallel light never exceeds one half this color focal difference. For objectives of the usual two-color-correction type, the total range of longitudinal chromatic aberration for wave lengths of the visible spectrum is of the order of $0.005\,f$ or less. Figure 9 (*a*) shows that, with $f=400$ mm and $A=30°$ or more, the tolerance in collimator refocusing is at least as great as ± 1 or 2 mm, provided ϵ does not exceed 0.2 mm, and these ranges are one or two times as large as the requisite one half of the chromatic variation in focal length. Usually there is ample provision for larger changes in F_c or for larger values of ϵ, and thus even from this consideration of convenience a collimator longer than 40 cm seems unnecessary for minimum-deviation measurements unless it is desired to limit individual errors to something less than approximately $\pm 1\times 10^{-6}$ in the computed index of refraction.

WASHINGTON, March 29, 1933.

U.S. Department of Commerce—Bureau of Standards

RESEARCH PAPER RP576

Part of Bureau of Standards Journal of Research, Vol. 11, July 1933

A 200-KILOCYCLE PIEZO OSCILLATOR

By E. G. Lapham

ABSTRACT

This paper describes a piezo oscillator which is used to control the frequency of the standard-frequency transmissions of the Bureau. The unit incorporates in its design a double temperature control of the quartz plate, temperature control of the oscillator and amplifier, and a clamped type of quartz-plate mounting.

CONTENTS

		Page
I.	Introduction	59
II.	Initial tests	59
III.	General arrangement	60
IV.	Quartz plate and holder	61
V.	Circuit arrangement	61
VI.	Temperature control	62
VII.	Results	64
VIII.	Acknowledgment	64

I. INTRODUCTION

This paper describes a piezo oscillator specially designed for constancy over periods of a few hours. It is used in controlling the frequency of the radio transmitter used in the Bureau's weekly standard-frequency transmissions. The transmissions are for 2 hours at a time, on a frequency of 5,000 kilocycles per second, and it is required that the accuracy be maintained at all times better than 1 cycle per second (1 part in 5,000,000). This imposes rigorous requirements upon the piezo oscillator used to control the frequency of the radio transmitter.

II. INITIAL TESTS

The piezo oscillators which were available at the beginning of the 5,000-kilocycle transmissions were used for several months. The frequency of the radio transmitter was constant to approximately 1 part in 1,000,000. Careful checking between the frequency monitor and the transmitter revealed three main sources of variation. The first was a transient effect which was caused by the reaction of the radio transmitter on the piezo oscillator. The magnitude of this variation was indeterminate because of its short duration. The second source of variation was the operation of the heater relays. This caused an abrupt frequency change of the order of 5 to 8 parts in 10^8. The third variation was a slow drift in the temperature of the quartz plate due to changes in room temperature, which caused the frequency to change at the rate of approximately 1 part in 10^6 per hour. This rate of variation would not continue indefinitely but it might continue for several hours.

The reaction of the radio transmitter on the piezo oscillator was noticeable immediately after keying the transmitter. While the transmitter was being keyed the plate current in the oscillator circuit of the piezo oscillator would vary in synchronism with the keying. At the termination of the keying a short time would elapse before the frequency of the standard reached its previous steady condition. The most evident solution was to improve the shielding around the standard and to further decrease the coupling between the amplifier and the oscillator.

The operation of the heater relays in the temperature control of the piezo oscillator was also found to produce an abrupt change in frequency in certain of the standards tested. The change in frequency was too abrupt to be due to any cyclic variation in temperature which might occur as the heat was applied. It was found to be due to a change in the capacity of the plate holder with respect to ground. This variation was found to be eliminated by proper grounding of the metal boxes surrounding the heaters and careful shielding of leads which passed through the heater compartment. These precautions were also effective in reducing the a.c. modulation which is often induced by the heaters when operated on alternating current.

The frequency variation which was most important was that due to a drift in the temperature of the quartz plate. The radio transmitter was at the time located in a temporary building. The room temperature varied between 15° and 35° C. The quartz plates which are used in the secondary standards have a temperature coefficient of frequency of approximately -20 parts in 10^6 per ° C. A change in the temperature of the quartz plate of 0.01° C. produces a change in frequency of 1 cycle in 5,000 kilocycles, which is the maximum tolerance. The single temperature controls with which the available secondary standards were equipped were not sufficiently constant when subjected to such wide variations in room temperature. There were three possible courses, any or all of which could be used to maintain a more constant frequency—(1) provide a quartz plate with a lower temperature coefficient of frequency, (2) provide additional temperature control for the piezo oscillator, and (3) provide a variable condenser to compensate for unavoidable temperature changes. The two latter courses were adopted in the design of a new piezo oscillator. A second temperature-controlled compartment surrounding the quartz plate and oscillator and amplifier circuit arrangements decreased the temperature variations so that only a very narrow range of frequency adjustment was required by (3)

III. GENERAL ARRANGEMENT OF PIEZO OSCILLATOR

The general arrangement of the piezo oscillator is shown in figures 1 and 2. Figure 1 is an exterior view. The filament and plate voltmeters and the oscillator plate-current meter are at the right. The two heater indicator lamps are located on the left-hand side of the panel. In the lower center the end of a slotted shaft is visible which is for small frequency adjustments. Guards for the two thermometers are on the top. The filament and plate batteries are mounted in a metal box, and connecting leads pass through a flexible metal sheath. The B batteries were later replaced by a rectifier.

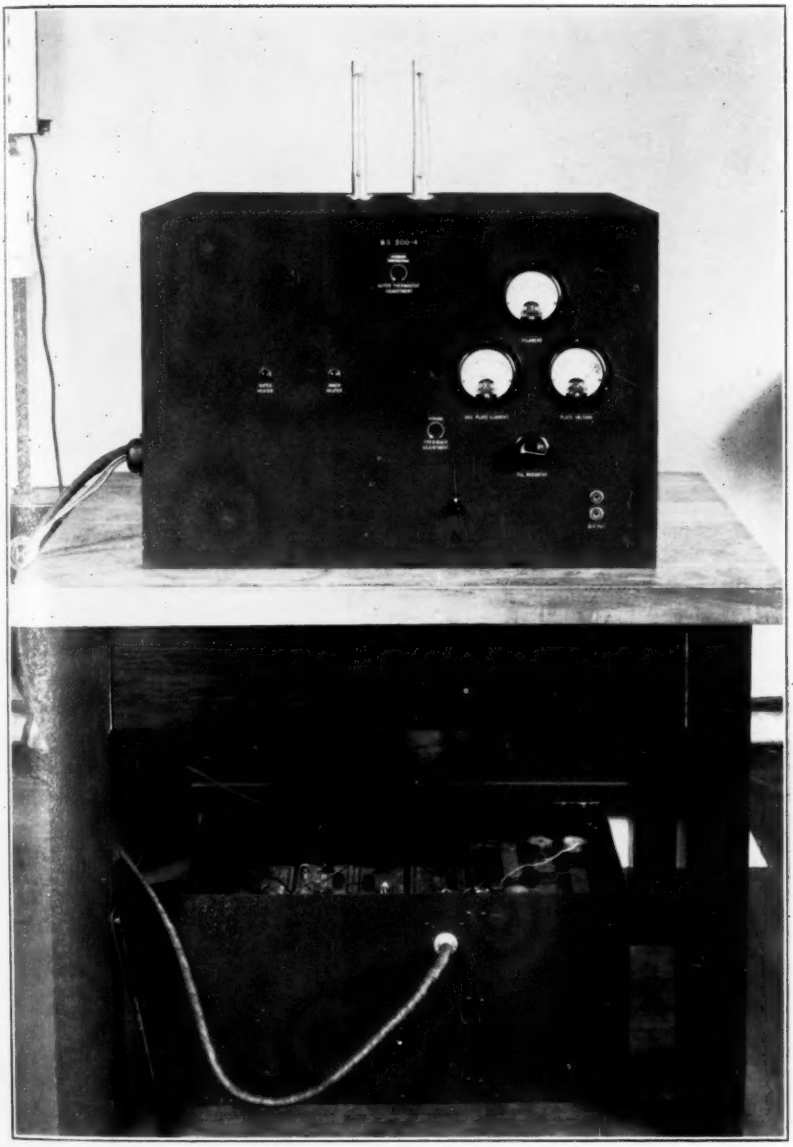

FIGURE 1.—*Front view of piezo oscillator and shielded battery compartment.*

UNIV OF MICH.

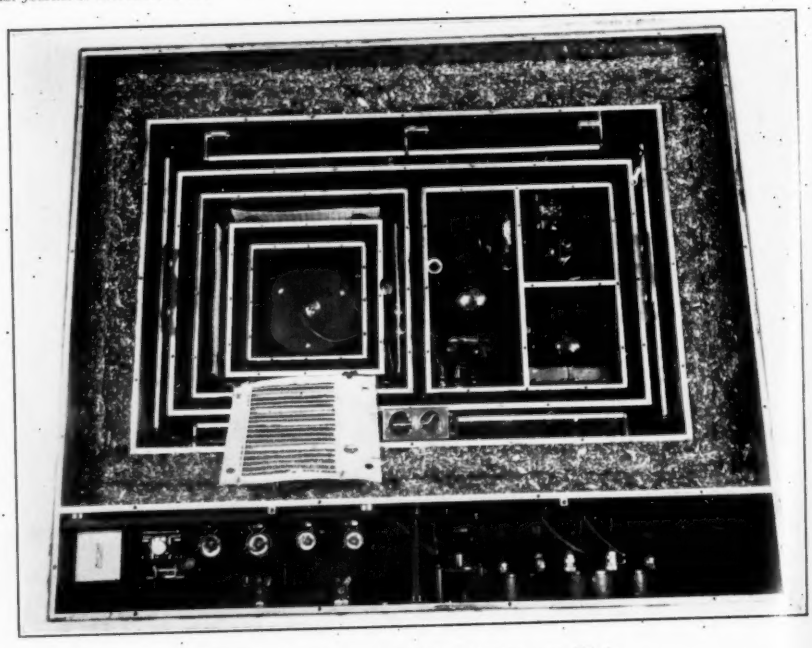

FIGURE 2.—*Interior view of piezo oscillator.*

The plate voltage on the oscillator tube was maintained at 90 volts by means of a UX874 voltage regulator tube. Figure 2 is an interior view. A 4-inch space between the front panel and the temperature-controlled compartment is provided in which the heater control equipment, terminal strip, and meters are located. The temperature control is divided into two parts. The oscillator and amplifier circuit arrangements are in the section at the right and the quartz plate is in the section at the left. The bimetallic thermostat in this view was later replaced by a mercury thermostat. The bimetallic thermostat was not sufficiently sensitive to be satisfactory for the outer temperature control.

IV. QUARTZ PLATE AND HOLDER

The piezo-electric element is a Curie-cut or zero-cut quartz plate. It is circular in shape and the dimensions are such that the fundamental frequency is 200 kilocycles per second at approximately 45° C. The quartz plate is held in position between the electrodes[1] by means of three screws which bear at the bottom of a V-shaped

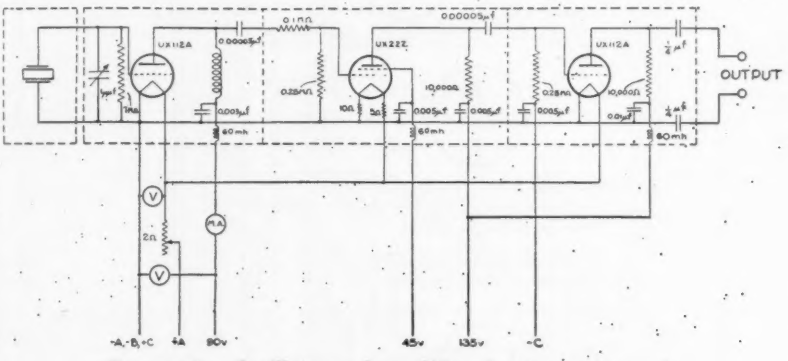

FIGURE 3.—*Oscillator and amplifier circuit arrangement.*

groove on the cylindrical surface of the plate midway between the plane faces.

V. CIRCUIT ARRANGEMENT

The circuit arrangement (fig. 3) is essentially the same as that used in previous secondary standards.[2] The quartz plate is connected between grid and filament of a UX112A tube and an untuned inductance is used as the plate impedance. The coupling to the first amplifier, a UX222 tube, is reduced considerably by the voltage divider arrangement indicated in the figure. This coupling amplifier is followed by another stage using a UX112A tube and straight capacity-resistance coupling. The manual frequency control consists of a 2-plate variable condenser connected in parallel with the quartz plate. The maximum capacity of this condenser is approximately 2 $\mu\mu$f. A very gradual adjustment of the frequency is provided by means of a 60 to 1 reduction through a friction drive and a set of gears.

---

[1] V. E. Heaton and E. G. Lapham, Quartz Plate Mountings and Temperature Control for Piezo Oscillators, Proc. I.R.E., vol. 20, p. 261, February 1932. B.S. Jour. Research, vol. 7 (RP366) October 1931.

[2] V. E. Heaton and W. H. Brattain, Design of a Portable Temperature-controlled Piezo Oscillator, Proc. I.R.E., vol. 18, p. 345, July 1930. B. S. Jour. Research, vol. 4 (RP153), March 1930.

VI. TEMPERATURE CONTROL

Figure 4 is a schematic diagram of the temperature control. It consists of two thermostatically-controlled compartments, one within the other. The outer compartment is operated at a temperature about 1.5° lower than the inner one. The quartz plate is located within the inner compartment so that it has a double temperature control. The oscillator and amplifier circuit arrangements are placed

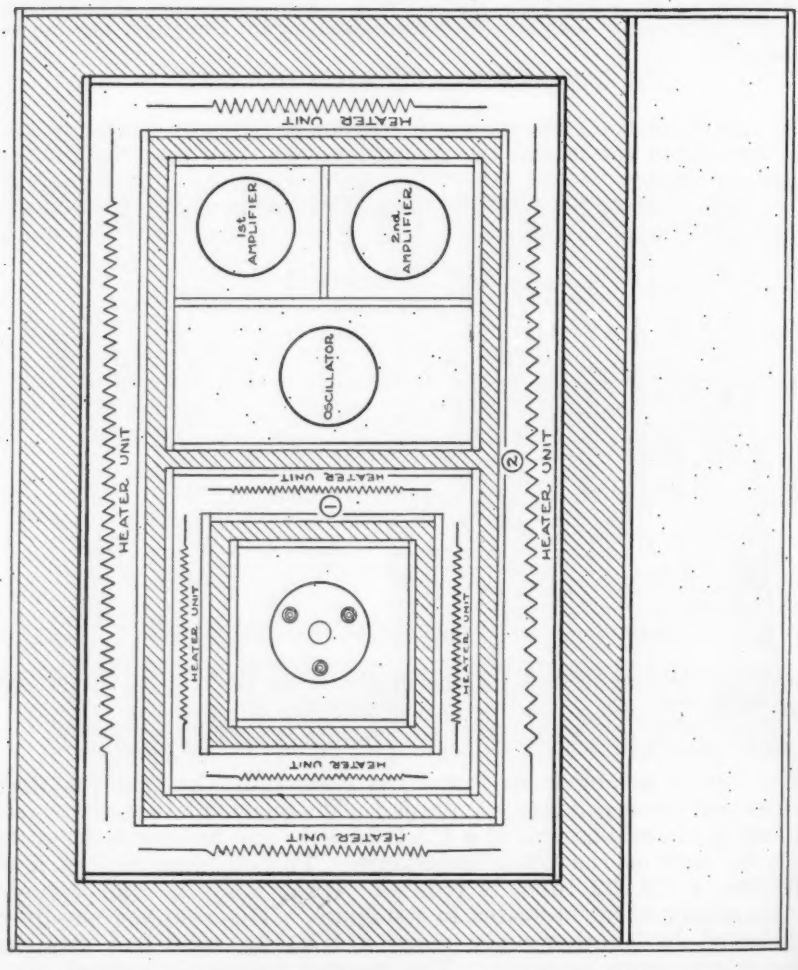

FIGURE 4.—*Schematic diagram of temperature control.*

within the outer temperature control only. Two cubical boxes, constructed of 3/16-inch aluminum, serve to equalize the temperature on all sides of the quartz plate. The two boxes are separated by three layers of ¼-inch felt, as indicated by the diagonal lines, which reduce the rate of flow of heat through the walls. The inner heaters are 1-ampere heater grids, one mounted on each wall of the temperature-controlled space. A 5-inch mercury thermostat is used to control the temperature. It is mounted vertically on the inner wall of the compartment between the heater and the heat-attenuating layers, in

the position indicated by the numeral *1* in the diagram. Additional layers of felt and another aluminum box separate this unit and the one containing the oscillator circuit arrangement from the outer heaters. The outer heaters are constructed of no. 28 nichrome wire wound into a spiral which is looped back and forth across an insulating framework. The temperature of this outer space is likewise controlled by a mercury thermostat which is mounted in an aluminum well in the position indicated by the numeral *2*. The extreme outer wall is composed of two thicknesses of ¾-inch hair-felt enclosed by a 3/16-inch aluminum box.

The heater control circuits are shown in figure 5. The relays are of the sensitive polarized type which operate very positively on 4 milliamperes direct current. The necessary voltage to operate the relays is furnished by a step-down transformer and a copper-oxide

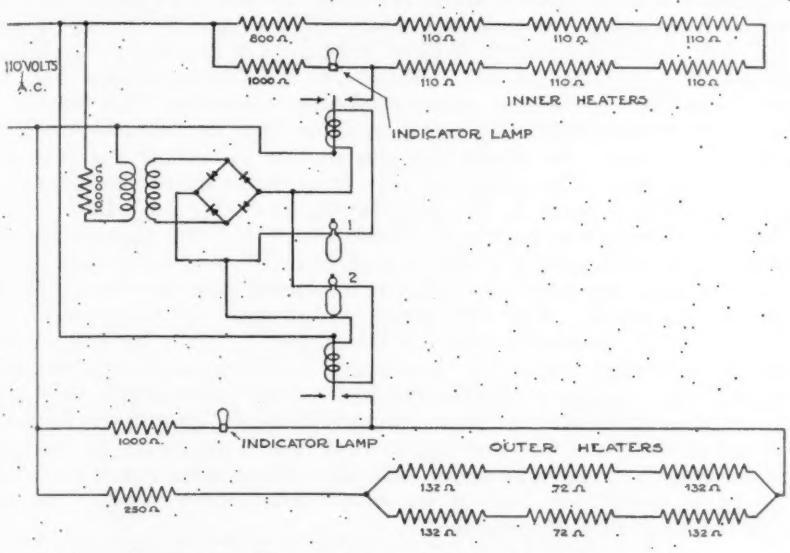

FIGURE 5.—*Temperature-control circuit arrangement.*

rectifier. The contacts on the relays were replaced by tungsten contacts so as to prevent burning and sticking.

The use of this piezo oscillator has shown one major limitation. The temperature of the quartz plate is slightly higher when the tubes are operating than when they are not. This fact makes it necessary to turn the oscillator on at least 24 hours before it is to be used in order to keep the frequency highly constant. The change in frequency due to the heat from the tubes is approximately 2 parts in 1,000,000. There are various ways in which this effect could be minimized. One would be to increase the thickness of felt between the tube compartment and the quartz plate compartment and decrease the heat attenuation between the tube compartment and the outer heater. The result would be that the heat from the tubes would be dissipated more rapidly to the outer temperature-controlled space and result in a lower temperature of the tube compartment, which would, accordingly, reduce the effect on the temperature of the quartz plate.

Several holes through the top of the box surrounding the tubes would also be effective in reducing the temperature effect upon the quartz plate. Another solution would be to have fixed heaters located in the compartment containing the tubes, and adjusted to furnish an amount of energy equal to that dissipated by them. The heaters could then be connected to the switch operating the tube filaments, so that when filaments were off the heaters would be on. The life of the tubes could thus be conserved without disturbing the temperature regulation.

VII. RESULTS

The piezo oscillator was completed in August 1931. During the first three months that it was in use to control the standard-frequency transmissions, the frequency drifted to a lower value so that several temperature adjustments were required in order to maintain the correct frequency. Such a frequency drift seems to be the normal behavior with this clamped type of holder. On December 1, 1931, a temperature adjustment was made and new tubes installed. For one year from that date this piezo oscillator controlled the standard-frequency transmitter each week without any further adjustments, except, of course, for slight changes in the condenser for fine frequency control. The range of this frequency-control condenser is approximately 3 parts in 10^6, and during this time only half of this total adjustment was required. This means that the piezo oscillator maintained its frequency within 1.5 parts in 10^6, and with the adjustment it was always possible to set the frequency to agreement with the primary standard. The frequency will remain constant within 2 parts in 10^8 for several hours. On December 1, 1932, the piezo oscillator was moved from the temporary building to the permanent transmitting station at Beltsville, Md. The unavoidable vibration encountered in the change caused an air-bubble to form in the mercury column of the outer thermostat, so that it was necessary to readjust this thermostat. At this same time new tubes were again installed. The piezo oscillator has given very satisfactory service in the standard-frequency transmissions.

VIII. ACKNOWLEDGEMENT

F. S. Ringler constructed the piezo oscillator described in this paper, and it is desired to acknowledge the many valuable suggestions which he contributed.

WASHINGTON, April 22, 1933.

U.S. Department of Commerce—Bureau of Standards

RESEARCH PAPER RP577

Part of Bureau of Standards Journal of Research, Vol. 11, July 1933

THE VISCOSITY OF OPTICAL GLASS

By W. H. Wadleigh

ABSTRACT

This is a report of a laboratory investigation of the viscosities of six optical glasses at high temperatures. A modified Searle type of concentric cylinder viscometer was used. The method of calibrating the viscometer is described, including the determination of frictional and "end effect" corrections. The important factors and formulas involved in the computation of viscosities from experimental data are given. A graph is shown of the logarithms of the viscosity values for a given glass plotted against the corresponding temperatures. Equations are given expressing the mathematical relations of viscosity to temperature. Included is a brief discussion of the viscosity changes resulting from volatilization and pot dilution during measurement, and of the consequent difficulty in determining the exact composition at the moment measurement is made.

CONTENTS

		Page
I.	Introduction	65
II.	Choice of method	65
III.	Description of apparatus	66
	1. Furnace	66
	2. Cylinders (crucible and stirrer)	66
	3. Driving mechanism	66
	4. Timing equipment	67
	5. Temperature measuring equipment	68
IV.	Equation for viscosity	68
V.	Evaluation of corrections	68
	1. The attainment of constant speed	69
	2. Friction corrections	69
	3. Evaluation of "end effect"	70
	4. Relation of effective load to r.p.m	72
VI.	Method of procedure for measuring viscosity of glass	72
	1. Adjustment of set-up	72
	2. Determination of bottom clearance D and "wetted height," h	73
VII.	Glasses studied	74
VIII.	Results	74
IX.	Summary and conclusions	78

I. INTRODUCTION

In the manufacture of optical glasses a knowledge of the viscosity-temperature relations is helpful in determining the most desirable melting and fining temperatures and conditions for stirring. The purpose of this report is to record results obtained by the modification of, and application to six optical glasses, of one of the common methods of measuring viscosities at high temperatures.

II. CHOICE OF METHOD

A brief résumé of the various methods used by earlier investigators is given by Washburn.[1] A survey of these methods of measuring

[1] E. W. Washburn, G. R. Shelton, and E. E. Libman, The Viscosities and Surface Tensions of Soda-Lime Glasses, Eng. Exp. Sta., University of Illinois, Bulletin no. 140, 1924.

viscosities had led earlier Bureau of Standards investigators [2] to adopt Searle's [3] modification of Margules' [4] method as the one seemingly best adapted to meet the requirements. This method depends on the measurement of the torque required to rotate the inner of two concentric cylinders, the outer cylinder being fixed and the material under test being confined between the two cylinders.

III. DESCRIPTION OF APPARATUS

A lateral view of the complete set-up is shown in figure 1.

1. FURNACE

The furnace was of the electrical resistance type, heated by three elements of 80 percent platinum-20 percent rhodium wire. These elements were supported by two disks and a cylinder of bonded artificial corundum forming the top, bottom, and sides of the heating chamber which was 12 cm deep by 7.6 cm in diameter. The assembled furnace was thoroughly insulated as shown in figure 1.

2. CYLINDERS (CRUCIBLE AND STIRRER)

The stationary cylinders or crucibles (c) were 6.2 cm in internal diameter and 9.0 cm in height and were so mounted as to prevent rotation. The stirrers, or rotating cylinders (Q) were closed-end tubes about 23 cm long. The portion immersed in the glass was ground to a flat-bottomed cylinder of 1.7 ± 0.0025 cm external diameter.

3. DRIVING MECHANISM

The driving mechanism is shown in the upper portion of figure 1. The hollow stirrer shaft (s) which carried the stirrer clamp (E) was mounted on ball bearings (u, u) and was rotated by means of the drum (f) which was 5.08 cm in diameter. On this drum were wound two fine braided silk cords which passed over adjustable, ball-bearing pulleys (a, a) to the driving masses (m, m). To keep the total driving weight constant, other sections of the cord continued to the floor.

In order to maintain a constant linear relation of machine friction to total pan load, the ball bearings on which pulleys (a, a) rotated were "run in" at about 1,000 r.p.m. for 3 hours with emery flour and kerosene, thoroughly cleaned, and then lubricated by touching 2 or 3 balls of each bearing with the best porpoise oil obtainable. The moment of inertia of the rotating system was increased by mounting a metal disk (M) on the upper end of the shaft (s).

It was found necessary also to alter the face of each pulley so that the cord, instead of running in a V-groove, ran over a cylindrical pulley face. The driving mechanism with its mounting was made adjustable horizontally and vertically by screws (A) and (B).

---

[2] L. A. Palmer, E. J. TePas, W. Scholl, and G. L. Bixby.
[3] G. F. G. Searle, A Simple Viscometer for Very Viscous Liquids, Proc. Camb. Phil. Soc., vol. 16, p. 000, 1912.
[4] Max Margules, Uber die Bestimmung des Reibung und Gleitungs Coefficienten aus ebener Bewegungen einer Flussigkeit; Sitzungsber. Akad.-Wiss. Wein., vol. 83, pt. 2, p. 585, 1881.

4. TIMING EQUIPMENT

The time-measuring apparatus was a stop watch, reading to 0.2 second and started and stopped automatically by an electromagnet

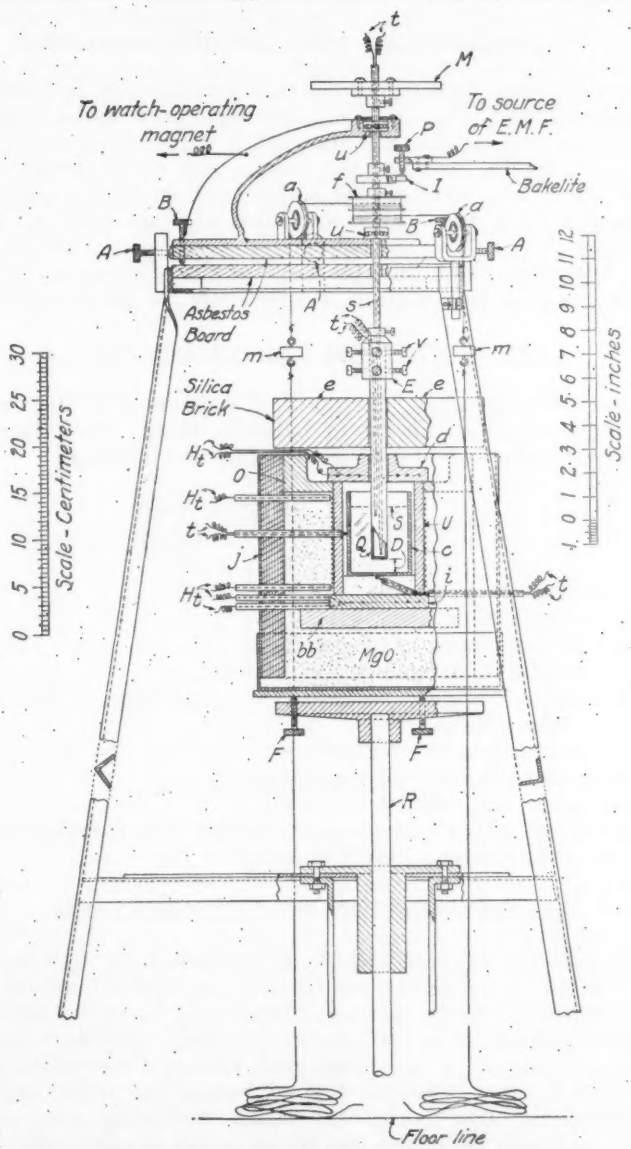

FIGURE 1.—*Lateral view of complete set-up.*

A and *B*, adjusting screws; *a*, pulley; *bb*, refractory; *c*, stationary cylinder or crucible; *D*, bottom clearance; *d*, inner cover; *E*, stirrer clamp; *e*, outer cover; *F*, leveling screws; *f*, drum; H_t leads to heating elements; *I*, rotating mercury contact; *i*, bottom heating plate; *j*, metal jacket; *M*, metal disk; *m*, driving masses; *O*, refractory; P, stationary contact; *Q*, rotating cylinder or stirrer; *R*, supporting shaft for furnace; *S*, glass surface; *s*, stirrer shaft; *t*, thermocouple leads; *U*, lateral heating unit; *u*, ball bearings; *v*, adjusting screws.

operated through the secondary of a telegraph relay. There were two breaks in the primary circuit of this relay. The tip of the sta-

tionary screw P and the mercury in an overfull iron trough I, mounted on the shaft (s), constituted the terminals of one break; the other, a knife switch, was operated manually. It was possible to measure the time required for from 1 to 8 complete revolutions.

5. TEMPERATURE MEASURING EQUIPMENT

The temperature-measuring equipment consisted of four platinum to platinum-rhodium thermocouples, a potentiometer and a cold-junction box of known and constant temperature. The hot junctions of two couples were placed inside of the stirrer, one at the bottom and the other at about the level of the upper surface of the molten glass. After placing these the stirrer was filled at least half full with pulverized corundum to prevent convection currents of air from reaching the hot junctions. The hot junctions of the other two couples were placed at the side and bottom, respectively, of the crucible, on the outside.

IV. EQUATION FOR VISCOSITY

The theoretical relation [5] for an ideal apparatus of the two coaxial cylinder type, having the liquid between them, when expanded to meet the conditions of test for this investigation becomes

$$\text{Viscosity, } \eta = \frac{30Wgr(d_2^2 - d_1^2)}{\pi^2(h+k)Nd_2^2d_1^2} \tag{1}$$

in which

η = viscosity in poises.
W = effective load.
g = the acceleration of gravity.
r = radius of drum + radius of cord.
h = wetted height, or depth of immersion of the stirrer in the glass.
N = revolutions per minute.
d_1 = outer diameter of the stirrer.
d_2 = inner diameter of the crucible.
k = "end effect" (a constant which is a function of d_1, and the "bottom clearance" D).

V. EVALUATION OF CORRECTIONS

Before making the necessary adjustments to attain constant speed, to determine the machine friction, or to make actual viscosity tests, it was necessary to aline pulleys (a, a) in such positions that (1) the plane of rotation of each pulley was truly vertical and contained the point of contact of the drum and the cord extending from the pulley to the drum; (2) the point of contact of the pulley and the cord was between the two horizontal planes enclosing that portion of the drum on which this cord was wound; and (3) the pulleys, placed on opposite sides of the drive shaft, were so located that their centers and the axis of this shaft were in a common vertical plane.

[5] E. W. Washburn, Univ. of Ill. Eng. Exp. Sta. Bull. 140, p. 12, April 1924.

1. THE ATTAINMENT OF CONSTANT SPEED

The device of the familiar Atwood machine was used in order to insure, during each test, a uniform speed (N) at which the resisting torque offered by the material under test just equalled that maintained by the effective load W. A rider, placed initially on one of the weights, M (fig. 1) was removed automatically at a time, determined by trial, such that the total remaining effective load was just able to maintain against the resisting torque of the viscous material under test, the velocity attained at the instant of removal of the rider. The proper point at which this rider should be removed was considered to have been determined when, following its removal at that point, the times required for the last 6 and for the last 8 revolutions were found to be in the ratio 6:8 (table 1). The attainment of this constancy of speed is essential since the computed value of viscosity is in each case directly proportional to the time required per revolution.

TABLE 1.—*Errors resulting from inconstancy in r.p.m.*

Trial no.	Rider travel	Time required for last—		$\frac{T_6}{T_8}$	Estimated time, T_8, at constant r.p.m.	Estimated residual error due to acceleration
		6 revs. T_6	8 revs. T_8			
	cm	*Sec.*	*Sec.*		*Sec.*	*Percent*
1a	1.0	8.2	11.2	0.732		5.2
1b	1.2	8.0	11.1	.731		2.6
1c	1.4	8.0	10.9	.734		2.6
1d	1.6	8.0	10.8	.741		2.6
1e	2.0	7.8	10.4	.750	7.8	0.0
2a	.5	18.3	23.7	.771		20.0
2b	.3	18.6	24.6	.756		8.4
2c	.2	18.75	25.1	.747		1.3
2d	.2+	18.73+	25.0	.749	18.70	.18

2. FRICTION CORRECTIONS

The machine friction, F, will vary, depending on the total load applied to the system. Obviously F could not be determined under conditions of actual test, for loads such as would be required to rotate the stirrer, because the resisting torque produced by the glass alone was not known. Therefore, it was necessary to use the empty viscometer and the set-up A shown in figure 2 rather than set-up B which was used in the actual tests of viscosity.

After the bearings had been adjusted determinations were made, for various values of L (fig. 2, A), of the corresponding values of the load difference, a', required to maintain in each case a uniform rate of rotation.[6] It was found that, for a given value of L, the friction $2(L+a)$ in set-up B was less than a'. The amount of this was determined and assumed to be true for all loads used in actual tests. Later in the investigation, when the bearings were recleaned and reset, new values were determined.

[6] At speeds in excess of 30 r.p.m. there was a slight variation from the linear relation between F and L.

3. EVALUATION OF "END EFFECT"

The "end effect", k, may be defined as a factor proportional to the resisting torque produced by the viscous material under test acting on the end of the stirrer. In order to evaluate k it was necessary to use a liquid of known viscosity. Accordingly a "simple viscous" petroleum oil (that is, obeying Poiseuille's law) and known as "Sunoco Golden", was chosen because, in the convenient temperature range 5° to 30° C., it had viscosity values of the same order of magnitude as those of molten glasses. Its viscosity-temperature relation could be expressed by the equation:[7]

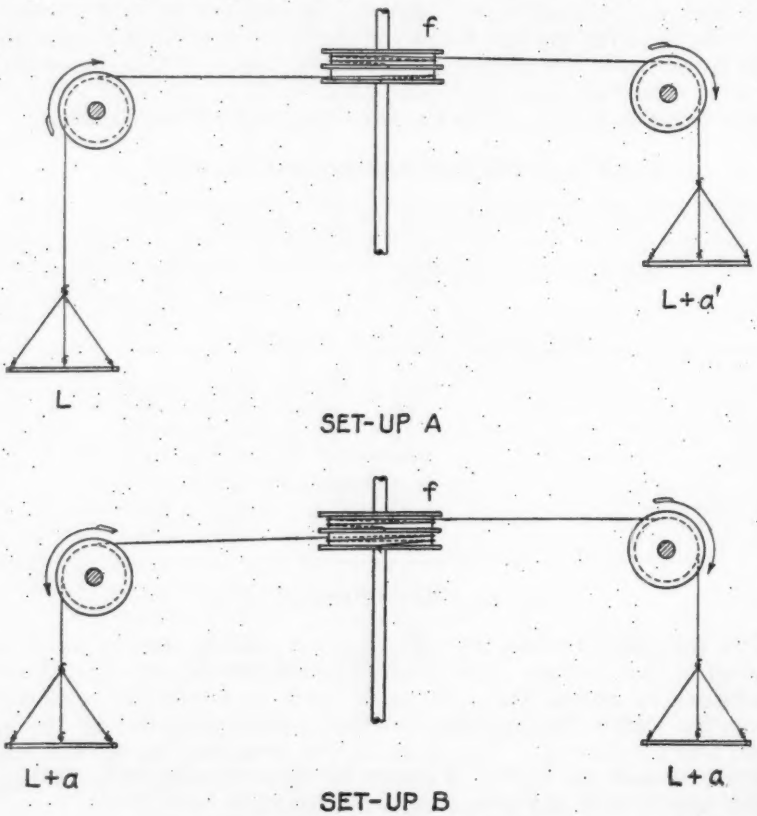

FIGURE 2.—*Diagrams of driving system.*

Set-up A shows arrangement for determining friction corrections for various loads and set-up B shows arrangement used in viscosity tests. a' effective driving weight, set-up A; $2(L+a)$; driving weight, set-up B: f, drum.

$$(\mathrm{Log}_{10}\eta - A)\ (T - B) = C \qquad (2)$$

in which

$A = -4.6392.$
$B = -71.3375.$
$C = 701.6.$
$T =$ temperature in °C.
$\eta =$ viscosity in poises.

When making determinations of k, the furnace (fig. 1) was replaced by a water bath, and the crucible by a glass cylinder whose dimen-

[7] Herschel, W. H., Viscosity and Temperature Changes, Oil and Gas J., vol. 25, p. 146, Dec. 2, 1926.

sions, except height, were approximately those of the refractory crucibles. Similarly, the refractory stirrer was replaced by a glass replica. The temperature of the oil in the glass cylinder was controlled by the water bath. In setting up the viscometer the stirrer was adjusted by means of screws, v (fig. 1), so as to rotate about its own axis, and that axis brought to a position vertical and concentric with the crucible. The clearance, D, at room temperature, between the end of the stirrer and the bottom of the crucible was then determined to ± 0.05 cm, which variation would not produce errors greater than 0.5 percent in computed values of viscosity.

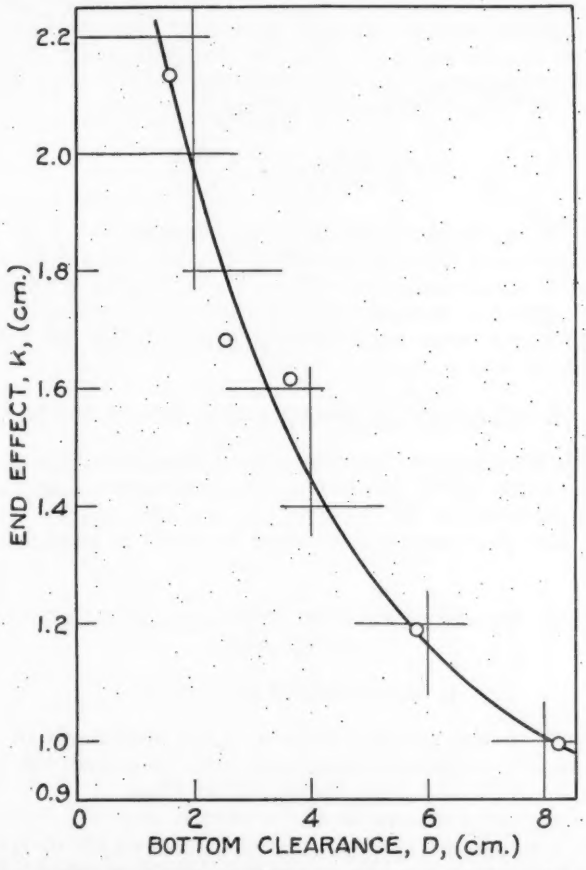

FIGURE 3.—*Showing "end effect" k as a function of bottom clearance D.*

From a consideration of the definition of unit viscosity and of equation (1) for viscosity, η, it can be shown that k is a function of d_1, d_2, and the bottom clearance D, but it cannot be thus shown whether k is or is not a function of h, N, or η. Although it had been shown previously by Proctor and Douglas [8] that k is not a function of h, N, or η, a number of tests were made, the results of which appear to be in accord with their conclusions. Therefore, since in any

[8] Proctor, R. F., and Douglas, R. W., Measurement of the Viscosity of Glass at High Temperatures by the Rotating Cylinger Viscometer, Proc. Phys. Soc. (Br.), vol. 41, pt. 5, no. 230, Aug. 15, 1929.

given test, d_1 and d_2 were also constant, the bottom clearance D remains as the only variable of which k may be a function. The form of this function was found by determining values of k corresponding to various values of D by substitution in equation (1), η being known from equation (2). These values of k were plotted (fig. 3) against the corresponding values of D, the best curve drawn through the points, and its equation determined as:

$$k = \frac{6.3}{(D+2.4)^{0.8}} \tag{3}$$

Theoretically, k is a function of d_1. Therefore, since the diameters of the refractory stirrers used in viscosity determinations differed slightly from the diameter (1.8 cm) of the calibrating glass stirrer, a modification of equation (3) was used, this modification being based on the work of Lillie.[9] Equation (3) then becomes:

$$k = \frac{6.3}{(D+2.4)^{0.8}} \cdot \left(\frac{d_1}{1.8}\right)^{1.18} \tag{4}$$

where d_1 is the diameter of the refractory stirrer.

It was found that closer duplication in results could be secured by stirring the oil immediately preceding the taking of readings, though this had the effect of increasing the apparent viscosity. Accordingly all determinations were immediately preceded by 20 turns of the stirrer at about 50 r.p.m.

4. RELATION OF EFFECTIVE LOAD TO R.P.M.

If glass, in the temperature range considered, is a "simple viscous" liquid, the values of W plotted against corresponding values of N should lie in a straight line passing through the origin. Any results which did not plot reasonably close to such a straight line were discarded.

VI. METHOD OF PROCEDURE FOR MEASURING VISCOSITY OF GLASS

1. ADJUSTMENT OF SET-UP

Preliminary to the actual viscosity tests, specimens of glass were molded in a form approximating the form assumed by the molten glass in the crucible and with the stirrer in place.

Having fastened a stirrer in the clamp E (fig. 1), the set-up was adjusted so that the stirrer was vertical, rotated about its own axis, and was concentric with the crucible. The furnace could then be lowered, the glass specimen inserted in the crucible, and again raised until the stirrer was in the preformed depression in the glass and in the same relative position occupied during a test. The top covers *d* and *e* (fig. 1) could then be put in place and the temperature raised to the temperature at which the glass was to be tested. In making a test it was necessary to determine the bottom clearance D and the "wettedheight" h, and to so adjust the apparatus that constant speed during a test would be assured.

[9] Lillie, H. R., Margules' Method of Measuring Viscosity Modified to Give Absolute Values, Phys. Rev., vol. 8, pp. 347 to 362, July 15, 1930.

2. DETERMINATION OF BOTTOM CLEARNACE *D* AND "WETTED HEIGHT" *h*

The bottom clearance D was checked occasionally by raising the furnace, while holding the temperature constant and with the molten glass in the crucible, until the bottom of the crucible just touched the stirrer. The furnace was then lowered a measured distance which determined the clearance D.

From figure 4 it is apparent that the wetted height, h, is equal to the total exposed length of the stirrer (H) minus the distance $L'+b$. This distance was determined by one of the following two methods.

At temperatures of 1,100° C. or above glass is a fairly good electrical conductor and this permitted the use of a gage (of cold length L) composed of two parallel platinum wires in series with a source of emf and a potential indicator. The gage was mounted on the viscometer stand so as to be vertically adjustable by means of a rack and pinion. After removing one of the furnace cover bricks (e, fig. 1) the gage was lowered through a hole in the cover, d (fig. 1), and the instant of contact of the lower ends of the wires with the glass was made evident by the indicator. The value of "b" (fig. 4) was determined by means of an "inside" caliper.

For temperatures below 1,100° C. a gage was made of a refractory tube attached to a hollow metal holder supporting it vertically from its upper end. The lower end of this gage was left open while the upper end was connected to a vacuum pump by means of a small copper tube. An ordinary glass U-tube manometer of the closed end type was connected to the line between the gage and pump. This gage also was adjusted vertically with the rack and pinion. With the pump in operation the gage was lowered until the manometer indicated contact of the lower end of the gage with the surface of the molten glass, when the distance b was measured.

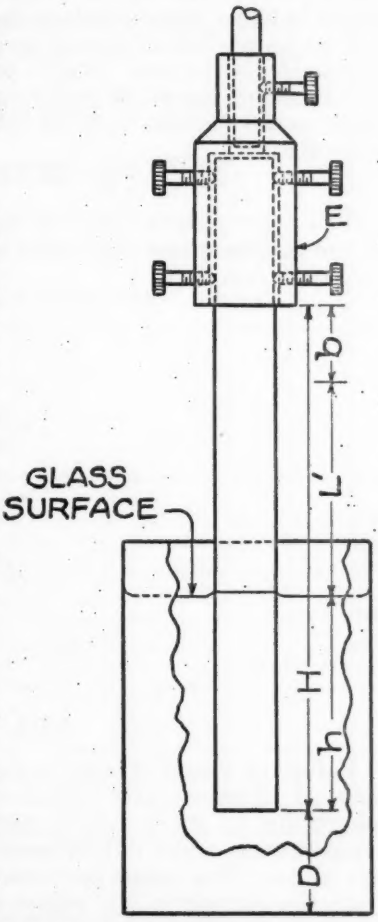

FIGURE 4.—*Sketch showing dimensions involved in determining "wetted height" h.*

Consistent values for $L'+b$ were difficult to obtain in spite of the most painstaking precautions. However, in 135 viscosity determinations, during the course of each of which from 2 to 4 measurements of $L'+b$ were made, the extreme variation was 0.13 cm, while the mean of all variations was 0.03 cm, or approximately 0.7 percent.

This would produce a corresponding mean error in the computed value of the viscosity of less than 0.5 percent.

In determining the wetted height it was necessary to take into consideration the increase in length of the stirrer, as well as of the two gages, caused by their thermal expansion when exposed to the furnace temperatures. The coefficients of thermal expansion of the stirrer, and of the wire or refractory of the two gages, was fairly definitely known. Nevertheless, the temperature gradients in the stirrers and gages not being known, certain tacit assumptions were necessary when calculating their lengths under test conditions. Unless changes in lengths of the gages and stirrer are taken into account, errors as large as 2.0 percent may be introduced into the computed value of viscosity.

VII. GLASSES STUDIED

The approximate chemical compositions and indices of refraction of the glasses whose viscosities were measured are given in table 2.

TABLE 2.—*Approximate compositions of the glasses tested*

Oxide	Kind of glass					
	Light barium crown	Light crown (soda-lime)	Boro-silicate crown	Dense flint	Medium flint	Barium flint
	Percent	*Percent*	*Percent*	*Percent*	*Percent*	*Percent*
SiO_2	47.5	74	65	41.0	45.5	45.5
Na_2O		12.5	8	.5	3.0	
K_2O	8.5	.2	12.5	6.5	5.0	8.0
B_2O_3	4.0		11.5			
ZnO	9.5		2.5			8.0
BaO	30.5		0.5			15.0
CaO		13.5				
PbO				52.0	46.5	23.5
Index of refraction	1.574	1.524	1.517	1.650	1.620	1.605

VIII. RESULTS

Values of viscosity were computed for any one glass from the results of all apparently satisfactory tests made on that glass. The logarithms of these values were plotted against the corresponding temperatures and the best possible initial graph was drawn through the plots. The mean percentage deviation of all computed values from the corresponding values shown by the initial graph was then determined. Following this a final graph was drawn (of which fig. 5 is an example) disregarding all those values whose percentage deviation was greater than four times the mean deviation.[10] Viscosity values for the glasses, tested at 900°, 1,000°, 1,100°, 1,200°, 1,300°, and 1,400° C. are given in table 3. In table 4 are given the equations (and the values of the constants involved), expressing these viscosity-temperature relations. These equations, except for borosilicate crown, are based on results obtained with crucibles and stirrers of porcelain designated as *A*.

[10] Goodwin, H. M., Precision Measurements and Graphical Methods, p. 21, McGraw-Hill Book Co.

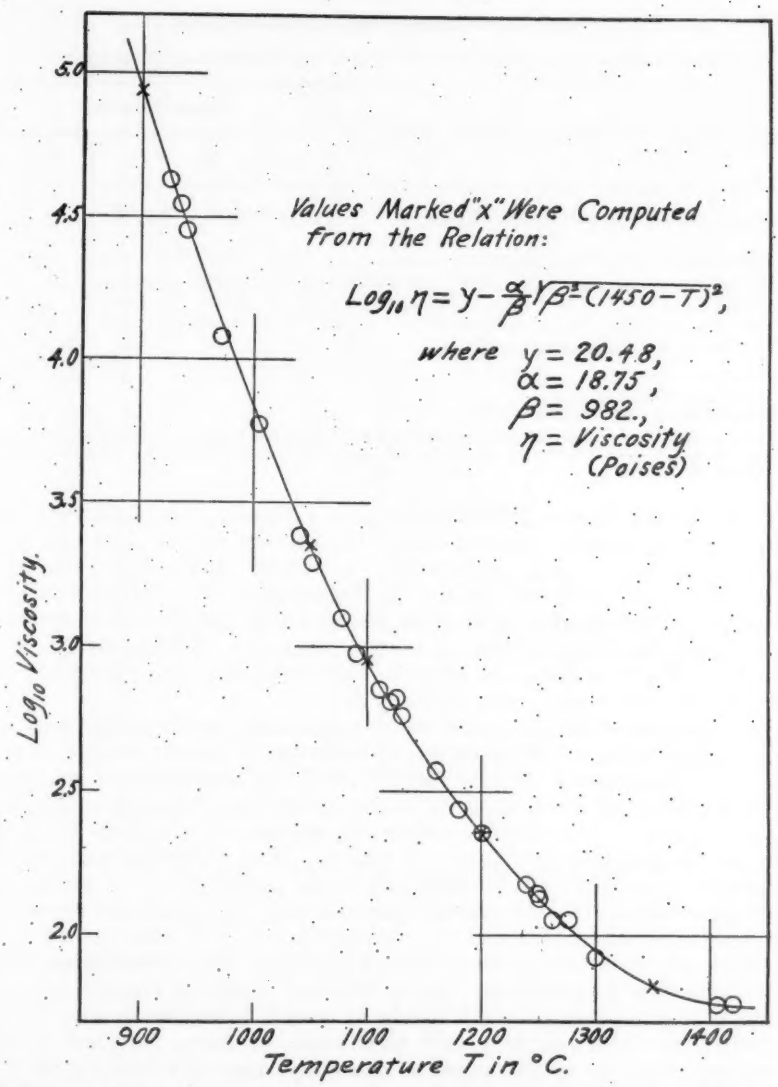

FIGURE 5.—*Showing log* $_{10}$ *of viscosity as a function of temperature in °C. for light barium crown glass.*

TABLE 3.—*Numbers of samples and determinations, and résumé of most probable viscosity values*

Kind of glass	Number of samples	Number of determinations	Viscosity at—					
			900°C.	1,000°C.	1,100°C.	1,200°C.	1,300°C.	1,400°C.
			Poises	*Poises*	*Poises*	*Poises*	*Poises*	*Poises*
Light barium crown	25	160	90,000±2,500	6,600±200	870±35	225±7	87±3	57±1
Light crown (soda-lime)	7	20	148,000±3,000	20,200±800	3,730±200	1,030±50	360±20	151±4
Borosilicate crown	6	30	----------	----------	(See table 5)			
Dense flint	7	21	6,600±200	1,525±35	460±25	186±6	88±3	47±1
Medium flint	2	9	----------	2,040±90	580±20	216±6	105±3	65±4
Barium flint	3	15	----------	8,000±275	1,500±50	385±15	140±5	76±2

TABLE 4.—*Viscosity-temperature relations*

[General equations expressing the viscosity-temperature relations of the glasses studied]

Kind of glass	Viscosity temperature relation [1]	Values of constants				
		α	β	γ	δ	ϵ
Light barium crown	$\text{Log}_{10}\eta=\gamma-\frac{\alpha}{\beta}\sqrt{\beta^2-(1{,}450-T)^2}$	18.75	982	20.48		
Soda-lime	$\text{Log}_{10}\eta=\frac{\beta}{(T+273.1)^2}-\alpha$	.727	8.13×10^6			
Borosilicate crown[2]	$\text{Log}_{10}\eta=\alpha+\beta(29-0.02T)+(29-0.02T)^2$	1.172	75.204	5.79		0.002
Dense flint	$\text{Log}_{10}\eta=\alpha+\beta\gamma^{-\epsilon T}$	.648	24.42	3.073		.002
Medium flint	$\text{Log}_{10}(\text{Log}_{10}\eta-\delta)=\alpha-\beta\gamma^{-\epsilon T}$	.9115	.0775	.3375	1.614	.002
Barium flint	$\text{Log}_{10}\eta=\alpha+\beta(\gamma-\epsilon T)^2$	1.75	1.77	3.1	2.14	.002

η = absolute viscosity in poises.
T=temperature in the Centigrade scale.

[2] Equation based on results obtained with crucible and stirrer of platinum and before heating to higher temperatures. Equation does not fit where T=1,400°, probably because there was a marked increase in voltatilization.

Early in the investigation it became apparent that selective volatilization of certain components of the glasses might alter the compositions of the glasses sufficiently to affect their viscosities, but there were no practical means of preventing it. Solution of the crucible by the molten glass was found to be another factor which could alter the composition as a test proceeds. Visible evidence of attack on the crucibles and stirrers was especially pronounced in the case of tests on borosilicate crown glass.

Accordingly a limited number of tests were made on borosilicate crown glass using (1) a porcelain of different composition and denser structure (designated as porcelain *B*); and (2) platinum coverings for those surfaces of crucible and stirrer otherwise exposed to contact with the glass. The effects on viscosity values and chemical composition are summarized in tables 5 and 6. The irregular and widely divergent viscosity values obtained with porcelain *A* as compared with those obtained with porcelain *B* and with the platinum protected containers, when considered in connection with the changes in composition, are believed to be sufficient evidence that crucible solution may introduce large errors. It is believed that the change in composition of glass sample no. 3 (table 6) tested in platinum was caused by selective volatilization, and that this, in turn, resulted in the increased viscosity of this glass as shown by the curves in figure 6.

It is regretted that time did not permit testing all of the glasses in platinum, or even in porcelain *B*, which would apparently have been a decided improvement over porcelain *A*, although (as stated previously) there was much more solution of porcelain by the borosilicate crown than by any of the other glasses. Therefore, when considering the values in tables 3, 5, and 6, it should be remembered that they apply to glasses the compositions of which, at the actual time of test, are not accurately known.

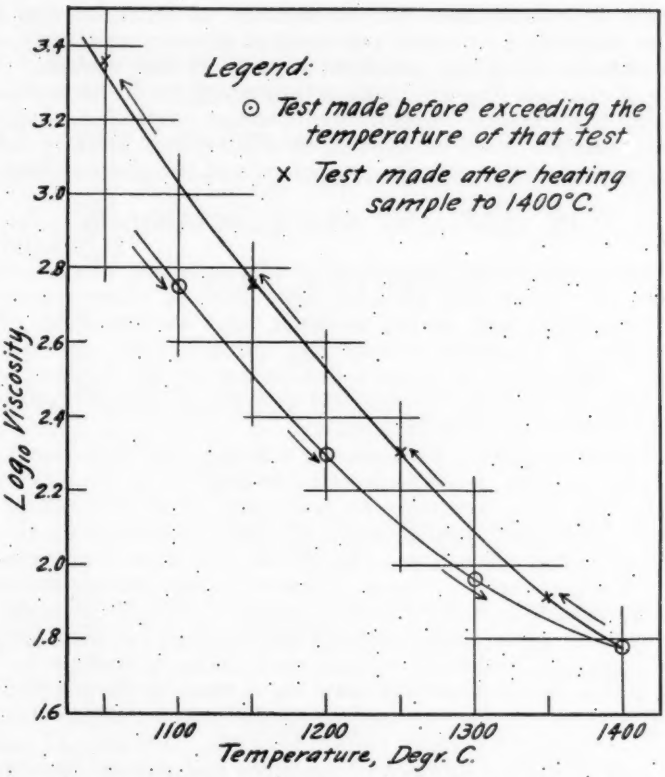

FIGURE 6.—*Showing change in viscosity of borosilicate crown glass (tested in platinum) due to volatilization.*

TABLE 5.—*Viscosity values*[1] *(poises), of borosilicate crown glass as measured in various crucibles*

Crucibles used	Number of samples	Number of determinations	Temperatures, ° C.				
			1,000	1,100	1,200	1,300	1,400
			Poises	*Poises*	*Poises*	*Poises*	*Poises*
Porcelain A	3	10	2,720±175	565±47	199±10	119±3	110±3
Platinum	1	10	[2] 2,000±10	560±11	200±6	90±2	60±1
Porcelain B	2	10	2,170±175	560±25	190±5	86±2	51±1

[1] Each of the above values of viscosity was determined before the sample was heated to higher temperatures.
[2] Value determined by extrapolation of log viscosity-temperature graph.

TABLE 6.—*Chemical analyses of variously treated borosilicate crown glasses*

Number of sample	Melt No.	Treatment	Analyses		
			SiO_2	R_2O_2	R_2O
			Percent	*Percent*	*Percent*
1 "control"	697	From molded sample [1] (before test)	65.8	0.3	19.6
2	668	After being held at 1,400° C. for 6 hours in crucible *A*	63.6	6.9	16.4
3	697	After being held at 1,400° C. for 9 hours in platinum crucible.	68.6	.4	18.0
4	697	After being held at 1,400° C. for 5 hours in crucible *B*	66.8	.6	18.6

[1] See pt. VI, 1, p. 72.

Changes in composition due to solution of crucibles and stirrers might be minimized by using porcelain of greater resistivity, or perhaps eliminated by using platinum containers and stirrers. This is not true of changes due to volatilization which could be avoided only by making the viscosity measurements under controlled conditions in which the sample could be kept in an atmosphere already saturated with the vapors of the volatile components of the glass under test.

IX. SUMMARY AND CONCLUSIONS

This paper reports an investigation of viscosities, at elevated temperatures, of six optical glasses—light barium crown; borosilicate crown; soda-lime; and dense, medium, and barium flint. Searle's modification of Margules' concentric cylinder type viscometer was adopted. The paper contains a description of the furnace, crucible and stirrers, driving mechanism, and timing and temperature-measuring equipment of the complete set-up.

The classical equation for viscosity was modified to adapt it to the apparatus. A fairly detailed description is given of the evaluation of certain factors and corrections such as production of constant speed, friction, "end effect", and relation of effective load to r.p.m., which evaluations it was necessary to establish prior to actual tests on the glasses. Further carefully made adjustments and measurements, such as the determination of the "wetted height" or depth of immersion of the stirrer in the glass, are necessary after the glass has been introduced into the apparatus and raised to the temperature of test.

The results of 255 viscosity tests on a total of 50 samples of the 6 optical glasses are summarized in equations expressing the mathematical relations of viscosity to temperature. Because of volatilization, as well as partial solution of crucibles and stirrers by the several glasses, especially borosilicate crown, the exact compositions of the glasses at the time of test are not known. An approximation of the importance of volatilization and solution as factors in viscosity determinations was obtained by a number of tests of the borosilicate crown glass in a crucible of special and more resistant porcelain, as well as with crucible and stirrer protected with platinum.

As a result of the investigation of the many factors involved in making viscosity determinations at high temperatures with the concentric cylinder type viscometer, it is believed that the information obtained enables the investigator to so evaluate and apply the necessary corrections as to make possible the obtaining of additional viscosity values of significant accuracy—insofar as the apparatus itself is concerned. It has been shown further that solution of crucible and stirrer by the glass, and volatilization of the glass, are factors of major importance because they may materially alter the composition of the glass during the course of a test. It should be a relatively simple matter to avoid contamination of the glass by solution of the container, but this is not true of changes due to volatilization. However, volatilization could conceivably be greatly minimized.

WASHINGTON, May 9, 1933.

U.S. DEPARTMENT OF COMMERCE—BUREAU OF STANDARDS

RESEARCH PAPER RP578

Part of Bureau of Standards Journal of Research, Vol. 11, July 1933

THE PRESENT STATUS OF THE STANDARDS OF THERMAL RADIATION MAINTAINED BY THE BUREAU OF STANDARDS

By W. W. Coblentz and R. Stair

ABSTRACT

The basis of the lamp standards of radiation, established and maintained by the Bureau of Standards since 1913, is the black body using the Stefan-Boltzmann constant of total radiation $\sigma = 5.70 \times 10^{-12}$ watt/cm^2/deg.^{4}

In this paper the present status of the value of the constant of total radiation is reviewed, and it is concluded that, for the present, the basis of the lamp calibration remains unchanged.

These carbon-filament lamp standards of thermal radiation maintained by the Bureau of Standards (S227) were intercompared after a lapse of 12 years and found in good agreement with the original standards which were established in 1913 by direct comparison with a black body.

Two reproductions of these standards which, according to published reports, showed rapid deterioration in radiant flux, were recalibrated. No deterioration, to 2 parts in 840, could be measured in the radiation emitted by one of these lamps which had been in use 8 years. In the other lamp an increase in radiant flux, amounting to about 1 percent, was found. This was caused by a hot spot in the filament, probably resulting from usage or perhaps by injury in shipment.

In a life test, a standard of radiation was operated for 245 hours before an increase in radiant flux became appreciable, and at the expiration of 300 hours this increase amounted to only 0.8 percent.

One section is devoted to the technique of operation, and specific directions are given to insure high precision.

CONTENTS

		Page
I.	Introduction	79
II.	Establishment of the reference standards of thermal radiation	80
III.	Intercomparison of the reference standards of thermal radiation	81
IV.	Constancy of lamp standards of thermal radiation	83
V.	Technique of operation	84
VI.	Bibliography	87

I. INTRODUCTION

For the convenience of those who desire to evaluate radiation stimuli in absolute units, during the past two decades the Bureau of Standards has been supplying standards of radiant intensity in the form of seasoned 115-volt carbon-filament incandescent lamps which have been standardized for radiant flux (microwatts per square centimeter).

Before the lamps are calibrated radiometrically they are seasoned and then measured for voltage at three or more designated currents in accordance with the accepted procedure in preparing similar standards of luminous intensity. The maximum voltage is always some 10 percent below the rated voltage.

176983—33—6

After the initial seasoning, experience indicates that such lamps are operable for 100 hours or more before they begin to change in radiant flux. Only when the lamps are operated above the calibration voltages is the surface of the filament likely to disintegrate, and only in very rare instances does the filament develop loose contacts at the lead-in wires, which defect is observable from the volt-ampere calibration supplied with the lamp.

At the International Congress on Light, which met in Copenhagen in August 1932, the Committee on Measurement and Standardization of Ultraviolet Radiation Used in Medicine recommended the evaluation of ultraviolet radiation stimuli on a physical (radiometric) basis, in absolute units (1)[1] by means of a nonselective radiometer (thermopile) and filters. The simplest and most reliable procedure for calibrating the radiometer is by means of a standard of thermal radiation. Obviously it would be desirable to use the same kind of standard of radiation in different laboratories, thus eliminating one source of uncertainty.

The object of the present communication is to present the results of an inquiry into the present status of the lamp standards of radiation maintained by this Bureau. Reproductions of these standards are being supplied to the several national laboratories looking forward to the time when there will be an international basis of comparison as now obtains in the lamp standards of luminous intensity.

II. ESTABLISHMENT OF THE REFERENCE STANDARDS OF THERMAL RADIATION

In view of the difficulties in making direct radiometric measurements in absolute value, the original carbon-filament lamp standards of radiation of the Bureau were obtained by direct comparison with a black body (at 1,000° to 1,150° C.), the radiant flux of which was calculated on the assumption that the Stefan-Boltzmann constant of total radiation is $\sigma = 5.7 \times 10^{-12}$ watt/cm^2/deg.^{4} (2) (9).

In making this initial comparison the standard lamps were placed at a distance of 1 m from the thermopiles, which were developed with continuous receiving surfaces (7) in order to reduce errors in calibrating them radiometrically. In part of this calibration the thermopiles were sighted alternately upon the black body (distance 30 to 75 cm) and then upon the lamps.

Subsequent measurements upon these lamps, made radiometrically with a thermopile that evaluated the radiant flux in absolute units, and also with a nocturnal radiation instrument, constructed for the United States Weather Bureau (2), showed a close agreement with the direct calibration against the black body.

It was, therefore, assumed that the radiant flux from the standard lamp is known with sufficient accuracy to meet the requirements of workers desiring to evaluate radiation stimuli in absolute units.

Concerning the Stefan-Boltzmann constant of total radiation, the value ($\sigma = 5.70 \times 10^{-12}$ watt/cm^2/deg.^{4}) used in that calibration is a trifle lower than more recent estimates ($\sigma = 5.71$ to 5.75) of this constant (9) in which corrections have been made for atmospheric absorption. However, the direct measurements (2) which do not

[1] Figures in parentheses here and throughout the text indicate references and notes given in the bibliography at the end of this paper.

depend upon the Stefan-Boltzmann constant, show no systematic difference from the initial comparison of the lamps against the black body in which the Stefan-Boltzmann constant was utilized.

From a recent survey of this question (9) it appears that the value [2] of the constant of total radiation ($\sigma = 5.70 \times 10^{-12}$ watt/cm^2/deg.^{4}), which formed the basis of the lamp calibration long before the more accurate determinations of this constant were available, is so close to the true value that it needs no consideration at the present time.

III. INTERCOMPARISON OF THE REFERENCE STANDARDS OF THERMAL RADIATION

The lamps issued as standards of thermal radiation, in absolute units, are seasoned in lots of 25 to 50. Those that qualify for constancy are marked for orientation, and the voltages are then measured at designated currents by means of the potentiometer outfit used in calibrating lamp standards of luminous intensity.

From each lot of calibrated lamps several are selected and added to the group of reference standards of radiation which, thereafter, are used only infrequently. Those in the earliest sets are rarely used. During the past 20 years, in addition to its working standards, this Bureau has accumulated and placed in reserve a group of 20 lamps as reference standards.

The first lot of 16 lamps that qualified for constancy, after seasoning, were calibrated directly against a black body as already described (2), and, of this group, lamps C-1, 2, 3, 12, 14, and 17 were set aside as reference standards. Five years later (1918) an intercomparison of lamps C-1, 2, 3, 12, 14, and 17, operated on 0.400 ampere, showed a deviation of 0 to 3 parts in 1,000 from the values of the radiant flux assigned to each lamp in 1913, which deviation is entirely within the errors of observation.

In October 1930, before undertaking a calibration of a new lot of lamps, the thermopile-galvanometer outfit was standardized (by R. Stair and J. M. Hogue) against all the standards which had been set aside up to that time, including the group of three lamps (C-1, 2, and 3) which had not been used for 12 years (1918). As shown in columns 4 and 6 of table 1 the average radiation sensitivity (galvanometer deflection) of the thermopile-galvanometer outfit, for the 9 standard lamps, was 1 cm deflection = 4.086 μw/cm^2, with a maximum deviation of 3 parts in 1,000, which is entirely within the experimental error of observation.

---

[2] The value of the Stefan-Boltzmann constant, determined with an absolute thermopile (2) after a recalculation (9) of all the observational data (using 10 copies of the same type of radiometer), taking into consideration all losses by reflection from the receivers as well as atmospheric absorption is $\sigma = (5.722 \pm 0.012) \times 10^{-12}$ watt/cm^2/deg.^{4}). This value contains two sets of data which depart by ± 2.8 percent from the mean of 20 sets of measurements, involving a total of about 600 separate determinations. Hence, these two sets have but little effect upon the average value.

The discussions, which emphasize the fact that this value of the radiation constant contains two extreme values, overlook the fact that the few wide departures from the mean value have the merit of showing the extreme range that is possible when use is made of a large number of copies (in this case 13 in all; several were known to be defective) of a particular type of radiometer. Since the observed value of the constant σ, may be systematically too high or too low, a good agreement among a few sets of measurements, made with one or two copies of a particular type of radiometer, is not a sufficient criterion for determining the accuracy of the absolute value. High precision in a few sets of readings is not necessarily an indication of the true value of the measurement.

A recent determination of the constant of total radiation by Hoare (Phil. Mag., vol. 13, p. 380, 1932) using a Callendar radiobalance, gives a value of $\sigma = 5.736 \times 10^{-12}$ watt/cm^2/deg.^{4}.

In a recent discussion of this subject, Birge (Phys. Rev., vol. 40, p. 207, 1932) points out that the directly observed values which range up to $\sigma = 5.79$, are inconsistent with the results derived indirectly by various equally reliable methods, which indicate a value of $\sigma = 5.714$. From this it appears that the calibration of the standards of radiation against a black body on the basis of $\sigma = 5.70$ is not far from the truth.

A comparison of columns 2 and 3 of this table shows that, within the above limits, there is no systematic difference in the radiation emitted by these lamps. Furthermore, the deviations of 0 to 3 parts in 1,000 are not systematically different from those observed on the same lamps when examined in 1918.

All the reference standards, selected from the different lots of new lamps are in close agreement, electrically and radiometrically, with the lamps originally calibrated against a black body. In addition to these reference standards, there are working standards for use in the laboratory. The "instructions" that are always supplied with the standards of thermal radiation (a pair of which should be used for certainty) suggest that the users likewise should provide themselves with working standards.

If a rapid deterioration took place in this type of lamp, as reported by Leighton and Leighton (3), it would have been observed long ago in the extensive intercomparisons of similar lamps when used as working standards of luminous intensity. It was because of the fact that this type of lamp was known to remain practically constant for 100 hours or more after the initial seasoning (10) that it was selected as a simple, convenient primary standard of thermal radiation in preference to flame standards (2). While its wide usage was only dimly foreseen, from the beginning it was realized that, owing to variations in atmospheric humidity, there would be small variations in the radiant flux. However, owing to absorption by the glass bulb, only a small amount of the total radiation emitted by such a lamp filament is of wave lengths longer than 4 μ. Hence, since atmospheric absorption by CO_2 and water vapor is weak for infrared wave lengths shorter than 4 μ, this error is probably small and negligible in comparison with other errors. This is supported by the fact that no marked variation in transmission through 1 to 2 m of air has been observed, assuming that the inverse square law holds for the radiation from a lamp filament.

TABLE 1.—*Determination of the radiation sensitivity of a thermopile-galvanometer radiometer in absolute units ($\mu w/cm^2$) by comparison with a series of carbon filament lamp standards of thermal radiation, operated on 0.400 ampere*

Lamp	Radiant flux at 2 m	Galvanometer deflection	Radiant flux to produce 1 cm deflection	Deviation from the average value	Deviation from average
1	2	3	4	5	6
	$\mu w/cm^2$	*cm*	$\mu w/cm^2$	$\mu w/cm^2$	*pts/1,000*
C-1	89.9	22.06	4.075	−0.011	−3
C-2	83.3	20.39	4.085	−.001	0
C-3	92.0	22.55	4.080	−.006	−1
C-17	89.0	21.72	4.098	+.012	+3
C-62	83.7	20.46	4.090	+.004	+1
C-73	81.7	20.03	4.079	−.007	−2
C-84	83.9	20.55	4.083	−.003	−1
C-85	86.2	22.00	4.100	+.014	+3
C-92	86.6	21.21	4.083	−.003	−1
Average			4.086		

IV. CONSTANCY OF LAMP STANDARDS OF THERMAL RADIATION

In this test two standards of thermal radiation, lamps C-125 and C-215, were rigidly mounted, side by side, at a fixed distance (2 m) from the thermopile. The rigid mounting was used to eliminate small, but unavoidable errors that occur in resetting the lamps. Lamp C-125 was used only for determining the radiation sensitivity of the thermopile-galvanometer radiometer, which varies slightly from day to day, and even during the day.

The radiant flux of lamp C-215, relative to that of lamp C-125, used as a standard, was determined after it had been burned, on 0.400 ampere (98.5 volts), for various intervals, amounting to a total of 296 hours. The milliammeter and the voltmeter were in circuit only while measurements were being made.

After operating C-215 for 62 hours, two sets of measurements, made on different days, were found in agreement to 1.5 parts in 1,000 with the average of the measurements made during the first 2 hours, and to within 1 part in 1,000 with the average of all the measure-

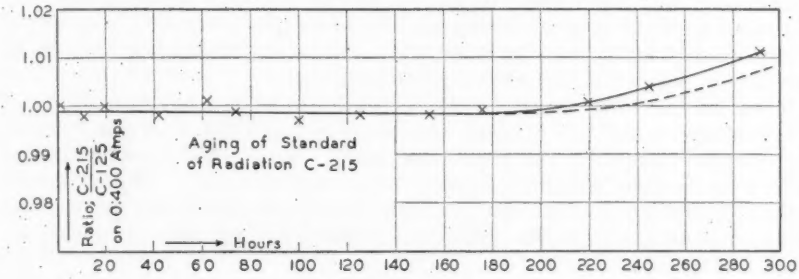

(FIGURE 1.)

ments made during the 62 hours. As shown in figure 1, these measurements include two poor sets (at 20 and 62 hours) obtained on windy days.

Not finding a definite change in the radiant flux on operating the lamp for 62 hours the radiometric procedure was then improved by keeping the galvanometer mirror adjusted on the zero of the scale reading (6) and by making a total of 7 sets of readings on the two lamps—4 sets on lamp C-215 with 3 intervening sets on lamp C-125 making (since each set included 15 galvanometer readings) a total of 105 observations, at the expiration of each period of burning.

The measurements, beginning at 74 hours' operation of the lamp and extending to 176 hours, showed no certain change in radiant flux (see fig. 1); and only after about 245 hours operation did an increase in radiant flux (on 0.400 ampere) become appreciable. The burning of the lamp was therefore continued to 291 hours (plus about 5 hours used in observations) when the increase in radiant flux appeared unmistakable. The lamps were then dismounted for a new volt-ampere calibration.

The result of this recalibration showed that the volt-ampere relation of the unused standard lamp C-125 remained unchanged, whereas the voltage of lamp C-215 after 296 hours' operation on 0.400 ampere had increased from 98.3 to 98.5 volts, or about 0.2 percent.

The dotted part of the curve in figure 1 indicates the change in radiant flux of lamp C-215, when the measurements are corrected for the same energy input in the lamp instead of for the same current (0.400 ampere). Even on this basis the increase in radiant flux of lamp C-215 by 300 hours' operation is less than 0.8 percent.

While this is a test of the constancy of but one lamp which may have shown an unusually good performance, numerous checks on our working standards and prolonged investigations of such lamps as standards of luminous intensity (10) indicate that, when properly used, the carbon filament lamp provides a satisfactory means for calibrating radiometers.

Seasoned tungsten-filament lamps have also been tried as standards, one objection to the use of which is the central glass support which may screen part of the incandescent filament.

Certain standards of radiation from this Bureau (viz, C-39 and C-40 issued in 1924 and C-69 in 1928) were reported by P. A. and W. G. Leighton (3) to deteriorate at the rate of about 0.5 percent per hour. In the case of lamp C-39, the decrease in radiant flux was reported to amount to 3.1 percent after burning 9 hours. These lamps were recalled and subjected to radiometric tests, using this Bureau's type of linear thermopile of bismuth-silver (7), connected with a highly shielded Thomson galvanometer (8), also with a high-sensitivity Weston d'Arsonval galvanometer.

Recalibration of lamp C-39 showed that it had not changed appreciably since its original calibration in 1924 (certified value 84.3 $\mu w/cm^2$; present value 84.1 $\mu w/cm^2$). Lamp C-69 was found to have a defective filament, easily observed visually. When recalibrated it showed an increased radiant flux over the initial calibration value of about 1 percent. Eleven hours' burning increased this by another percent.

Considered as a whole, there is no evidence, either radiometrically or from many years of investigation of such lamps as standards of light (10) indicating a deterioration of 0.5 percent per hour. The defect found in lamp C-69, though unusual and unavoidable, shows the importance of keeping such lamps properly inspected and using them only for reference standards, against which working standards are compared.

V. TECHNIQUE OF OPERATION

The carbon filament lamp standards of radiation, as already stated, are issued because years of experience in their use as standards of light (10), and as sources in optical pyrometry, show that they are more dependable and constant than any other means of standardization yet attempted.

They provide a simple and accurate means for calibrating photoelectrical and photochemical dosage intensity meters (4), and radiation stimuli used in biological (5) or photochemical problems.

Of the 180 or more standard lamps, issued during the past 20 years, the first intimation of unsatisfactory performance, as noted, appeared during the past year (3).

From the foregoing tests of these particular lamps, it appears that the unsatisfactory performance was more likely in the auxiliary apparatus than in the lamps.

For example, as stated in the instructions issued with each lamp, owing to slow warming of the glass bulb and the support of the filament, the radiation emitted will increase (rather than decrease) slightly in intensity during the first 5 minutes after starting. It is consequently difficult to attribute the observed decrease in intensity (reported to be 0.5 percent per hour, at least on first operation) (3) to a change in the lamp, rather than to a decrease in the radiation sensitivity of the radiometric outfit. For it is commonly observed, at the beginning of a series of measurements, especially if the radiometric apparatus has not been used for some time, that the radiation sensitivity is subject to a small change. In our experience, the constancy (of the sensitivity) of the radiometric outfit is less reliable than the lamp. Unless the laboratory is favorably situated, traffic and meteorological conditions must be unusually steady to permit radiometric measurements with this type of instrument (thermopiles in air) to an absolute accuracy much higher than 1 percent. Although the actual measurements may appear more precise (12), high precision in a set of measurements does not necessarily indicate high accuracy in absolute value.

A change in radiation sensitivity may result from a number of causes: (*a*) Fatigue of the d'Arsonval galvanometer suspension when deflections are large and in only one direction; (*b*) lack of uniformity of the galvanometer field, accompanied with a shift of the zero reading [3]; (*c*) heating of the thermopile junctions by the Peltier current; (*d*) change in temperature conditions between the shutter and the background of the lamp; (*e*) creeping of the zero reading of the ammeter; and (*f*) a general "warming up" of the whole radiometric outfit which probably includes a number of unexplained factors.

In the days when bolometers were used some of these difficulties were overcome, unknowingly, by keeping the bridge balanced by suitable shunts in the battery circuit. In precise readiometry with a thermopile, which in itself requires no impressed emf, the simplest procedure to keep the circuit balanced is to introduce an auxiliary control current, from a dry battery, through an external circuit (6).

In regard to the standard itself, as is well known, the radiation from an incandescent lamp is not uniform in all directions; hence, the bulb is marked for alignment with respect to the radiometer. If the filament becomes obviously displaced relative to these marks on the bulb (which happened on one occasion) in shipping, or by rough usage in the laboratory, the certified calibration cannot, of course, be depended on. The lamp with displaced filament, mentioned above, retained its volt-ampere relationship but was 3.4 percent above calibration value in radiant flux.

Specific instructions for mounting and using standards of radiation are sent with each lamp. These include the alignment of the lamp with the radiometer, which is accomplished by screwing the lamp into a socket (approved by underwriters) that is held in an upright support. This permits adjusting the lamp about a vertical axis, but which cannot reflect light into the radiometer. The socket itself need not be shielded from the radiometer, but the inside should be inspected to ascertain that the insulation has not become defective.

[3] For example, caused by a change of level or rotation of the coil in the field of the permanent magnets, or by rotation of the astatic magnet system in the field of the control magnets of a highly shielded Thomson galvanometer.

The calibration is based on the whole incandescent lamp being exposed to the radiometer. Sufficient time (about 5 minutes) must be allowed for the glass base which supports the filament to attain a uniform temperature before starting the radiometric readings, otherwise errors will be introduced into the energy measurements. In order to reduce this heating, the lamp is purposely supported "base down."

In cleaning the bulb the glass may become electrified by rubbing, and cause the filament to adhere to it. Hence, before lighting the lamp, it should be ascertained that the filament does not adhere to the glass.

To eliminate errors arising from heating by the lamp, the shutter (about 15 by 20 cm) used between the lamp and the thermopile consists of two sheets of aluminum, between which is mounted a sheet of asbestos about 5 mm thick. The side of this shutter toward the lamp is unpainted and kept highly reflecting to reduce absorption of radiation from the lamp. The side toward the radiometer is painted a dull black to minimize reflection.

Other precautions of advantage are: A black cloth, about 1 m square should be placed at a distance of about 1 m to the rear of the standard lamp; and an opaque (heavy cardboard) shield about 1 m square, with an open window about 10 cm wide and 15 cm high, should be placed about 25 cm in front of the lamp. Facing the opening in this shield, the radiometer is placed at a distance of 1 or 2 m from the lamp.

The shutter is mounted between the shield and the lamp, preferably close to the shield. This maintains constant temperature conditions between the radiometer and the shield when the shutter is opened and closed.

Before lighting the lamp, the amount of radiation falling upon the radiometer from the background of the lamp is determined by opening and closing the shutter. This test may be applied at any time provided the lamp has been given sufficient time to come to room temperature. The correction to the observed galvanometer deflection may be positive or negative depending upon the temperature of (radiation from) the background relative to that of the shutter.

It is desirable to make the measurements in a dimly lighted room, to avoid errors from changing sunlight, falling upon the thermopile or surroundings, thus varying the temperature and causing air currents near the radiometer.

The best results are to be obtained by operating the lamp between the certified maximum and minimum calibration values of current or voltage. If the measurement of current be made when a voltmeter is connected across the terminals of the lamp, a correction may have to be made for the part of the current shunted around the lamp. To avoid changes in voltmeter and ammeter calibrations, these instruments should be placed in the same direction (N–S) as when calibrated and no iron or rheostats should be nearer than 50 cm.

It may be stated in conclusion that the evaluation of the radiation stimulus in absolute units, as given in the Bureau's calibration is probably as accurate as the numerous other factors that enter present-day applications. When these other uncertainties have been overcome, it will be desirable to increase the accuracy of the radiometric evaluation either by null methods, in which the galvanometer is

used merely as an indicator (rather than as a precision electric current meter as now used); or, by evaluation of the radiation stimulus by means of an absolute thermopile (2) calibrated directly against a black body instead of using it to determine the Stefan-Boltzmann constant.

VI. BIBLIOGRAPHY

1. W. W. Coblentz, The Copenhagen Meeting of the Second International Congress on Light, Science, vol. 76, p. 412, November 4, 1932.
2. W. W. Coblentz, Measurements on Standards of Radiation in Absolute Value, B.S.Bull. (S227), vol. 11, p. 87, 1914. See also B.S.Bull. (S262), vol. 12, p. 580, 1916.
   W. W. Colbentz and W. B. Emerson, Studies of Instruments for Measuring Radiant Energy in Absolute Value: An Absolute Thermopile, B.S.Bull. (S261), vol. 12, p. 503, 1916.
3. P. A. Leighton and W. G. Leighton, Some Remarks on the Use of Thermopiles for Absolute Measurement of Radiant Energy. J.Phys. Chem., vol. 36, p. 1882, 1932.
   Recomparison of Standards of Radiation, B.S.Tech. News Bull., No. 190, p. 14, February 1933.
4. W. W. Coblentz, R. Stair, and J. M. Hogue, Measurements of Ultraviolet Solar Radiation in Various Localities, B.S.Jour. Research, vol. 10 (R.P. 517), p. 79, 1933.
5. W. W. Coblentz, R. Stair, and J. M. Hogue, Tests of a Balanced Thermocouple and Filter Radiometer as a Standard Ultraviolet Dosage Intensity Meter, B.S.Jour. Research, vol. 8, (R.P.450), p. 759, 1932.
6. W. W. Coblentz, R. Stair, and J. M. Hogue, A Balanced Thermocouple and Filter Method of Ultraviolet Radiometry, with practical applications, B.S. Jour. Research, vol. 7 (RP370), p. 723, 1931.
7. W. W. Coblentz, Various Modifications of Bismuth Silver Thermopiles Having a Continuous Absorbing Surface, B.S.Bull., vol. 11 (S229), p. 131, 1914.
8. W. W. Coblentz, Sensitivity and Magnetic Shielding Tests of Thomson Galvanometers for Use in Radiometry, B.S.Bull., vol. 13 (S282), p. 423, 1916.
9. W. W. Coblentz, Present Status of the Determination of the Constant of Total Radiation from a Black Body, B.S.Bull. (S262), vol. 12, p. 553, 1916.
   W. W. Coblentz, Constants of Radiation of a Uniformly Heated Enclosure B.S. Sci. Papers (S357), vol. 15, p. 529, 1920.
   W. W. Coblentz, Present Status of the Constants and Verification of the Laws of Thermal Radiation of a Uniformly Heated Enclosure, B.S. Sci. Papers (S406), vol. 17, p. 8, 1921.
10. E. B. Rosa and G. W. Middlekauff, Carbon Filament Lamps as Photometric Standards, Proc. Amer. Inst. Elect. Engrs., vol. 29, p. 1191, 1910.
    J. F. Meyer, Maintenance of the International Candle by Means of Carbon-filament Incandenscent Electric Lamps, Recuil des Travaux de la Commission Internationale de l'Eclairage, Cambridge, 1931.
11. According to a recent estimate by Dr. W. G. Leighton the total time that lamp C-39 had been operated was 35 hours, and lamp C-69 for 5¼ hours.
12. Without desiring to be pessimistic one of the writers (W.W.C.), after over 3 decades of experience in radiometry, ventures the suggestion that workers in this field should feel happy if they can attain anywhere near this accuracy (viz, 1 percent).

WASHINGTON, May 10, 1933.

U.S. Department of Commerce—Bureau of Standards
RESEARCH PAPER RP579
Part of Bureau of Standards Journal of Research, Vol. 11, July 1933

NOTE ON AN IMPROVED CHAIN-PACKED DISTILLING COLUMN [1]

By Sylvester T. Schicktanz [2]

ABSTRACT

A description of an automatically controlled, chain-packed column capable of giving approximately 100 percent pure benzene and ethylene chloride, which boil 3.42° C. apart, from an initial charge of a 50 mole percent mixture of the two. This still is small enough to be installed in an ordinary sized laboratory.

In a previous paper [3] a detailed description has been given of the construction, operation, and efficiency of various forms of laboratory stills for the fractional distillation of liquids. A still with a 35-foot column packed with jack-chain had a higher efficiency than any of the other stills. Such a still is, however, expensive to construct and because of its height cannot be erected in an ordinary laboratory.

The purpose of this note is to describe a still with a chain-packed column of high efficiency, which can be erected in any laboratory of the usual height. The still is in every respect similar to those described in the previous paper except that a column packed with jewelers brass locket chain, size nos. 13 to 18, is employed.

A 3-liter still pot, supporting a column 2.5 cm in diameter and 250 cm long, requires approximately 3,600 feet of chain for filling. This filling should be uniformly distributed throughout, since any congested section in the column will cause flooding to occur before the most efficient operating conditions are reached. The over-all height of a still using this length of column is 322 cm, and the still can be readily installed in a room 344 cm high.

This still, running at a rate of 0.5 ml of distillate per minute, with a reflux ratio of 22 : 1, a vapor velocity of 7.57 m per minute, and having a "hold up" of 180 ml, readily separates a mixture of benzene and ethylene chloride. Starting with 1,500 ml of a 50 mole percent mixture of benzene and ethylene chloride, substances having boiling points differing by only 3.42° C., it was possible to obtain 450 ml of almost pure benzene as distillate and 350 ml of almost pure ethylene chloride as residue (fig. 1). Thus 53 percent of the charge was obtained as pure benzene and pure ethylene chloride. This percentage could be increased readily by either decreasing the amount of liquid held in the column or increasing the volume of the charge. In increasing the volume of the charge it is necessary to keep the evaporat-

[1] Financial assistance has been received from the research fund of the American Petroleum Institute. This work is part of project no. 6, The Separation, Identification, and Determination of the Constituents of Petroleum.
[2] Research associate representing the American Petroleum Institute.
[3] Johannes H. Bruun and Sylvester T. Schicktanz, Laboratory Rectifying Stills of Glass, B.S.Jour. Research, vol. 7, p. 852, 1931.

ing surface of the liquid small enough so that upon brisk boiling the evaporating liquid does not cause continual flooding in the column. The 2.5-cm column was found to be approximately the right size to take care of the evaporation from the surface of the liquid exposed in a 3-liter round-bottom flask. Larger charges than this could be distilled satisfactorily through this column, if an elongated pot was used, thus keeping the surface area approximately the same.

In a column of this type the difference in pressure between the still head and the still pot is one of the controlling factors in obtaining the maximum efficiency. It was found that with a column 2.5 cm in diameter and 250 cm long the maximum efficiency was obtained when using a pressure difference of 26 mm of Hg, whereas in a smaller column, 2 cm in diameter, and of the same length, a pressure difference of 15 mm gave the maximum efficiency. In order to maintain this

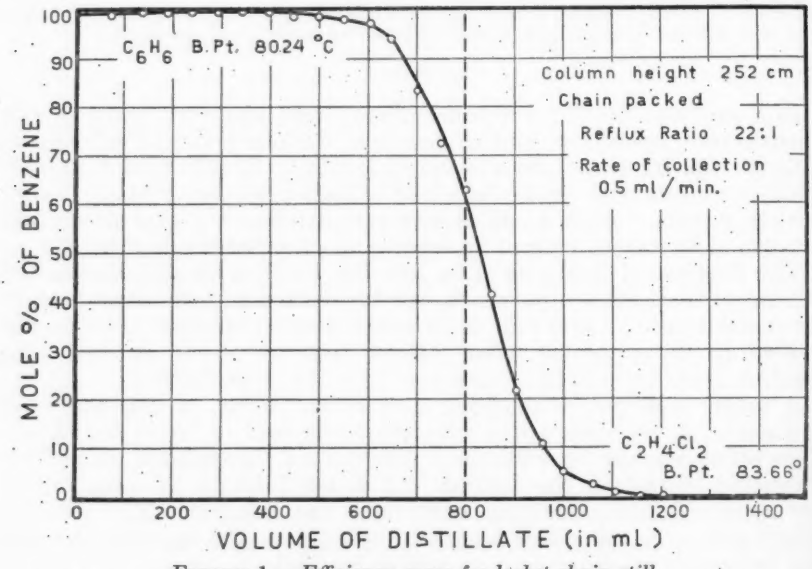

FIGURE 1.—*Efficiency curve for locket-chain still.*

Ordinate.—Mole percent of benzene in distillate.
Abscissa.—Total volume of distillate collected.

pressure at the value found most efficient for the still in question, the current in the coil, which heats the still-pot, is automatically controlled. The pressure difference is indicated by means of a differential manometer, one end of which is attached to the pot and the other to the still head. Two contact points are placed 1 mm apart in the high side of the manometer and one contact in the mercury proper. The two contacts control the high and low voltage regulators which are actuated by means of mercury relays. The voltage controls are nothing more than fixed resistances placed in the line, as illustrated in figure 2. When the mercury in the manometer (M) makes contact with the high contact point, a resistance (R_1) is thrown into series with the still-pot heater coil (S) by breaking the contact in relay (A), thereby decreasing the potential drop across the coil itself; and when the mercury breaks contact with the low point, the circuit through (A_1) is closed and a resistance (R_2) is thrown in parallel with rheostat (R_3)

which controls the heating coil, thereby increasing the potential across the heater.

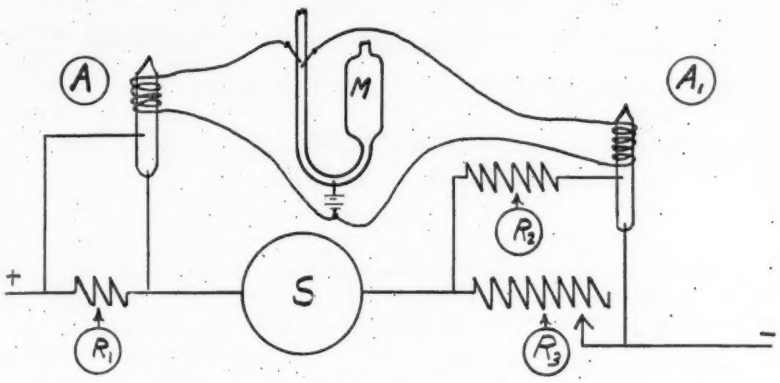

FIGURE 2.—*Diagram of automatically controlled heater unit for still pot.*

Mercury relays, without moving parts, were used since currents of from 4 to 6 amperes had to be broken. The relay is illustrated in figure 3; *A* is a 10-mm pyrex tube, *B* is the solenoid consisting of 600 ohms of enameled silk-covered copper wire No. 33, *C* and *C'* are two sealed-in tungsten contact points, and *D* is a soft-iron plunger. The relay is assembled and then evacuated and sealed off in order to prevent the mercury from fouling the contact points when operating under heavy loads.

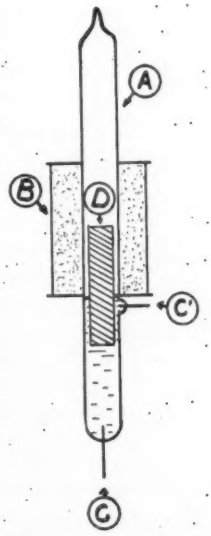

FIGURE 3.—*Diagram of mercury relay.*

To prevent sparking at the contact points, caused by the slow moving mercury boundary in the manometer, it was found desirable to use alternating current instead of direct current, thus obviating the expense of installing a vacuum tube hook-up. The reflux ratio is another important factor in operating a still efficiently. The greater the ratio the more efficient the separation. In the 2.5 cm column a 22:1 ratio gave initially 99.1 percent pure benzene ($n_D^{25.2}$ 1.4972 as compared to $n_D^{25.2}$ 1.4976 benzene initially used for the charge). An 11:1 ratio gave only 96 percent benzene.

The column should be run with no lateral heat loss, since the most efficient separation occurs when there is a uniform temperature gradient along the column. Hot and cold spots in the column cause flooding which decreases the efficiency. The same method of controling the temperature gradient is used on the packed column as was used on the plate stills.[4]

Table 1 shows the results obtained when using different types of columns and different packings.

[4] See footnote 3, p. 89.

TABLE 1.—*Separation of benzene and ethylene chloride using different distilling columns*

Type of still	Size of chain	Rate of distillation	Reflux ratio	Purity of initial fraction
		ml/min.		*Percent*
30-plate		1.0	10:1	78.0
Do		.75	20:1	84.0
Packed	22 jack-chain	1.0	10:1	80.0
Do	24 double jack-chain	1.0	10:1	83.3
Do	Locket chain	1.0	11:1	96.0
Do	do	.5	22:1	99.1

The efficiency is increased as we go from the jack-chain to the double jack-chain and to jewelers brass locket chain in accordance with the increase of effective surface exposed in the column.

WASHINGTON, April 13, 1933.

U.S. Department of Commerce—Bureau of Standards
RESEARCH PAPER RP580
Part of Bureau of Standards Journal of Research, Vol. 11, July 1933

EQUIPMENT FOR TESTING CURRENT TRANSFORMERS

By Francis B. Silsbee, Ray L. Smith, Nyna L. Forman, and John H. Park

ABSTRACT

The equipment and test procedure developed at the Bureau of Standards for measuring the ratio and phase angle of current transformers up to currents of 12,000 amperes at power frequencies are described in detail. Data are given to show the accuracy of the standard current transformer used in the higher ranges, and the effectiveness of the shaping of the heavy-current circuit so as to minimize errors from stray magnetic fields.

CONTENTS

	Page
I. Introduction	93
II. Method	95
III. Description of apparatus	99
1. General arrangement	99
2. Standard transformer	104
3. Adjustable standard resistor	110
4. Mutual inductor	113
5. Vibration galvanometers	114
IV. Test procedure	115
V. Conclusions	118
Appendix A.—Calculation of the magnetic field around the test transformer "cage"	119

I. INTRODUCTION

The steady and rapid increase in the use of electric power in recent years has involved a corresponding increase in the number and importance of the locations where large amounts of alternating-current power or energy must be accurately measured for purposes of billing or control. In such metering it has become universal practice to avoid connecting the measuring apparatus directly to the power circuits, and to use instead instrument transformers which serve to reproduce in their secondary circuits a replica on a reduced scale of the currents and voltages applied to their primary circuits. This practice offers the very great advantages of a reduction in life hazard, an economy in the cost and size of the measuring instruments proper and a very great increase in the flexibility and convenience in switchboard wiring and in protective relay operation. The instrument transformers, however, introduce an additional step in the measurement process and it becomes necessary in precise work to determine experimentally the exactness with which the current and voltage transformers reproduce to the proper scale the magnitude and phase relations of the primary currents and voltages, respectively.

As is the case with almost any kind of measurement, it is much easier to compare the ratio and phase angle of one transformer with those of another transformer of the same nominal ratio than it is to determine the ratio and phase angle of a single transformer directly.

Convenient types of apparatus for accomplishing the former comparisons have been on the market for some years and are now widely used by power companies to check the transformers installed for important metering work in terms of standard transformers of the same range. The testing of these standard transformers is done in turn at one of the more elaborately equipped laboratories maintained for the purpose by the larger power companies, by the transformer manufacturers, by public-utility commissions, or by the Federal Government.

The equipment and methods used for this purpose at the Bureau of Standards at Washington have been modified and enlarged from time to time to keep pace with the increasing demands in accuracy and range of the transformers to be tested. The object of this paper is to describe the equipment and methods [1] now in use at this Bureau in the hope that the data given may be of assistance to other laboratory workers who may wish to install apparatus for similar work.

The accuracy needed in this class of testing should, if possible, be so high that errors in the certified values will be negligibly small in comparison with the inaccuracy likely to occur in the next step in the measurement process; that is, in the comparison in the field between the standard transformer and the working transformer. A limit to the possible accuracy is, of course, set by the repeatability of the transformer under test. This limit is influenced by a number of factors, among which are changes in the magnetic condition of the core as a result of previous operation, uncertainties in the temperature of the transformer windings and hence in their resistance, and uncertainty in the exactness with which the burden used in the field is duplicated in the test. In the case of hole-type current transformers additional uncertainty arises because of differences in the position of the primary conductor in the hole, and in the position of the return lead. The magnitude of the changes in calibration resulting from these effects depends greatly upon the type of transformer, but may amount to several tenths of 1 percent.

The sensitivity of the present equipment is such that a change of 0.01 percent in ratio and 0.3 minute in phase angle is definitely detectable even at a secondary current as small as 0.5 ampere. Changes in the performance of the transformer under test are therefore often noted. The accuracy of the equipment, since it involves the calibration of resistance standards of widely different values with the additional liability to errors from skin effect and residual self-inductance, is, perhaps, not as high as the precision mentioned above would indicate. The accuracy limits printed on the Bureau's certificate form (viz, 0.1 percent in ratio and 3 minutes in phase angle) are, however, certainly very conservative. In reducing the observed values all corrections are normally carried to the nearest 0.005 percent and 0.1 minute and the resulting values are then rounded off in the certificate to the nearest 0.01 percent and 1 minute.

The present equipment is intended only for tests of transformers having the conventional 5-ampere secondary current rating. The measuring apparatus can be used for primary currents from 1 ampere to 12,000 amperes, but the ratings of the motor-generator sets available

[1] These developments have been the work of a very considerable number of individuals, both laboratory workers and mechanicians. In the former group mention should be made of P. G. Agnew, J. L. Fearing, J. M. Cork, F. M. Defandorf, and R. D. Wyckoff; in the latter, E. A. Baker, J. Ludewig, J. M. S. Kaufman, and E. A. Tibballs.

for energizing the circuits limit the testing to 6,000 amperes at 50 cycles, 7,500 amperes at 25 cycles, and 12,000 amperes at 60 cycles.

II. METHOD

The present equipment is based on the "resistance" method,[2] which is applied directly to the transformer under test for currents up to 2,500 amperes. For higher currents, use is made of a standard multiple-range transformer which is first calibrated by the resistance method on a low range and used on a higher range as a standard with which the transformer under test is then compared.

The essential circuits of the resistance method are shown schematically in figure 1. A current I_1 flows from the supply transformer through the primary of the transformer under test and through a fixed resistor R_1 of the 4-terminal type. The secondary current I_2

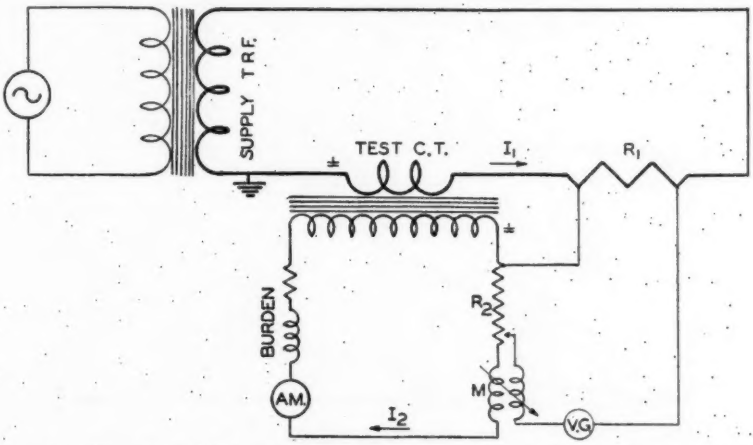

FIGURE 1.—*Circuits used in direct test of a current transformer by the resistance method.*

flows through an adjustable 4-terminal resistor R_2, through the primary winding of a mutual inductor M, and through an additional impedance, which is adjusted at the beginning of the test so as to make the resistance and the reactance of the entire secondary circuit, external to the transformer, equal to those of the burden with which the transformer is to be used in service.

Although the resistors R_1 and R_2 are made as noninductive as feasible, they have slight residual inductances L_1 and L_2, respectively. The impedance drops produced by the primary and the secondary currents are therefore $I_1(R_1+j\omega L_1)$ and $I_2(R_2+j\omega(L_2-M))$, respectively, M being considered positive when its induced emf opposes $\omega L_2 I_2$. The two circuits are connected so that these two drops oppose each other and any net difference circulates current through the vibration galvanometer *V.G.* The potential taps of the secondary standard resistor and the position of the coils of the mutual inductor are then adjusted until the galvanometer shows no deflection.

[2] For a discussion of various possible methods, see F. B. Silsbee, Trans. Am. Inst. Elec. Eng., vol. 43 p. 282, 1924.

The vector relations existing when a balance is obtained are indicated [3] in figure 2, and, on equating the magnitude and the phase of the two opposing voltages give the two equations

$$\frac{R_1 I_1}{\cos \theta_1} = \frac{R_2 I_2}{\cos (\alpha - \theta_2)} \tag{1}$$

and

$$\beta + \theta_2 = \alpha + \theta_1 \tag{2}$$

where

$$\tan \theta_1 = \frac{\omega L_1}{R_1} \tag{3}$$

$$\tan \theta_2 = \frac{\omega L_2}{R_2} \tag{4}$$

and

$$\alpha = \tan^{-1} \frac{\omega(M - L_2)}{R_2} + \tan^{-1} \frac{\omega L_2}{R_2} \tag{5}$$

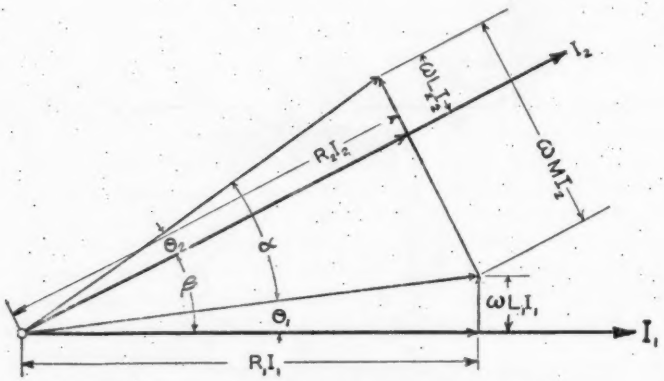

FIGURE 2.—*Vector diagram of resistance method.*

Equations (1) and (2) may be rearranged and put into more convenient form by introducing some approximations which, however, do not introduce errors of more than 0.01 percent in ratio or 0.1 minute in phase angle provided θ_1 and θ_2 do not exceed 5 minutes and 1 minute, respectively, and that β is not greater than 2 degrees. This process gives

$$n = \frac{I_1}{I_2} = \frac{R_2}{R_1} \cdot \frac{1}{\cos \beta} \tag{6}$$

$$\beta = \frac{\omega M}{R_2} + \theta_1 - \theta_2 \tag{7}$$

In equation (7) if M is expressed in henries and R_2 in ohms, β, θ_1, and θ_2 should be in radians. Since 1 radian = 3,438 minutes, equation (7) may be written

$$\beta = \frac{0.003438\ M\omega}{R_2} + \theta_1 - \theta_2 \tag{7a}$$

if M is in microhenries, R_2 in ohms and β, θ_1 and θ_2 are in minutes.

[3] For the sake of clearness the phase angles are greatly exaggerated in figure 2. The current vectors are drawn to correspond to the arrows in figure 1 and not with regard to their magnetic effect on the transformer core.

When the multiple-range transformer is used as a standard, the circuits are as shown in figure 3. It is evident that the impedance drop in the resistor R_3 plays the same role in this circuit that the impedance drop in the resistor R_1 does in that of figure 1. Also as a matter of definition, the secondary current I_3 of the standard transformer is related to the primary current I_1 by the vector relation.

$$I_3 = \frac{I_1}{n_s}(\cos \beta_s + j \sin \beta_s) \tag{8}$$

where n_s and β_s are the ratio and phase angle, respectively, of the standard transformer. Substituting this value in the expression for the impedance drop in the fixed standard resistor having resistance R_3 and phase angle θ_3 gives

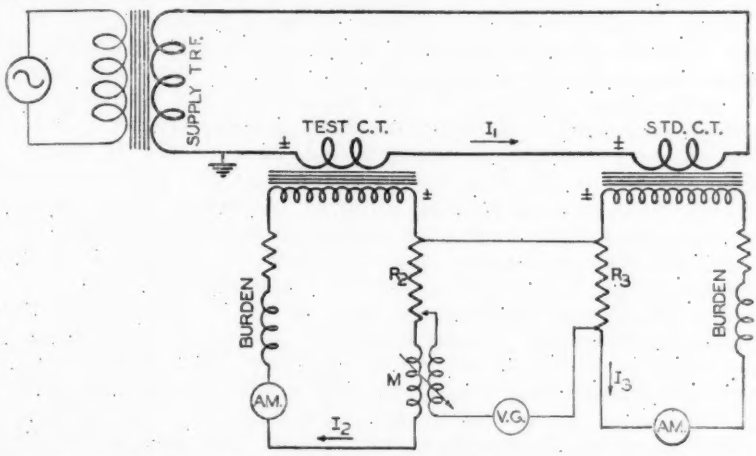

FIGURE 3.—*Circuits used in testing a current transformer by comparison with the standard current transformer.*

$$E_3 = I_3 R_3(1 + j \tan \theta_3) = \frac{I_1 R_3 \cos \beta_s}{n_s}\left\{1 - \tan \theta_3 \tan \beta_s + j(\tan \theta_3 + \tan \beta_s)\right\}$$
$$= \frac{I_1 R_3}{n_s}\left\{1 + j \tan (\theta_3 + \beta_s)\right\} \ldots\ldots \text{approx.} \tag{9}$$

the approximation being very exact since θ_3 and β_s are very small angles (less than 1 minute and 5 minutes, respectively, in the present equipment). The corresponding drop in figure 1 is

$$E_1 = I_1 R_1(1 + j \tan \theta_1) \tag{9a}$$

A comparison of (9a) and (9) shows that we need merely replace R_1 by $\frac{R_3}{n_s}$, and θ_1 by $\theta_3 + \beta_s$ to obtain the final equations for the circuits of figure 3. This process yields for the ratio and phase angle of the transformer under test

$$n_x = \frac{R_2 n_s}{R_3} \frac{1}{\cos \beta_x} \tag{10}$$

$$\beta_x = \frac{\omega M}{R_2} + \theta_3 + \beta_s - \theta_2 \tag{11}$$

When the standard transformer is connected for currents which can be carried by an available primary standard resistor, n_s and β_s can be directly observed by the resistance method. When the standard transformer is connected for ranges higher than those at which direct tests in terms of resistance can be made, the proper values of n_s and β_s must be determined by suitably modifying the results of tests at lower ranges.

The fundamental principle on which this determination can be based is that when the primary turns of a current transformer are changed from a series connection to a parallel one, the secondary winding, frequency, burden, and secondary current remaining the same, the phase angle will be unchanged and the ratio will be changed in inverse proportion to the number of series primary turns in use. It has been found experimentally without exception in a very great number of transformers tested at this Bureau that this principle holds to the same precision as that with which the transformer will repeat its performance if the connections are unchanged. The only combination of conditions which would be expected to cause the principle to fail is (1) that the impedance of the primary sections which are used in parallel shall differ so materially as to cause the currents which flow in each such section to be also materially different, and (2) that the mutual inductances of the sections in question on the secondary winding shall also be materially different.

In the multirange transformer used at the Bureau of Standards the secondary winding is distributed very uniformly around the ring core punchings so that there can be only very little difference in the mutual inductance between it and any conductor linking with the core, thus avoiding condition (2). Furthermore, any serious inequality in current distribution which might exist among the parallel paths in the primary winding would cause the net magnetomotive force to be different at different azimuths around the axis of the transformer. An exploring coil arranged to be placed in various azimuths at a constant radius from the axis of the transformer, serves as a convenient indicator of the distribution of leakage flux and hence of nonuniform magnetomotive force, and thus gives warning of the existence of condition (1).

A second principle which affords a partial check on the foregoing is that if the sections of the secondary winding are changed from parallel to series, and the impedance of the external burden is increased at the same time in proportion to the square of the ratio of the new to the old number of series secondary turns, the number of series primary turns remaining unchanged; then at the same frequency, and the same secondary ampere turns the phase angle of the transformer will be unchanged and the ratio will be increased in proportion to the increase in the number of series secondary turns.

A second and independent check on the validity of the stepping-up process is obtained by testing the multiple-range transformer on the higher range at low values of secondary current. The corresponding primary current will then not overload the primary standard resistors, and the values thus observed should agree with those inferred from the performance on the lower range at the same low secondary cur-

rent. If such an agreement is observed, the transformer can then be used as a standard at higher currents with good assurance that the conditions required for the principle to be applicable are satisfied. The extent to which the standard transformer built for this work satisfies the conditions and exemplifies these principles will appear in a later section of this paper.

III. DESCRIPTION OF APPARATUS

1. GENERAL ARRANGEMENT

Figure 4 (p. 100) shows the general arrangement and figure 5 (p. 101) a wiring diagram of the equipment as installed at the Bureau of Standards in the spring of 1930. Two independent primary, or heavy-current circuits are provided; that at *XW* for transformers having ranges up to 500 amperes, and that at *KOS* for transformers of higher range. The secondary circuits of the transformer under test and of the standard transformer are located on the L-shaped table *BENG* at a considerable distance from *U* and *O* to avoid errors from the stray magnetic fields produced by the large primary currents. The leads *R*, connecting each of these circuits to its respective transformer, are formed of a length of no. 0000 A.W.G. stranded wire placed inside of a copper tube 1.5 inches in diameter and 0.0625 inch thick. This large cross section of conductor serves to keep down the resistance of the circuit, while the tubular construction gives good mechanical stiffness and incidentally makes all stray field effects in or from these conductors entirely negligible. The switchboard *T* furnishes a source of supply for the various circuits and also contains the terminals of trunk lines connecting the laboratory with the main distribution board of the Electrical Building.

For most tests power is obtained from one or another of several motor-generator sets located in another part of the building. These sets are driven by d.c. motors which are supplied by storage batteries, thus securing very constant frequency and current. Control of the fields of both motor and generator is obtained through a remote-control system,[4] outlets from which are provided on the switchboard. These motor-generator sets range in capacity from 3 to 15 kva at 120 or 240 volts, and can be overexcited to give an open-circuit voltage of over 300 volts. The wave form is very closely sinusoidal at excitations above one fourth of normal.

For currents exceeding 6,000 amperes at 60 cycles use is made of a 100 kva motor-generator set, normally used for the life testing of incandescent lamps. This machine is driven by a 60-cycle synchronous motor from circuits of the local power company. By its use currents up to 12,000 amperes are obtainable, but only at the fixed frequency of 60 cycles per second.

The 500-ampere primary circuit (*XW* in figs. 4 and 5) is supplied by two 3 kva 120/60 to 2/4 volt 60-cycle step-down transformers *Y*. The secondaries of these transformers are permanently connected in series with each other and with a rheostat. This consists of four fixed sections of 0.025 ohm each in parallel with a 3-dial rheostat section which has a minimum resistance of 0.025 ohm. The last-mentioned section is located under the table at *J* (fig. 4), where it is accessible to operator

[4] Agnew, P. G., Stannard, W. H., and Fearing, J. L., B.S. Bull., vol. 13 (S291), p. 581, 1916–17.

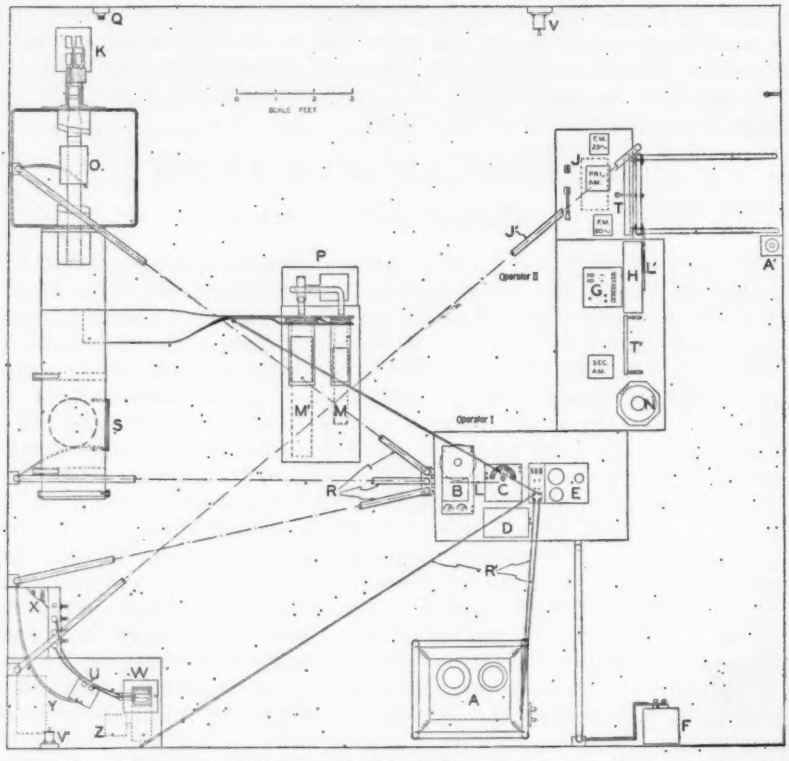

FIGURE 4.—*Arrangement of apparatus for testing current transformers up to 12,000 amperes.*

A, 25- and 60-cycle vibration galvanometers.
A', d.c. galvanometer.
B, mutual inductor.
C, secondary standard resistor for test transformer.
D, secondary standard resistor for standard transformer.
E, mercury cup selector switch.
F, air-core inductors.
G, adjustable resistance and d.c. galvonometer key panel.
H, Wheatstone bridge for measuring burden.
J, 3-dial rheostat for low-current primary circuit.
J', leads connecting *J* in parallel with *X*.
K, supply transformer for high-current primary circuit.
L, scale for vibration galvanometers.
L', scale for d.c. galvanometer.
M, 1,000-ampere oil-cooled standard resistor.
M', 2,500-ampere oil-cooled standard resistor.
N, variable inductor 10 microhenries.
O, transformer under test, range up to 12,000 amperes.
P, oil pump and motor.
Q, terminal board for primary of supply transformer.
R, secondary leads from transformers to measuring apparatus.
R', galvanometer circuit leads.
S, standard transformer.
T, supply panel.
T', secondary panel.
U, transformer under test range up to 500 amperes.
V, main supply switch.
V', low-current supply switch.
W, air-cooled standard resistor.
X, rheostat for low-current primary circuit.
Y, supply transformers for low-current primary circuit.
Z, blower for cooling standard resistor.

II. The fixed sections are located at X above the step-down transformers and can be connected in parallel with the 3-dial section by single-pole knife switches. For each test the primary circuit is completed through the transformer under test U and the primary air-cooled standard resistor W by flexible leads of dynamo brush cable.

The precision resistors used in this primary circuit are of the air-cooled type[5] and range in resistance from 0.05 to 0.001 ohm. They

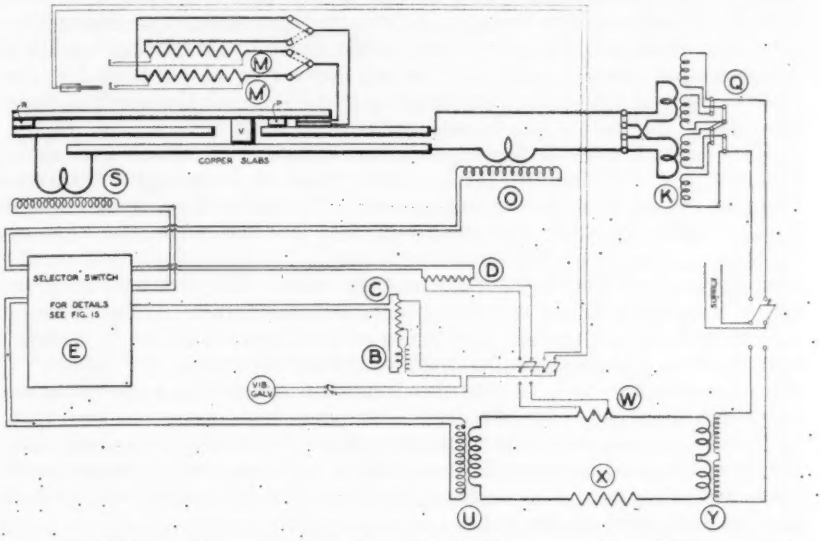

FIGURE 5.—*Wiring diagram of apparatus for testing current transformers up to 12,000 amperes.*

(Circled letters are the same as those shown in fig. 4.)
Ⓑ, mutual inductor.
Ⓒ, secondary standard resistor for test transformer.
Ⓓ, secondary standard resistor for standard transformer,
Ⓔ, mercury cup selector switch.
Ⓚ, supply transformer for high-current primary circuit.
Ⓜ, 1,000-ampere oil-cooled standard resistor.
Ⓜ′, 2-500-ampere oil-cooled standard resistor.
Ⓞ, transformer under test, range up to 12,000 amperes.
Ⓠ, terminal board for primary of supply transformer.
Ⓢ, standard transformer.
Ⓤ, transformer under test, range up to 500 amperes.
Ⓦ, air-cooled standard resistor.
Ⓧ, rheostat for low-current primary circuit.
Ⓨ, supply transformers for low-current primary circuit.

are designed to operate with a voltage drop of 0.5 volt and at this load have a temperature rise of about 5° C. Cooling is provided by a blast of air from a motor-driven centrifugal blower Z, which is located under the table which supports the standard resistor and the transformer under test. The air stream from the blower passes up a duct and through a hole $4\frac{5}{16}$ inches (11 cm) square in the table top. The standard resistor is placed over this hole when in use.

The standard resistor M (figs. 4 and 5) has a resistance of 0.0005 ohm and at its rated current (1,000 amperes) has a drop between its

[5] For a more detailed description of these standard resistors see F. B. Silsbee, B.S. Jour. Research, vol. 4, (RP133), p. 91, January 1930.

potential terminals of 0.5 volt. The larger resistor M' is rated to carry 2,500 amperes and has two sets of potential terminals corresponding to resistances of 0.00025 and 0.00020 ohm. The total power dissipation in the larger resistor between its current terminals is about 2 kw. The transfer of this heat from the resistor metal itself is effected by a stream of oil which is forced through a narrow annular passage on each side of the resistor metal by a motor-driven centrifugal pump. Under normal conditions the speed of the pump is 1,800 rpm and the oil flow is 20 gallons per minute (1,200 cm^3 per second). Since the oil passages are about $\frac{5}{32}$ inch (4 mm) wide, the oil velocity is about 2 feet (60 cm) per second and the temperature rise of the resistor metal above that of the outlet cooling oil is 11° C., at the normal rate of transfer of 1.7 watts per square inch (0.26 w/cm^2).

The inductance of these precision resistors is small and definite because the working metal has the form of a straight thin-walled circular cylinder of sheet manganin. The current returns through a copper cylinder which is inside of and coaxial with the manganin cylinder. The potential leads are attached to the outer surface of the resistor and are tied tightly against the tube. The disturbing effect of stray magnetic fields on the effective inductance of the resistor is minimized by using four complete sets of potential leads which are attached to the manganin cylinder along elements 90° apart[6] and which are connected, at suitable junction points, in parallel through equal resistances. The effective 4-terminal resistance can be adjusted as closely as desired to the nominal value by moving a tap lead along a single resistor of about 0.2 ohm, which is connected between such of these junction points as to place it effectively in parallel with a length of $\frac{3}{4}$ inch (2 cm) of the tube.

The 12,000-ampere primary circuit includes the step-down supply transformer K (figs. 4 and 5) a "cage" in which the transformer under test, O, is located, the multirange standard transformer S, and the 2,500-ampere and 1,000-ampere primary standard resistors M' and M.

The supply transformer is rated 480/240/120 to 4/2 volts, 25 cycles and has a 1-hour rated capacity of 20 kva. The primary windings can be connected in series, series-parallel, or parallel by a suitable arrangement of links on the terminal board Q. The secondary terminals are arranged for series or parallel connection by heavy copper terminal blocks and spacers. The greater voltage available with the series connection is needed only in tests of transformers of less than 1,000-ampere rating. At 60 cycles it is, of course, possible to operate this transformer at voltages considerably above the nominal rating and thus overcome the increased reactance offered by the circuit at the higher frequency.

The design of the primary circuit at the place where the transformer under test is located presented a rather difficult problem. Most transformers of the ranges tested in this circuit are used with a single primary turn, and in service are usually in a bus compartment at a considerable distance from the conductors carrying the return current in the other phases. Consequently it seemed desirable to have the return lead in the test circuit so placed as to have the least possible

[6] The resistances of these potential leads are checked periodically and before every important test in order to detect the development of any poor contact or an open circuit. For a more detailed description of these shunts see F. B. Silsbee, B.S. Jour. Research, vol. 4, (RP133), p. 91, January 1930.

effect on the transformer under test. On the other hand, the use of a wide primary loop would increase the kilovolt-amperes required from the motor-generator sets, and the resulting large stray magnetic field would constitute a potential source of error by reason of its effect in the primary standard resistors and the secondary mutual inductor. The distance from this inductor to the transformer under test was limited both by the size of the room and by the necessity of keeping down the resistance, and hence the length, of the leads connecting the transformer secondary with the inductor.

A fairly satisfactory escape from this dilemma was found in the construction shown just to the left of the supply transformer K in figure 6. The outgoing current passes through a conductor, not visible in the figure, which lies along the axis of the cagelike structure surrounding the transformer O under test, and after passing through the standard transformer or one of the standard resistors, returns through the 4 outer copper slabs which are connected in parallel by 2 vertical end slabs. The length of this "cage" is 36 inches and the "radius" approximately 20 inches. The reactance of this section of the circuit is about 190 microhms at 60 cycles and is a major part of the total impedance of the heavy current circuit. As is shown in appendix A, such a construction reduces the stray magnetic field at locations only a few feet away from the axis to a small fraction of that which would be produced by a single loop. Tests with an exploring coil at a distance of 40 inches from the axis of the cage showed a magnetic field of only 0.14 gauss with 1,000 amperes flowing. At the location of the mutual inductor the stray field was only 0.005 gauss per 1,000 amperes. At the same time the magnetic field at the core of the transformer under test is closely similar to that which would exist if the return conductor were at a very great distance.

Except in the neighborhood of the transformer under test, the heavy-current circuit is formed of wide copper slabs placed as close together as possible. For the circuit to the standard transformer which is designed for the full-rated current, these slabs are 20 inches wide by ½ inch thick and are spaced about 1 inch on centers. In the branch circuit to the oil-cooled resistors, which have a maximum rating of 2,500 amperes, the slabs are 10 inches wide by ¼ inch thick and are separated by only the thickness of a strip of varnished cambric. These slabs twist through an angle of 90° in a length of 2 feet in passing from the main slabs which are horizontal to the vertical terminals of the primary resistors. It was found feasible to bend the copper cold in this manner and thus avoid several joints.

The uppermost 20-inch slab is mounted on hinges so that it can be lifted back away from the other conductors. This gives access to the top of the standard current transformer and to the studs connecting its primary conductors to the upper transformer terminal. It is also possible by inserting either bakelite or copper spacers in the proper gaps at points R, V, P (figs. 5 and 6), to obtain any of the circuit combinations listed in table 1. A similar set of insulating or conducting spacers enables either or both standard resistors M and M' to be connected in series with the 10-inch slabs.

TABLE 1.—*Circuit combinations possible with primary circuit shown in figures 5 and 6*

Circuit combination	Between slabs at R	Between upper and lower slabs at V	Between upper and center slabs at P
Test transformer and standard resistor only	Bakelite	Copper	Bakelite.
Test and standard transformers only	Copper	Bakelite	Copper.
Test and standard transformers and standard resistors	do	do	Bakelite.

2. STANDARD TRANSFORMER

The standard transformer was designed so as to satisfy as completely as possible the requirements outlined above for having the same ratio factor and phase angle on different primary connections. The core is of silicon-steel ring punchings 12 1/16 inches (20.7 cm) outside diameter, 7 3/16 inches (19.8 cm) inside diameter, and 0.014 inch (0.36 mm) thickness. The core contains 36 pounds (17 kg) of this material and forms a stack 2 1/8 inches (5.4 cm) thick. While the use of the newer nickel-iron alloys would have reduced the magnitude of the phase-angle and ratio errors, it was felt that they would not have been so small that corrections could have been neglected entirely. The mere reduction in the magnitude of the corrections was not considered a sufficient improvement to justify the very considerably greater cost of a core of nickel-iron alloy.

The secondary winding has a total of 2,400 turns of no. 12 A.W.G. single cotton and enamel covered wire. To minimize the danger of breakdown of insulation between turns, the winding is formed of 20 sectors each subtending an angle of 18° around the periphery of the core. Each sector is insulated from the core and from the adjacent sectors by at least two thicknesses of varnished cambric. Each of the sectors contains three separate coils, also carefully insulated, which have 96, 20, and 4 turns, respectively. The terminals of the 60 coils thus formed are brought to the outside of the secondary winding and there grouped to form 12 windings, of which 4 have 480 turns each, 4 have 20 turns each, and 4 have 100 turns each. In this grouping the five individual coils which are joined in series to form a winding are selected from sectors spaced 72° apart. Consequently the magnetomotive force produced by any one winding is distributed equally over five equidistant sectors of the core. Because 5 is not a factor of 24 (the number of primary turns), this spacing of the secondary sectors prevents any secondary winding from having a materially closer coupling to any one group of primary turns than to any of the others.

At the terminal board each 20-turn winding is joined in series between the 480-turn and the 100-turn windings which are located in the same set of five sectors. There are thus formed in effect 4 equal sections, each having a total of 600 turns with taps at 500 turns and at 480 turns. Links are provided for readily changing taps and also for connecting the four sections in series, series-parallel or parallel. It is thus possible to obtain a uniform turn distribution with 480, 500, 600, 960, 1,000, 1,200, 1,920, 2,000, or 2,400 turns. The resistance of the complete winding is about 4 ohms. The weight of the secondary copper is about 47 pounds (22 kg). The core and secondary

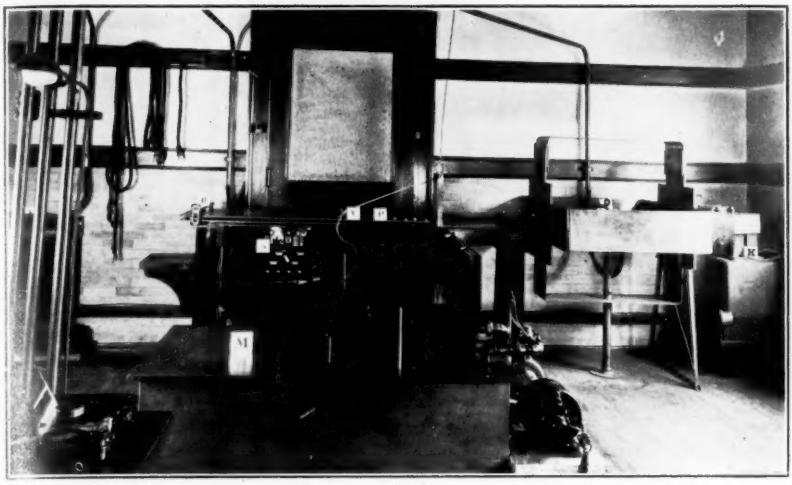

FIGURE 6.—*Primary circuit for testing current transformers, range up to 12,000 amperes.*

S, Standard current transformer; O, Transformer under test; K, Supply transformer; M, Tank containing oil-cooled standard resistors.

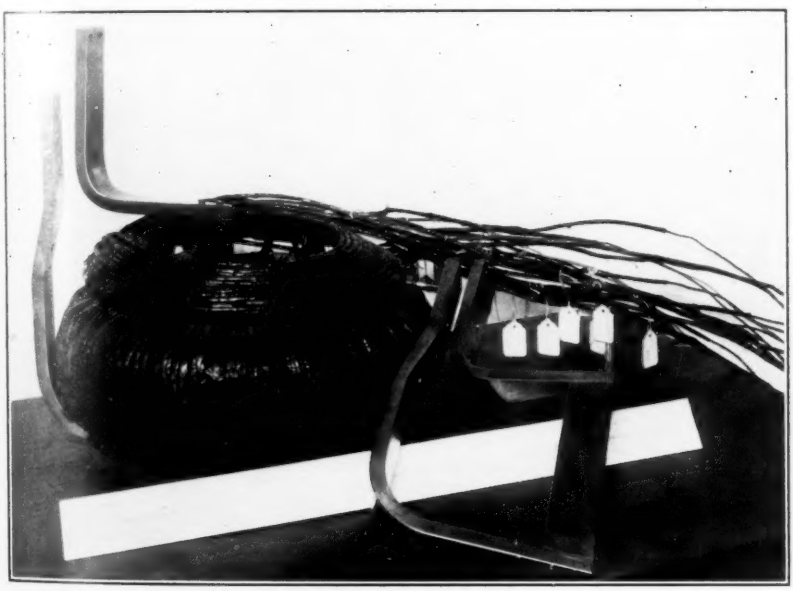

FIGURE 7.—*Completed wound core of standard current transformer showing the secondary winding and two primary turns, one in its normal position.*

UNIV. OF MICH.

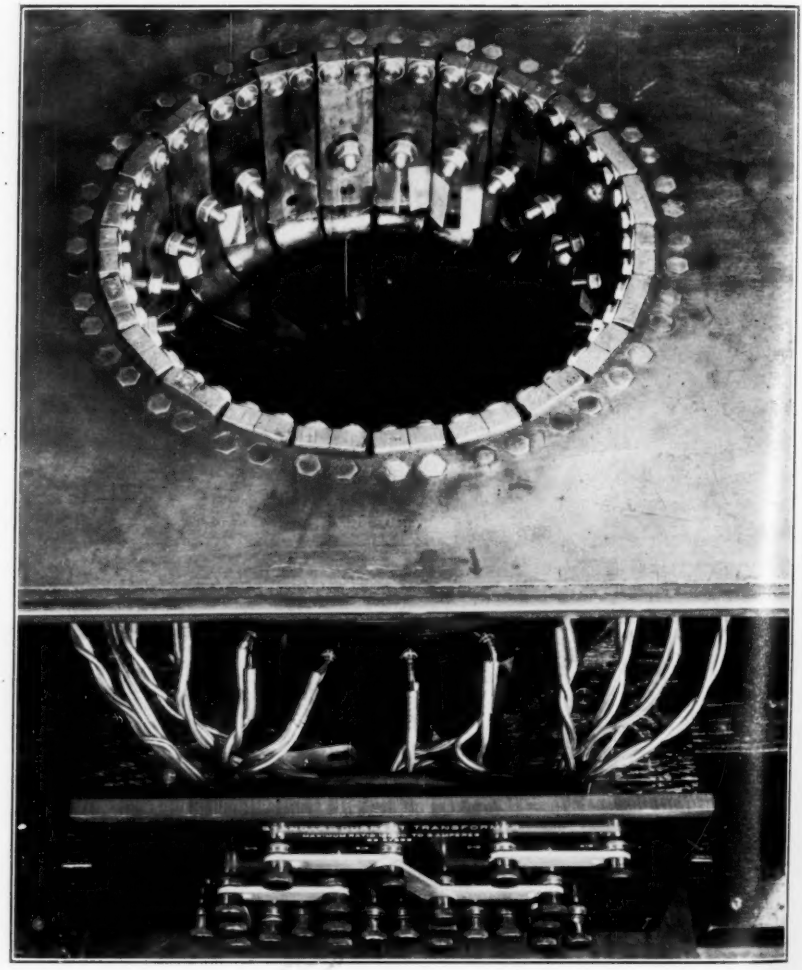

FIGURE 8.—*Completed standard current transformer in place.*

winding were vacuum impregnated[7] with insulating compound to form a very solid permanent unit. Figure 7 shows the completed secondary winding with the leads which connect the separate coils to form the windings.

As a further safeguard against failure of the secondary insulation, two safety spark gaps are provided. These are shunted around two of the 480-turn windings and break down at a potential difference of only a few hundred volts, thus short circuiting the winding and relieving it of electric stress in case the external secondary circuit should be accidentally opened.

Figure 8 shows the external appearance of the completed transformer as seen from above with the 24 primary turns which encircle the core and secondary winding connected in parallel to the upper terminal slab. Figure 9 shows a vertical cross section. The openings in the upper and lower terminal slabs (*D* and *E* in fig. 9) are machined to form regular polygons of 24 sides; that in the upper slab being observable in figure 8. Each primary turn consists of a sector-shaped bar which passes through the central opening in the transformer and two L-shaped pieces, such as *B* and *C* in figure 9. Two complete turns are shown in figure 7.

Each of the sector-shaped bars has a left-hand twist of 15° between its end faces. Because of this each outer bar *C* lies opposite that face of the polygon *F* which is next, in a counterclockwise direction (as seen from above), to the face which is opposite the inner bar *B* of the same turn. The result of this twist is that if a bolt is inserted at *b*, it pulls the *C* bar of one turn into contact with the *B* bar of the next turn, thus connecting the two turns in series. The upper L-shaped pieces, *B*, extend through an opening in the lower terminal slab *E*, and can be pulled into contact with the upper slab *D*, if desired by two ¼-inch cap screws. The lower L-shaped pieces *C*, extend only high enough to permit of connection to the cast copper flange *F* which in turn is bolted to the lower terminal slab *E*.

Removal of the cap screws and the insertion of a thin strip of insulating material at *e* serves to insulate this junction from either terminal of the transformer, the bar *C* springing enough if bolt *a* is absent to be held out of contact with flange *F*. As many adjacent turns as desired may thus be connected in series. Each group of such series turns is connected to the terminal slabs by screws at *a* and *e* at the end bars of the group, and is thus put in parallel with other similar groups. The number of series primary turns of the transformer may thus be made equal to any of the eight integral factors of 24.

The joints at *m* and *d* are silver-soldered. The joints *d* had to be soldered after the core and secondary winding were in place. It was found that the primary bars could be heated to the brazing temperature very conveniently by sending about 7,000 amperes through them. This electric heating avoided the risk of injuring the secondary winding which would have been incurred if the joints had been brazed with a gas flame.

The primary turns are insulated from the secondary windings by the ¼-inch bakelite ring *f* on which the secondary winding rests and by cylindrical shields of 1/32-inch sheet bakelite at *g* and *h*. The bars

[7] Through the courtesy of the General Electric Co., the impregnating process was carried out at their West Lynn works.

A are spaced apart by 1/32-inch bakelite strips, *j*, and are anchored symmetrically by the cap screws which fasten the bars *C* to the bakelite ring *k*.

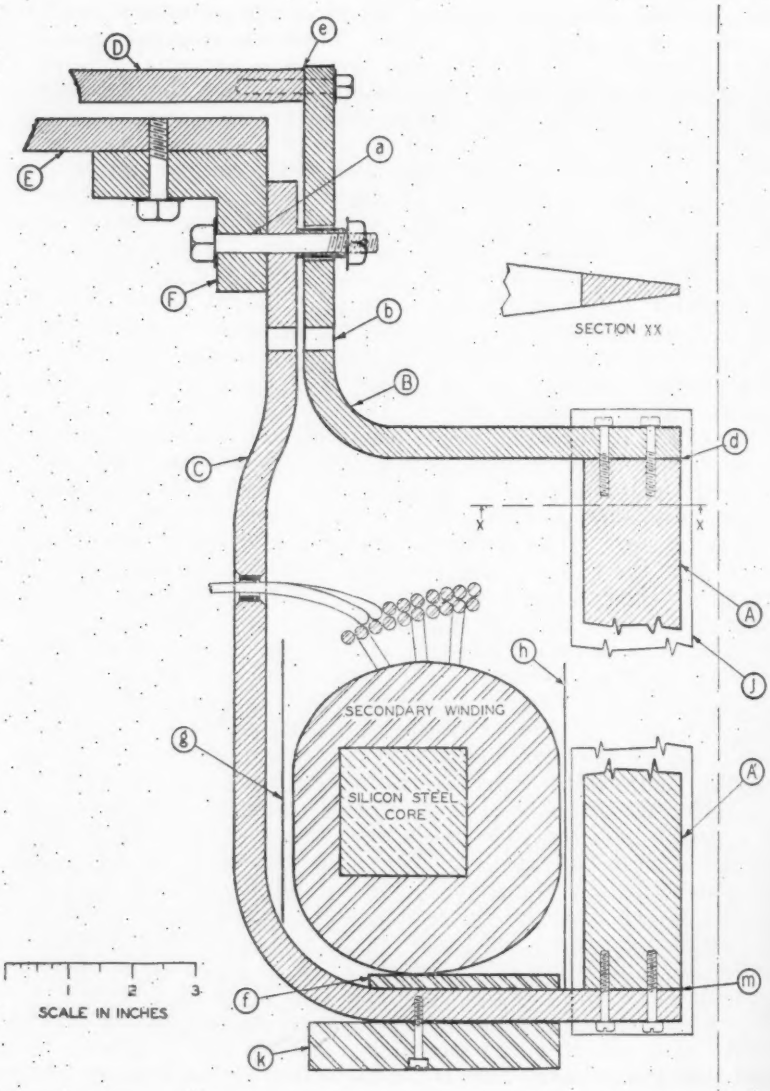

FIGURE 9.—*Vertical cross section of standard current transformer.*
(Bars *A-B* are part of the next turn adjacent to that formed by bars *A'-C*.)

As will be noted from figure 9, there is a considerable clearance in a vertical direction between the secondary winding and the primary turns. This spacing was allowed to permit of soldering the upper joint without damage to the insulation, although it materially increases the primary leakage reactance. The reactance of the

primary, when all 24 turns are in series and the secondary is short-circuited, is 7,400 microhms at 60 cycles, while the effective resistance is 2,360. The resistance computed from the dimensions of the bars and the resistivity of copper is 840 microhms and the losses in the short-circuited secondary may account for a resistance of perhaps 400. The excess of 1,120 microhms remaining is presumably mainly due to skin effect. All the contact surfaces both of the bars and of the faces of the two 24-sided polygonal openings in the terminal slabs are gold plated, with the result that the resistance of the average contact is only 2.5 microhms.

Of the two factors which might combine to introduce an error when the transformer is used on a higher range than that on which it was calibrated, the first (inequality in current distribution among the primary turns) has been studied in some detail. The variations in contact resistance among the various parallel paths ordinarily do not amount to more than 4 microhms, or about 4 per cent of the total resistance of a single primary turn. In order that the length of path and hence the resistance offered to the portions of current flowing to the several primary turns may be as nearly equalized as possible, the two terminal slabs are extended in opposite directions from the transformer, so that, at any instant, the current after passing through the primary winding flows away from the transformer in the same absolute direction as that in which it approached. As a result the system, as regards resistance, is symmetrical about a plane passing through the axis of the transformer at right angles to the axis of the terminal slabs. The transformer is, of course, also symmetrical about the plane containing its axis and that of the slabs. The result of this twofold symmetry is that the resistances of the current paths are the same for the four quadrants into which these planes divide the transformer. Unfortunately the current in the uppermost horizontal slab does not completely neutralize the magnetic effects of the currents in the two slabs below it, and the resulting voltages induced in the primary turns somewhat affect the current distribution.

Curve *A* of figure 10 shows the distribution of current among the various bars at 25 cycles per second, when all 24 were connected in parallel, as indicated by measuring the impedance drop on a length of about 7 inches of each bar by an a. c. potentiometer. The axis of the terminal slabs lies between bars 1 and 2 and between bars 13 and 14.

The use of an exploring coil (100 turns of 10 cm^2 area located 1 cm outside of the outer bars) gives a more convenient though less direct measurement of the distribution of current and magnetomotive force around the transformer. The coil is placed in succession opposite the center of each primary bar, the plane of the coil being radial so that the tangential component of the magnetic field is effective in inducing an electromotive force in it. This induced voltage is balanced by that induced in a mutual inductor carrying the secondary current of the transformer. The results are expressed as the leakage field intensity in gilberts per centimeter, per primary ampere turn.

In figure 10, curve *C* gives the result obtained when all 24 primary turns were connected in series and necessarily carried the same current. The fluctuations from bar to bar can be explained in part as resulting from slight inequalities in the location (both radially

and tangentially) of the individual primary bars, and in part from similar inequalities in the spacing of the sectors of secondary winding. The small absolute magnitude of this stray field is made evident by the arrows which indicate that the maximum field intensity is less than 3 percent of that existing just inside of the primary turns.

Curve *B* was obtained when all 24 turns were in parallel. The differences between curves *B* and *C* are presumably the result of differences in the magnitude of the current flowing in the several bars and of the stray magnetic field of the loop formed by the terminal slabs at the top. To greatly exaggerate these inequalities curve *D* was obtained when 23 turns were connected in series, bar no. 2 being

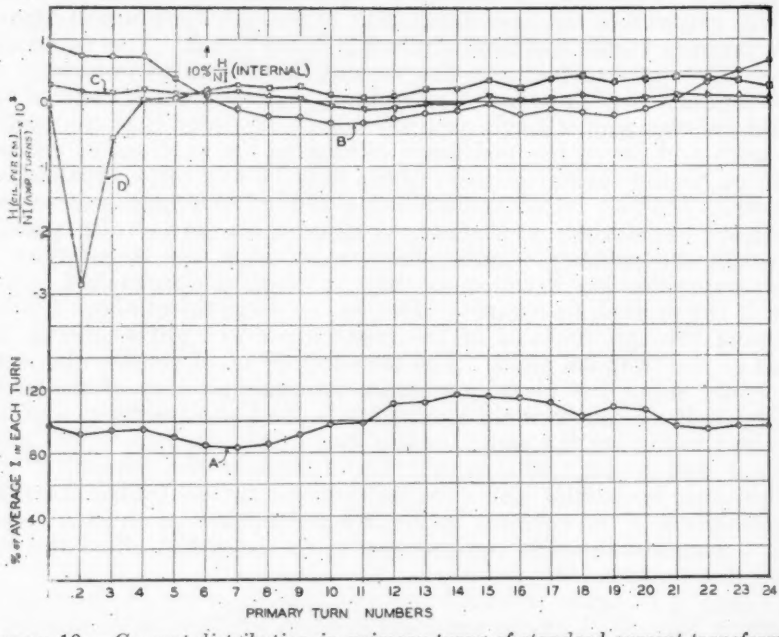
10% H/NI (INTERNAL)
C
B
D
A
% of AVERAGE I in EACH TURN
120
80
40
1 2 3 4 5 6 7 8 9 10 11 12 13 14 15 16 17 18 19 20 21 22 23 24
PRIMARY TURN NUMBERS

FIGURE 10.—*Current distribution in primary turns of standard current transformer and stray magnetic field around transformer.*

Curve *A*, percent of average current per turn in each turn when all turns are in parallel.
Curve *B*, tangential magnetic field outside at central plane of each turn when all turns are in parallel.
Curve *C*, tangential magnetic field outside at central plane of each turn when all turns are in series.
Curve *D*, tangential magnetic field outside at central plane of each turn when 23 turns are in series (turn no. 2 being disconnected).

omitted from the circuit. The stray field opposite this bar is seen to be six times the greatest difference between the normal curves *C* and *B*, yet the ratio factor and phase angle of the transformer as a whole were found to be the same as under normal conditions to within 0.01 percent and 0.1 minute.

The second factor (inequalities in the coupling between individual primary bars and the secondary winding) was checked experimentally by measurements of ratio factor and phase angle when only one primary turn was used. Under these conditions the transformer operates with only 500 ampere turns and has a correspondingly mediocre performance, but of the six representative primary turns measured there was no departure from the mean exceeding 0.03 percent in ratio factor or 2 minutes in phase angle. Since each primary

turn only contributes one twenty-fourth of the total magnetomotive force, the slight inequalities in current distribution and coupling would not be expected to combine to make the ratio factor with turns in parallel differ appreciably from that with turns in series.

An alternative basis can be obtained from the following data for judging the degree to which this transformer satisfies the requirements outlined above as being necessary and sufficient for the correct extrapolation of its ratio and phase angle to higher ranges of current. When used with only 500 secondary turns the ratio and phase angle may be directly measured by the resistance method for all 8 combinations of primary turns. The results of such a series of measurements are given in tables 2 and 3 for ratio factor and phase angle respectively. The changes in these quantities with change in primary grouping are seen to be less than 0.02 percent and 1 minute respectively.

TABLE 2.—*Ratio factor of standard transformer with 500 secondary turns and burden of 96μh and 0.284 ohm*

Ratio	Secondary current in amperes					
	0.5	1	2	3	4	5
500/1	1.0001$_6$	1.0002$_2$	1.0002$_4$	1.0002$_5$	1.0002$_2$	1.0002$_0$
500/2	1.0001$_4$	1.0002$_2$	1.0002$_1$	1.0002$_2$	1.0002$_3$	1.0001$_9$
500/3	1.0001$_9$	1.0002$_4$	1.0002$_5$	1.0002$_5$	1.0002$_5$	1.0002$_3$
500/4	1.0002$_1$	1.0002$_7$	1.0002$_9$	1.0003$_1$	1.0003$_1$	1.0002$_9$
500/6	1.0002$_5$	1.0002$_8$	1.0003$_1$	1.0003$_0$	1.0003$_0$	1.0002$_6$
500/8	----------	1.0003$_0$	1.0003$_2$	1.0003$_1$	1.0003$_0$	1.0003$_0$
500/12	1.0003$_2$	1.0003$_5$	1.0003$_8$	1.0003$_6$	1.0003$_3$	1.0002$_9$
500/24	1.0002$_7$	1.0003$_0$	1.0003$_2$	1.0003$_2$	1.0003$_2$	1.0003$_0$

TABLE 3.—*Phase angle (in minutes) of standard transformer with 500 secondary turns and burden of 96μh and 0.284 ohm*

Ratio	Secondary current in amperes					
	0.5	1	2	3	4	5
500/1	11.1	9.1	7.3	6.4	5.9	5.4
500/2	11.3	9.4	7.5	6.6	5.9	5.5
500/3	10.9	9.1	7.2	6.3	5.7	5.3
500/4	11.4	9.6	7.5	6.6	5.9	5.5
500/6	10.5	9.2	7.4	6.4	5.8	5.4
500/8	----------	9.3	7.5	6.6	5.8	5.5
500/12	10.7	9.4	7.5	6.5	5.9	5.5
500/24	11.0	9.5	7.6	6.6	6.0	5.5

The agreement of the transformer with the second general principle set forth above is shown by figure 11, in which values of secondary ampere-turns are plotted as abscissas and values of ratio factor and phase angle as ordinates. Data were obtained for three different numbers of secondary turns and for each the external burden was kept proportional to the square of the number of secondary turns. It is seen that the observed points all lie on a common curve, thus strengthening the validity of the extrapolation to higher currents.

3. ADJUSTABLE STANDARD RESISTOR

The adjustable standard resistor used in the secondary circuit of the transformer under test is shown diagrammatically in figure 12. The general mechanical arrangement is indicated in (*a*) while the connections are shown schematically in (*b*).

The resistor consists of a closed loop of resistance alloy. Coarse adjustment (in steps of 0.01 ohm) is obtained by plugs (as at *EF*) which fix the points at which the current enters and leaves the loop (as in an Ayrton shunt); while two steps of fine adjustment are obtained by sliding the two potential taps on the opposite side of the loop.

Between *A* and *B* (shown at the bottom of figure 12(*b*)) is a strip of resistance alloy 0.78 inch (2 cm) wide, 0.01 inch (0.027 cm) thick, and 55 inches (139 cm) long. This has a resistance of about 0.118 ohm and carries the bulk of the secondary current. With the plugs

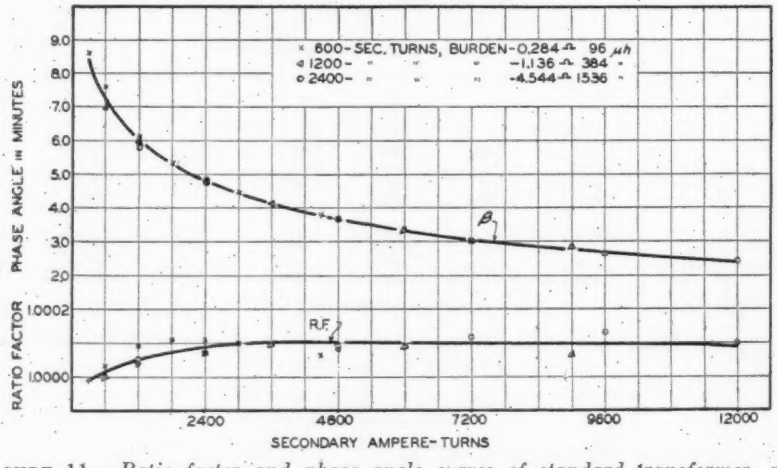

FIGURE 11.—*Ratio factor and phase angle curves of standard transformer, primary consisting of two groups of turns in parallel, each group having 12 turns in series.*

as shown, the current enters this strip at *E* and leaves at *F*. In parallel with *AB* is a second circuit GP_1P_2H which has a resistance of 10.7 ohms. One of the potential terminals P_1 is connected to a sliding contact on a 0.1 ohm slide "wire" [8] 21 cm long, which forms one end of this shunt circuit, while the other P_2 connects to the contact arm which runs over the set of 13 studs separated by 0.1-ohm coils which form the other end of the circuit GP_1P_2H. Between the slide wire and the studs is a fixed coil of 9.4 ohms.

If R_p denotes the resistance of the branch *GH* between the potential taps P_1 and P_2, R_c the resistance of the branch *AB* between the plugs *E* and *F*, and *S* the total resistance of the entire closed loop of resistance material GP_1P_2HBFAG, the resistance of the two circuits in parallel between branch points *E* and *F* is given by $R_c(S-R_c)/S$. The fraction of this resistance which is spanned by the taps P_1P_2 is

[8] This slide "wire" is formed of an alloy strip 0.027 cm thick and 0.36 cm wide set on edge and bent into the form of a circular arc of 8 cm radius. The contactor touches the edge of the strip as shown in section at *XX* of figure 12.

$R_p/S-R_c$. Hence the effective resistance R_2 of the 4-terminal combination, using E and F (or C_1 and C_2) as current terminals and P_1 and P_2 as potential terminals, is

$$R_2=\frac{R_pR_c}{S} \tag{12}$$

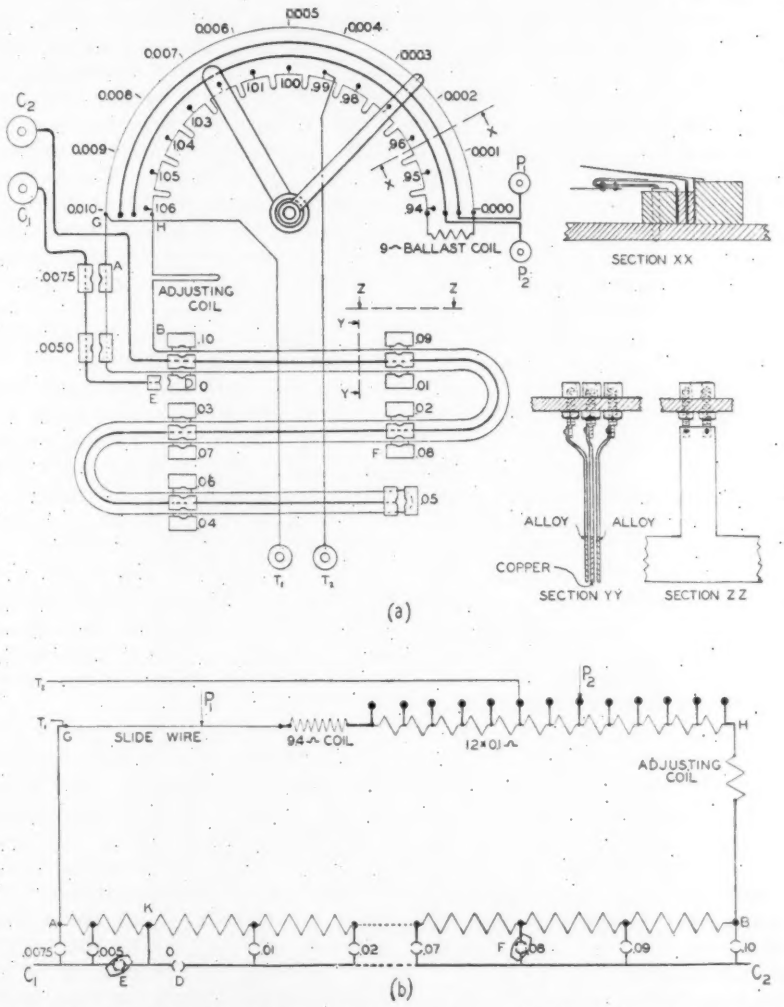

FIGURE 12.—*Standard resistor used in secondary circuit of transformer under test.*

Since S is independent of the settings of the plugs or sliders, the effective resistance for any given setting of R_c is proportional to the resistance R_p between P_1 and P_2. The inner end of the slide wire is marked "0" and the central stud is marked "1.00." The resistance of the branch circuit between these points is adjusted to be 10 ohms. Consequently each step of the contact arm P_2 changes

R_p and hence R_2 by 1 percent. The entire range of the slider is also 1 percent, and as it is furnished with a 100-division scale, settings can be read to 0.1 division or 0.001 percent.

An adjusting coil of about 0.16 ohm is inserted between H and B and serves to make the total resistance S exactly 1,000 times the resistance (0.01097) of R_c between adjacent plug taps. When P_1 and P_2 are set to read 100 percent and, therefore, $R_p = 10$ ohms, the effective 4-terminal resistance is by equation (12) exactly 0.01 ohm for each step between plugs E and F. The plug blocks marked 0.005 and 0.0075 to the left of E in figure 12 (b) allow of increasing the resistance above that corresponding to the plug at F by the fractional steps indicated. In use the plugs are so inserted that the nominal resistance is equal to the product of the resistance of the primary standard resistor multiplied by the transformer ratio. The settings of P_1 and P_2 then indicate directly the true ratio of the transformer in terms of its nominal ratio. This resistor has the additional merit that the resistance inserted in the secondary circuit of the transformer under test is only slightly greater (10 percent) than the effective 4-terminal resistance needed for the measurement.

A number of precautions have been taken to minimize the effective inductance of the apparatus. As shown in cross section at YY (fig. 12) the alloy strip is doubled back on itself and a copper strip constituting the lead DC_2 of figure 12 (b) is placed between the two alloy strips separated only by thin mica insulation. The inductance of this arrangment of conductors can be computed for each plug position, and the phase angle of the resistor is about 0.3 minute at 60 cycles. The 9.4-ohm coil and the 0.1-ohm steps in the high-resistance branch circuit are wound bifilar. As shown in the section on XX, the contact arms to the slide wire and to the studs serve merely to bridge across to one of the two copper arcs which connect to the potential binding posts. In this way, no loops of appreciable area are formed in the potential circuit for any position of the contact arms and the resistor is therefore not subject to inductive effects from stray magnetic fields.

To facilitate measuring its 4-terminal resistance by means of a Kelvin double bridge, additional potential terminals T_1T_2 are permanently soldered to the end of the slide wire and to the "0.99" stud. The use of these test terminals eliminates the four sliding contacts with their possible variations in resistance from the ratio-arm circuits of the double bridge. The initial calibration of the apparatus can be accomplished by the use of two potentiometers, by the Mathiessen-Hockin method, or, when the contacts are in good condition, by careful work with the double bridge, using the normal potential terminals. Periodic checks to verify the constancy of the effective resistance can then be made with the double bridge, using the test terminals.

The resistor has its maximum resistance at a temperature of 14° C. and decreases by 0.01 percent for a temperature rise of 13° C. above this point. For the most precise work it is therefore necessary to apply a correction for these resistance changes, allowing also for the temperature rise produced by the current, which is about 6° C. at 5 amperes.

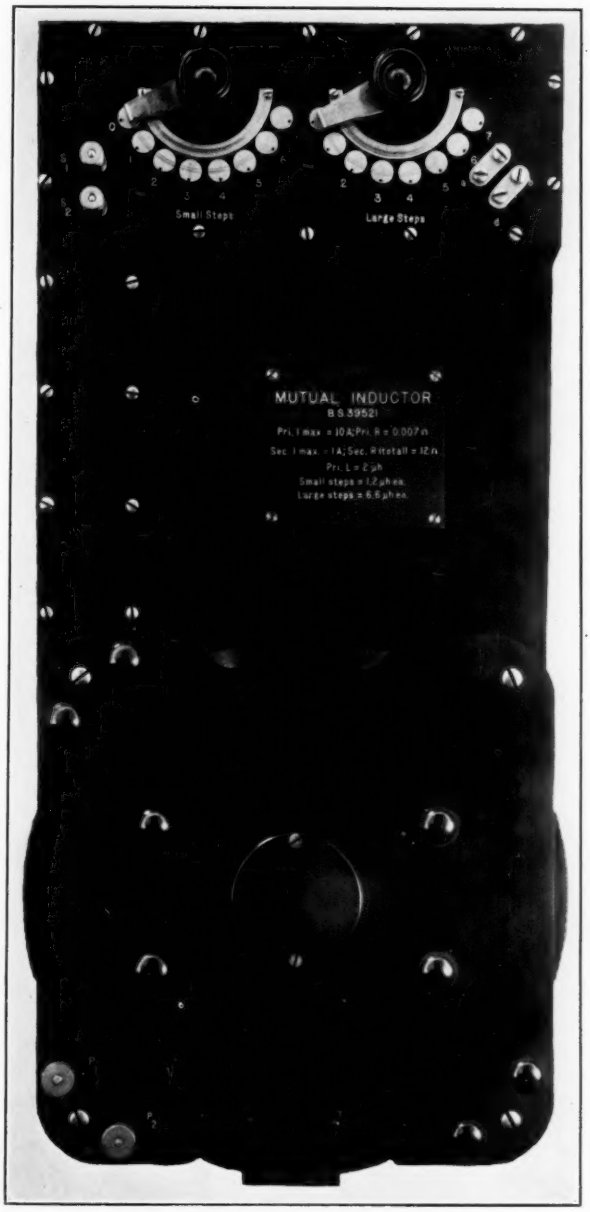
Small Steps
Large Steps
MUTUAL INDUCTOR
B.S.39521
Pri. I max. = 10 A; Pri. R = 0.007 Ω
Sec. I max. = 1 A; Sec. R total = 12 Ω
Pri. L = 2 μh
Small steps = 1.2 μhen.
Large steps = 6.6 μhen.

FIGURE 13.—*Mutual inductor.*

UNIV. OF MICH.

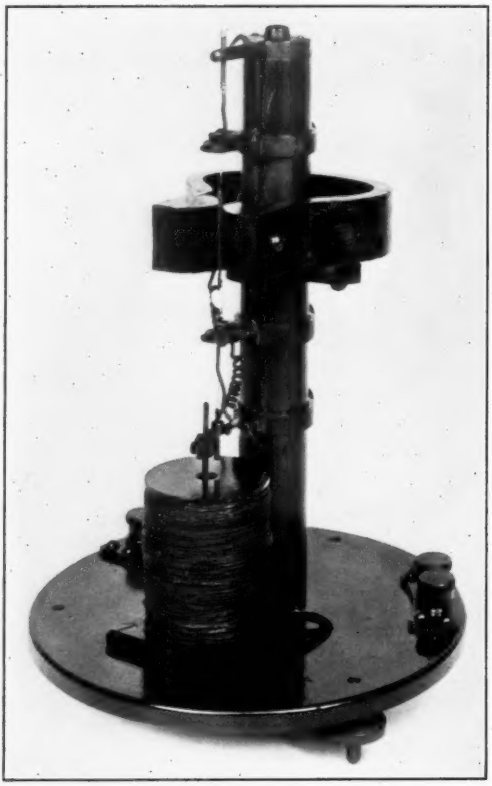

FIGURE 14.—*Vibration galvanometer used for 25-cycle tests, as equipped with solenoid for remote tuning.*

4. MUTUAL INDUCTOR

The mutual inductor (fig. 13) used to measure the phase angle of the transformer under test has a maximum value of 56 μh. The primary circuit has a resistance of 0.007 ohm and an inductance of only 2 μh. The burden thus imposed on the transformer under test is very small and can readily be allowed for in making up the total burden to any desired value. The secondary circuit is composed of three parts: (1) A set of 7 fixed sections each giving 6.6 μh, (2) a set of 7 fixed sections each giving 1.2 μh, and (3) an adjustable coil mounted so that it can be moved with respect to the fixed coils. The mutual inductance between this third section and the primary may be varied continuously from -1.0 μh through zero to $+1.3$ μh.

The arrangement of primary and movable secondary coils is, in general, similar to that described by Brooks and Weaver,[9] and the molded bakelite parts in which the coils are mounted are identical with those used in the Brooks inductometers regularly manufactured by the Leeds & Northrup Co. Because of the small number of turns needed for the low range of this instrument, and the space required for the fixed sections of the secondary winding, the primary turns do not occupy the entire winding space, and the scale law is not quite so linear as in a normal inductor.

The primary windings consist of four turns, one in each recess of the upper and lower plates. To minimize skin effect and eddy currents this winding is made of litzendraht wire having 189 strands (3 by 3 by 3 by 7) of no. 32 enamel-covered copper wire. The two turns in the lower plate lie against the outer wall of the recesses while those in the upper plate are located at the inner edge of the normal winding space.

The secondary winding on the movable disk consists of eight turns of no. 17 litzendraht wire. Four turns are wound pancake fashion in the central plane of each oval, the turns being spaced radially with heavy cord. The fixed sections are wound with a stranded conductor formed of seven no. 24 copper wires each insulated with enamel and silk. Each of the 7 strands forms 1 of the 7 steps of the appropriate section of the winding, and by reason of this construction the several steps differ in mutual inductance by less than one half percent. The small steps consist of 8 turns, 4 turns being wound outside of the single primary turn in each recess of the upper plate. The large steps consist of 40 turns, 20 turns being wound inside of the single primary turn in each recess of the lower plate.

The terminals of the various sections of the secondary winding are brought to a terminal block mounted 8 inches away from the nearest point of any coil to avoid magnetic coupling between the connecting leads and the primary turns. Two dial switches serve to insert any desired number of the fixed steps in series with the movable coil. For purposes of calibration, links and plug sockets are provided by which the secondary electromotive force of the movable coil can be opposed in succession to that of each small fixed step, and also so that the movable coil, together with the first five small steps, can be opposed to each one of the large steps. In this way the relative values of mutual inductance of the steps and of the movable coil can be readily determined. The calibration of the scale of the movable coil relative

[9] Brooks, H. B., and Weaver, F. C., B.S.Bull. vol. 16 (S290), p. 569, 1916.

to some one scale point can be made by opposing its electromotive force to the resistance drop in a calibrated slide wire which is carrying a current in quadrature with that flowing in the primary of the mutual inductor. A single direct measurement of the mutual inductance, when all sections of the secondary are aiding, then completes the calibration of the apparatus.

The scale engraved on the movable disk is laid off in uniform divisions subtending 1° each, and is probably decidedly more accurate than would be the case if an attempt had been made to lay it off electrically to fit the scale law of the apparatus. Errors from parallax are minimized by using a special form of fiducial mark. A block of plate glass 0.5 inch (1.3 cm) thick is embedded in the upper plate of the inductor. The index mark consists of a fine radial line etched on the lower surface of this glass block which is close to the scale. A small "*X*" mark etched on the upper surface of the block directly above the index mark enables the observer to place his eye in line with these two marks and insures that his line of sight is always at the same definite angle with the scale.

5. VIBRATION GALVANOMETERS

The vibration galvanometers used to indicate the balance of alternating potential drops are of the moving-coil type. One of these, used for 25-cycle tests, was built in the instrument shop of the Bureau of Standards. The other galvanometer, which is used for tests at 60 and at 50 cycles, was built by Robert W. Paul, Ltd., but has been greatly modified to adapt it to the present work. The 25-cycle galvanometer is shown in figure 14. The moving coil of each galvanometer consists of 10 turns of no. 32 A.W.G. enameled wire stretched taut between suspensions of copper strip. Rough adjustment of the natural frequency of vibration of the coil is obtained by adjusting the distance between the clamps which hold the suspensions. The lower end of the lower suspension strip carries a small iron plunger which hangs inside a solenoid. Adjustment of the direct current flowing in this solenoid changes the pull exerted on the suspension and affords fine adjustment of the natural frequency of the instrument. Thus tuning for maximum sensitivity becomes a very simple process, for the solenoid current may be adjusted while the observer is watching the amplitude of the deflection.

The sensitivity of each galvanometer is about 0.3 mm/μv at its terminals with a scale distance of 1 m. The sensitivity drops to about one half of this value for a change of 8 percent in frequency. The resistance of each galvanometer is about 1 ohm.

The galvanometers are mounted on a special support to avoid disturbance from external mechanical shocks. This support consists of a large concrete block (12 by 16 by 25 inches) which is hung on four large helical steel springs. The natural frequency of oscillation of this system is very low and the small impulses of higher frequency which are transmitted to it are effectively absorbed by a layer of hair felt about 1 inch (2.5 cm) thick which is placed between the top of the concrete block and the board on which the galvanometers stand.

IV. TEST PROCEDURE

When a current transformer is received for test the insulation between primary and secondary windings is first tested with a 1,000-volt megger. Its primary terminals are then connected in series in the primary circuit (fig. 5) appropriate to the range of the transformer. A standard resistor capable of carrying the rated primary current of the transformer is also connected in this circuit. The value of secondary standard resistor to use is thus fixed as equal to the product of the resistance of the primary resistor multiplied by the ratio of the transformer. If the primary current exceeds 2,500 amperes, the primary shunt is not used, but the primary terminals of the standard transformer are so connected as to give it about the same primary current rating as that of the transformer under test. A 5-ampere resistor (R_3) of convenient value is connected to the secondary terminals of the standard transformer. The value of the standard resistor (R_2) in the secondary of the transformer under test is then determined from the equation $R_2 = R_3\, n_x/n_s$ where n_x is the nominal ratio of the transformer under test, and n_s is the nominal ratio of the standard transformer.

The resistance of the secondary circuit of the transformer under test is then measured with a Wheatstone bridge to make sure that it is definite and not abnormally high as the result of broken wires or poor contacts. In this measurement the bridge current is kept very small (less than 10 milliamperes) to avoid magnetizing the transformer appreciably.

The next step in the test is the adjustment of the secondary burden to duplicate that specified by the customer. The desired inductance is made up by including in the circuit the proper combination of air-cored reactance coils. A set of eight such coils wound with 0.162-inch square wire gives values of inductance up to 1,100 μh in steps of 10 μh, with a time constant ranging from 0.002_5 to 0.017 second. Other coils of somewhat lower time constant are available to give burdens up to 8,000 μh. Fine adjustment of the inductance is obtained by two inductors of the Brooks type which have ranges of 1,100 and 10 μh, respectively.

The resistance of the burden is adjusted by a set of fixed resistors connected to a set of contact plugs which give a range of 1.1 ohm in steps of 0.01 ohm. The smallest step can be bridged by a continuously adjustable resistor formed by a mercury column 0.12 inch (3 mm) in diameter and 8 inches (20 cm) long. An amalgamated copper wire forced down into the mercury effectively short-circuits any desired fraction of the mercury resistor. The resistance of the burden is adjusted experimentally to the desired value as shown by the Wheatstone bridge, thus allowing for changes in the resistance of the circuit resulting from temperatures changes. This adjustment is made to an accuracy of about 0.001 ohm. The mercury-cup selector switch (fig. 15) with its two sets of links provides a convenient means of making connections between either of the current transformer secondaries, the Wheatstone bridge, and the burden. The shunt S when applied to the bridge ratio arm A serves to make the total resistance of the arm XY, including the lead to Y, equal to the nominal value of A. Arms R and B are of much higher resistance so that the lead from Z to R has a negligible effect.

The secondary precision resistor, the primary winding of the mutual inductor and a certain amount of lead resistance are necessarily in the secondary circuit of the transformer under test. This minimum burden for a resistance setting of 0.05 ohm is 0.11 ohm. When the

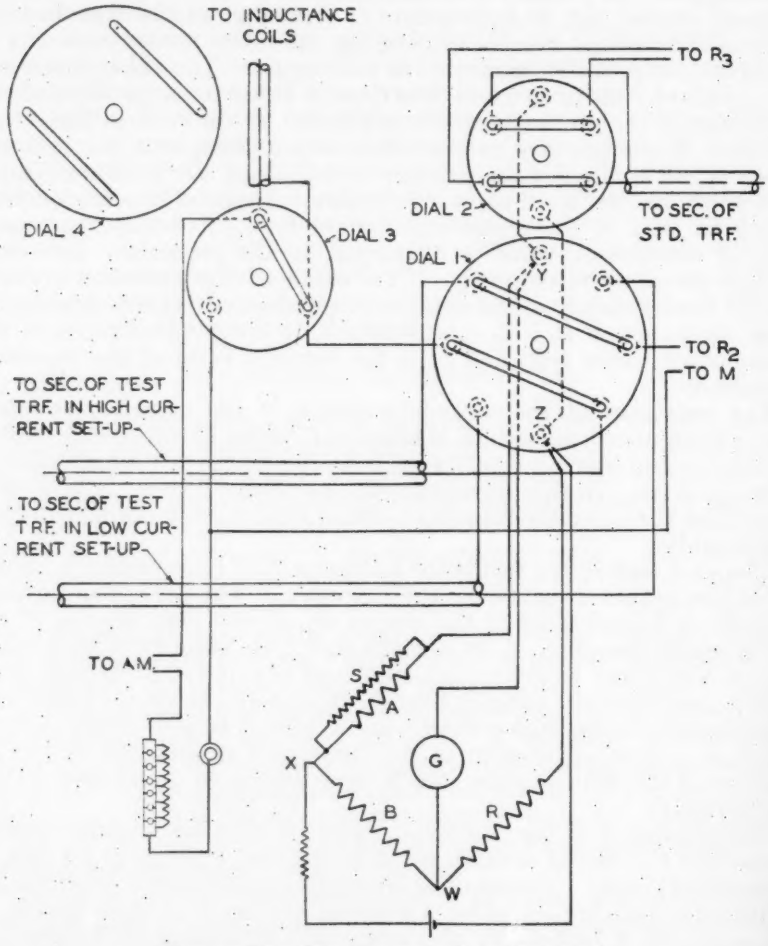

FIGURE 15.—*Mercury cup selector switches.*

Dial *1* as shown, secondary of high-current transformer to measuring circuit (consisting of adjustable mutual inductor and secondary resistor).
Dial *1* rotated 45° clockwise, secondary of high-current transformer to bridge.
Dial *1* rotated 90° clockwise, secondary of low-current transformer to bridge.
Dial *1* rotated 135° clockwise secondary of low-current transformer to measuring circuit.
Dial *4* replacing dial *1*, measuring circuit to bridge.
Dial *2* as shown, secondary standard transformer to its standard resistor.
Dial *2* rotated 60° clockwise, secondary winding of standard transformer to bridge.
Dial *2* rotated 120° clockwise, external secondary circuit of standard transformer to bridge.
Dial *3* as shown, burden inductors shorted.
Dial *3* rotated 120° clockwise, inductors and adjustable resistor shorted.
Dial *3* rotated 240° clockwise, adjustable resistor shorted.
Dial *3* left out, inductors and adjustable resistor in secondary circuit.

burden specified by the customer is less than this it becomes necessary to make two tests on the transformer, the first with the minimum feasible burden and the second with a burden greater than the minimum by an amount equal to the excess of the minimum burden over

the specified burden. Using these two sets of data, linear extrapolation will give with reasonable certainty the ratio and phase angle which the transformer would have on the specified burden. As has been pointed out elsewhere [10] there is little gain to the user from specifying very low transformer burdens.

It is frequently feasible to use in the test the actual instruments which will later be used with the transformer. The resistance of the standard resistor, mutual inductor, etc., must then be allowed for by correspondingly reducing the test lead resistance below the customer's value. If this specified value is 0.1 ohm or more it is usually possible to make the test in this way. Other things being equal, it is, of course, desirable for the highest accuracy to use the actual secondary instruments because their impedance may depart slightly from the typical values stated by their maker. Furthermore, the inductance of most instruments changes somewhat with the position of the pointer and, if iron is present, with the frequency and the current. It is not practicable to duplicate these changes using simple air-cored inductors.

As a final preliminary step the transformer is demagnetized, usually by connecting the secondary circuit between the sliding contact and one end of a potentiometer-type slide-wire rheostat while the transformer primary is open. The voltage applied to the transformer is raised until a current of 5 amperes is reached, or until a rapid increase in current for a small increase in applied voltage indicates that the knee of the magnetization curve has been passed. The applied voltage is then reduced very gradually to zero, at first by the generator field control and later by the slide rheostat. In the case of transformers of very high range it is sometimes necessary to apply as much as 350 volts at 25 cycles to reach the desired flux density. In cases where the customer wishes to know the ratio and phase angle of the transformer in the condition in which it was used in some preceding measurements, this demagnetizing process and the measurement of secondary resistance are, of course, omitted.

After these preliminaries are completed, the transformer secondary is connected to the burden circuit by the links at the mercury-cup selector switch. The supply switch is closed and the generator voltage raised by the field control until a secondary current of 5 amperes is reached. Operator II (fig. 4) adjusts frequency and current to the proper values and operator I adjusts the secondary standard resistor and the mutual inductor until a balance is obtained on the vibration galvanometer. The settings are recorded, operator II reduces the current to 4 amperes, and another setting is made. Further successive settings are then made with the secondary current at 3, 2, 1, and 0.5 amperes. Because of the small deflection produced by 0.5 or 1 ampere in a 5-ampere ammeter, the adjustment of current for these points is usually based on the indication of an ammeter of suitable range inserted in the primary circuit and short-circuited during the remainder of the test. After the balance has been obtained at the 0.5-ampere point, the operators exchange places and make a second set of balances at increasing values of current. Any differences exceeding 0.02 percent or 0.5 minute between the two sets of results indicate the need for a repeat test to locate the origin of the differences.

[10] Silsbee, F. B., Elec. World, vol. 81, p. 1082, May 12, 1923.

After the series of alternating-current balances has been satisfactorily completed, the resistance of the burden is again measured to make certain that it has not changed appreciably. If a gradual drift in the ratio has been noted, the resistance of the secondary winding may be measured again to obtain a basis for estimating its temperature rise during the run.

The computation of the results includes the averaging of the two settings at each value of current; the correcting of the apparent ratio factor, as read from the dials of the precision resistor in the secondary, by the calibration correction to the primary and secondary resistors and by the effects of room temperature and current in further changing their resistance. The phase angle is computed by equation (7a) from the mutual inductance as read from the calibration curve, the frequency and the setting of the secondary resistor.

The computations as made by one observer are checked independently by the other. The values of ratio and phase angle are then plotted as ordinates against secondary current as abscissas to make certain that they yield a smooth curve of normal shape. As a further check against errors, the results are carefully scrutinized independently by a third member of the staff, familiar with current-transformer performance, and when possible are compared with the old records of data obtained in the course of any previous test of the same transformer. The formal certificate is then prepared and proof read twice against the original data sheet before issuance.

V. CONCLUSIONS

Experience with the various parts of the equipment here described has led to the following general conclusions:

1. The resistance method for the absolute measurement of the ratio and phase angle of current transformers is readily capable of giving sufficient accuracy for present-day purposes, at least up to 2,500 amperes.

2. The design of suitable primary resistance standards is the limiting factor in the method and has become difficult and expensive when the range of currents has reached 1,500 amperes.

3. The use of a standard multirange transformer, tested with its primary turns in some groupings and used as a standard with its primary turns in other groupings of higher range, is feasible and accurate, and is preferable to the resistance method for currents above 1,000 amperes.

4. The uniformity of secondary winding which can be obtained with a ring core is the main factor in securing good performance in such standard transformers. Because of this excellent uniformity, the need for equality of current distribution in the primary is less necessary than might be anticipated. This is fortunate because contact resistance and the inductive action of the current in the terminal slabs prove to be serious obstacles to obtaining uniformity of primary current.

5. The number of primary sections (24) in the present transformer is probably larger than is necessary for most purposes, and with fewer turns the difficulties of construction would be materially decreased.

6. The arrangement of the primary leads is of increasingly great importance with increasing current rating in certain types of current

transformer, and an arrangement, such as the present "cage", which eliminates the effect of the return lead, would seem to be the logical form to use with standard transformers in testing laboratories.

APPENDIX A—CALCULATION OF THE MAGNETIC FIELD AROUND THE TEST TRANSFORMER "CAGE"

Figure 16 shows in cross section four infinitely long straight linear conductors, *A*, *B*, *C*, and *D*, connected in parallel to constitute the return for the single lead *O*. This structure approximates the "cage" in which the current transformer is placed for test. Three features

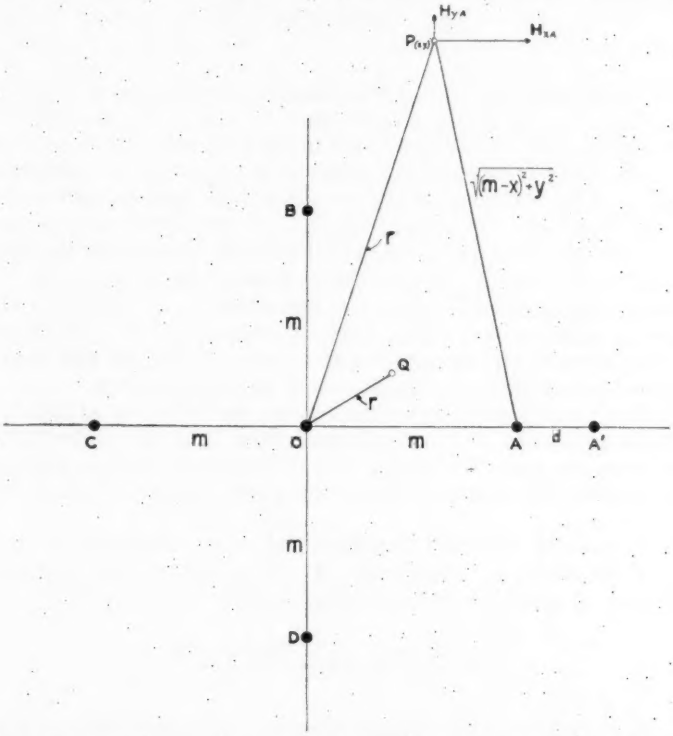

FIGURE 16.—*Diagrammatic cross section of test transformer "cage".*

of the magnetic field produced by such a structure are discussed below:

1. When a current I flows outward from the plane of the paper in conductor O, what is the magnetic field at a point P distant from the central conductor by an amount r, which is much greater than the distance m between each return conductor and O?

From the Biot-Savart equation for the field due to a long straight conductor, $H=2I/r$, we may immediately write down the contributions to the X and Y components of H produced by each of the five conductors. Thus for conductor A carrying a current $I/4$

$$H_{XA}=\frac{+Iy}{2[(x-m)^2+y^2]} \text{ and } H_{YA}=\frac{-I(x-m)}{2[(x-m)^2+y^2]} \qquad (1A)$$

Summing up these contributions, including terms of the fourth order in $\frac{m}{r}$, gives

$$H_x=\frac{-2Iym^4}{r^6}\left[3+4\frac{y^2}{r^2}-8\frac{(x^4+y^4)}{r^4}\right] \tag{2A}$$

$$H_y=\frac{2Ixm^4}{r^6}\left[3+4\frac{x^2}{r^2}-8\frac{(x^4+y^4)}{r^4}\right] \tag{3A}$$

and for the resultant field from this total current I

$$H=\sqrt{H_x^2+H_y^2}=\frac{2Im^4}{r^5} \tag{4A}$$

Terms of lower order in m/r vanish completely, and it is interesting to note that the intensity of the resultant field is (to fourth-order terms) independent of the direction in which point P lies with respect to the axes, but varies as the inverse fifth power of the distance from the origin. The direction of the resultant field will be radial at points where $H_x/H_y=x/y$. On inserting the values from equations (2A) and (3A) in this condition, we find that the field is radial for $x=\pm(\sqrt{2}+1)y$ or $x=\pm(\sqrt{2}-1)y$. These conditions correspond to lines making an angle of 22.5° with the coordinate axes through the side conductors. Conversely the field is tangential if $H_x/H_y=-y/x$, which corresponds to cases when the point P lies on the coordinate axes or on lines making an angle of 45° with these axes.

The effectiveness of this arrangement in reducing stray field appears from equation (4A) which indicates that at a distance $r=5$ times m from the axis, the field is only 0.16 percent of that which would be produced by the central conductor alone, the return lead being at a great distance.

For comparison we may consider the field produced if the entire current I returned in conductor A. Combining the contributions from O and A gives to second order terms

$$H_x=\frac{4I_mxy}{r^4} \quad H_y=\frac{2I_m(y^2-x^2)}{r^4}$$

and the resultant field $H=\frac{2Im}{r^2}$

In this case at $r=5$ times m we have a field 0.2 of that due to the central conductor alone, and hence 125 times as great as that produced by the 4-conductor arrangement.

2. With a total current I flowing in the outer four conductors only (assuming it equally divided among them and returning at an infinite distance) what is the magnetic field at a point Q located so near the origin that r is much less than m? The contributions of the four conductors may be tabulated as before, expanded in terms of r/m, and on summing these contributions, we get to terms of second order in r/m

$$H_x=\frac{2Iy}{m^4}(3x^2-y^2) \tag{5A}$$

$$H_y = \frac{2Ix}{m^4}(x^2 - 3y^2) \tag{6A}$$

The resultant field is then

$$H = \frac{2Ir^3}{m^4} \tag{7A}$$

and is, to this approximation at least, independent of the direction of O from O. An analysis similar to that of case I shows that the resultant field of the four outer conductors is tangential when O is on the coordinate axes or on lines at 45° from these, while the field is radial at points half-way between.

The intensity of the field at the center is zero and, at a distance r from the axis, the ratio of the field due to the four outer conductors only to that due to the same current flowing in a central conductor, is r^4/m^4. Since the radius, m, of the cage used is about four times that of the usual current transformer, the field intensity at the point where the core is placed, due to the return bars, is less than 0.4 percent of that of the central conductor. Of course, the line integral of this field around the core is rigorously zero with any configuration of return conductors not passing through the opening in the core.

3. When it is desired that the assemblage of return leads shall produce a magnetic field at the axis equal to that which would be produced by a single return conductor at a given large distance R from the axis, what should be the location A' of one of the bars? Since equal currents in A, B, C, D combine to give zero field at O, the field at O due to equal currents in A', B, C and D will be the same as that due to a current in A' returning in A only. This field is for a current $I/4$

$$H_{A'} = \frac{2I}{4}\left(\frac{1}{m} + \frac{1}{m+d}\right) \tag{8A}$$

The desired field is

$$H_D = \frac{2I}{R} \tag{9A}$$

Hence d can be found by equating these values, which yields

$$\frac{1}{m+d} = \frac{1}{m} + \frac{4}{R} \tag{10A}$$

If A' lies farther from the axis than A as shown, d is positive and R is negative; that is, the equivalent single return is on the opposite side of the axis from A. For the cage used m=50 cm and d can be adjusted from +10 to —30 cm. The effective range of R is therefore from —1,200 through infinity to +133 cm.

If conductors B and D are removed equation (8A) becomes

$$H_{A'} = \frac{2I}{2}\left(\frac{1}{m} + \frac{1}{m+d}\right) \tag{11A}$$

and (10A) becomes

$$\frac{1}{m+d}=\frac{1}{m}+\frac{2}{R}$$

The minimum value of R is thus brought down to 67 cm and by using one conductor A' only, still smaller values can be obtained.

The field at points near but not on the axis is, of course, not exactly the same when the cage is in use as when a real distant single return conductor is present. The difference is, however, not very great and the resulting differences in the performance of a current transformer are probably negligible.

WASHINGTON, May 15, 1933.

U.S. Department of Commerce—Bureau of Standards

RESEARCH PAPER RP581

Part of Bureau of Standards Journal of Research, Vol. 11, July 1933

PHASE SYNCHRONIZATION IN DIRECTIVE ANTENNA ARRAYS WITH PARTICULAR APPLICATION TO THE RADIO RANGE BEACON [1]

By F. G. Kear

ABSTRACT

With the development of the TL antenna system for use with the radio range beacon a new problem was encountered. It became necessary to provide a positive means of stabilizing the space pattern. Slight detuning of the antennas would alter the course indications. The extent to which detuning affects the pattern is demonstrated in detail and the limits to which the tuning must be maintained are shown to be very rigid. To overcome this difficulty two types of excitation systems have been developed in which the stability of the space pattern is independent of the antenna tuning to a marked degree. Either a parallel connected pair of lines 90° in electrical length or a series connection of lines 180° in length is shown to possess this characteristic.

Experimental data on several types of lines show the system to be practical for use along the airways, and no sacrifice of the desirable features of the TL antenna is required. Tests of the system on actual airway range beacons show it to be satisfactory.

CONTENTS

	Page
I. Introduction	123
II. Effect of phasing on the space pattern	124
III. Analysis of current and voltage relations	125
IV. Building out sections	131
V. Experimental work	131
1. Laboratory tests	131
2. Tests on the antenna system	132
3. Tests on parallel connection	133
4. Tests on series connection	136
5. Tuning methods	137
VI. Conclusions	138
VII. Appendix	138

I. INTRODUCTION

In order to eliminate the fluctuations of radio range-beacon courses during the hours of darkness this Bureau recently developed, for the Research Division of the Aeronautics Branch, Department of Commerce, a new type of transmitting antenna system which has been named the TL antenna. This research has been described in a recent paper.[2] Briefly, this sytem consisted of substituting for the loop antennas previously used, two pairs of vertical antennas producing the same radiated space pattern in the ground plane as that created by the loop antennas, but of which the electric field was substantially vertically polarized. It was shown that this system was practically free from night fluctuation effects and also possessed other desirable

[1] The substance of this paper has been submitted to the Massachusetts Institute of Technology in partial fulfillment of the requirements of a doctorate thesis. Copies of the complete thesis will be on file in the Library of the Institute.

[2] H. Diamond, The Cause and Elimination of Night Effects in Radio Range-beacon Reception, B.S. Jour. Research, vol. 10 (RP513), p. 7, January 1933.

features. However, the space pattern produced by these antennas was essentially unstable in that it was dependent upon all tuning adjustments remaining constant. To overcome this difficulty an excitation system has been developed which synchronizes the cur-

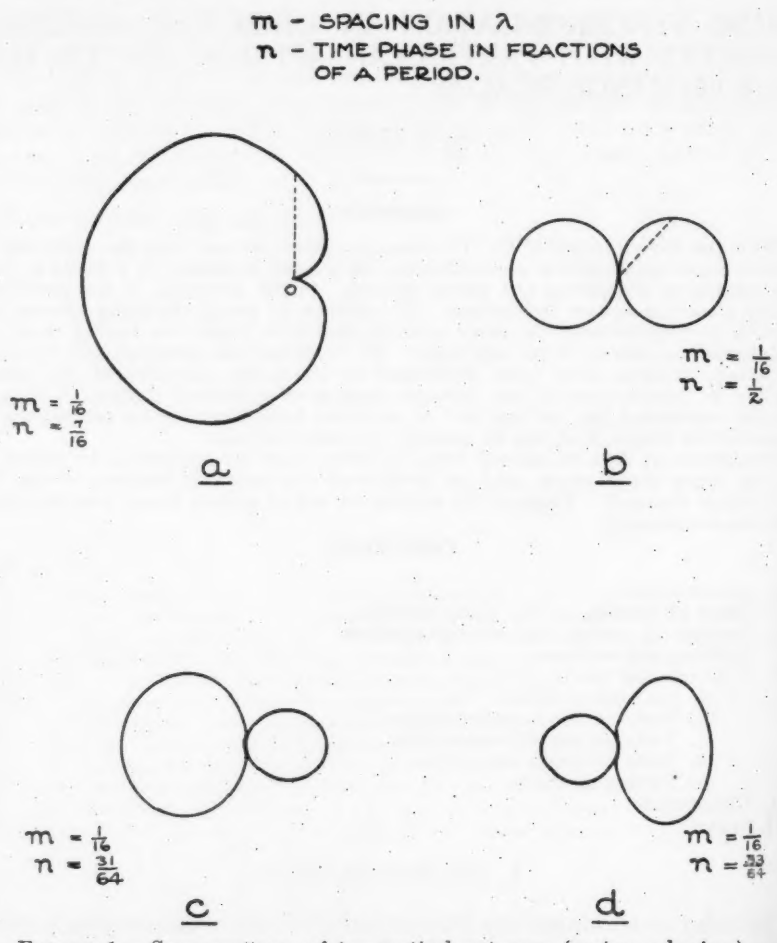

FIGURE 1.—*Space patterns of two vertical antennas (various phasings).*

rents in each pair of antennas to an extent which makes their stability comparable to that of the loop antenna.

II. EFFECT OF PHASING ON THE SPACE PATTERN

The directional characteristics of antenna arrays have been discussed at length in various papers.[3] These analyses, however, deal chiefly with antennas whose separation is a large fraction of a wave length and of which the phasing is changed in similar fractions. In the range-beacon system the antenna separation varies from 400 to 600 feet depending upon the ground available, which corresponds to

[3] For example: A. M. Foster, Directive Diagrams of Antenna Arrays, Bell System Tech. J, vol. 5, p. 292, 1926.

possible separations of from one eleventh to one sixth wave length for the frequency band employed. In addition to this, the so-called "on course" zone is created by the intersection of two independent space patterns. These two factors require that the phase of the currents be kept within much closer limits than is necessary with the customary directional array.

The general equation for the space pattern of two antennas in the ground plane is

$$E = K\,[\cos\,(\pi m \cos\theta + \pi n)]$$

(where only the terms necessary for indicating the pattern are included). E is the intensity at constant radius and at an angle of θ degrees from

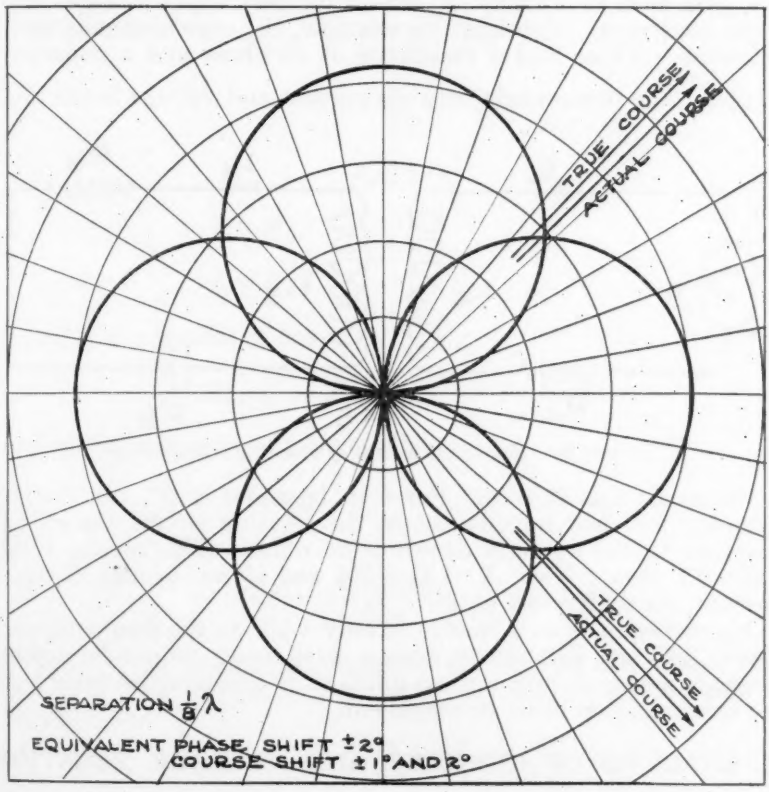

FIGURE 2.—*Effect of slight phase shift on space pattern.*

an arbitrary zero. m is the spacing of the two antennas in wave lengths or fractions thereof while n is the time phase in fractions of a period. Two sets of phase relations are commonly employed with such an antenna group. The first is $m+n=1/2$ which results in a cardioid pattern. The second is $n=1/2$ and $m<1/2$. This gives the figure-of-eight pattern. These are illustrated in figure 1 (*a*) and (*b*).

In range-beacon work the figure-of-eight is most commonly employed with some slight change in the value of n to permit course bending. This variation is described in footnote 2. For a change of phase from the correct value the pattern is altered considerably.

Figure 1 (*c*) and (*d*) show the extent of this change in the figure-of-eight pattern for phase variations of 5°, and for antennas spaced one sixteenth wave length. This is the spacing of the antennas at the College Park range beacon It is obvious that a change of this magnitude will not be allowable.

Since some change of phase will undoubtedly occur because of changing antenna constants, it is necessary to determine within what limits such changes are permissible. Figure 2 shows a space pattern for the range beacon with a 2° change of phase of one antenna. This shifts the course indication from 1° to 2°, which is as much as can be tolerated. A phase shift of 2° was therefore selected as the maximum permissible shift.

A total shift of 2° may be caused by very slight changes in the circuit constants. Consider, for example, the cage antennas used at Bellefonte. These had a resistance of 10 ohms and a capacity of 500 $\mu\mu$f. The phase angle between current and voltage is arc tan $\frac{X}{R}$.

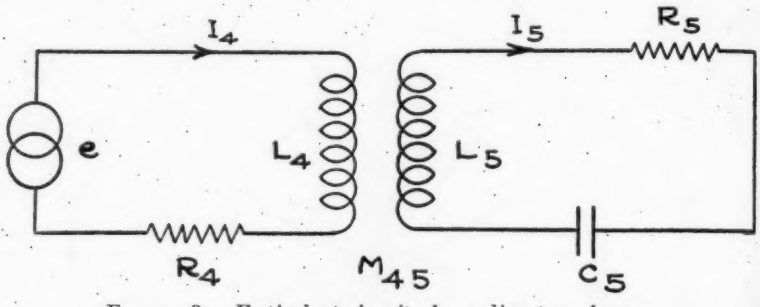

FIGURE 3.—*Equivalent circuit of coupling transformer.*

At resonance this is zero. For θ to be equal to 2°, tan $\theta = 0.035$. Assuming matched impedances in the exciting circuit the effective resistance in the antenna circuit is 20 ohms. This means a value of $X = 0.7$ ohm. Now $X = |X_L - X_c|$ and if we assume X_L to be constant, then $\Delta X_c = 0.7$ ohm.

This corresponds to a change of only 1 $\mu\mu$f at the frequencies employed. A cage antanna or even a steel tower cannot be expected to remain constant within these limits so in consequence some means of synchronization must be employed.

III. ANALYSIS OF CURRENT AND VOLTAGE RELATIONS

The first step toward securing a suitable circuit was the design of a coupling system which had maximum inherent stability. The transmission lines used with the TL antenna consisted of a pair of rubber-covered wires surrounded by a metallic sheath. It had a low surge impedance and required impedance matching transformers at each end. (The line characteristics are discussed in detail later.) Instead of using coupling transformers, such as are frequently adopted for radio circuits, and matching impedances by securing coupling conditions of $\omega^2 M^2 = R_1 R_2$, transformers with a very high degree of coupling and high self-inductance were employed. It can readily be shown that if the $\frac{\omega L}{R}$ of each coil is very large compared to the load imped-

ances and if the coupling coefficient is high, a transformer will act purely as an impedance-matching device in which the ratio of transformation (turns ratio) is equal to the square root of the ratio of impedances to be matched. For example, consider the circuit of figure 3. We may write the following relations:

$$e = Z_4 I_4 + Z_{45} I_5$$

$$O = Z_{45} I_4 + Z_5 I_5$$

whence

$$I_4 = \frac{Z_5 e}{Z_4 Z_5 - Z_{45}^2}$$

$$I_5 = -\frac{Z_{45} e}{Z_4 Z_5 - Z_{45}^2}$$

$$\frac{I_5}{I_4} = -\frac{Z_{45}}{Z_5} = -\frac{j\omega M_{45}}{R_5 + j\omega L_5}$$

but

$$j\omega L_5 \gg R_5$$

$$L_4 = K n_4^2$$

$$L_5 = K n_5^2$$

where K is a geometric constant

$$M_{45} = C\sqrt{L_4 L_5} = C\sqrt{K^2 n_4^2 n_5^2} = CK n_4 n_5$$

where C is the coefficient of coupling.

$$\frac{I_5}{I_4} = -\frac{j\omega M_{45}}{j\omega L_5}$$

$$= -\frac{M_{45}}{L_5} = -\frac{CK n_4 n_5}{K n_5^2} \cong -\frac{n_4}{n_5} \text{ (as } C \cong 1)$$

Under these conditions, therefore, the current in the secondary is related to that in the primary solely by means of the turns ratio. Furthermore

$$I_4 = \frac{(R_5 + jX_5)e}{(R_4 + jX_4)(R_5 + jX_5) + X_{45}^2}$$

$$= \frac{e}{(R_4 + jX_4) + \frac{X_{45}^2}{(R_5 + jX_5)}}$$

$$= \frac{e}{(R_4 + jX_4) + \frac{X_{45}^2}{R_5^2 + X_5^2}(R_5 - jX_5)}$$

$$=\frac{e}{(R+\varphi R_5)+j(X_4-\varphi X_5)}$$

where

$$\phi=\frac{X_{45}^2}{R_5^2+X_5^2} \text{ and since } X_5^2 \gg R_5^2$$

$$=\frac{X_{45}^2}{X_5^2}$$

$$=\frac{M_{45}^2}{L_5^2}=\frac{(CKn_4n_5)^2}{(Kn_5^2)^2}=\frac{C^2n_4^2}{n_5^2}\cong\frac{n_4^2}{n_5^2}$$

The impedances therefore are reflected through the circuit by a constant proportional to the square of the turns ratio. Now should the coefficient of coupling be unity ($C=1$)

$$\phi X_5=\frac{X_{45}^2}{X_5^2}\times X_5$$

$$=\frac{X_{45}^2}{X_5}\cong\frac{K^2n_4^2n_5^2}{Kn_5^2}$$

$$=Kn_4^2=X_4$$

and

$$j(X_4-\phi X_5)=j(X_4-X_4)=0$$

So for unity coupling the inductances do not affect the circuit. Should the coupling be less than unity there will remain some of the inductive terms which can be removed by making X_5 (or X_4) capacitative to the amount of such discrepancy. For high coefficients of coupling (90 percent is secured on the coils in actual use) the ratio of transformation is not altered greatly and is compensated for by the method of tuning. This analysis neglects the effect of capacity coupling between circuits. For the lines in use the voltages and frequencies were low enough so that the capacity could be neglected. The resulting circuit is shown in figure 4(*a*). By replacing the transformers with their equivalent leakage reactance the circuit now simplifies to that of figure 4(*b*). The series circuit at the end of each line is much easier to deal with in considering synchronization than would be a parallel circuit.

Since the relation between primary and secondary currents in the transformer is fixed, if the transformer primary currents in two opposite lines are synchronized the antenna currents will also be synchronized. That allows the circuit under consideration to be simplified still further to that of figure 4(*c*). When this simplification is made, there is at once apparent a very simple method of attack. Consider the ratio of sending end voltage to receiving end current; that is, the transfer impedance. This is

$$Z_{TR}=\frac{E_S}{I_R}=Z_R\cosh\gamma l+Z_o\sinh\gamma l\ ^4$$

where γ is the propagation constant of the line per unit length, Z_o the surge impedance and Z_R the load impedance.

---

[4] Everitt, communication engineering, McGraw Hill Co. (book).

Now, in general, a change of Z_R will result in a change of Z_{TR}. However, if cosh $\gamma l = 0$, Z_{TR} is independent of the load, and the current-voltage relation is determined solely by Z_0. For a line with negligible attenuation cosh $\gamma l \cong \cos \beta l$, a circular function which is zero for $\beta l =$ any odd multiple of $\frac{\pi}{2}$. Consequently, if the line is 90 electrical degrees long and has a low attenuation, $Z_{TR} = jZ_0$ and the load current will bear a constant relation to the sending voltage.

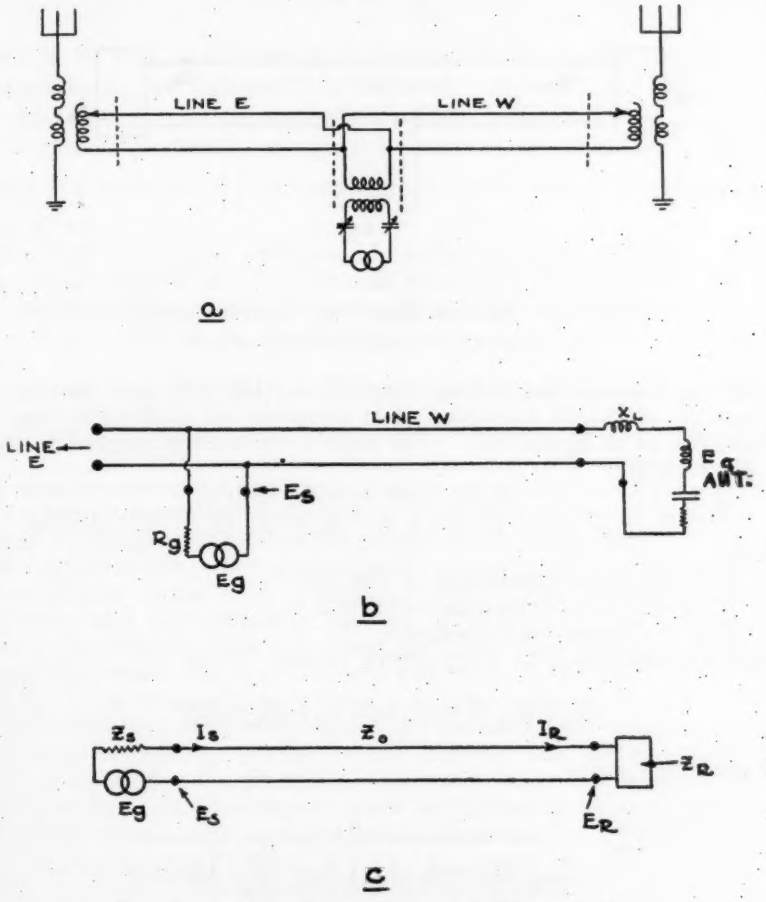

FIGURE 4.—*Antennas excited by parallel connections.*
a, actual circuit; *b*, first simplification; and *c*, final circuit analyzed.

Since this applies to each line supplied from E_S, the relation of I_{R1} to I_{R2} is constant regardless of antenna tuning. I_{R1} will, of course, change for a change of Z_{R1}, but at the same time E_S is constrained to follow such a change and I_{R2} is changed likewise. The result is total synchronization of the two currents.

There is also an alternative method of attack. The loop antennas are free from phase shift, since the two sides of the loop form a continuous series circuit. We may similarly connect the transmission lines in series as in figure 5(*a*). The hybrid coil at E_S is employed

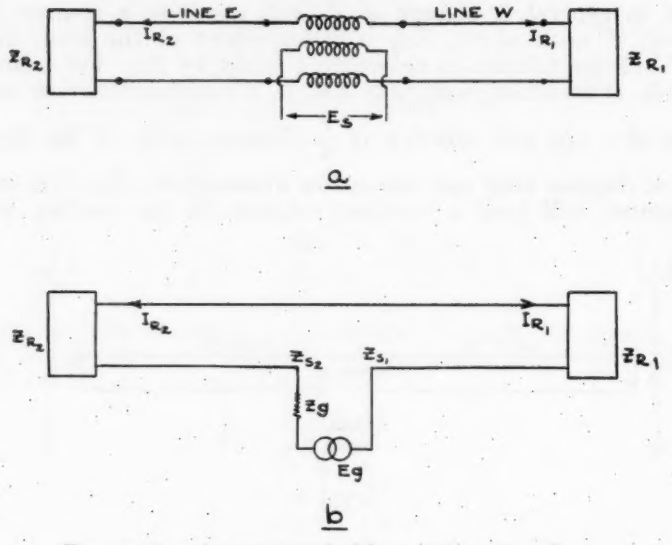

FIGURE 5.—*Antennas excited by a series connection.*

a, actual circuit; and *b*, equivalent circuit analyzed.

merely to balance the voltage applied to the lines and prevent an unbalance of sheath currents. For purposes of analysis it may be considered as in figure 5(*b*). For such a circuit the current is given by the equation:

$$I_{S1}=\frac{E_g[Z_o \cosh \gamma e + Z_{R1} \sinh \gamma e]}{Z_o(Z_{R1}+Z_{S2}+Z_g) \cosh \gamma e + [Z_o^2 + Z_{R1}(Z_{S2}+Z_g)] \sinh \gamma e}$$

where

Z_o is the surge impedance of the line

Z_{S2} is the input impedance of line 2

Z_g is the generator impedance.

Assume antenna 2 to be properly tuned. Then

$$Z_{S_2}=R_{S_2},\ Z_g=R_g \text{ and } R_g+R_{S_2}=Z_S\underline{|0^0}$$

We may now write

$$I_{R_1}=\frac{E_g}{(Z_R+Z_S) \cosh \gamma l + \left(Z_o+\frac{Z_R Z_S}{Z_o}\right) \sinh \gamma l}$$

$$=\frac{E_g Z_o}{Z_o(Z_R+Z_S) \cosh \gamma l + (Z_o^2+Z_R Z_S) \sinh \gamma l}$$

and since $I_{S_1}=I_{S_2}=I_g$

$$\frac{I_S}{I_{R_1}}=\frac{Z_o \cosh \gamma l + Z_{R_1} \sinh \gamma l}{Z_o}$$

$$\frac{I_S}{I_{R_1}}=\cosh \gamma l + \frac{Z_{R_1}}{Z_o} \sinh \gamma l$$

For the line which is properly terminated

$$\frac{I_s}{I_{R_2}} = \cosh \gamma l + \sinh \gamma l$$

Hence

$$\frac{I_{R_1}}{I_{R_2}} = \frac{\cosh \gamma l + \sinh \gamma l}{\cosh \gamma l + \frac{Z_{R_1}}{Z_o} \sinh \gamma l}$$

That is to say, the phase and magnitude of I_{R_1} will change with respect to I_{R_2} as antenna 1 is detuned. Now if $\sinh \gamma l << \cosh \gamma l$ this change will be negligible. This means a very short line (a simple series circuit) or again if the attenuation is small, any line which is a multiple of $\frac{\lambda}{2}$ in length, since under that condition $\sinh \gamma l \cong j \sin \beta l = 0$.

For half wave lines connected in series we may, therefore, expect synchronization of the two antenna currents. Both the quarter and the half wave lines were tested experimentally to determine how closely they would conform to the theory.

IV. BUILDING-OUT SECTIONS

As has previously been stated, the separation of the antennas in the airway installations varies from 400 to 600 feet. From the exciting transformer to the antenna, therefore, is usually less than a quarter wave length considering the phase velocities of the lines used. It would be possible to use sufficient line to make the length a quarter or a half wave length as desired and coil the portion in excess of the actual length at the base of each antenna. This is quite expensive, however, and also inflexible should a change in transmitting frequency be made. To avoid this, the lines were cut to the length required to reach the antennas and were then built out to the desired length by artificial lines within the range-beacon house. These building-out sections were designed for the same propagation constant and surge impedance as the actual lines so that no discontinuities were introduced. Furthermore, the low voltage and current on the lines permitted small compact units occupying much less space than the actual cable. One such section is illustrated in figure 6.

V. EXPERIMENTAL WORK

1. LABORATORY TESTS

First tests on this method of synchronizing were made in the laboratory where control of the circuit parameters was possible. Two types of transmission line were available, the first consisted of two strands of no. 14 rubber-covered wire in an enclosing lead sheath and the second two no. 12 rubber-covered wires within first a lead and next a steel sheath (Parkway cable). Since the first was easier to handle it was used for most of the tests although the greatly reduced losses in the Parkway cable made its use desirable in the final arrangement. The characteristics of these lines will be found in the appendix.

Using two sections of line each 120 feet long and connected in series (see fig. 7), the change of phase of receiving end currents was observed as a load on the end of one line was changed. This observation was made on a cathode-ray oscillograph and a shift of 5° from the correct phase could readily be observed. These lines were approximately 40° long and no synchronization was noticed. They were then built out with suitable sections to half-wave lines and further observations made. It was now possible to vary Z_R from the correct value of $75\underline{|0}°$ to $120\underline{|33}°$ and $120\overline{|10}°$ without losing synchronization. The fact that beyond these limits synchronizing action was lost was ascribed to the relatively high loss of this type of line.

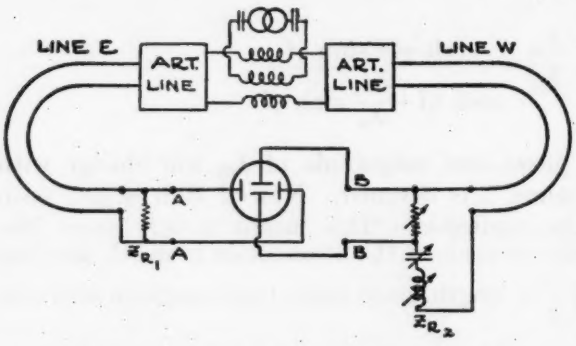

FIGURE 7.—*Circuit for oscillographic study.*

A similar set of tests was made with a parallel connection of the lines built out to a quarter wave length. The results were about the same; if anything, somewhat better. It was therefore concluded to try the same circuits on an actual antenna system.

2. TESTS ON THE ANTENNA SYSTEM

There were at College Park two pairs of vertical antennas 40 feet high and separated 220 feet from each other. These were excited by means of the transmission lines built out to various lengths and the synchronizing action studied. The coupling unit is illustrated in figure 8, which shows the compact nature of the arrangement.

To determine the degree of synchronization two antennas were excited, and the voltage induced in a third antenna, equidistant from the other two, was measured by means of a milliammeter inserted in its base. If the phase is correct and the currents in the antennas are equal there will be no current apparent in the third antenna. However, a slight unbalance of magnitude or phase will cause the milliammeter to indicate. For example, if each antenna independently (I_n and I_s in fig. 9) causes 100 ma of current to flow in the test antenna, then a phase difference of 2° from the true 180° relationship will cause a current of 3 ma when both antennas are excited (I_R in fig. 9). These

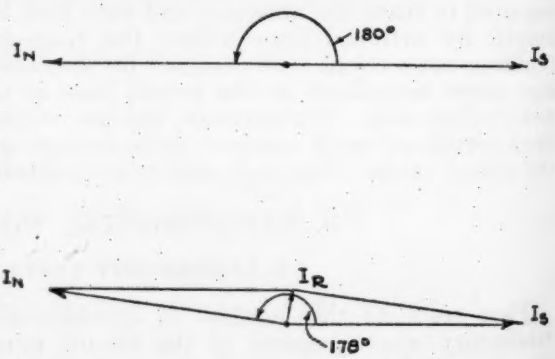

FIGURE 9.—*Phase relations in test antenna.*

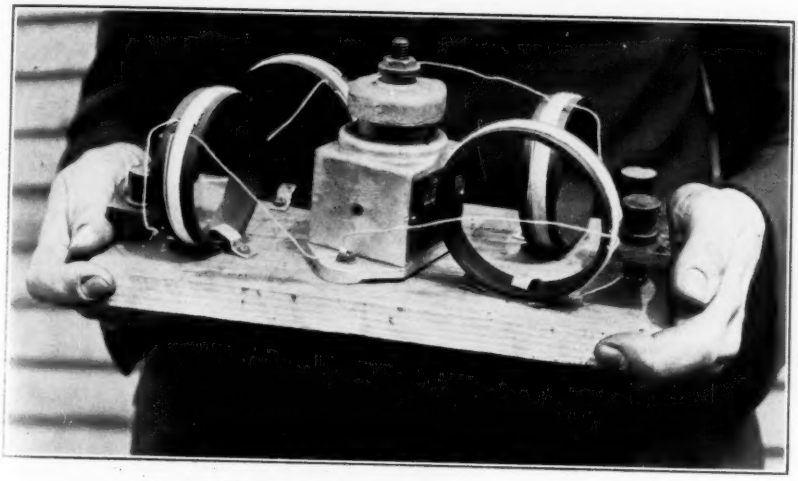

FIGURE 6.—*Building-out section.*

FIGURE 8.—*Coupling unit with matching transformers.*

currents could easily be read on the meter employed and since 2° is the variation which is chosen for the maximum allowable deviation, the method of observation was adequate. Previous experience with this method of adjustment had also shown it to be satisfactory.[5]

3. TESTS ON PARALLEL CONNECTION

With the parallel connection of figure 4, a series of tests were made with various line lengths. The graph of figure 10 gives a comparison between the lines formerly in use (40°) and the 90° lines. With the former the instability was very serious. Slight swinging of the antenna in the wind caused large changes in phase. With the 90° lines the antennas could not only be detuned until the reactance was ± 15 percent of the antenna resistance without dephasing, but even when definitely beyond the zone of control no changing of phase was

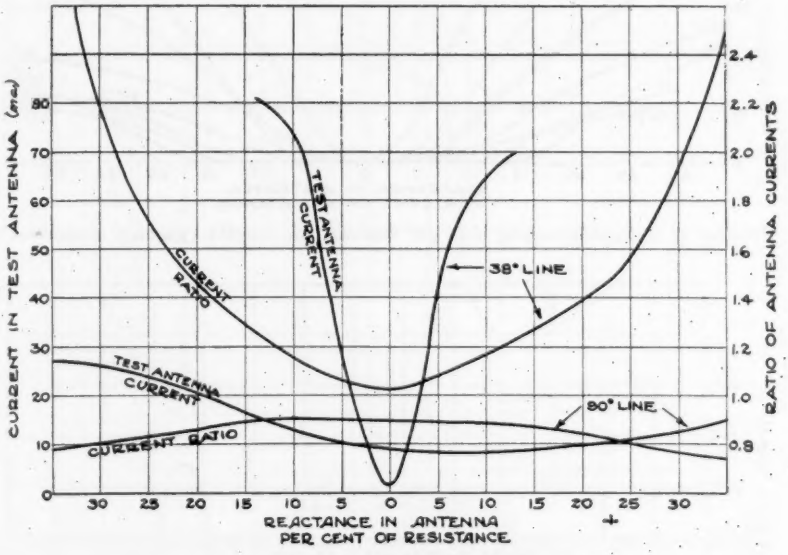

FIGURE 10.—*Synchronization data (lines in parallel).*

observed with a swinging antenna. In figure 10 the current flowing in the third antenna (the test antenna) is plotted against the amount of detuning of one of the antennas of the array with the other antenna in correct tune. For the 38° line a change of less than 2 percent in reactance caused a change of current of more than 3 ma. For the 90° line a change of reactance of ± 15 percent was necessary before the test antenna current changed 3 ma. Unfortunately in this test the ratio of currents in the antennas of the array did not equal unity, consequently there was no zero current condition but merely a minimum. The ratio of antenna currents plotted on the same graph indicates the existence of this condition. The data of figure 11, and those which follow it, were secured with an equality of currents in the two antennas under test, consequently the curves go through a zero rather than a minimum.

[5] See footnote 2, p. 123.

Tests were next conducted to determine the optimum line length and the allowable deviation from correct length. Figures 11 and 12 give the results of these tests. It will be noted that the optimum length is

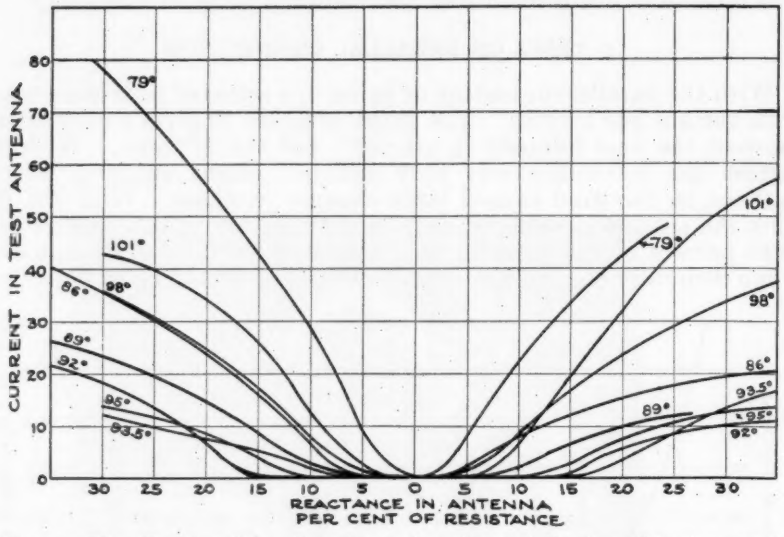

FIGURE 11.—*Synchronizing data for various line lengths (parallel connection).*

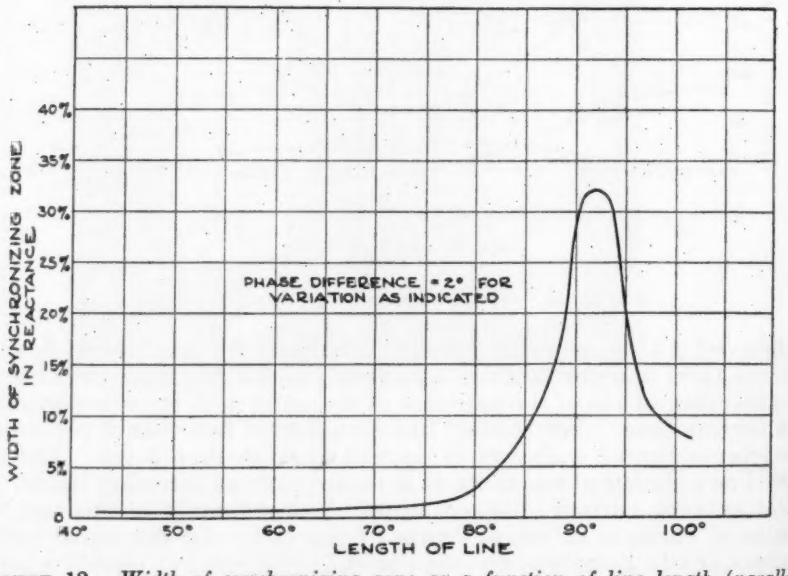

FIGURE 12.—*Width of synchronizing zone as a function of line length (parallel connection).*

93° and not 90°. It is apparent that the exact length is not important. Several degrees difference is possible with good synchronism. This means that the north line may be 98° and the south line 88°, with the resultant antenna currents synchronizing at 170° instead of 180°.

As a result of this feature the method of course bending described in footnote 2 may be applied without sacrificing the action of the lines in maintaining the pattern.

Further analysis of the data used in plotting figure 11 reveals another interesting fact. Figure 11 was plotted so that the curves are all approximately symmetrical about an arbitrary zero reactance point. As a matter of fact the location of the minimum shifts with line lengths. Lines which are greater than the optimum length have a minimum in the negative reactance side of tuning. Lines which are short have their minimum in the positive reactance side. The location of these minima with respect to line length is plotted in figure 13. In adjusting the line length it can immediately be determined whether the line under test is too long or too short by merely noting the center of maximum synchronization with respect to resonance, and referring

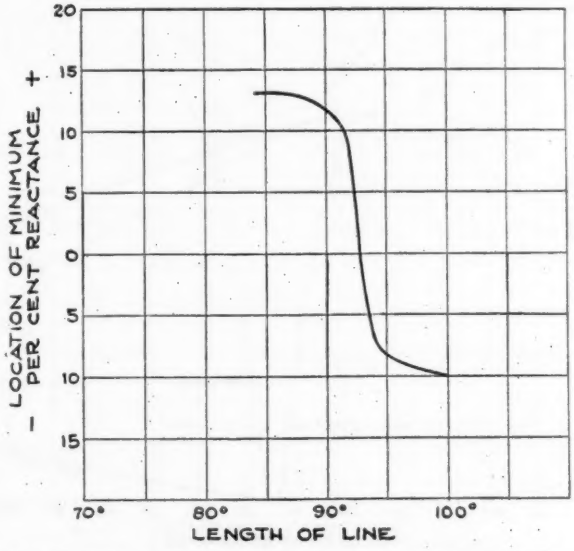

FIGURE 13.—*Location of minimum versus line length (parallel connection).*

to the curve. This is of great assistance in the installation of such a system where it is desired to use the maximum possible synchronization.

A final set of curves is given in figure 14 for the case of lines with very low attenuation. This is approximately the type of line used on the airways and the range of synchronizing action makes the resulting antenna system comparable in stability with the loop antennas. The antenna currents in the north and south antennas are plotted on this graph as a function of the amount of detuning. The relative values of these currents are of interest in that when synchronization is secured the currents rise and fall together. With no synchronization the reverse is true, making the space pattern depart even further from the desired shape.

Two other details were investigated. A line with nonuniform structure was substituted for the uniform line. About half of the line had a surge impedance of 75 ohms and the remainder 55 ohms. This had no apparent effect upon the synchronizing action. The effect of mismatch

of the antenna to the line which was similar in nature was also studied. It was found that any tuning adjustment which roughly matched the impedances within plus or minus 15 percent, operated very well. From these results it is safe to say that the system is decidedly non-critical in its action and consequently field installations can be made under adverse conditions with reasonable certainty of successful operation.

4. TESTS ON SERIES CONNECTION

Tests similar to those made for the parallel connection were made for the series case. The action was in accord with the theory, when allowance was made for the loss due to relatively high attenuation. The maximum amount of detuning permissible was then ± 12.5 percent as compared with ± 16 percent for similar lines connected in parallel.

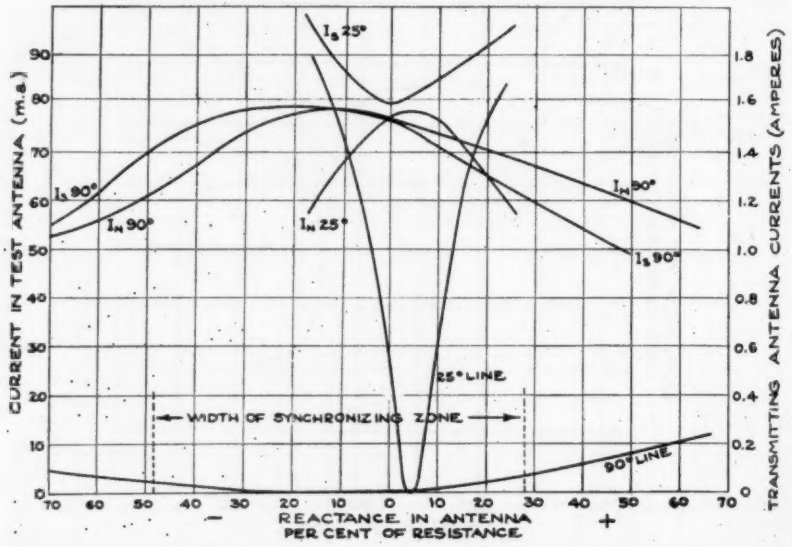

FIGURE 14.—*Synchronizing data. Low loss lines. (Parallel connection.)*

The increased loss because of greater line length no doubt caused some of this reduction. Furthermore, with the series connection the current is essentially of a circulating nature through the two antennas. Because of this the effect of sheath capacity would be more serious than in the parallel connection. Open wire lines would probably be preferable for series use.

Figures 15 and 16 show graphically the action of the series lines. They should be compared with figures 11 and 12 of the parallel line curves, since the same type of line was used in the two cases. The parallel connection seems to be preferable, as it operates over a wider range, requires less line length, and has a simpler exciting circuit. However, both methods are satisfactory. For use in the airway installations the 90° line has been adopted as a standard.

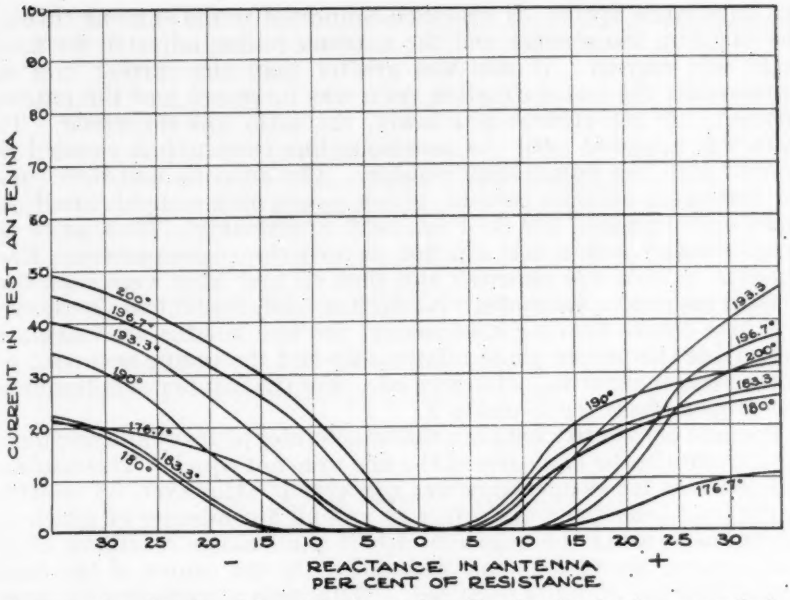

FIGURE 15.—*Synchronizing data for various line lengths (series connection).*

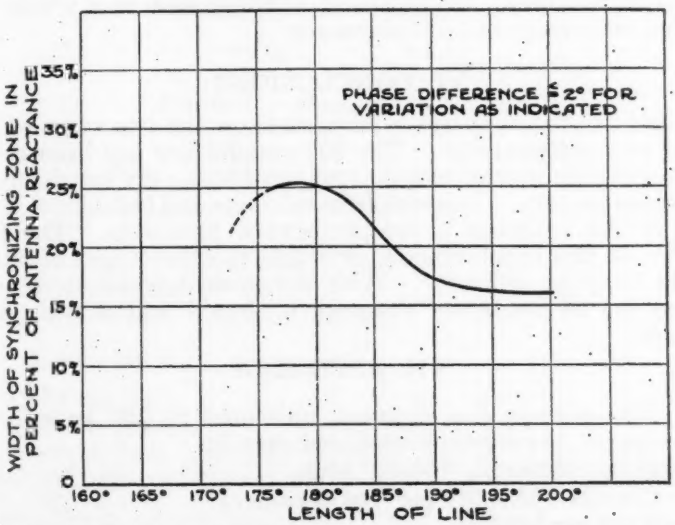

FIGURE 16.—*Width of synchronizing zone as a function of line length (series connection).*

5. TUNING METHODS

Since the tuning adjustments are no longer critical, almost any uniform procedure may be adopted. At College Park the procedure was as follows: Three lines were terminated in their surge impedance; that is, a noninductive resistor of the proper value. The line being adjusted was first terminated in its impedance and the current into

the impedance noted. It was then connected to the antenna through the coupling transformer and the antenna tuning adjusted for maximum line current. If this was greater than the current into the termination the transformation ratio was increased and the antenna retuned. If the current was lower, the ratio was decreased. The ratio was adjusted until the maximum line current just equaled the current into the terminating resistor. The antenna was then tuned for maximum antenna current, which meant only a slight misadjustment and increased the field intensity appreciably. Because of the synchronizing action this did not disturb the space pattern. Each antenna in turn was adjusted and then all four lines were connected to their respective antennas. No further readjustment was necessary.

Where course bending is necessary, the line lengths are calculated to provide the proper phase relationship and the tuning is carried out in the same manner as just described. For the manner of determining the proper phase see footnote 2.

Because of capacity between the transformer primary and secondary the currents in the two wires of the line were not equal. This made no difference as far as operation was concerned. However, by inserting in the lead from the transformer to ground a condenser of which the reactance equaled the negative of half the leakage reactance of the transformer, the nodal point was shifted to the center of the transformer and the currents balanced. With such a condenser the meter readings of the currents into the four antennas all balance and it is an easier matter to check the operation of the system as a whole. It is an added refinement but not necessary.

VI. CONCLUSIONS

The results of the experimental work show the two types of line to operate very satisfactorily. The 90° parallel line has been tested in actual service for several months and provides a very satisfactory and stable space pattern. It is simple to calculate and install and it makes tuning of the antennas a straightforward procedure. The further extension of this synchronizing principle to other types of antennas presents no great difficulty. With the present trend to directional antennas on all frequency channels it should find a wide field of usefulness.

VII. APPENDIX

Transmission line constants measured at 290 kc/sec.

1. 2-wire no. 14 rubber-covered lead sheath:
   Surge impedance $Z_o = 53.5\underline{|0°}$ ohm.
   $\gamma = 0.00138 + j0.00577$ per foot of cable.
   $\alpha = 0.138$ per 100 feet.
   $\beta = 33°$ per 100 feet.
   Phase velocity, 59,400 miles/sec.
   Attenuation, 3.76 db per 100 feet.

2. Parkway cable no. 12 rubber-covered wire, lead and steel sheaths:
Surge impedance $Z_0 = 69\underline{/0°}$.
$\gamma = 0.00014 + j0.00362$.
$\beta = 20.7°$ per 100 feet.
$\alpha = 0.014$ per 100 feet.
Phase velocity, 92,800 miles/sec.
Building-out sections (computed for 290 kc/sec.).
Parallel connection, Parkway cable.
Length of line 24° 40′,
Length of section 65°20′ (for 90° line).

$Z_1 = Z_2 = Z_0 \tanh \frac{\theta}{2} = j69 \tan 32°40'$ (attenuation neglected) $= j44.6$ ohm.

$L_1 = L_2 = 25.2$ μh.
Each coil of H-section is then 12.6 μh (fig. 17).

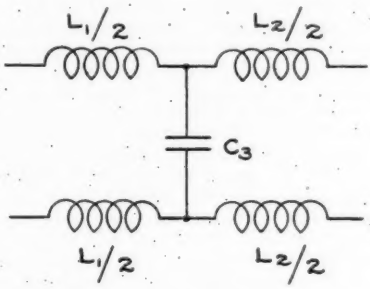

FIGURE 17.—*Equivalent* H-*section.*

$$Z_3 = \frac{Z_0}{\sinh \theta} \cong -j \frac{70}{\sin 65°20'}$$
$$= -j77.2 \text{ ohm.}$$
$C_3 = 0.007_3$ μf

Series connection. Lead cable.
For 115 feet of line $\beta l = 38°$.
Length of section = 142° for 180° line.

$$Z_1 = Z_2 = Z_0 \tan h \frac{\theta}{2}.$$
$$= j\ 54 \tan 71°.$$
$$= j\ 156.8 \text{ ohms.}$$
$L_1 = L_2 = 81.9$ μh
Each coil of H-section = 41. μh.

$$Z_3 = \frac{Z_0}{\sinh \theta} \cong -j \frac{54}{\sin 142°}$$
$$= -j87.7 \text{ ohm.}$$
$C_3 = 0.0063$ μf.

Other sections were computed similarly.

WASHINGTON, May 12, 1933.

U.S. Department of Commerce—Bureau of Standards

RESEARCH PAPER RP582

Part of Bureau of Standards Journal of Research, Vol. 11, July 1933

CONTINUOUS MEASUREMENTS OF THE VIRTUAL HEIGHTS OF THE IONOSPHERE

By T. R. Gilliland

ABSTRACT

This paper is a report of continuous measurements of the virtual heights of the ionized regions of the upper atmosphere. Short pulses of radio-frequency energy are sent out by a transmitter operating on 4,100 kc per second. The time interval required for the pulses to go up to the ionosphere and back is recorded photographically in the same room by means of an oscillograph. The revolving mirror of the oscillograph and the chopper wheel which makes the transmitter pulses are driven on the same shaft by a synchronous motor. Records are shown which indicate the variability especially at night. In the morning and afternoon reflections come from the *F* region showing virtual heights around 240 km. However, during the middle of the day the reflection often splits into two components and the 240-km reflection becomes weak and disappears. The remaining component often rises during the middle of the day to 300 or 320 km and then drops gradually to join the 240-km component which reappears before sunset. Records are given which show the rapid appearance and disappearance of reflection at night from both the *E* and *F* regions. An increase in ionization is probably responsible for the reappearance of *E* reflections of the type shown. However, *F* reflections which gradually become strong at night may possibly be explained by recombination in the lower part of the *F* region which exposes a more strongly ionized upper part. It is pointed out that the changes are so abrupt and irregular that data taken over a longer period and for other frequencies will be necessary before it is possible to establish the relative importance of such things as magnetic storms, meteor showers, sun spots, or thunderstorms.

CONTENTS

		Page
I.	Introduction	141
II.	Results	143
III.	Conclusions	146

I. INTRODUCTION

This paper is presented as a brief report on experimental results obtained in the measurement of the virtual heights of the ionosphere with a continuous recorder between November 1932 and March 1933. The frequency used was 4,100 kc per second. This work was done at the Bureau of Standards transmitting station near Beltsville, Md. It is desired to show the type of record obtained and to point out the variability from day to day. Results in the past where measurements were made manually have shown the need for continuous records which give a more complete picture of the changes actually occurring.

Briefly, the system used consists of a radio transmitter, receiving set, and galvanometer oscillograph with photographic attachment.

The transmitter is made to send out short pulses of radio-frequency energy at regular intervals by means of a chopper driven by a synchronous motor. Besides the direct path from transmitter to receiver the pulse also may arrive by one or more paths from the ionosphere. The pulses received are passed through the oscillograph and by means of a synchronous revolving mirror the pattern is projected onto the moving photographic paper in such a manner that only the top portion of the pulse is recorded. Since the path length for the direct pulse is fixed it will cause a straight line to be recorded, but as the virtual height of the ionosphere changes the path lengths for the other impulses will change and the corresponding traces will shift with respect to the fixed or "ground" trace. The distance on the record from any trace to the ground trace will be a measure of the virtual height for the corresponding reflection. The system is similar to that described in a previous publication [1] except that in the present arrangement the revolving mirror of the oscillograph and the chopper controlling the transmitter are attached to the same shaft, the transmitting and receiving sets being in the same room. No trouble is experienced with overloading or blocking in the receiving

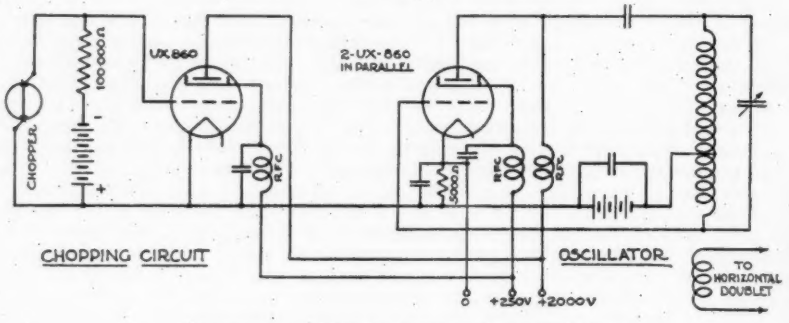

FIGURE 1.—*Circuit diagram of transmitter.*

Closing of chopper contacts causes plate current to flow in chopping tube. This decreases the negative bias on the oscillator grid so that oscillation takes place.

set from the direct pulse. This consolidation of the apparatus has material advantages of convenience.

The transmitter consists of two 75-watt tubes of the screen-grid type (UX–860) connected in parallel in a Hartley oscillator circuit. A single tube of the same type is connected between the chopper and the oscillator grid circuit to avoid trouble from radio-frequency currents at the chopper contacts (fig. 1). A half-wave horizontal doublet is used for transmitting, while receiving is done with an "L" type antenna.

The receiving equipment consists of a tuned radio-frequency broadcast receiving set preceded by a high-frequency converter. The galvanometer oscillograph element of the fixed magnet type, the moving coil of the dynamic loudspeaker, a copper-oxide rectifier and a 1-μf condenser are all connected in series in the output of the receiving set. The condenser, although not essential, serves to sharpen the pulses somewhat, thus giving narrower traces. No shift in the

[1] T. R. Gilliland and G. W. Kenrick, Preliminary Note on an Automatic Recorder Giving a Continuous Height Record of the Kennelly-Heaviside Layer, B. S. Jour. Research, vol. 7, p. 783, November 1931; Proc. I. R. E., vol. 20, p. 54, March 1932.

beginning time of the pulses could be detected with the addition of the condenser so that no change in accuracy of the records should be expected.

Helical gears with a ratio of 16 to 31 are used between the chopper-mirror shaft and the synchronous drive motor, giving slightly over 15 pulses per second. The odd gear ratio is employed to eliminate spurious results caused by noises occurring at power line frequency. The resolution obtained with the slower mirror speed is also more desirable. Recording is done on photographic paper moving at 4 cm per hour. On the vertical scale 1.5 cm represents 100 km in virtual height. Unevenness in the base line of some of the earlier records is caused by irregularities of the chopper brushes, but the virtual height can be measured for any instant by measuring vertically from the ground trace for that time. Since the beginning side of the peaks of the pulse pattern are almost at right angles to the zero-current line the virtual height may be determined by measuring from the lower edge of the ground trace to the lower edge of the reflection trace. It should be kept in mind that with this type of recorder the photographic paper moves in a direction parallel to the axis of the revolving mirror, and perpendicular to the zero current line projected by this mirror. The portion of the pulse pattern recorded was usually below the top of the peaks, so that each trace appears as a double line. Where the trace appears single only the top of the peak is being recorded. The double trace might be mistaken for actual splitting, but the latter phenomenon is so irregular that little confusion should result. A recent improvement has been the substitution of a spherical lens for the conventional cylindrical lens in the oscillograph optical system. By this method the light from a considerable portion of the top part of the peak can be concentrated into a single bright spot on the paper, thus doing away with the double trace. Recording is done with the incandescent oscillograph lamp working at two thirds normal voltage.

Recently other workers have used a gaseous discharge tube in place of the galvanometer oscillograph in the synchronous method of recording.[2] [3] Since the speed of response with both types seems to be limited by the radio receiver it appears that the galvanometer oscillograph is at no great disadvantage unless it is desired to sacrifice selectivity. The oscillograph is of assistance when it is desired to monitor reception visually.

II. RESULTS

The changes that occur at night are the most striking and the extreme variability from night to night makes it impossible to choose any record that can be called typical. In the daytime during the period of these observations reflections on this frequency usually came from the *F* layer [4] showing virtual heights ranging between 220

[2] Rukop and Wolf, Eine leistungsfahrige Einrichtung fur Messungen an der Heavisideschichten, Zeits. für tech. Phys., vol. 13, p. 132, 1932.

[3] H. R. Mimno and P. H. Wang, New Devices for Recording Kennelly-Heaviside Layer Reflections (abstract), Phys. Rev., vol. 41, p. 395, 1932.

[4] It has been shown that stratification exists in the ionosphere and the region showing virtual heights ordinarily of the order of 100 to 120 km has been called the E layer, while the region giving a virtual height of 200 km or more has been called the *F* layer. This designation was originated by Professor Appleton who first pointed out the existence of stratification. It is likely, in the light of more recent work, that other strata exist at times.

and 320 km. Figure 2 is an example of a record taken during the daytime (Dec. 18). Here the rapid drop is noted in the morning. The trace near the top of the record is a multiple of the first reflection indicating that pulse energy has made two round trips between the ground and the ionosphere. Splitting into two components which has been frequently observed by other workers and attributed to double refraction in the earth's magnetic field is noted at about 0800 and again at 1700 E.S.T. Here the component with the greater retardation is seen to rise and fall rapidly. This phenomenon is more clearly seen in some of the records that follow. At about 1820 the virtual height increases rapidly until the trace moves off scale. The rapid drop in the morning and the rise at night indicated in this record are not observed on all days. Frequently the drop in the morning and more often the rise at night will be gradual. Occasionally reflections continue throughout the night with the virtual height not greater than 500 km. In figure 2 reflections from the E layer are noted between 1900 and 2115 E.S.T. giving a virtual height ranging from 120 to 170 km.

In most of the daytime records it is noted that the height is greater at noon than for just after sunrise and before sunset. On some days the records indicate that splitting is occurring and one component (F_2) with the longer retardation frequently giving a height of 280 to 320 km becomes predominant near noon while the other component (F_1) at 220 to 240 km shows in the morning and afternoon. Occasionally F_1 shows intermittent weak reflections during the middle of the day when F_2 is strong. This is illustrated by figure 3. Figure 4 shows the two components separating at about 0800. F_1 disappears during the middle of the day but reappears at 1400 and joins F_2 at about 1610. It is possible that F_2 is the stronger at times even in the morning and afternoon, but the receiving system cannot resolve it immediately after a very strong F_1 reflection. The virtual heights for F_2 increase during the middle of the day sometimes going as high as 800 km with the peak usually occurring between 1100 and 1300 E.S.T.[5]

Figure 5 shows the momentary appearance of reflection at 0133 on November 30. The virtual height drops rapidly to 370 km, the total time for appearance and disappearance being 10 minutes. Changes after sunrise are noted at the right where the retardation of one component increases and decreases rapidly. Rapid changes of this type are also noted on the morning of January 21 (fig. 10).

Figure 6 shows interesting changes on the evening of December 28. At 1738 reflections begin to appear from a virtual height of 190 km. During the next 15 minutes the height changes to 115 km where it remains for about 3¼ hours except for momentary increases in height at about 1855 and 2030. These increases are practically coincident with appearance of reflections from the F layer. At 1855 the F-layer reflection is only momentary while at 2030 the time for appearance and disappearance covers about 10 minutes. The F-layer ionization is probably present during the entire time but shows only during momentary decreases in E-layer ionization.

[5] In a paper now in preparation describing work here on various frequencies, S. S. Kirby, L. V. Berkner, and D. M. Stuart have suggested that splitting of this type is due to stratification in the F region and that the high virtual heights of the F_2 component during the day are due to a critical phenomenon in the lower F_1 region much the same as that observed for the E layer about 1,000 kc lower in frequency. They have shown that where this critical effect is in evidence on 4,100 kc the virtual heights for F_2 will decrease from the extremely high values as frequency is increased above 4,100 kc.

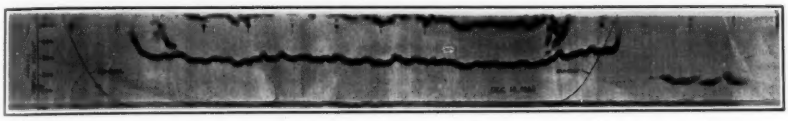

FIGURE 2.—*Record taken during daytime.*

Note slight increase in height during middle of the day. E-region reflections appear after sunset: All times are United States eastern standard time. All records are for 4,100 kc per second.

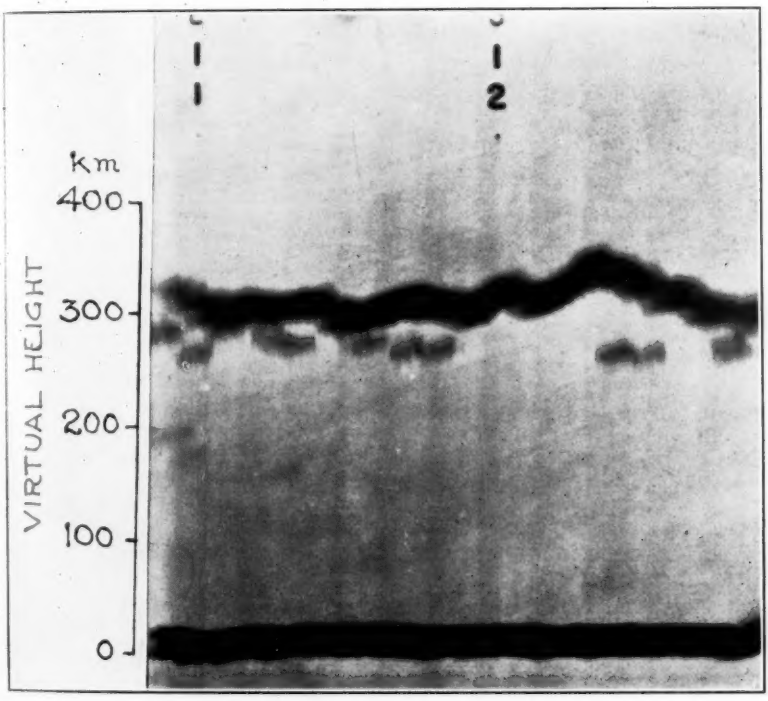

FIGURE 3.—*Record showing two components during the noon hour.*

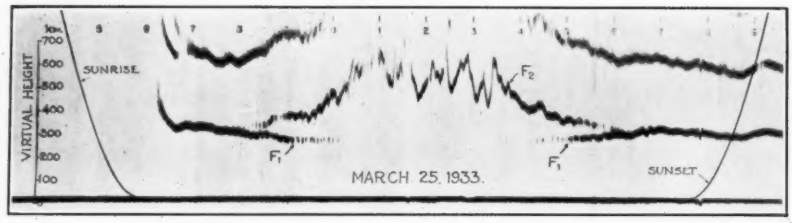

FIGURE 4.—*Record showing separation of the two components in the morning and joining again before sunset.*

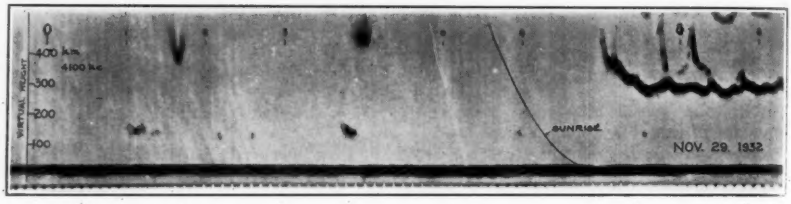

FIGURE 5.—*Record showing momentary appearance of reflection at night.*
Also note rapid changes of component with greater retardation after sunrise.

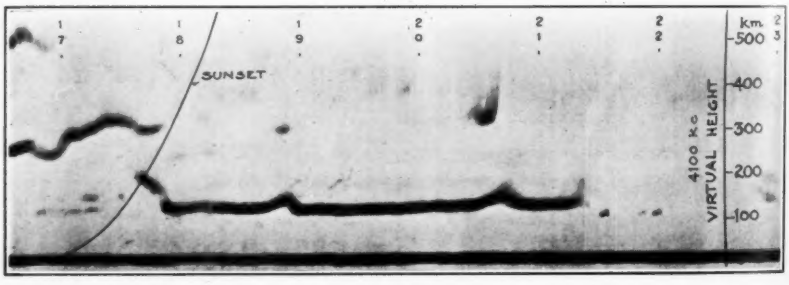

FIGURE 6.—*Record showing appearance of F-region reflections coincident with changes in E region.*

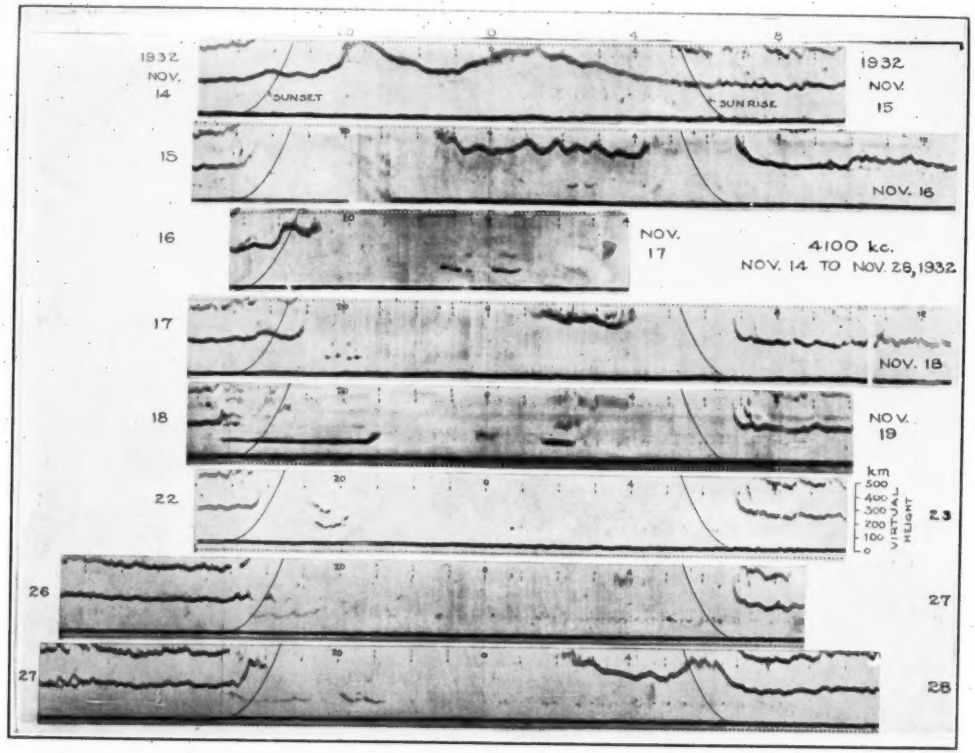

FIGURE 7.—*Maximum of Leonid meteor shower occurred on night of November 14–15.*

The 14th and 16th are days of magnetic character 1. Record for morning of November 23 shows virtual height decreasing at the rate of 1.1 km per second for 90 seconds. The next record shows still more rapid change.

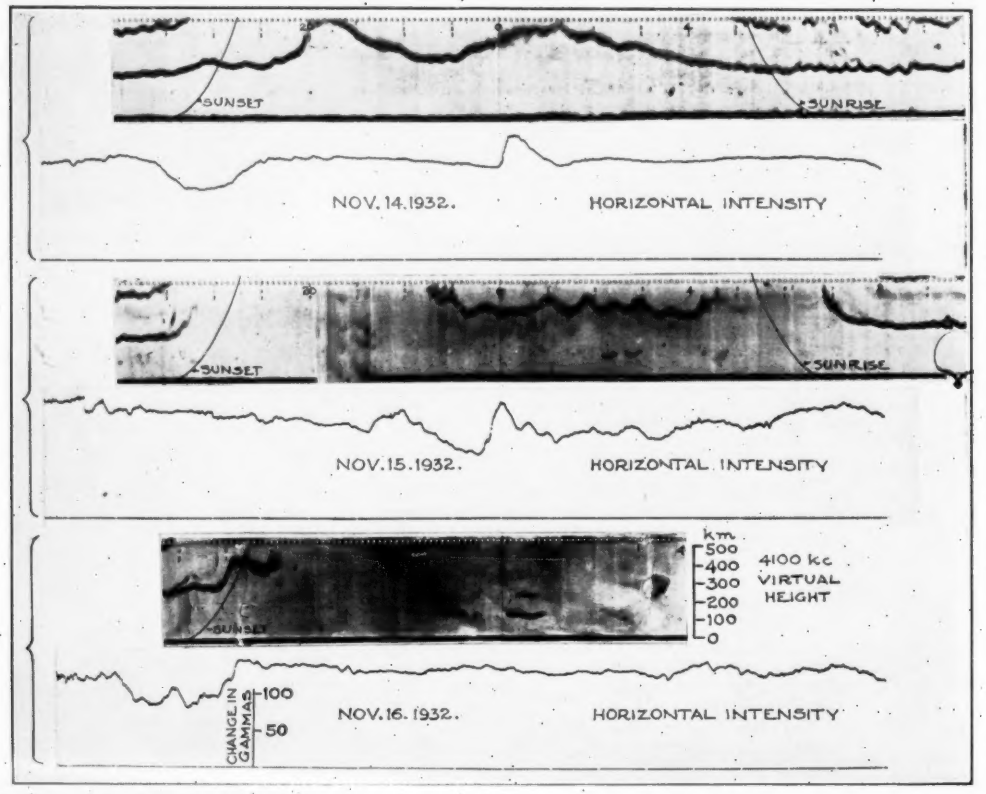

FIGURE 8.—*Records of November 14, 15, and 16 replotted with curves of horizontal intensity of earth's magnetic field.*

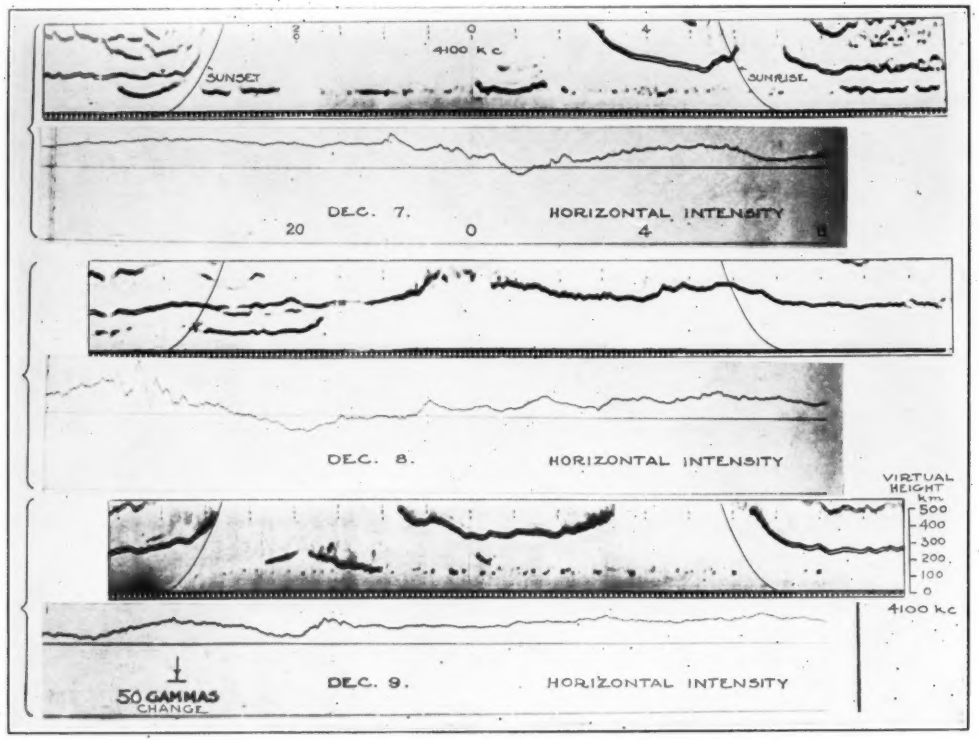

FIGURE 9.—*Records for 3 days plotted with magnetic records.*

Magnetic storm is indicated by rapid change in horizontal intensity beginning just before 1,600 on the 8th. Note strong reflections at night from both E and F regions.

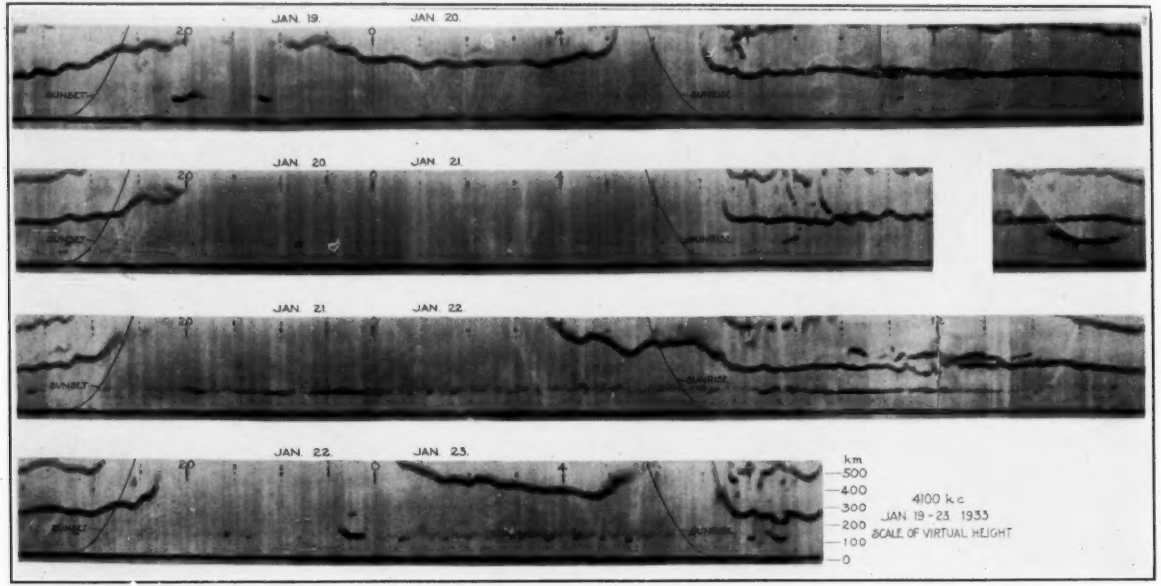

FIGURE 10.—*Records for 4 consecutive days.*

The 20th and 22d are days of magnetic character 1, while the 19th, 21st, and 23d are zero days.

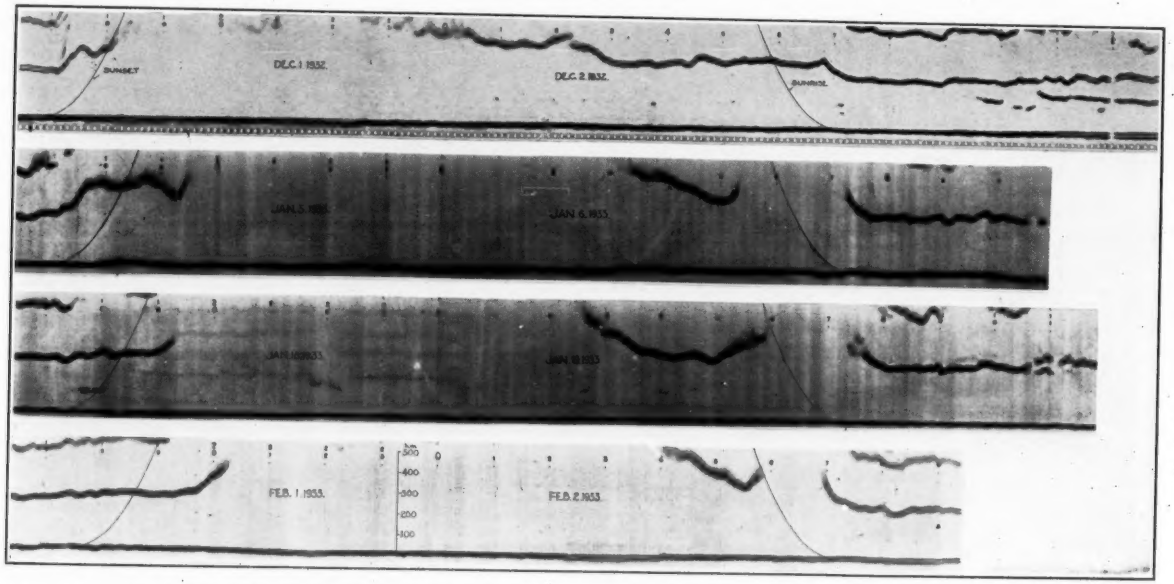

FIGURE 11.—*Records showing reflection at night from the upper region without evidence of strong reflections from the lower region.*

January 6 has magnetic character 1. Others are zero days.

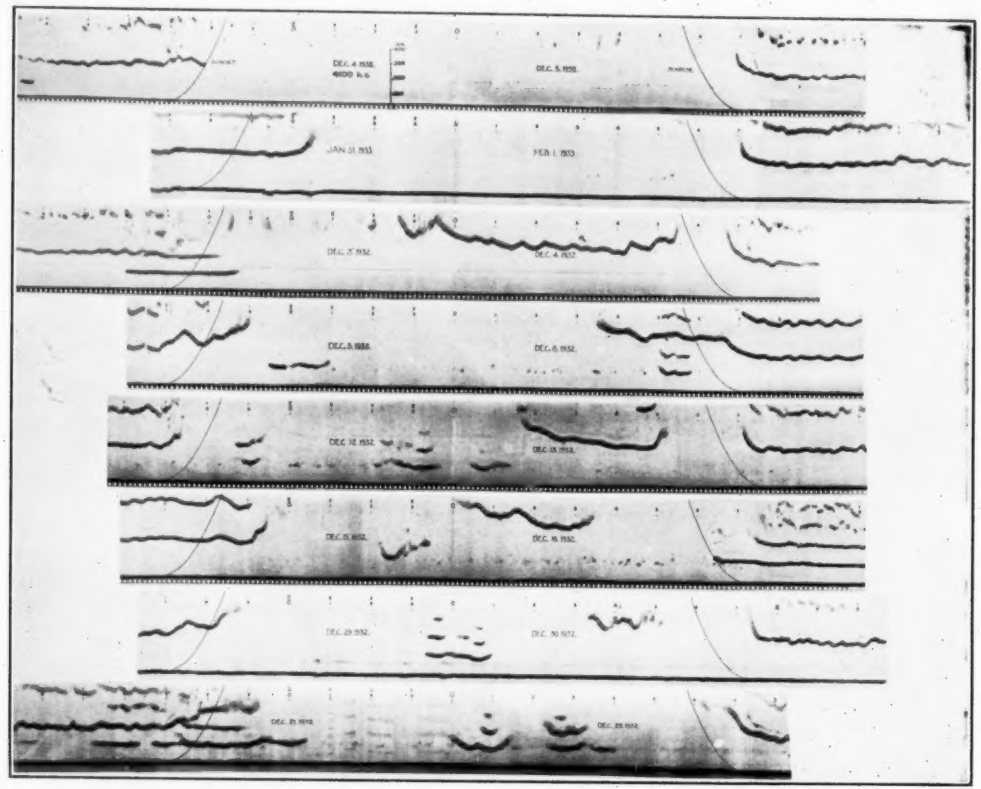

FIGURE 12.—*Records chosen to indicate variability from night to night.*

The first two records give only slight indication of reflection at night. The third to seventh records inclusive show appearance of both E and F reflections while the last record shows strong reflections from only the E region during the night. December 15 has magnetic character 1. Others are zero days.

Records taken between November 14 and 27, 1932, are shown in figure 7. The 14th and 16th were of magnetic character 1[6], while the other days of November were zero days. The maximum of the Leonid meteor shower occurred on the 14th. For the purpose of showing the complexity rather than for demonstrating any definite correlation, the records of November 14, 15, and 16 are reproduced in figure 8 with records of horizontal intensity of the earth's magnetic field. The night of November 14–15 was the first during this series that reflections continued throughout the night. Strangely enough there are practically no *E*-layer reflections visible on this record. It is possible that any *E*-layer ionization due to meteors was of such short duration that reflections failed to register. *E*-layer reflections are more in evidence on most other nights. Rapid changes in virtual height on this frequency are most likely to occur at sunrise and sunset, although such changes occur at other times when this frequency is near a critical value. The record for the morning of November 23, (fig. 7) shows the virtual height decreasing at the rate of 1.1 km per second for 90 seconds. The next record shows a much more rapid change but it is impossible to determine the rate of drop accurately because of the slow rate of movement of the film.

Records taken on December 7, 8, and 9 are shown with magnetic records in figure 9. The 7th and 9th are zero days, while the 8th has magnetic character 1. A magnetic storm is indicated by the rapid change in horizontal intensity beginning just before 1600 on the 8th.

Records obtained for four consecutive days from January 19 to January 23 are shown in figure 10. The Cheltenham Observatory gives the 20th and 22d with character 1, while the 19th, 21st, and 23d are zero days.

The changes which have been observed in the ionosphere are so abrupt and irregular that it has been found very difficult to show in just what way they are connected with other phenomena, such as magnetic storms, meteor showers, sunspots, or thunderstorms. It is likely that still other factors will be necessary to explain all the changes observed. It is thought advisable to await the accumulation of data over a longer period of time and on other frequencies in order that a more complete study may be made.

The reappearance of reflections at night suggests an increase in ionization, especially where strong reflections from the *E*-layer suddenly occur. The first record of figure 9 shows a strong E reflection beginning just after midnight and lasting until about 0200. At 0245 reflections appear from the upper region. Although these latter reflections may be explained by changing of the gradient of ionization in the *F* layer, as mentioned below, it is possible that ionization has merely passed through the *E*-layer critical value for the frequency used and long retardation and high absorption are occurring between the disappearance of the lower reflection and the appearance of the higher one. Another critical value is reached about 0600 and long retardation again occurs. At shortly after 0700 reflections again appear with sunrise. This occurs again on the third record earlier in the night.

Schafer and Goodall[7] have noted the reappearance of reflections at night from the E layer. They mention that a changing gradient

[6] Zero magnetic character indicates quiet day, no. 1, moderately disturbed, and no. 2, severely disturbed. Magnetic records supplied by the Cheltenham (Md.) Observatory of the Coast and Geodetic Survey.

[7] J. P. Schafer and W. M. Goodall, Kennelly-Heaviside layer studies employing a rapid method of virtual height determination, Proc.I.R.E., vol. 20, p. 1131, July 1932.

of ionization may explain this reappearance, but they believe that an increase in ionization is more likely. The latter viewpoint would be supported by changes of the type shown in the first and third records of figure 9, where the appearance of strong reflections is sudden. In figure 11 are four records showing reflections at night from the upper layer without evidence of strong reflections from the lower layer. Here an increase in ionization may not be occurring. Possibly as recombination begins after sunset a critical value is reached in the lower part of the F layer so that high absorption and long retardation result. However, as recombination proceeds farther an upper, more richly ionized part of this region, where recombination is less rapid, begins to return energy. As conditions get farther from the critical value the virtual height is frequently seen to be as low as 280 km. The ionization in this upper region appears to reach another critical value just before sunrise.

Figure 12 contains records chosen to indicate the variability from night to night. The first two records give only slight indication of reflections at night. Note the rapid opening and closing of the split reflection at 1700 on the first record. The third to seventh records inclusive show appearance of reflections from both E and F layers, while the last record shows strong reflections from only the E layer during the night.

III. CONCLUSIONS

Of greatest interest perhaps is the reappearance of strong reflections at night from both E and F layers. Some of these reflections indicate sudden increases in ionization, while others suggest that recombination in a lower part of the region exposes the upper part where ionization is richer.

Many of the changes observed are very sudden, and strong reflections from the E layer may appear at almost any hour. Various explanations have been offered in the past, including sun spots, meteor showers, and thunderstorms. Comparisons are also made between such results and changes in the earth's magnetic field. Although certain peculiarities, such as strong E reflections, are observed at magnetically disturbed times quite similar phenomena are observed when no unusual magnetic changes are in evidence. Since the changes in the ionosphere are so frequent and so rapid it is impossible, with the small amount of data at hand, to show definitely just how important each factor is.

None of the explanations yet offered seems to explain satisfactorily the extremely high ionization frequently observed at night. Although E-layer reflections appear at almost any time, they occur most frequently around the time of sunset or shortly after on this frequency during the period of these observations.

This method offers a convenient means for studying the physical properties of the upper atmosphere and should prove helpful in the solution of certain radio transmission problems. With data of this type taken over a longer period and on other frequencies it is hoped that it will be possible to obtain a more exact picture of the changes which occur in the ionosphere and to determine some of the agencies responsible for these changes.

WASHINGTON, April 18, 1933.

U.S. Department of Commerce—Bureau of Standards

RESEARCH PAPER RP583

Part of Bureau of Standards Journal of Research, Vol. 11, July 1933

THE EFFECTS OF ATMOSPHERIC MOISTURE ON THE PHYSICAL PROPERTIES OF VEGETABLE AND CHROME TANNED CALF LEATHERS

W. D. Evans and C. L. Critchfield

ABSTRACT

Data are presented giving the changes in tensile strength, stretch, load at failure, area, thickness, and moisture content with changes in relative humidity for vegetable and chrome-tanned calf leathers.

The differences between the behaviors of chrome- and vegetable-tanned leathers are accounted for by the difference between the amounts of protein material in the leathers.

The mechanism of the effect of absorbed moisture on the strength of leather is discussed.

CONTENTS

		Page
I.	Introduction	147
II.	Description of leathers used	148
III.	Methods of tests	148
	1. Strength and stretch tests	148
	2. Moisture content	150
	3. Rate of adsorption	151
	4. Area change	151
IV.	Results	153
	1. Strength and stretch tests	153
	2. Moisture content	155
	3. Rate of adsorption	157
	4. Area change	157
V.	Discussion	159
VI.	Summary	162

I. INTRODUCTION

Water vapor is always present in small amounts in the atmosphere. Usually referred to as "humidity", this water vapor affects the physical properties of materials with which it is in contact. This is particularly noticeable in the case of materials of an organic and fibrous nature, such as wool, cotton, silk, wood, paper, and leather.

For convenience, the water-vapor concentration in the air is usually referred to as a percent of the vapor pressure of pure water at that temperature, or "percent relative humidity." This arbitrary designation has been quite universally adopted, since measurements referred to it are found to be more nearly independent of change with temperature than those referred to the absolute humidity or actual vapor pressure of water.

There are two principal types of tannage—chrome and vegetable. Chrome-tanned leather is tanned with basic chromium salts and usually contains from 5 to 10 parts tanning material (as Cr_2O_3) per

100 parts of hide substance. Vegetable-tanned leather is tanned with extracts of certain vegetable materials and usually contains from 50 to 80 parts tannin per 100 of hide substance.

There is quite a difference between the behavior of these two types of leather as affected by water vapor. Wilson and Kern studied the variations in strength, stretch,[1] and area,[2] for both leathers, but used a limited number of samples. Veitch, Frey, and Leinbach [3] studied the strength and stretch of vegetable tanned calf leather alone at humidities of 35, 55, and 75 percent. In this work a further study has been made of the effects of atmospheric moisture on the properties of both types of leather.

II. DESCRIPTION OF LEATHERS USED

One chrome-tanned and one vegetable-tanned calfskin were used in these tests. The skins were commercially tanned and finished. Their analyses are given in table 1.

The chrome-tanned calfskin was divided into two sides. One of these sides was degreased with petroleum ether. The rest of the leather was used as finished by the manufacturer.

TABLE 1.—*Chemical analyses of leathers used*

[Results expressed in percent, excepting for degree of tannage]

	Vegetable-tanned calf leather		Chrome-tanned calf leather	
Moisture		8.04		11.45
Petroleum ether extract		6.83		2.10
Hide substance		42.60		68.30
Total ash	0.85			9.26
Soluble ash	.72			------
Insoluble ash		0.13		------
Water solubles		6.49		------
Soluble tans	2.10			------
Soluble nontans	4.39			------
Cr_2O_3		-------	5.87	
Fe_2O_3		-------	.06	
Al_2O_3		-------	1.77	
Combined tannin [1]		35.91		------
Other organic matter [1]		-------		8.89
Total		100.00		100.00
Degree of tannage [2]		84.30		------

[1] Determined by difference.
[2] Grams combined tannin per 100 g hide substance.

III. METHODS OF TESTS

1. STRENGTH AND STRETCH TESTS

The skins were cut into strips 6 inches long by 1¼ inches wide, parallel to the backbone. The strips were stamped out with a die into standard tensile strength samples [4] (fig. 1). A number was stamped

[1] Wilson, J. A., and Kern, E. J., Variation in Tensile Strength of Calf Leather with Relative Humidity, J. Am. Leather Chem. Assoc., vol. 21, p. 250, 1926.
[2] Wilson, J. A., and Kern, E. J., Area Change of Shoe Leather with Relative Humidity, J. Am. Leather Chem. Assoc., vol. 21, p. 351, 1926.
[3] Veitch, F. P., Frey, R. W., and Leinbach, L. R., Influence of Atmospheric Humidity on the Strength and Stretch of Leather, J. Am. Leather Chem. Assoc., vol. 17, p. 492, 1922.
[4] Federal specification no. 37.

on each strip to identify it. The strips were marked with gage marks 2 inches apart and the thickness measured in four places. The thickness was estimated to one ten thousandth of an inch on a Randall and Stickney gage reading directly to thousandths of an inch. A constant load of 1 kg was applied to the measuring foot which had an area of 1 cm^2.

The strips of each skin were divided into three groups according to strength as indicated by Wilson's chart of strength variation over a calfskin.[5] Then each side of skin no. 1 (chrome calf) was divided into 5 lots of 17 strips each, and skin no. 2 (vegetable calf) was divided into 9 lots of 13 strips each. Each strength group was divided evenly among the various lots so that each lot was as nearly as possible representative of the whole skin.

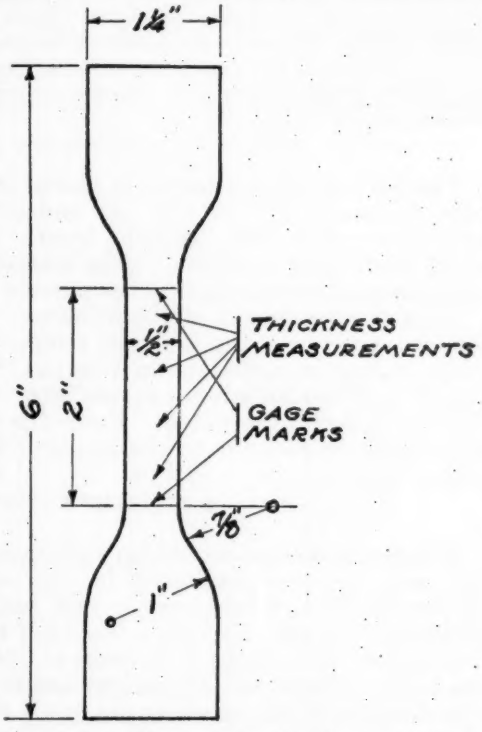

FIGURE 1.—*Diagram showing shape and size of tensile test specimens.*

Half-liter bottles were used for conditioning. The corks were paraffined to prevent the passage of moisture and hooks were screwed into the lower ends. Saturated salt solutions with an excess of salt were put in the bottoms of the bottles and the strips suspended in pairs from the hooks.

One lot each of the normal and degreased chrome calf leather from skin no. 1 was placed over dry phosphorus pentoxide for the 0 percent relative humidity conditions. The other 8 lots, 4 each of the normal and degreased leather, were placed over salt solutions maintaining the humidities 32.9, 52, 75.7, and 97.1 percent.

The nine lots of strips from skin no. 2, vegetable-tanned calfskin, were conditioned in a like manner at humidities of 0, 9, 20, 32.9, 52, 75.7, 83.8, and 97.1 percent.

Saturated salt solutions in a closed system at a definite temperature tend to maintain a constant concentration of water vapor in the atmosphere over them. The salt used in these tests and the humidities they maintain are given in table 2. These values were taken from the International Critical Tables.[6] Those salts listed at 20° and 23° were used as being the same at 21°. This introduces but a slight error.

[5] Wilson, J. A., Chemistry of Leather Manufacture, Am. Chem. Soc. Monograph Series, vol. 2, p. 1063 (2d ed.), 1929.
[6] Int. Crit. Tables, vol. 1, pp. 67–68.

TABLE 2.—*Relative humidities over saturated salt solutions*

	Relative humidity	Temperature
		° C.
Phosphoric acid ($H_3PO_4.1/2\ H_2O$)	9	23.5
Potassium acetate (CH_3COOK)	20	20.0
Magnesium chloride ($MgCl_2$)	32.9	21.0
Potassium carbonate (K_2CO_3)	43.5	21.0
Sodium dichromate ($Na_2Cr_2O_7$)	52	20.0
Sodium chloride (NaCl)	75.7	21.0
	74.3	43.0
	74.0	60.0
Potassium bromide (KBr)	83.8	21.0
Potassium nitrate (KNO_3)	94.2	21.0
Potassium sulphate (K_2SO_4)	97.1	21.0

The bottles and leather were placed in a room kept at a constant temperature of 21° C. At the end of a month the bottles were opened one at a time, and the length, width, and thickness of the strips were again measured. The leather was replaced in the bottles after having been exposed to the outside air less than 1 minute.

After 2 more weeks of conditioning, the bottles were removed a few at a time from the constant temperature room, opened, and the strips broken immediately on a vertical Scott testing machine. The stretch at 2,000 pounds per square inch, the stretch at failure, and the load at failure were noted. From the breaking load and the area and thickness data the tensile strength was calculated in pounds per square inch.

2. MOISTURE CONTENT

The method used to obtain moisture contents was substantially the same as that employed in the strength tests. Leather was suspended in a bottle over a salt solution until equilibrium was obtained. It was put into a weighing bottle and the weight taken. The leather was dried for 24 hours at 100° C. in an electric oven and the loss in weight and dry weight noted. The moisture content was calculated as grams of water per 100 g of dry leather. This method of determining the moisture content was adopted because it is that used by the American Leather Chemists Association. The salts used to maintain humidities were the same as those used in the strength tests. (See table 2.)

For purposes of comparison the moisture contents of several other leathers were measured. Humidities were maintained over sulphuric acid solutions [7] of various concentrations. The leathers used other than the vegetable and chrome tanned calf leathers were:

1. Natural quebracho-tanned steer hide leather.
2. Chestnut-tanned steer hide leather.
3. Degreased alum-tanned cowhide leather.
4. Dehydrated and deashed hide substance (in strips).

[7] Wilson, R. E., Humidity Control by Means of Sulphuric Acid Solutions, Ind. Engr. Chem., vol. 13, p. 226, 1921.

3. RATE OF ADSORPTION

The rate of adsorption was measured for each leather in a small closed system with no induced circulation of air.

A hole was bored through the cork of a wide-mouthed bottle and a small piece of glass tubing inserted. A piece of fine copper wire was run through a paraffined cork small enough to stopper the glass tubing. The leather was suspended from the wire inside the bottle. Conditioning agents were kept in the bottom of the bottle (fig. 2). When weighings were to be made the bottle was set on a bridge in the balance, the cork removed from the glass tubing, and the cork, wire, and leather weighed together from the balance pan hook. This arrangement permitted keeping a record of the change in weight of the sample without removing it from contact with the conditioning atmosphere.

The suspended sample was placed in a bottle over phosphorus pentoxide until dryness was attained as indicated by constant weight. It was immediately transferred to another bottle in which there was a saturated solution of potassium sulphate (97 percent relative humidity). The sample was weighed at frequent intervals until approximate equilibrium was reached.

The reverse procedure was followed with the chrome-tanned calfskin to obtain a desorption curve. The vegetable-tanned calfskin molded too badly at the high humidity to allow these measurements.

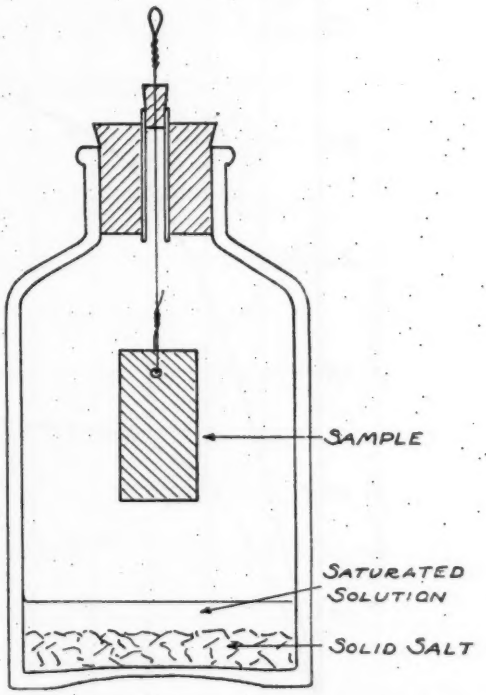

FIGURE 2.—*Diagram of apparatus used in adsorption-rate measurements.*

4. AREA CHANGE

A flat, horizontal, moisture-proofed box was equipped with a plate-glass cover. An inch and a half below the glass and parallel with it a brass screen was fixed. Three samples of vegetable-tanned calf leather and two samples of chrome-tanned calf leather were cut into circles approximately 10 cm in diameter. Two sets of gage marks were made at right angles to each other on the samples. The leather was put on the brass screen. Humidifying solutions were kept in an enameled pan in the bottom of the box. The removable cover was sealed in place with clamps and stopcock grease.

Measurements were made by means of a movable flat scale and a piece of optical glass 2 inches thick with plane parallel faces. Two lines parallel to each other were etched on opposite faces of the glass

identifying a plane perpendicular to the plane of the faces. The glass was placed on the plate-glass cover of the box in such a way that one of the gage marks on a sample and a point on the scale were made to coincide with the line of sight of the etched lines. The glass was moved and sighted on the corresponding gage mark and a scale reading made. From the lengths thus measured the change in area

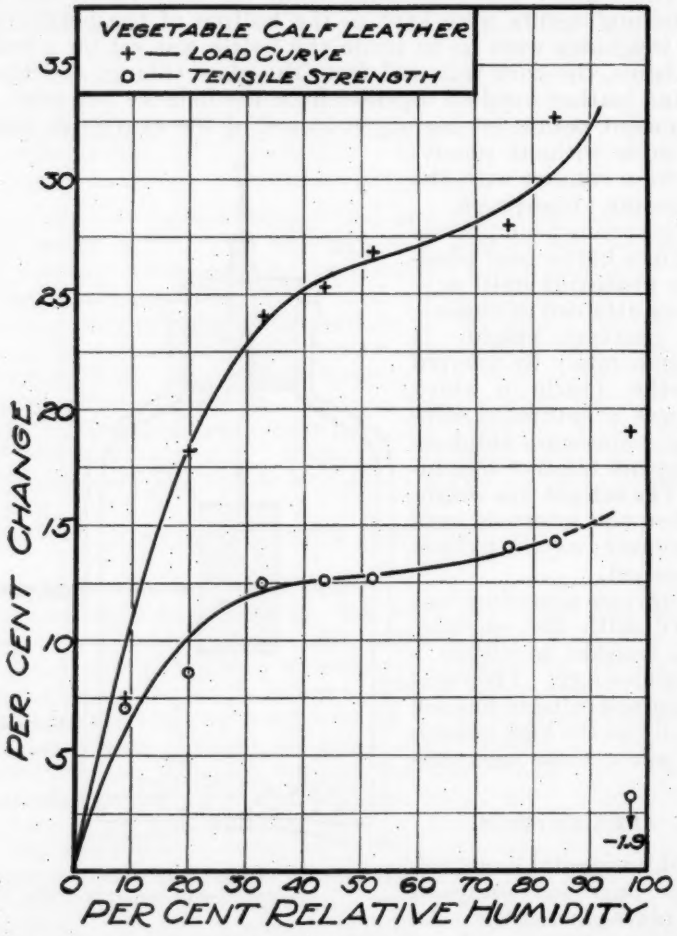

FIGURE 3.—*Percent changes in breaking load and tensile strength with change in relative humidity of vegetable-tanned calf leather.*

of the leather between different relative humidities was calculated. Readings were taken at humidities of 0, 33, 52, 75, and 94 percent. The samples were conditioned a month or over for each measurement although practically no change in area was observable after 5 days. Concentrated sulphuric acid was used to obtain 0 percent relative humidity. The salts used to maintain the other humidities are given in table 2.

This method of procedure allowed a record to be kept of the dimensional changes of a piece of leather over a period of time without rolling, stretching, flexing, or touching it in any way during the course of the experiments.

IV. RESULTS

1. STRENGTH AND STRETCH TESTS

The results of the strength and stretch tests are presented in tables 3 and 4. It will be seen by inspection that the change in properties is

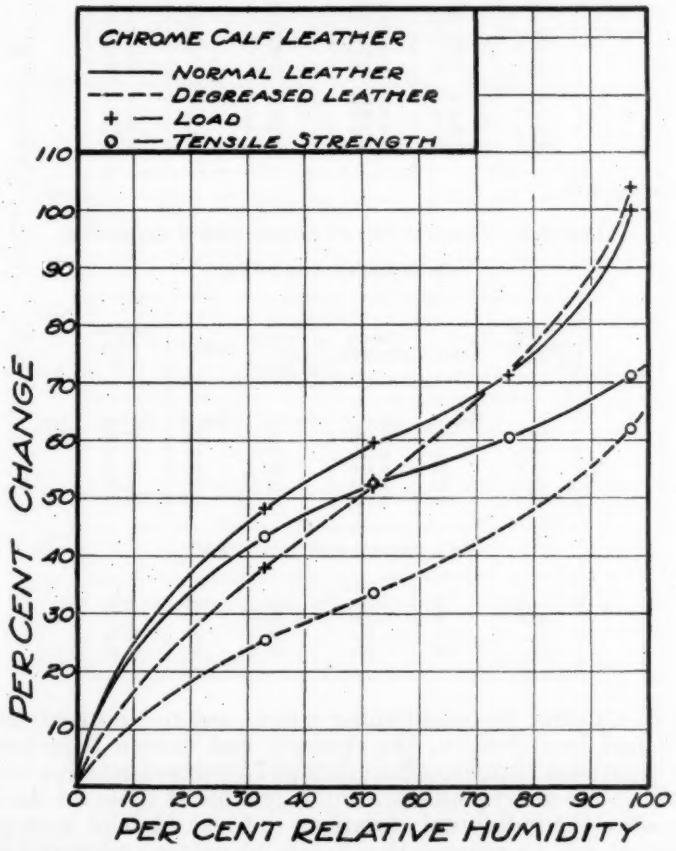

FIGURE 4.—*Percent changes in breaking load and tensile strength with change in relative humidity of chrome-tanned calf leather.*

much more pronounced for the chrome than for the vegetable-tanned leather.

In figures 3 and 4, the percent changes in load and tensile strength with relative humidity are shown graphically. The percent change in tensile strength is less than the percent change in load, since the change in the former is partly compensated for by the change in cross-sectional area. The load values are the better for the purpose of

comparison, since the tensile strength values introduce another variable, cross-sectional area, which for a given sample of leather is not under the control of the observer and may be studied separately.

TABLE 3.—*Physical tests on vegetable-tanned calf leather*

Relative humidity, 21° C.	Load at failure	Tensile strength	Stretch at load of 2,000 lb./in.²	Stretch at failure	Increase in thickness
	Pounds	*Lb./in.²*	*Percent*	*Percent*	*Percent*
0	74.7	4,630	16	30	0.00
9	80.3	4,960	17	32	1.39
20	88.3	5,030	18	38	2.03
32.9	92.7	5,210	19	33	2.30
43.5	93.6	5,215	19	34	2.81
52	94.7	5,220	19	34	2.85
75.7	95.6	5,280	21	36	4.60
83.8	99.1	5,290	20	37	6.01
[1] 97.1	[1] 89.0	[1] 4,540	21	36	9.63

[1] Leather badly molded.

TABLE 4.—*Physical tests on chrome-tanned calf leather*

A. NORMAL LEATHER

Relative humidity, 21° C.	Load at failure	Tensile strength	Stretch at load of 2,000 lb./in.²	Stretch	Increase in thickness
	Pounds	*Lb./in.²*	*Percent*	*Percent*	*Percent*
0	52	3,170	19	34	0.00
32.9	77	4,550	25	46	1.55
52	83	4,840	23	46	1.87
75.7	89	5,080	24	48	4.23
97.1	104	5,420	25	50	14.05
B. DEGREASED LEATHER					
0	53	3,250	16	26	0.00
32.9	73	4,070	22	41	3.95
52	79	4,340	23	43	4.74
97.1	108	5,270	25	54	15.87

Due to an error in conditioning which was not noticed until the samples had been broken, the strength and stretch determinations for the degreased chrome calf leather at 75 percent relative humidity were lost. The other points are not as reliable as those for the normal leather since the individual variations in breaking load were greater. However, it will be noticed that below 50 percent relative humidity the change in load is less for the degreased than for the normal leather, while above this humidity the reverse is true. The change in cross-sectional area was greater for the degreased than for the normal leather; consequently, the tensile strength change is less.

The vegetable calf leather at 97 percent relative humidity molded badly. This resulted in a loss in breaking strength which, in combination with the greatly increased cross-sectional area, was sufficient to give the leather a tensile strength less than that observed at 0 percent relative humidity.

2. MOISTURE CONTENT

The moisture contents of the normal chrome and vegetable-tanned calf leathers at 21° C. at different relative humidities are shown graphically in figure 5. The moisture contents are plotted as grams of water per 100 g of dry leather. The moisture contents of the degreased samples were practically the same as those of the normal leather.

The moisture content of leather dried over phosphorus pentoxide is given as being 0 percent. Actually, such leather upon being heated

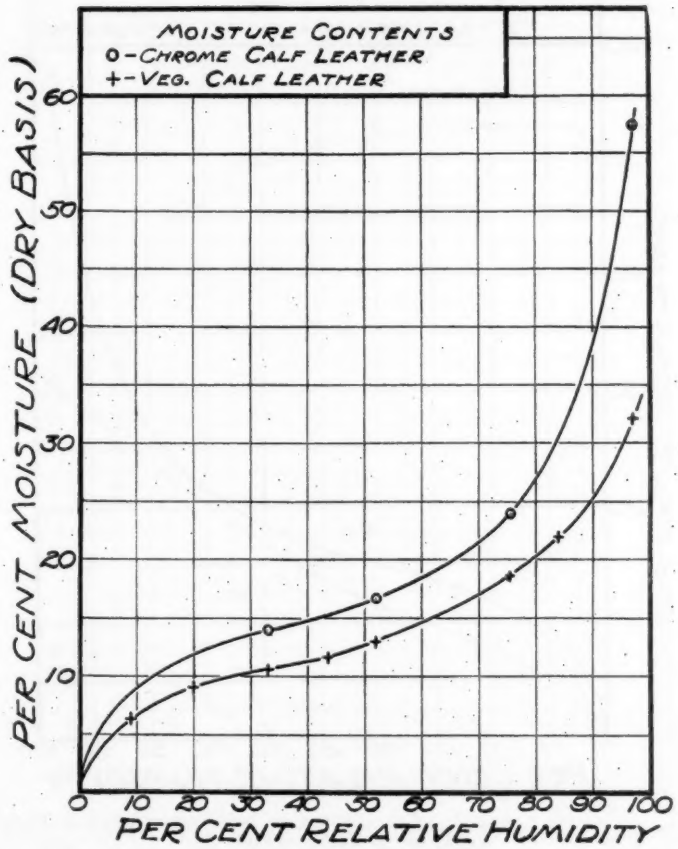

FIGURE 5.—*Change of moisture content with change in relative humidity of chrome- and vegetable-tanned calf leathers.*

at 100° C. showed a loss in weight of from 0.3 to 0.8 percent. Wilson [8] reports this as adsorbed water. The authors believe that such is not the case; that this is a permanent loss in weight due to a change in composition of the leather. Phosphorus pentoxide in a closed system maintains over itself a relative humidity below 0.0001 percent, for all practical purposes, 0 percent. Drying at 100° C. is a substitution

[8] Wilson, J. A., Chemistry of Leather Manufacture, Am. Chem. Soc. Monograph Series, vol. 2, p. 1071, 1929.

for this condition, approximately correct in most cases. This method is to be preferred wherever possible because of its greater convenience and rapidity. However, there are cases where it is inapplicable or only approximately valid. That this is true for leather is shown by the difficulties of the American Leather Chemist's Association Committee [9] and other investigators [10] in providing an accurate or reproducible method for the determination of moisture in leather. Veitch and Jarrell [11] have also shown that vegetable tanned leather heated at 100° loses weight continuously. As evidence that the composition

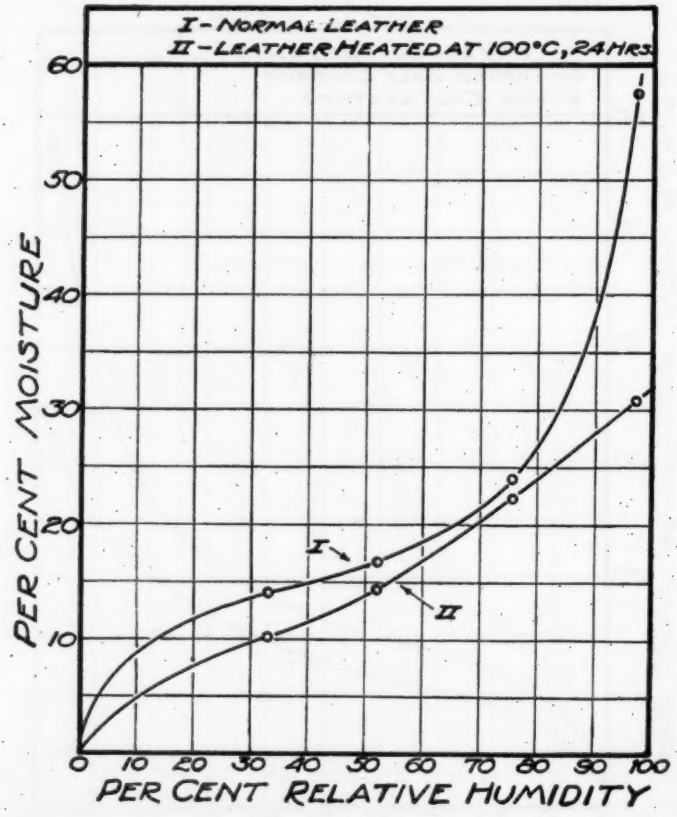

FIGURE 6.—*Adsorptive capacity of chrome-tanned calf leather before and after being heated for 24 hours at 100° C.*

of chrome-tanned leather is changed by heating, the data in figure 6 are presented.

Chrome-tanned calf leather was conditioned over saturated salt solutions until equilibrium was attained. This leather was then dried at 100° C. for 24 hours and the moisture content calculated on this dry basis (curve 1, fig. 6). The leather was reconditioned over

[9] American Leather Chemists Association Committee Report on Humidity, J. Am. Leather Chem. Assoc., vol. 15, p. 529; vol. 17, p. 262; vol. 21, p. 435; vol. 22, p. 265.
[10] Veitch, F. P., and Jarrell, T. D., J. Am. Leather Chem. Assoc., vol. 16, p. 547; vol. 19, p. 568; vol. 20, p. 334.
[11] Veitch, F. P., and Jarrell, T. D., J. Am. Leather. Chem. Assoc., vol. 16, p. 547.

the same salt solutions. The new moisture contents are given in curve 2, figure 6. The leather never regained its original weight, the application of heat inhibiting the readsorption of water under the same conditions.

3. RATE OF ADSORPTION

As previously described, leather was dried over phosphorus pentoxide and then exposed to an atmosphere of 97 per cent relative humidity the change in weight being noted at intervals. The results are presented in figure 7. The moisture, as a percent of the total change in

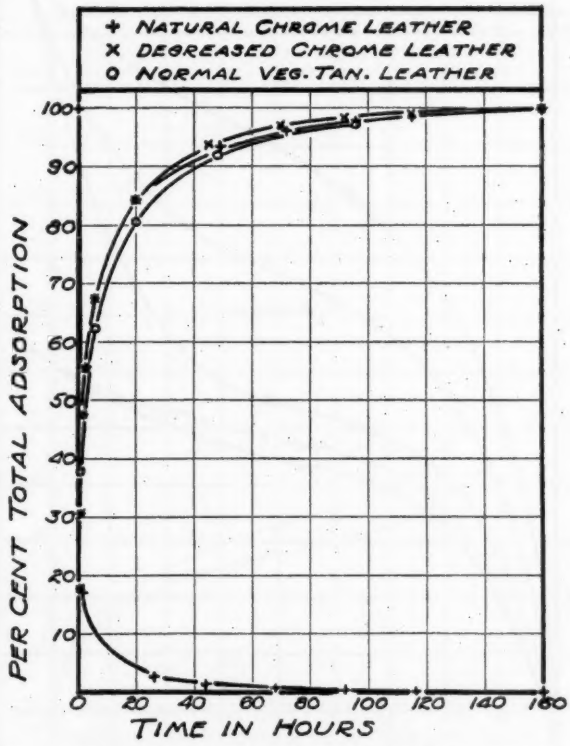

FIGURE 7.—*Rate of adsorption of calf leather in still air.*

weight of the sample, is plotted against the time in hours. Practically no change in weight was observable from 150 to 200 hours. The drying curve for normal chrome tanned calf leather is also shown in figure 7.

4. AREA CHANGE

Change in area is shown as a function of relative humidity in figure 8. The most striking feature of this graph is the large hysteresis effect shown by the chrome calf leather. The small arrow heads show the direction in which conditioning was proceeding. Much less hysteresis was exhibited by the vegetable-tanned calf leather.

No investigator has observed moisture content hysteresis of sufficient extent to account for this effect.[12] It is suggested that when the moisture conditions are changed an internal stress is set up in the leather which does not entirely equalize itself, but will rapidly do so if the leather is bent, handled, or coiled. This would account for the failure of Wilson and Kern [13] to detect this effect since they used strips of leather which were coiled and uncoiled during the course of their

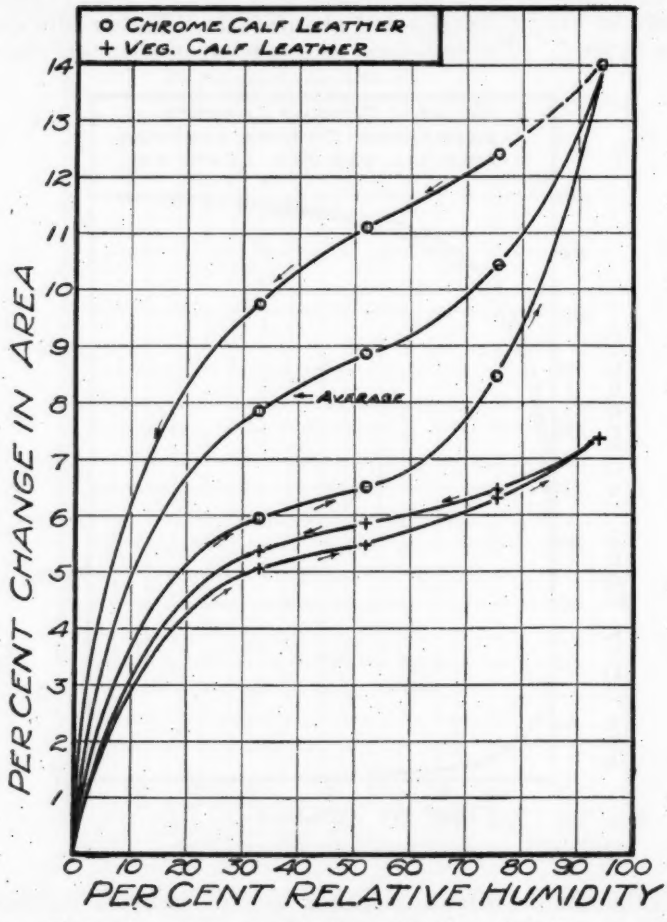

FIGURE 8.—*Change in surface area with change in relative humidity of vegetable- and chrome-tanned calf leathers.*

experiments. The differences between the behaviors of the chrome- and vegetable-tanned leathers may perhaps be accounted for by the looser structure of the former, the greater range of variation, and the larger percent of protein material.

Change in cross-sectional area with relative humidity is shown in figure 9. The values for the linear change on the surface which were

[12] L. Meunier and K. Le Viet, J. Intern. Soc. Leather Trades' Chem., vol. 14, p. 524, 1930.
[13] See footnote 2, p. 148

used in calculation are the averages of those obtained by approaching a humidity from each side of the equilibrium. The thickness changes are the averages of those noted in the strength tests. The change in cross-sectional area is quite different from the change in surface area, due to the greater change in thickness with relative humidity as compared with change in length. Since the fibers are oriented more or less parallel to the grain, the probable explanation for this is the greater swelling of the fibers in a direction perpendicular to their length. This effect would be more noticeable, since the thickness measurements were made with the leather under a compression of 1 kg/cm^2.

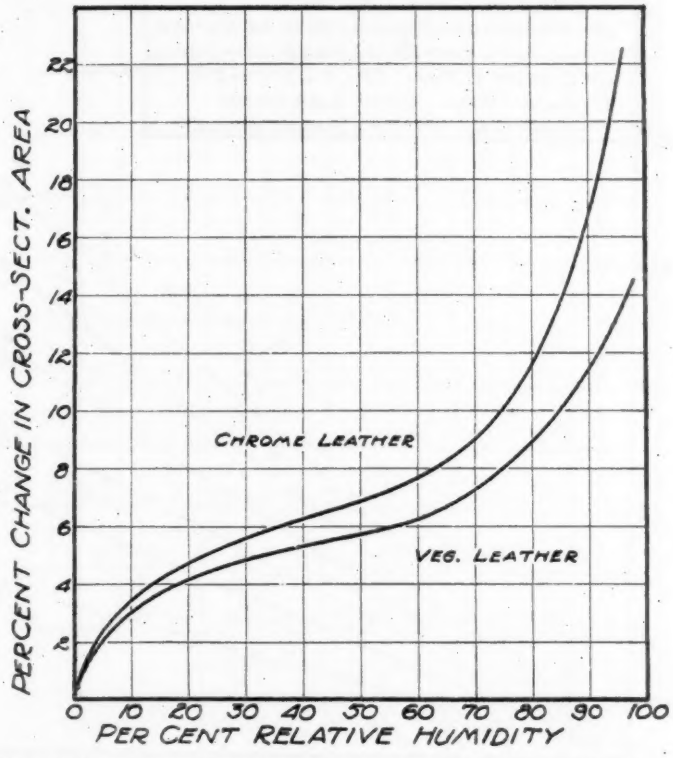

FIGURE 9.—*Change in cross-sectional area with change in relative humidity of vegetable- and chrome-tanned calf leathers.*

V. DISCUSSION

During the previous paragraphs emphasis has been laid principally on the relationships existing between the various properties studied and the relative humidity. It should be remembered that this is a secondary relationship. The variations studied depend upon the moisture content of the leather which in its turn depends upon the relative humidity.

If the moisture content of a sample of leather at a definite temperature is plotted against the corresponding relative humidities, a sigmoid curve characteristic of this material is the result.

The ability of a leather to adsorb water seems to depend principally on the amount of hide substance in the leather. This is augmented or interfered with by the presence of other materials. In figure 10 the percent moisture at 10, 20, 30, 40, 50, and 60 percent relative humidity, 30° C., of six leathers is plotted against the percent hide substance of the leathers. The result is a series of nearly straight lines passing through the origin. This is quite surprising considering that the effects of grease, uncombined tannin, nontans, added salts, etc., have

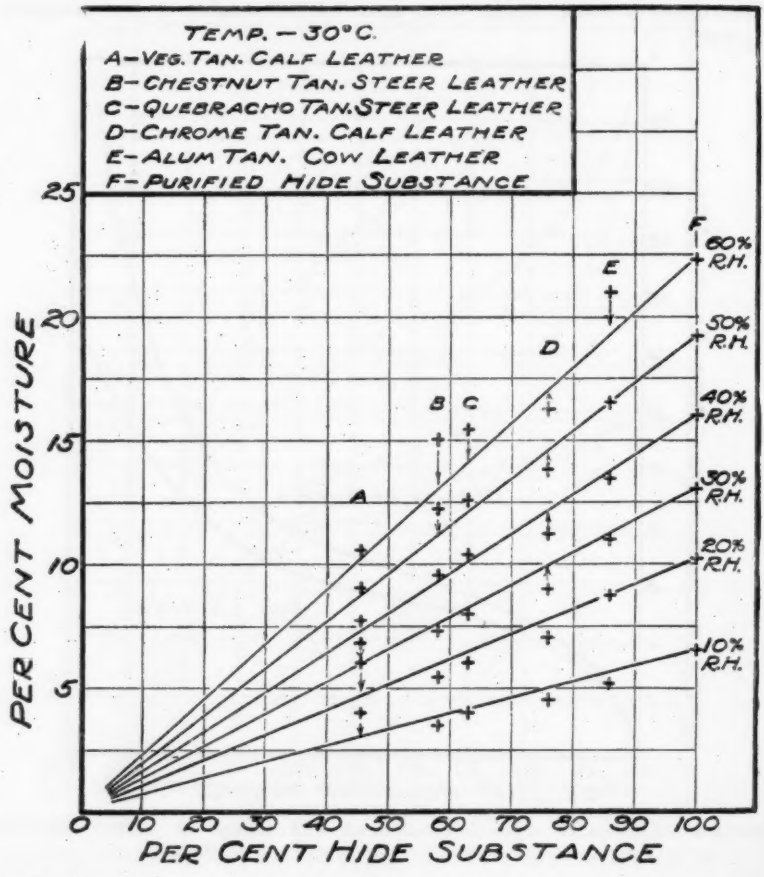

FIGURE 10.—*Relation between adsorptive capacity and constitution of various leathers.*

been entirely disregarded. Above 60 percent relative humidity the effect of salts becomes too great to be disregarded, particularly in the case of the alum-tanned leather. As the percent of hide substance decreases the effects of the other materials mentioned are, of course, augmented.

In figure 11, the percent changes in load and area for the chrome- and vegetable-tanned calf leathers are plotted against the percent changes in moisture content. The points shown represent relative humidities of 10, 20, 30, etc., up to 90 percent. The shape of the

corresponding curves is very similar, suggesting merely a change in scale. This change of scale is probably governed by the amount of protein material in the dry leather. It is interesting to notice that lines drawn between the points representing the corresponding relative humidities result in a series of nearly parallel lines.

Wilson and Kern [14] state that the effect of moisture on the strength of leather is due to the lubricating effect of the adsorbed water. However, this curve, shown in figure 11, is a sigmoid, suggesting that the adsorbed water has a compound effect which may be analyzed as in the succeeding paragraphs.

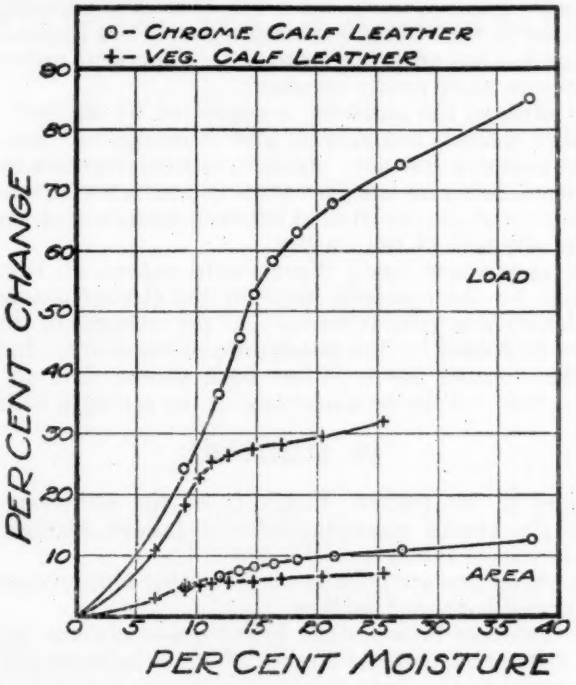

FIGURE 11.—*Changes in breaking load and surface area with change in moisture content of vegetable- and chrome-tanned calf leathers.*

If the stretch of leather at constant load per unit of cross-sectional area is plotted against the moisture content, a rapid increase in ease of stretch is noticed between 0 and 15 percent moisture, after which there is little change. This increase in case of stretch may account for a similar increase in strength.

When a sample of leather is put under tension it does not fail instantaneously. If the sample is held in immovable jaws under a proper tension, the pull of the leather itself will in time be sufficient to break it. First the snapping of individual fibers will be heard, continuing possibly for several minutes. Then the leather will start to tear slowly from one edge. This tearing will increase in speed as

[14] See footnote 1, p. 148.

more and more tension is placed on fewer and fewer fibers. Finally, when the sample has broken, the torn ends will be seen to consist of a mass of long silky fibers, each pulled from the opposite side of the plane of failure.

The above-described behavior of leather subjected to strain suggests a certain mechanism for the failure of leather as affected by moisture. When a piece of dry leather is put under tension, the stress is not evenly distributed on all the fibers, as witnessed by the snapping of individual fibers as the limit of strength is approached. As the moisture content increases, a more equable distribution of the load between the fibers is obtained due to the greater stretch of the leather. This effect becomes greater the greater the moisture content, giving the first sharp rise in the strength-moisture curve, but approaches a limit when the leather has adsorbed from 10 to 15 percent moisture and the stretch becomes more nearly constant.

Another effect of the moisture is suggested by the fact that failure of the leather consists not only of fiber breakage but also of slippage of the fibers past one another. As the moisture increases in the leather the fibers swell, bringing one fiber more in contact with another. This would tend to increase the friction between them and at the same time increase the strength of the leather.

The two above-mentioned effects, with others, all taken together may account for the complex shape of the strength-moisture curve. If this explanation is valid it means that the strength of the fiber itself may not be increased by the adsorption of moisture. Indeed, in the case of other animal fibers, it has been shown that an increase in moisture content will cause a decrease in the strength of the fiber.[15]

VI. SUMMARY

1. Changes in the relative humidity of the atmosphere result in changes in the tensile strength, load at failure, stretch, area, and moisture content of leather.

2. These variations are more pronounced for chrome-tanned leather than for vegetable-tanned leather.

3. The differences between the behaviors of chrome and vegetable tanned leathers are attributed to the difference between the amounts of protein material in the leathers.

4. A speculation is made concerning the probable mechanism of the effect of adsorbed moisture on the strength of leather.

WASHINGTON, May 15, 1933.

[15] Speakman, J. B., J. Soc. Chem. Ind., vol. 49; T209, 1930.